Comparative analysis of desiccation responses in three *Xerophyta* species at two stages of seedling development

Mamosa Ngcala

Thesis Presented for the Degree of

DOCTOR OF PHILOSOPHY and DOCTOR RERUM NATURALIUM

in the

Department of Molecular and Cell biology and

Institute for Biochemistry and Biology,

Faculty of Science

UNIVERSITY OF CAPE TOWN and UNIVERSITY OF POTSDAM

December 2024

ABSTRACT

Vegetative desiccation tolerance (VDT) is a rare trait among flowering plants, enabling the adult tissues of certain species, known collectively as resurrection plants, to survive near-total water loss and revive upon rehydration. This study used a seedling model to investigate VDT at two developmental stages, pre-leaf and two-leaf stage, across three *Xerophyta* species: the poikilochlorophyllous *Xerophyta schlechteri*, and *X. humilis, and* the homoiochlorophyllous *X. elegans*. By analyzing changes in cellular ultrastructure, gene expression, and metabolite and lipid concentrations, the aim was to identify core conserved VDT mechanisms in these three *Xerophyta* species, as well as differences between poikilochlorophyllous and homoiochlorophyllous species in the same genus. Transcriptomic analysis showed that the key seed master maturation transcription factors (TFs) *ABI3A* and *ABI5A*, were up-regulated in dry pre-leaf seedlings but no expression was detected in two-leaf seedlings. In contrast, the ABRE binding factor, *ABFA*, was highly expressed in dry tissues at all developmental stages across all species, suggesting a potential role in VDT. A three-way comparison was used to identify gene orthogroups (OGs) that showed the same response to desiccation across all three *Xerophyta* species: these 370 up-regulated and 335 down-regulated OGs potentially represented a core set of desiccation-responsive genes in *Xerophyta* species. Promoter regions of these core OGs were enriched with binding sites for *Xerophyta* specific expanded TF families, including Heat Shock Factors (HSFs), A-T hook factors (AHLs), and C_2H_2 Zinc Finger Proteins (ZATs). The gene ontology enrichment showed that the HSF, AHL, and ZAT-motif containing OGs that were up-regulated are involved in water deprivation, abscisic acid response, and oxidative stress response processes, whereas the down-regulated OGs are involved in growth and development related processes. Notably, some of the up-regulated HSF motif-containing target OGs included WRKY TFs, stachyose synthase, and solanesyl-diphosphate synthase 2, which are involved in stress-related functions enhancing VDT. Metabolite analysis demonstrated that the osmoprotectants proline, sucrose, and trehalose accumulated in dry tissues at both developmental stages of all three *Xerophyta* species. Moreover, differences in cellular ultrastructure including chloroplast organization were investigated by transmission electron microscopy, comparing a detailed dehydration-rehydration time course of poikilochlorophyllous *X. schlechteri* to homoiochlorophyllous *X. elegans.* This analysis revealed that desiccation-induced ultrastructural changes, such as vacuolation, chloroplast centralization, and starch degradation, typically observed in adult tissues, were also prevalent in the two-leaf seedlings of *X. elegans* and *X. schlechteri*. Notably,

complete disassembly of the thylakoid membranes was observed in *X. schlechteri* but not in *X. elegans*. These results align with the significant reduction of monogalactosyldiacylglycerol, a major galactolipid involved in chloroplast function. The results of this study highlight differences between the poikilochlorophylly and homoiochlorophylly strategies, as well as conserved molecular responses to desiccation in *Xerophyta* species, providing insights into the evolution of VDT.

DECLARATION

I declare that this thesis is solely my own work, and it has not been previously submitted for any degree or examination at any other university. Unless otherwise indicated by reference or acknowledgment, all content presented herein is entirely of my own creation.

ACKNOWLEDGEMENTS

I am deeply grateful to my supervisors, Prof. Nicola Illing, A/Prof Rob Ingle, Prof. Zoran Nikoloski, and Dr. Rafe Lyall, for their endless support and guidance throughout my PhD journey. Special thanks to Rafe for the invaluable assistance provided in analyzing my RNA-Seq data. During moments when bioinformatics analysis "showed me flames", your willingness to listen and offer help without hesitation or judgment was truly appreciated.

I extend my sincere thanks to Saleh Alseekh and Michael Wittenberg for their assistance with GC-MS/LC-MS analysis. I am also grateful to Mohamed Jaffer from the TEM unit at UCT and Prof. Otto Baumann from the University of Potsdam in Germany, for providing me with excellent training in TEM. Additionally, thanks to Keren Cooper for aiding in the sectioning of resin blocks during the initial stages of my TEM work and Isla for assistance with processing some of the TEM samples. Special appreciation to Christine, Caroline and Kelly for their help with RNA extractions from the "problematic" early-stage seedlings.

To all members of lab 426, thank you for your support and the memorable moments we shared together. This journey would not have been as fulfilling without these special connections. Michael and Eugene, I appreciate the help you provided in some aspects of my data analysis.

Buyani, my partner in yonkinto, thank you for such a significant role in this journey and making it more bearable. All those long hours we spent in the library writing up, even working on Sundays and public holidays, have finally paid off. I am grateful for your steadfast support.

I am sincerely thankful to my family—my beloved mom and two sisters, as well as my dearest friends, for their unwavering love and patience throughout my PhD journey. Your constant prayers and support have been my anchor.

This research would not have been possible without the generous financial support from the National Research Foundation, the UCT Faculty of Science Equity Scholarship, and the European Union's Horizon 2020 Research and Innovation programme (RESIST project).

Above all, I would like to thank God for the strength, resilience, and for the peace that surpasses all understanding when everything was going south. I am grateful for the growth experienced.

TABLE OF CONTENTS

ABSTRACT ..... *ii*

DECLARATION ..... *iv*

ACKNOWLEDGEMENTS ..... *v*

CHAPTER 1 ..... *1*

Desiccation Tolerance in Resurrection Plants *1*

1.1 Introduction *1*

1.1.1 Damaging Effects of Water Loss on Plants 1

1.1.2 Adaptive Strategies of Plants to Water loss 2

1.2 Desiccation Tolerance *2*

1.2.1 Mechanisms underlying Desiccation Tolerance in Seeds 3

1.2.2 Regulation of the Seed Maturation Program 4

1.3 Vegetative Desiccation Tolerance in Resurrection Plants *7*

1.3.1 Morphological, Biochemical and Cellular Responses 8

1.3.2 Abscisic Acid 9

1.3.3 Protective Molecules that enable Vegetative Desiccation tolerance 11

1.3.3.1 Protective Proteins 11

1.3.3.1.1 Late Embryogenesis Abundant Proteins 11

1.3.3.1.2 Heat Shock Proteins 12

1.3.3.1.3 Early Light-Inducible Proteins 14

1.3.3.2 Antioxidant Defence System 15

1.3.3.3 Accumulation of Soluble Sugars 15

1.4 Xerophyta Resurrection Plants *16*

1.5 Aims and Objectives *18*

CHAPTER 2 ..... *20*

Ultrastructural Analysis of Two-Leaf Seedlings of Xerophyta elegans and Xerophyta schlechteri during Desiccation and Rehydration *20*

2.1.1 Introduction 20

2.1.2 Aim and Objectives of the Study 21

2.2 Methods and Materials *23*

2.2.1 Seed Germination and Drying Down Experiments 23

2.2.2 Sample Preparation for Cellular Ultrastructure 23

2.2.3 Trimming and Sectioning 24

2.2.4 Staining 24

2.2.5 Imaging and Quantification 25

2.3 Results 26

2.3.1 Similar Ultrastructural Changes Observed in two Independent Experiments 26

2.3.2 Changes in the Ultrastructure of *X. elegans* and *X. schlechteri* Leaf Cells in Response to Desiccation and Rehydration 28
2.3.3 Chloroplast Ultrastructural Changes in the Two-Leaf Tissues of *X. elegans* and *X. schlechteri* during Desiccation and Rehydration 32
2.4 Discussion 39
2.5 Conclusion 42
CHAPTER 3 ..... *43*
Comparison of the Transcriptome Response to Desiccation in Three Xerophyta Species at Two Stages of Seedling Development *43*
3.1 Introduction *43*
3.1.1 Aim and Objectives 45
3.2 Materials and Methods *46*
3.2.1 Genome size estimation 46
3.2.1.1 Plant material 46
3.2.1.2 Preparation of Nuclear Suspension Samples 46
3.2.1.3 Analysis of Nuclear DNA Content 46
3.2.2 Transcriptomic Analysis 47
3.2.2.1 Plant Material 47
3.2.2.2 Seed Sterilization 47
3.2.2.3 Seed Germination 47
3.2.2.4 Seedling Survival Experiments 48
3.2.2.5 Comparative Transcriptomics 48
3.2.2.6 RNA Extraction from *Xerophyta* Seedlings 49
3.2.2.7 RNA Extraction from Two-leaf Seedlings using a Modified TRIzol/Zymo-Spin Method 49
3.2.2.8 RNA Extraction from Pre-leaf Seedlings using the Footitt Method 50
3.2.2.9 RNA Agarose Gel Electrophoresis 50
3.2.2.10 Library Construction, Sequencing, and Quality Checks 50
3.2.2.11 RNA Read Mapping and Read Counts 51
3.2.2.12 Differential Gene Expression Analysis 51
3.2.2.13 Orthogroup Analysis 51
3.2.2.14 Gene Ontology Enrichment 53
3.2.2.15 Promoter Motif Enrichment Analysis 53
3.3 Results *54*
3.3.1 Estimation of Genome Sizes for Five *Xerophyta* Species 54
3.3.2 Survival of Early and Late-stage Seedlings to Desiccation 55
3.3.3 Gene Expression Analysis in *X. humilis* Tissues 58
3.3.4 The Expression of the *LAFL* network genes, *ABI5* and *ABFs* in *X. humilis* 59
3.3.5 Cross-species Expression of the LAFL, ABI5 and ABF Genes in Early- and Late-stage *Xerophyta* Seedlings 68
3.3.6 Analysis of Differential Gene Expression in Desiccated Tissues of *Xerophyta* Seedlings 70
3.3.7 GO term Enrichment Analysis 72
3.3.8 Orthogroup and Gene Ontology Analyses 75

3.3.9 Motif Enrichment Analysis 82
3.3.9.1 Enrichment of HSF motifs in *Xerophyta* genes 83
3.3.9.2 Enrichment of AHL motifs in *Xerophyta* genes 87
3.3.9.3 Enrichment of ZAT motifs in *Xerophyta* Promoter Genes 90
3.4 Discussion 94
3.5 Conclusion 99
CHAPTER 4 101
The Analysis of Metabolites and Lipids in Hydrated and Desiccated Seedlings of three Xerophyta Species 101
4.1 Introduction 101
4.1.1 Aim and Objectives 104
4.2 Materials and Methods 107
4.2.1 Seed Sterilization, Seed Germination and Drying Down Experiments 107
4.2.2 Metabolite and Lipid Extractions 107
4.2.3 GC-MS for Primary Metabolite Analysis 108
4.2.4 LC-MS for Secondary Metabolite Analysis 108
4.2.5 LC-MS for Lipid Analysis 109
4.2.6 Processing of Raw Chromatograms 109
4.2.7 Statistical Analysis 110
4.3 Results 110
4.3.1 Metabolite and Lipid Profiles in the Early and Late-stage Seedlings 110
4.3.2 Changes in the Abundance of Primary Metabolites during Desiccation 114
4.3.3 Changes in the Abundance of Secondary Metabolites during Desiccation 116
4.3.4 Changes in Lipid Profiles in *Xerophyta* Species during Desiccation 119
4.3.5 Differences between the Homoichlorophyllous and Poikilochlorophyllous *Xerophyta* Species 121
4.3.5.1 Variations in the Abundance of Secondary Metabolites in *Xerophyta* Seedlings 121
4.3.5.2 Variations in the Abundance of Lipid Profiles in *Xerophyta* Seedlings 123
4.4 Discussion 126
4.5 Conclusion 130
CHAPTER 5 131
General Discussion and Conclusions 131
Conserved Core Metabolic Responses to Desiccation Identified in *Xerophyta* Seedlings 132
Homoiochlorophyllous versus Poikilochlorophyllous species 134
Identification of Core Transcriptional Regulators in Dry *Xerophyta* Seedlings 137
5.1 Limitations of the Study and Future Work 139
5.2 Concluding Remarks 140
REFERENCES 142

APPENDICES... *158*

CHAPTER 1

Desiccation Tolerance in Resurrection Plants

1.1 Introduction

Water is critical for the growth and development of plants, playing an indispensable role in physiological and biochemical processes. In the absence of water, plants undergo a transition in their relative water content (RWC), moving from a fully hydrated (80-100% RWC) to mildly dehydrated (70-80% RWC), moderately dehydrated (50-70% RWC), severely dehydrated (30-50% RWC) and eventually to a desiccated state (<30% RWC) (Q. Zhang & Bartels, 2018). Most plants experience significant physiological stress as their water content declines from the mildly to moderately dehydrated states, leading to disruptions in cellular function and growth (Bohnert et al., 1995). As sessile organisms, plants cannot escape from adverse environmental conditions, instead, they have evolved a diverse array of adaptive mechanisms to withstand and survive periods of water deficiency. These adaptations range from morphological changes, such as reduced leaf area and increased root depth, to biochemical and physiological responses, including osmotic adjustment, the accumulation of protective metabolites, and the activation of stress-responsive genes. Understanding the adaptive mechanisms employed by plants under water-limited conditions provides valuable insights into their survival strategies and resilience. This knowledge is not only crucial for advancing our comprehension of plant biology but also for developing innovative approaches to enhance crop tolerance to drought and other abiotic stresses, which is increasingly important in the context of global climate change and the growing demand for agricultural productivity.

1.1.1 Damaging Effects of Water Loss on Plants

The loss of water in plants leads to a series of adverse effects that can ultimately cause wilting and death. In vegetative tissues, one of the earliest responses to water deficit is the cessation of carbon dioxide (CO_2) fixation due to stomatal closure (Charuvi et al., 2019; Farrant, 2000). This closure limits the consumption by the Calvin cycle of adenosine triphosphate (ATP) and nicotinamide adenine dinucleotide phosphate hydrogen (NADPH) generated by the light-dependent reactions of photosynthesis, which leads to over-reduction of electron transport chain. Continued light absorption leads to the production and accumulation of reactive oxygen species (ROS) as excess electrons react with oxygen (Basu et al., 2016; Farrant, 2000). Some of the common ROS generated in this process include superoxide radical anion (O_2^-), hydrogen peroxide (H_2O_2), and the hydroxyl radical ($OH\cdot$) (Alscher et al., 2002; Smirnoff, 1993). The

excessive accumulation of these ROS results in oxidative stress, which severely damages key components of photosynthetic machinery such as photosystems I and II, as well other cellular constituents such as proteins, lipids, and nucleic acids (Mundree et al., 2002). In addition to oxidative damage, water deficiency in plants results in a loss of cell turgor, leading to impaired cellular function. It also causes the formation of molecular aggregates, protein denaturation, and degradation (Ligterink et al., 2015), further compromising cellular integrity and metabolism. Moreover, dehydration can cause membrane fusion and loss of cellular compartmentalization, resulting in cell death (Oliver et al., 2020). All these effects not only disrupt the plant's photosynthetic capacity but also affect overall plant health, highlighting the critical need for mechanisms that can protect against and mitigate the impacts of dehydration.

1.1.2 Adaptive Strategies of Plants to Water loss

Plants have evolved various mechanisms to cope with water-limiting conditions. One of the primary strategies involves morphological and structural changes, including stomatal closure to reduce water loss through transpiration and enhance root growth to improve water absorption from the soil (Liu et al., 2019). In addition, plants also accumulate osmoprotectants, such as amino acids, protective sugars, and betaines. By accumulating osmoprotectants, they can maintain cell turgor through osmotic adjustment, which helps cells retain their shape and function (Liu et al., 2019). The ability of plant cells to maintain their shape and the resistance of their internal contents are other factors enabling the plants to survive dehydration (Basu et al., 2016).

While these adaptations are effective against mild to moderate dehydration stress, prolonged stress that significantly reduces the RWC will usually be fatal for most angiosperms. However, some plants possess specialized adaptation strategies that enable them to survive even severe desiccation. These plants are said to be desiccation tolerant, capable of maintaining cellular integrity and functionality under extremely dry conditions.

1.2 Desiccation Tolerance

Desiccation tolerance (DT) is the ability of certain organisms to survive severe dryness, with water content dropping below 0.1 g H_2O g^{-1} dry mass, and to subsequently resume normal physiological processes upon rehydration (Alpert, 2005; Oliver et al., 2000). DT emerged early in the history of life on land and is commonly found in less complex clades including

bryophytes, lichens, and algae, indicating that it was likely present in the common ancestor of all terrestrial plants (Kranner et al., 2008; Oliver et al., 2000). The ability of adult tissues to tolerate desiccation was lost as plants developed vascular systems (Oliver et al., 2005). However, this trait re-evolved in lycophytes, ferns, and at least 13 different lineages of angiosperms (Fig. 1.1; Gaff & Oliver, 2013), though it is rare overall, having been reported from some 135 species. In contrast, the DT trait has persisted throughout the evolution of land plants in reproductive structures such as spores, and eventually seeds (Oliver et al., 2020).

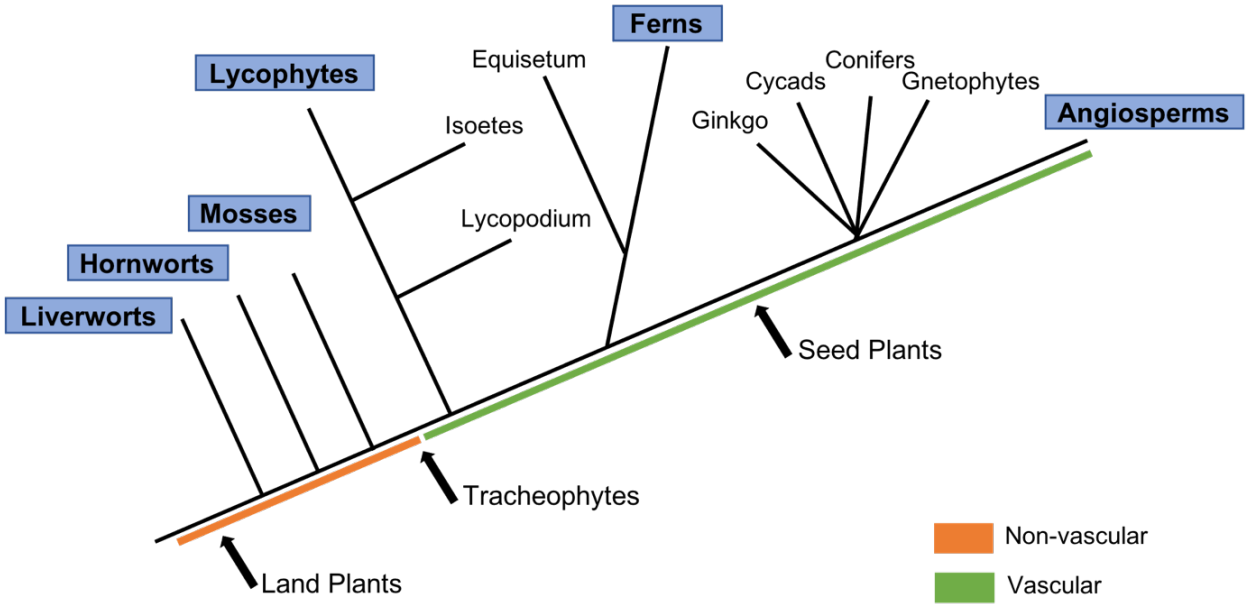

Figure 1.1. The evolutionary occurrence of desiccation tolerant species. The orange line represents the evolutionary timeline of primitive non-vascular land plants, while the green line shows the lineage of vascular plants, indicating the point at which vegetative desiccation tolerance was lost during the evolution of tracheophytes. Labels in the boxes highlight major clades that include known desiccation-tolerant members. Figure modified from Oliver et al. 2000 and Oliver et al. 2020.

1.2.1 Mechanisms underlying Desiccation Tolerance in Seeds

The vast majority of angiosperms produce seeds that are desiccation tolerant, and only a few have desiccation sensitive (recalcitrant) seeds. Seeds that can withstand prolonged periods of desiccation and still remain viable are termed “orthodox” seeds (Gaff & Oliver, 2013). This ability to withstand desiccation is acquired during the late maturation phase of embryogenesis in seeds.

The process of embryo development consists of two main phases; morphogenesis and maturation (Braybrook & Harada, 2008; Harada, 2001). Morphogenesis is characterised by tissue patterning, achieved through a well organised cell division and cell differentiation (Harada, 2001). This is then followed by the maturation phase, which can be divided into early and late phases. During early maturation, the embryo experiences rapid cellular division and expansion (Armenta-Medina et al., 2021). Additionally, the seed acquires storage compounds such as carbohydrates, proteins, and oils, which protect the embryo from desiccation, and also serve as nutrient reserves during seedling germination prior to the onset of photosynthetic activity (Fig. 1.2; Armenta-Medina et al., 2021; Braybrook & Harada, 2008). Subsequently, the embryo transitions into the late maturation phase, characterised by water loss (desiccation) and establishment of seed dormancy (Leprince et al., 2017). It is during this phase that late embryogenesis abundant (LEA) proteins and non-reducing sugars such as sucrose and raffinose family oligosaccharides (RFOs) accumulate (Fig. 1.2; Angelovici et al., 2010). All these function in protecting cellular structures and membranes during desiccation.

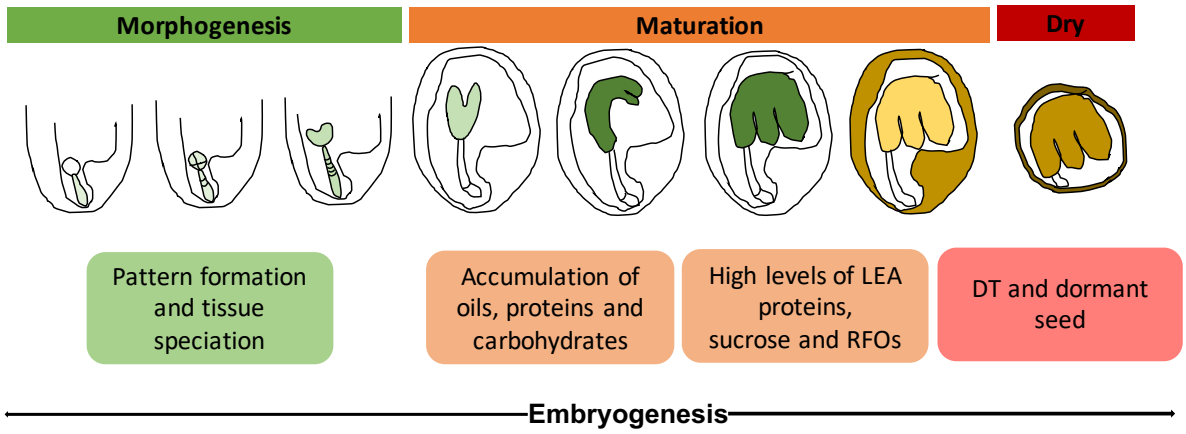

Figure 1.2. Schematic representation of *Arabidopsis thaliana* seed development. The images depict different stages of embryo development in Arabidopsis seeds. The late stage of embryo development is characterized by the deposition of storage reserves and loss of water, preparing the seed for desiccation and dormancy.

1.2.2 Regulation of the Seed Maturation Program

The seed maturation process is regulated by the LAFL network, a master regulatory network of transcription factors, including *LEAFY COTYLEDON 1 (LEC1), LEC2, ABSCISIC ACID INSENSITIVE 3 (ABI3)*, and *FUSCA 3 (FUS3).* This network is activated by developmental cues and abscisic acid (ABA) signalling (Kwong et al., 2003). LEC1 is a CCAAT-box binding

factor, also known as NF-Y, and belongs to the HAP3 family, whereas LEC2, FUS3 and ABI3 are B3 domain-containing transcription factors (TFs) (Kwong et al., 2003). LEC1, LEC2 and FUS3 play important roles in embryo development and early maturation phases (Braybrook & Harada, 2008). Loss-of-function in *lec1* and *lec2* mutants results in several effects on embryo development, such as loss of embryo organs identity, and defects in reserve accumulation (Brand et al., 2019), therefore emphasizing the critical roles played by *LEC* genes in the control of embryo development.

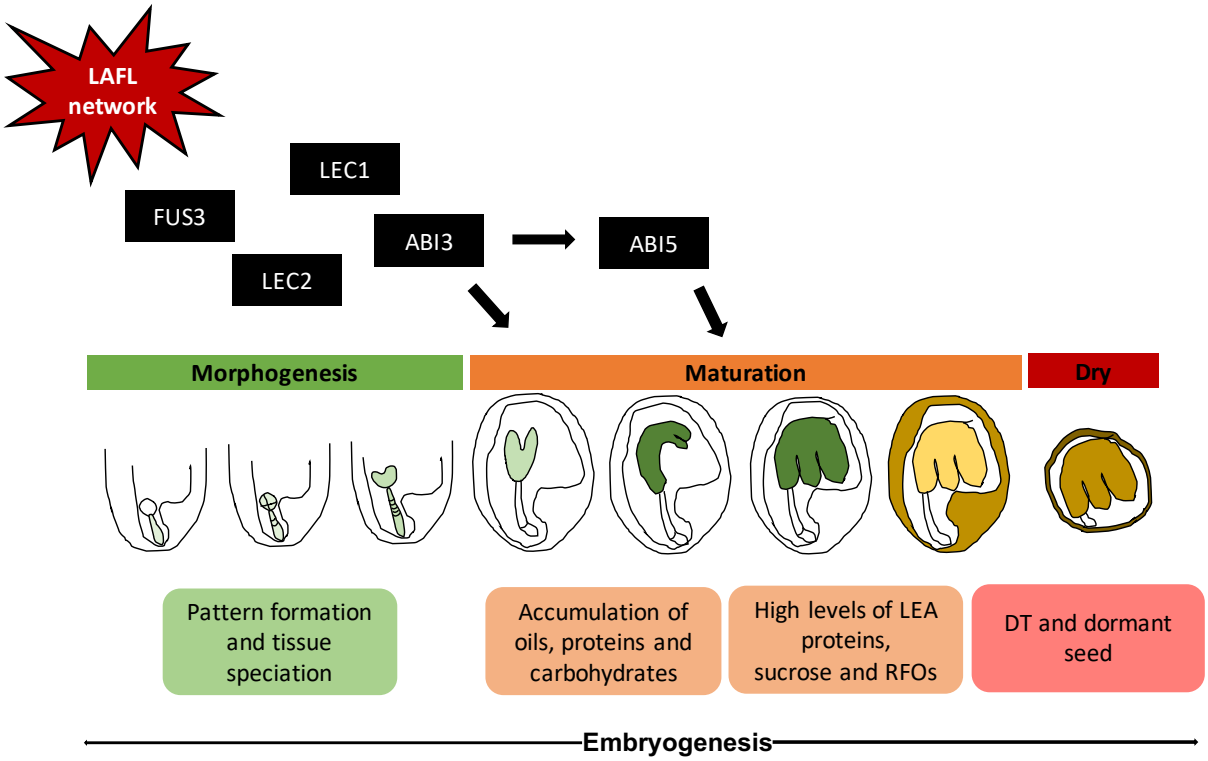

Figure 1.3. Schematic representation of Arabidopsis seed development regulated by the seed master LAFL regulators. The images show different stages of embryo development in Arabidopsis seeds. LEC1, LEC2 and FUS3 are involved in the morphogenesis phase, while ABI3 and ABI5 mainly regulate processes in the maturation phase. The late stage of embryo development is characterized by the deposition of storage reserves and loss of water, preparing the seed for desiccation and dormancy.

ABI3 is induced by water loss during the late maturation phase, and thus thought to play an important role in seed DT acquisition. ABI3 contains four conserved domains; the N-terminal A domain which is rich in acidic residues (A) and three basic domains (B1, B2 and B3). The A domain functions in transcription activation (Nakamura et al., 2001). The B1 domain is essential for interaction with bZIP TFs; B2 regulates some LEAs and storage protein genes through interacting with other TFs; and the B3 domain is the DNA-binding domain that is

highly conserved (Hill et al., 1996; Nakamura et al., 2001; Suzuki et al., 1997). Most plants, including *Arabidopsis*, encode a single copy of the ABI3 gene, which contains all four functional domains (Fig. 1.4). In contrast, *Xerophyta humilis* and *X. viscosa* have four paralogs of the *ABI3* gene: *ABI3A*, *ABI3B*, *ABI3C*, and *ABI3D*. The presence of multiple copies of ABI3 gene is uncommon, as most angiosperms typically encode only a single copy (Lyall et al., 2020). Among these paralogs in *Xerophyta* species, ABI3A contains all four domains, while ABI3B, ABI3C, and ABI3D each have a truncated B3 domain due to the presence of a stop codon directly after the B2 domain (Fig. 1.4; Lyall et al., 2020). However, these three ABI3 proteins can still regulate gene expression possibly through interacting with other TFs mediated by B1 and B2 domains (Lyall et al., 2020). The B1 domain in ABI3 enables it to interact with other proteins particularly ABI5 (Nakamura et al., 2001). ABI5 is a member of the ABA-responsive (group A) bZIP family of TFs that acts downstream of the LAFL network. Similar to ABI3, ABI5 plays a crucial role in the acquisition of DT in seeds.

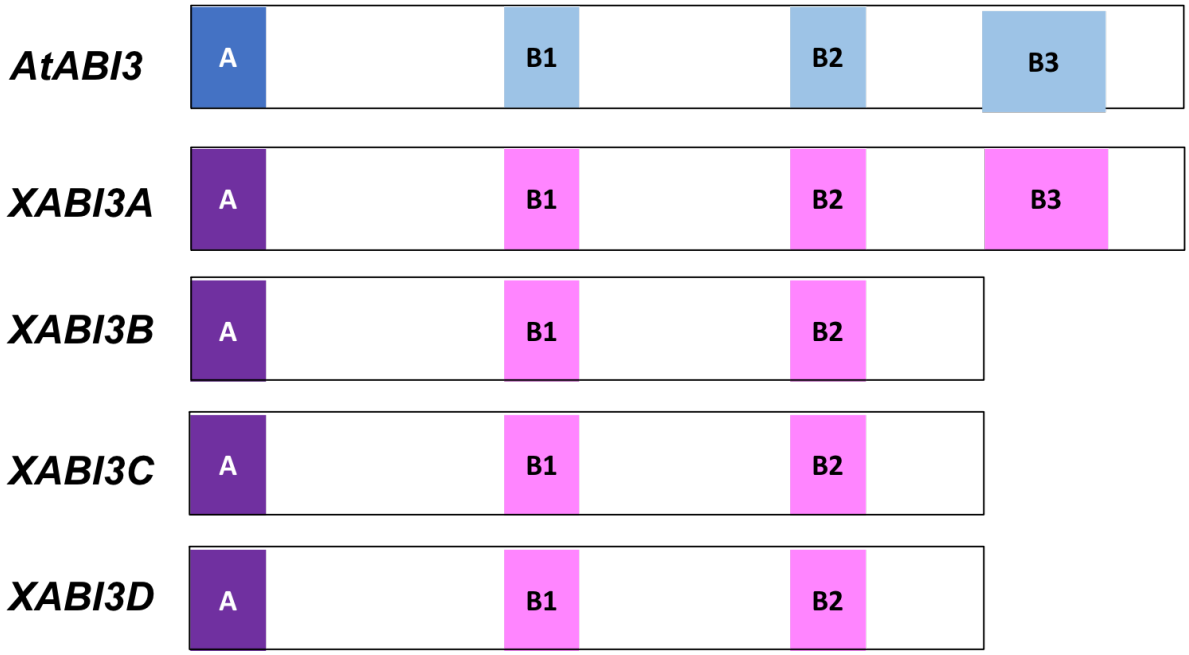

Figure 1.4. A schematic representation of structural domains of the ABI3 proteins in *Arabidopsis thaliana* and *Xerophyta* species, highlighting the loss of the B3 domain in *Xerophyta*. *Xerophyta* species contain four ABI3 copies, three of which (ABIB-D) are truncated. The acidic (A), and basic B1, B2 and B3 domains are indicated by the shaded areas. The blue-shaded regions represent *Arabidopsis*, while the purple/pink regions correspond to *Xerophyta* domains.

1.3 Vegetative Desiccation Tolerance in Resurrection Plants

There are approximately 330 vascular plant species exhibiting vegetative desiccation tolerance (VDT) in their adult tissues, and these are collectively known as resurrection plants. This group, which includes both monocot and eudicots, is primarily found in arid and semi-arid regions of tropical climates characterised by hot and dry conditions. Resurrection plants are predominantly distributed across the southern hemisphere, notably in Southern and Eastern Africa, South America, and Western Australia (Gaff & Oliver, 2013; Oliver et al., 2020). There are few species belonging to the Gesneriaceae family such as *Haberlea rhodopensis* and *Boea hygrometrica*, that are found in the northern hemisphere, particularly in temperate regions of Asia and Europe that experience extremely cold winters (Mitra et al., 2013). This suggests their ability to tolerate both dry and cold conditions. Most resurrection plant species are typically found in rocky areas with shallow soil, high temperatures, and shortage of rainfall (Marks et al., 2021; Porembski & Barthlott, 2000). However, *Lindernia brevidens* is an exceptional example which flourishes in habitats with high humidity (Phillips et al., 2008).

The trade-off for possessing DT is slower growth rates and smaller plant sizes. Furthermore, it is worth mentioning that the ability of resurrection plants to recover from desiccation upon water availability depends on the rate at which water loss happens. The most suitable method for resurrection plants to recover from desiccation is if they are subjected to slow drying (Gechev et al., 2012; Zhang & Bartels, 2018). This is evident in *X. humilis, Myrothamnus flabellifolius* and *B. hygrometrica* resurrection plants, which lose their viability when rapidly dried, but are able to recover when dried slowly (Farrant et al., 1999; Zhu et al., 2015). This makes sense as gradual drying gives these plants enough time to induce their protective mechanisms. Notably, some plants have the capacity to activate their set of protective mechanisms when subjected to rapid drying. For example, *Craterostigma wilmsii* is able to revive from rapid desiccation, however, it suffers prominent cellular damages compared to when dried under slow conditions, but these can be repaired upon rehydration (Farrant et al., 1999).

The study of resurrection plants has gained great interest over the years, and research studies have documented various mechanisms ranging from morphological and physiological adjustments, to changes in metabolic processes, activity of antioxidant systems, and transcriptional reprogramming. These protective mechanisms enable resurrection plants to withstand extremely dry conditions and resume normal physiological and metabolic process

upon rehydration. These studies have undoubtedly provided us with great insights on DT mechanisms in resurrection plants, with some of these adaptive strategies discussed below.

1.3.1 Morphological, Biochemical and Cellular Responses

The primary strategies used by resurrection plants involve adjustments in the leaves. These include leaf folding or leaf curling to reduce the surface area and exposure to light (Sherwin & Farrant, 1998). Many resurrection plants curl their leaves toward the adaxial surface, resulting in a grey-green appearance due to dense epidermal hairs on the abaxial surface. This curling and dense arrangement of epidermal hairs are defensive mechanisms that reduce the absorption of radiation, thereby mitigating photoinhibition and ROS production (Mitra et al., 2013). Additionally, these plants accumulate anthocyanins and carotenoid pigments which act as "sunscreens," protecting against light-induced damage by reducing light absorption (Sherwin & Farrant, 1998). This adaptation process is reversible upon rehydration (Yu et al., 2024). The reversible nature of leaf curling or folding in resurrection plants correlates with the dynamic folding of their cell walls.

Cell wall folding is a controlled and reversible process observed in some resurrection plant cells during desiccation (Mitra et al., 2013). It allows plant cells to alter their shape, maintaining contact with the plasma membrane, which contracts during dry conditions and expands during rehydration at specific sites. This mechanism helps to alleviate detrimental mechanical stresses and prevents severe structural damage (Liu et al., 2024). In species like *C. wilmsii*, extensive cell wall folding reduces cell size, preventing plasma membrane withdrawal (Farrant, 2000). Conversely, in *M. flabellifolius,* under similar drying conditions, cell wall folding is less pronounced (Farrant, 2000), indicating potential species-specific variations in the extent of this adaptation.

The ability of resurrection plants to fold their cell walls is facilitated by changes in the compositions of these walls. This process involves a mechanism known as "plasticization," highlighting the importance of arabinose-rich polymers such as pectin-arabinans, arabinogalactan proteins, and arabinoxylans (Moore et al., 2008). These polymers are crucial as they impart flexibility necessary for plants to endure dehydration and subsequent rehydration (Moore et al., 2008, 2013).

1.3.2 Abscisic Acid

ABA is an important phytohormone and signalling molecule within plants that is involved in response to many abiotic stresses including osmotic stress, high salinity, and water loss, as well as in seed maturation and dormancy (Uno et al., 2000). ABA coordinates a complex signalling pathway that enables plants to respond to developmental cues and survive under adverse environmental conditions.

1.3.2.1 ABA Signalling Pathway

ABA functions through a conserved signal transduction pathway regulated by SNF1-related protein kinase 2 (SnRK2), group A protein phosphatase 2Cs (PP2Cs), and ABA receptors (Sun et al., 2020). These receptors, including PYRABACTIN RESISTANCE 1 (PYR1), PYR1-like proteins (PYLs), and members of the regulatory components of ABA receptors (RCARs) family, are important in disrupting the inhibitory interaction between SnRK2 kinases and PP2Cs (Ma et al., 2009).

Underpinning the role of ABA in stress response, it is known that many genes exhibit increased expression levels in response to various abiotic stresses, and ABA is responsible for inducing some of these genes. These ABA-inducible genes typically contain ABA-responsive elements (ABREs) in their promoter regions (Nakashima & Yamaguchi-Shinozaki, 2013). TFs from the group A bZIP family, specifically ABRE-biding proteins (AREB)/ABF TFs, bind to these ABREs, thereby initiating the transcription of downstream stress-responsive genes. Among these targets are genes encoding LEA proteins and other TFs or proteins vital for stress adaptation (Nakashima & Yamaguchi-Shinozaki, 2013).

The activation of AREB/ABF TFs is critically dependent on post-translational modifications, specifically phosphorylation by members of SnRK2 family (Uno et al., 2000). In the presence of ABA, the PYR1/PYL/RCAR receptors can inhibit the interaction between SnRK2 kinases and PP2Cs (Fig. 1.5). This inhibition prevents the dephosphorylation of SnRK2 kinases by PP2Cs, resulting in the activation of SnRK2 kinases, which then phosphorylate and activate AREB/ABF TFs, eliciting stress response. In the absence of ABA, PP2Cs act as negative regulators by dephosphorylating SnRK2 kinases, thereby maintaining them in an inactive state (Sun et al., 2020). This inhibition prevents the activation of stress-responsive genes, thus illustrating the importance of ABA in modulating plant responses to stress conditions including desiccation.

The ABA signalling pathway enables plants to adapt and survive when subjected to extreme environmental conditions. For instance, during periods of water scarcity, ABA promotes the closure of stomata in guard cells to maintain water in plants (Nakashima & Yamaguchi-Shinozaki, 2013). In addition, ABA contributes to the accumulation of compatible solutes such as proline, as evidenced in *Arabidopsis thaliana* (Shrestha et al., 2021). Moreover, it plays a pivotal role in the synthesis of seed proteins like LEA proteins, crucial for the protection of seeds during desiccation (Zamora-Briseño & de Jiménez, 2016). ABA is also integral to the activation of heat shock factors (HSF), which regulate the expression of heat shock proteins (HSPs), protecting proteins under stress conditions (Huang et al., 2016). Increased levels of ABA have been observed in several resurrection plants such as *X. schlechteri* (Gabier et al., 2021), *Sporobolus stapfianus* (Yobi et al., 2017), and *Selaginella pulvinate* (Yu et al., 2024), implying a conserved role in VDT.

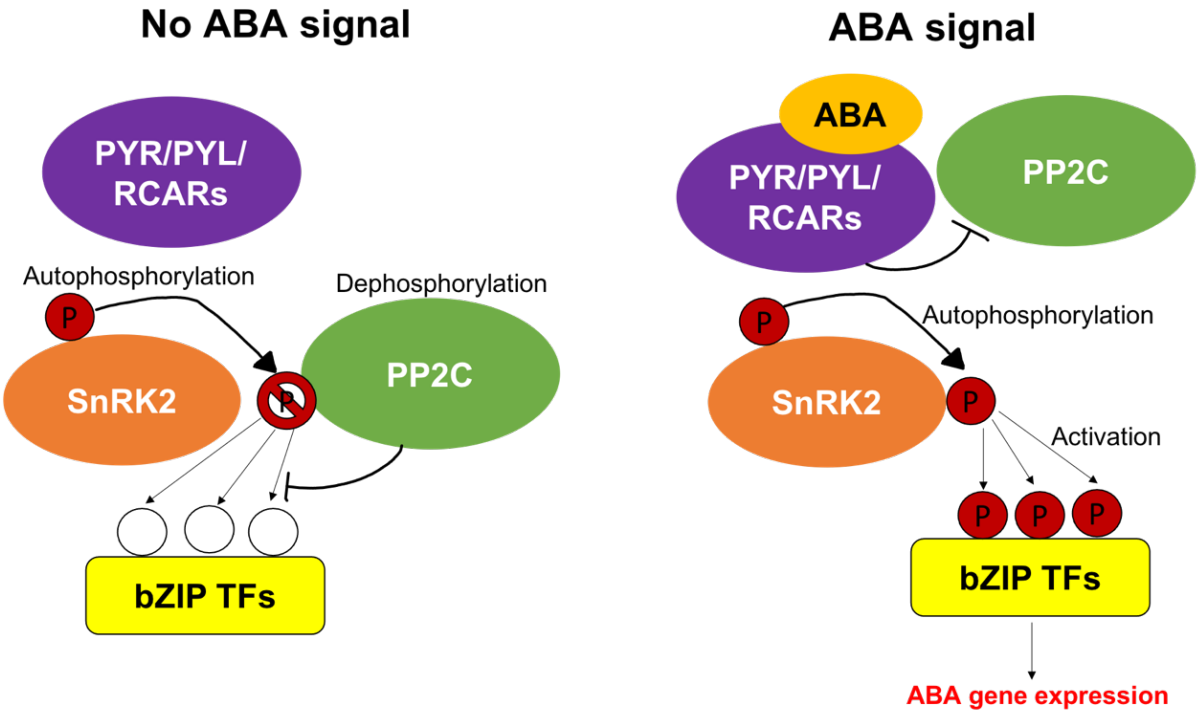

Figure 1.5. The abscisic acid signalling pathway. In the absence of ABA, PP2C dephosphorylates and inhibits SnRK2, preventing the activation of bZIP transcription factors. Upon ABA binding, PYR/PYL/RCARs receptors inhibit the interaction between PP2C and SnRK2. This inhibition allows SNRK2 to remain phosphorylated active, leading to the activation of bZIP transcription factors and the subsequent expression of ABA responsive genes. Diagram modified from Cuming, 2019 and Yu et al. 2024.

1.3.3 Protective Molecules that enable Vegetative Desiccation tolerance

1.3.3.1 Protective Proteins

Proteins synthesised in response to desiccation may serve directly as protectants during drying and rehydrating processes, or function as enzymes that aid in the production of other protective substances, such as antioxidants. Among the most studied protective compounds are LEAs, HSPs, early light induced proteins (ELIPs), and antioxidative defence systems.

1.3.3.1.1 Late Embryogenesis Abundant Proteins

LEA proteins represent a large and diverse group of highly hydrophilic proteins that protect cellular integrity and function during exposure to different abiotic stresses, including desiccation. LEAs belong to the class of hydrophilins due to their high hydrophilicity, as indicated by a hydrophilicity index greater than 1 and a glycine content exceeding 6% (Battaglia et al., 2008). These proteins were first identified at very high levels in cotton, *Gossypium hirsutum,* during the maturation phase of embryogenesis (Dure et al., 1981), hence the name "late embryogenesis abundant" proteins. Their accumulation during this phase is believed to be crucial for the acquisition of DT in seeds. However, the presence of LEA proteins is not confined to seeds alone; their expression is also significantly elevated in vegetative tissues of both desiccation sensitive and desiccation tolerant plants. This underscores their role in plant responses to water deficit conditions. Notably, in resurrection plant species such as *X. humilis* (Illing et al., 2005), *H. rhodopensis* (Gechev et al., 2013), and *S. pulvinata* (Yu et al., 2024), high levels of transcripts encoding LEA proteins have been observed in desiccated tissues.

The hydrophilic nature of LEA proteins allows them to form hydration shells around molecules, effectively functioning as molecular chaperones (Oliver et al., 2020). This capability is critical for retaining cellular water and preserving the structure of enzymes and other components of the cell, thereby preventing denaturation under stress (Banerjee & Roychoudhury, 2016). LEA proteins are also thought to contribute to the preservation of chromatin structure during desiccation and play roles in DNA repair and chromatin remodelling (Banerjee & Roychoudhury, 2016). Furthermore, it was found that LEAs are involved in the formation of the glassy matrix in the cytoplasm, which helps stabilize cellular structures during desiccation (Buitink & Leprince, 2004).

LEA proteins are remarkably diverse and are classified into several groups based on the similarities in their amino acid sequences (Illing et al., 2005). Group 1 LEA proteins are identified by a conserved motif of 20 amino acids: GGQTRREQLGEEGYSQMGRK (Cuming et al., 1999). Group 2 LEA proteins, commonly known as dehydrins, are the most extensively studied. These proteins are highly hydrophilic and are characterized by a lysine-rich conserved motif of 15 amino acids, known as the K-segment: EKKGIMDKIKEKLPG (Bartels et al., 2008). Group 3 LEA proteins feature a repeating motif of 11 amino acids (TAQAAKEKAGE) (Dure, 1993). Group 4 LEA proteins are found in both vascular (angiosperms and gymnosperms) and non-vascular plants (bryophytes) (Battaglia et al., 2008). Unlike the first three groups, group 4 and other LEA groups (groups 6, 7, 8 and 10), exhibit less obvious conservation, though they can still be classified based on their partially conserved motifs and chemical properties (Battaglia et al., 2008).

While LEAs are expressed both during seed maturation and in response to stress in vegetative tissues, it has been shown that the seed specific LEA proteins that accumulate may differ from those in non-seed tissues. For example, members of LEA protein groups 1 and 6 are significantly expressed during seed maturation but show low expression levels in the roots or leaves of *A. thaliana* (Illing et al., 2005). Conversely, group 2 LEA proteins are specifically associated with abiotic stress response in vegetative tissues (Banerjee & Roychoudhury, 2016; Illing et al., 2005).

1.3.3.1.2 Heat Shock Proteins

HSPs are a large class of protective proteins that are believed to act as molecular chaperones. Although HSPs were originally described in relation to elevated temperatures, research has shown that these proteins are also induced by a wide range of stresses, including cold stress, salinity stress, and drought stress (Vierling, 1991). They play important roles in preventing protein aggregation, membrane stabilization, and maintaining protein structure under stress conditions (Liu et al., 2019). Furthermore, HSPs are also found in unstressed cells where they act as molecular chaperones (Waters, 2013). These proteins function in maintaining cellular balance, supporting cell function under both favourable and adverse growth conditions (Wang et al., 2004).

There are five prevalent families of HSPs that are conservatively recognized as molecular chaperones based on their molecular weights, such as HSP100, HSP90, HSP70, HSP60 and

small HSP (sHSP) (Wang et al., 2004; Waters, 2013). All these facilitate a wide diversity of important processes in different organisms.

HSP100 proteins are present in bacteria, yeast and plants, but are absent in animals or humans (Zolkiewski et al., 2012). Different members of the HSP100 family exhibit a unique capability to rescue stress-damaged proteins from a previously aggregated state by resolubilizing them. Additionally, they recycle polypeptides that are marked for degradation (Zolkiewski et al., 2012). HSP90 proteins function in facilitating maturation of signalling molecules and genetic buffering (Wang et al., 2004). HSP70s are ATP-dependent proteins that prevent protein aggregation and aid in refolding of misfolded proteins under both normal and stressful conditions (Frydman, 2001). They are also integral to signal transduction processes and transcriptional activation. Some members of this family are constitutively expressed (70-kDA heat-shock cognate), and these are involved in the folding of newly synthesized polypeptides and translocation of precursor proteins (Wang et al., 2004). Other family members of the HSP70 family are induced only in response to abiotic stress and are critical for the refolding and proteolytic degradation of misfolded proteins (Frydman, 2001).

The HSP60 proteins, often located in the mitochondria, are critical for the folding and assembly of newly imported proteins into functional oligomeric complexes (Wang et al., 2004). Lastly, the sHSP family consists of a numerous and diverse group of proteins with low molecular weights, most in the range of 15-22 kDa (Waters, 2013). Unlike other HSPs that depend on ATP, sHSPs act as ATP-independent molecular chaperones, binding proteins denatured by stress to prevent irreversible aggregation (Waters & Vierling, 2020).

The expression patterns of HSPs in resurrection plants vary across different species. For instance, in the vegetative tissues of *C. plantagineum*, constitutive expression of sHSPs was observed in both hydrated and desiccated states (Alamillo et al., 1995). Conversely, in *B. hygrometrica,* although some sHSP transcripts were present in hydrated samples, their expression was significantly up-regulated in response to desiccation in dry tissues (Zhang et al., 2013). In *H. rhodopensis*, no constitutive sHSP expression was detected in control samples; instead, sHSP expression was only activated in tissues subjected to desiccation under high temperatures (Mihailova et al., 2023).

Although HSPs are not unique to resurrection plants, newly synthesised sHSPs during the late stages of desiccation, when RWC drops below 20%, are particularly interesting. This unique expression pattern in resurrection plants, absent in drought-sensitive species which cannot survive extreme water loss, provides crucial insights into the molecular basis of desiccation tolerance (Mihailova et al., 2023).

1.3.3.1.3 Early Light-Inducible Proteins

ELIPs are small, nuclear-encoded proteins found in the thylakoid membranes of both prokaryotes and eukaryotes (Adamska et al., 2001). These proteins are crucially involved in responding to environmental stressors such as light stress and dehydration (Montané & Kloppstech, 2000). The discovery of ELIPs dates back to 1980s when they were found to be rapidly induced in etiolated seedlings upon light exposure (Meyer & Kloppstech, 1984). This significant finding underscored their importance in protecting the photosynthetic apparatus from light-induced damage.

ELIPs belong to a family of closely related proteins characterized by shared structural features. This family includes the three-helix ELIPs, the two-helix stress-enhanced proteins, and the one-helix proteins, as well as high-light induced proteins and small Cab-like proteins (reviewed in Adamska et al., 1997). Their structural similarities and conserved sequences indicate a common evolutionary origin.

The primary role of ELIPs is to protect photosynthetic machinery from photooxidative damage. This is achieved through the transient binding of free chlorophyll and preventing the formation of free radicals by acting as sinks for excitation energy (Adamska et al., 2001; Liu et al., 2019). Additionally, ELIPs are pivotal in protecting resurrection plants from photoinhibition during desiccation. Increased expression levels of ELIPs have been documented in several resurrection plants including *C. plantagineum* (Bartels et al., 1992), *H. rhodopensis* (Gechev et al., 2013) and *S. stapfianus* (Yobi et al., 2017), during desiccation. Unlike LEA proteins, which are also expressed in the dry tissues of desiccation sensitive plants, ELIPs are notably more abundant in resurrection plants. This enrichment highlights the crucial role of ELIPs in enabling these plants to withstand desiccation stress and regain functionality upon rehydration.

1.3.3.2 Antioxidant Defence System

Maintaining a strong antioxidant system is important for preventing oxidative damage induced by ROS accumulation during dehydration in plant cells. This antioxidant defence system comprises both non-enzymatic and enzymatic components. The enzymatic antioxidant system includes several key enzymes such as superoxide dismutase, catalase, peroxidase, and glutathione reductase (Alscher et al., 2002). These enzymes are activated during desiccation and other abiotic stresses, where they play important roles in scavenging ROS and mitigating cellular damage caused by oxidative stress (Jaleel et al., 2009). Numerous studies on resurrection plants have observed increased activity of these antioxidant enzymes in response to desiccation. These include *S. pulvinate*, *X. humilis*, *X. viscosa*, *C. wilmsii*, *M. flabellifolius*, and *Eragrostis nindensis* (Farrant, 2000; Illing et al., 2005; Sherwin & Farrant, 1998; Yu et al., 2024), indicating their importance in desiccation response.

The non-enzymatic antioxidant system in desiccation tolerant plants employs low molecular weight compounds such as tocopherols, carotenoids, polyphenols, ascorbate and reduced glutathione to combat ROS in plant cells (Oliver et al., 2020). High levels of antioxidants, including ascorbate, glutathione, and tocopherols have been observed in *S. stapfianus* (Oliver et al., 2011; Yobi et al., 2017), while tocopherols have been detected in *B. hygrometrica* (Zhu et al., 2015), and carotenoids in the tissues of *X. schlechteri* (Radermacher et al., 2019). Additionally, the air-dried leaves of *H. rhodopensis* exhibit substantially high concentrations of both enzymatic and non-enzymatic antioxidants, such as ascorbate, flavonoids, ascorbate peroxidase and glutathione reductase (Georgieva et al., 2017).

1.3.3.3 Accumulation of Soluble Sugars

The accumulation of soluble sugars is a common response in plants experiencing stress, and resurrection plants are no exception (Ingram & Bartels, 1996). Among these sugars, sucrose, a disaccharide, is particularly prevalent. It functions as a water replacement molecule, stabilizing macromolecules within the cytoplasm (Vicré et al., 2004). During periods of water deficit, increased levels of sucrose protect cellular membranes by preventing their fusion (Oliver et al., 2020). Furthermore, the accumulation of sucrose leads to the formation of a glassy matrix through a process known as vitrification (Oliver et al., 2000). This highly viscous, super-saturated liquid state is a phenomenon observed in all desiccation tolerant cells. The glassy matrix is composed of a mixture of non-reducing sugars, proteins, amino acids and organic acids, which can differ between species and various tissues (Buitink & Leprince, 2004). The

primary function of this viscous vitreous phase is to reduce molecular mobility, thereby stabilizing cellular structures under desiccation stress (Buitink & Leprince, 2004). In addition, the cytoplasmic glass state inhibits chemical reactivity inside the cells, significantly decreasing the potential for cellular damage during periods of severe dehydration (Oliver et al., 2020).

Moreover, increased abundance of other sugars, such as raffinose and trehalose, in desiccated tissues, is also linked to conferring cellular protection against desiccation (Farrant, 2007). Trehalose is a disaccharide sugar that enhances the safeguarding effect of sucrose in drying tissue of most resurrection plants (Ghasempour et al., 1998). It has been postulated that raffinose prevents sucrose crystallization under dry conditions (Müller et al., 1997). Elevated levels of both raffinose and sucrose have been detected in diverse resurrection plant tissues from five different families; Velloziaceae, Poaceae, Gesneriaceae, Liliaceae and Cyperaceae (Ghasempour et al., 1998), therefore confirming that these sugars act as agents of desiccation tolerance in various species.

1.4 *Xerophyta* Resurrection Plants

Xerophyta is a genus of flowering plants belonging to the family Velloziaceae. Native to Madagascar, the Arabian Pennisula, and Africa (Behnke et al., 2013), these species are predominantly found in arid regions. This study focuses on several species within the monocotyledonous *Xerophyta* genus: *X. elegans*, *X. schlechteri* and *X. humilis.* Despite sharing a common genus, these species grow in different habitats and employ distinct mechanisms for VDT. For example, *X. elegans*, (previously known as *Talbotia elegans*), typically grows in rocky and shady areas, predominantly found in the Drakensberg mountains of KwaZulu Natal and the Mpumalanga provinces in South Africa (Fig. 1.5). During desiccation, *X. elegans* retains its chlorophyll and thylakoid membranes, a characteristic referred to as being homoiochlorophyllous, which helps it maintain its photosynthetic machinery in a ready state for rapid recovery. In contrast, *X. schlechteri* (incorrectly referred to as *X. viscosa* in Costa et al. 2017b) and *X. humilis* plants are poikilochlorophyllous, meaning that they dismantle their thylakoid membranes during desiccation to minimize the harmful effects of ROS. This strategy helps them conserve energy and protect vital cellular components during prolonged periods of dryness. *X. schlechteri* is native to parts of Limpopo and Mpumalanga provinces in South Africa, whereas *X. humilis* has a broader distribution across the Southern African region, including areas in Botswana, Namibia, and the northern parts of South Africa (Fig. 1.6). It is

worth mentioning that these two species grow in areas of full sun not in shade, which is probably why they break down chlorophyll during desiccation.

A number of studies focusing on DT mechanisms in these three *Xerophyta* species have been documented. These studies range from physiological and ultrastructural changes, to changes in the transcriptome, proteome, metabolites and lipids in these species during water deficit conditions (Artur et al., 2019; Collett et al., 2004; Dace et al., 1998; Farrant, 2000; Gabier et al., 2021; Hilhorst et al., 2017; Ingle et al., 2008; Lyall et al., 2020; Radermacher et al., 2019; Tshabuse et al., 2018). While these studies have provided valuable information on the various mechanisms of DT in individual *Xerophyta* species, none of them have conducted a comparative analysis across multiple species. A comparative analysis would be crucial for identifying conserved mechanisms of VDT, potentially uncovering fundamental principles that could apply to other plants as well. Moreover, these studies primarily focused on adult plant tissues, which presents certain challenges. First, the extended time required for the plants to grow can significantly delay experimental progress. Second, and most importantly, there is considerable heterogeneity in water content across the plant, and even within a single leaf during the drying process, which can complicate the interpretation of results. The rate at which plants dry down is additionally complicated by the size of the pot and the amount of soil in which they are grown in.

Using a seedling model could effectively address these challenges. Seedlings are easy to germinate from seed, grow more quickly, and dry more rapidly and uniformly compared to adult plants. Further, the seedling model is advantageous because it can be set up under controlled experimental conditions which provides an opportunity to obtain reproducible data more efficiently, facilitating a deeper understanding of the mechanisms underlying DT.

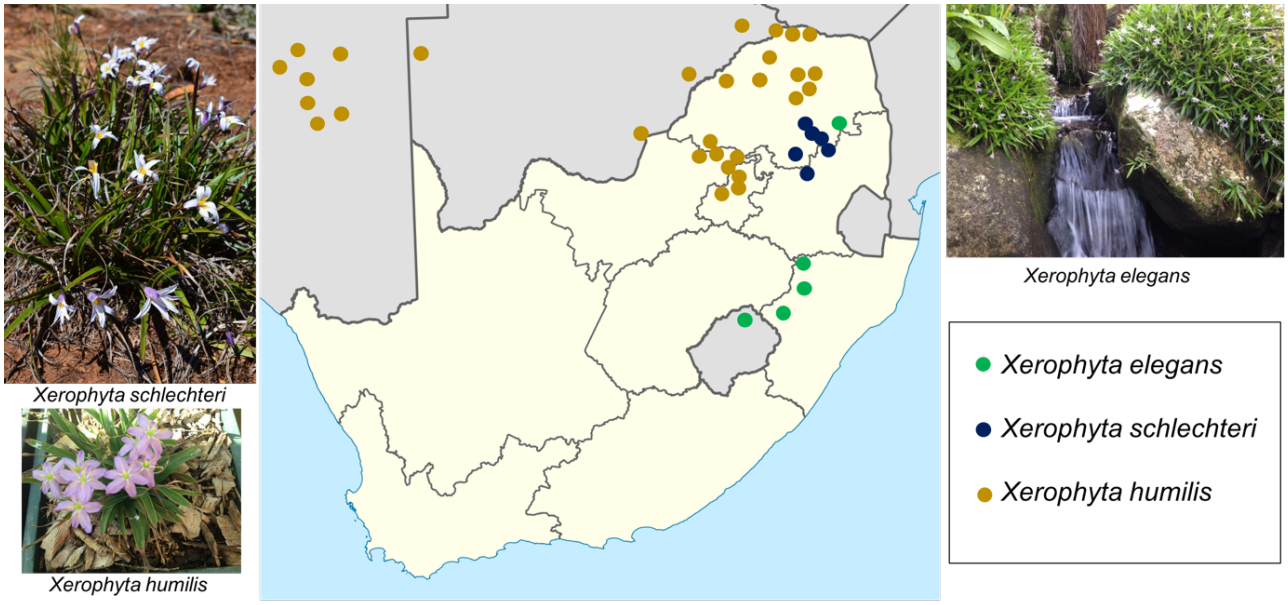

Figure 1.6. A map showing distribution of *Xerophyta elegans*, *Xerophyta schlechteri* and *Xerophyta humilis* in Southern Africa. The green-, blue- and gold-coloured circles on the map represent *X. elegans*, *X. schlechteri* and *X. humilis*, respectively.

1.5 Aims and Objectives

The primary aim of this study was to conduct a comparative analysis of the desiccation responses in three *Xerophyta* species: *X. elegans*, *X. schlechteri* and *X. humilis,* at early (pre-leaf) and late (two-leaf) stages of seedling development. This investigation sought to understand the VDT strategies that enable these species to survive desiccation, with a focus on identifying both conserved and species-specific mechanisms. A challenge with the existing data on *Xerophyta* species is that cross-species comparisons are difficult, as these species have been subjected to different experimental conditions. The advantage of our three-species approach is that all plants were exposed to the same growth and stress conditions, making direct comparisons between species more reliable. This consistency ensures that the observed differences are due to species-specific adaptations rather than variations in experimental conditions. The specific aims and objectives are outlined in each chapter of the thesis, however, the overall objectives are summarised below.

Objectives:

(i) Ultrastructural Analysis:

- To utilize Transmission Electron Microscopy (TEM) to examine and compare the ultrastructural changes in a time course series of desiccating and rehydrating seedlings of *X. elegans* and *X. schlechteri* at the two-leaf stage

(ii) Transcriptomic Analysis

- To perform RNA sequencing (RNA-Seq) to examine changes in transcriptome expression profiles in the three *Xerophyta* species at early and late stages of seedling development in response to desiccation

(iii) Metabolomic/lipidomic Analyses

- To perform metabolome and lipidome analyses using Gas Chromatography-Mass Spectrometry (GC-MS) and Liquid Chromatography-Mass Spectrometry (LC-MS) to investigate desiccation-induced changes in primary metabolites, secondary metabolites, and lipid profiles in the three *Xerophyta* species at two developmental stages. This was performed in parallel with the RNA-Seq analysis.

CHAPTER 2

Ultrastructural Analysis of Two-Leaf Seedlings of *Xerophyta elegans* and *Xerophyta schlechteri* during Desiccation and Rehydration

2.1.1 Introduction

An essential survival strategy during desiccation involves mitigating the damage caused by ROS accumulation. Poikilochlorophyllous resurrection plants such as *S. stapfianas, X. viscosa* and *X. humilis*, employ a unique approach to address this challenge by breaking down chlorophyll as their leaves desiccate, and dismantling the thylakoid membranes within chloroplasts (Cooper & Farrant, 2002; Ingle et al., 2008; Quartacci et al., 1997; Tuba et al., 1998). While effective in minimizing ROS, a significant drawback of this strategy is that the photosynthetic system needs to be rebuilt *de novo* upon rehydration, resulting in a slower recovery rate (Tuba et al., 1998).

In contrast, homoiochlorophyllous resurrection plants like *X. elegans*, *C. pumilum, and M. flabellifolius* maintain their chlorophyll and thylakoid membranes largely intact during desiccation (Hallam & Gaff, 1918; Moore et al., 2005; Oung et al., 2022). This preservation allows them to recover more rapidly when water becomes available again (Kranner et al., 2002). However, this strategy comes at the cost of increased vulnerability to oxidative stress caused by the accumulation of ROS. As a result, homoiochlorophyllous plants employ additional protective mechanisms, such as leaf folding to reduce light exposure, synthesis of anthocyanins, enhancement of their antioxidant systems to counteract oxidative stress damage (Alscher et al., 2002). These adaptations highlight the diverse strategies employed by resurrection plants to survive and recover from desiccation stress.

Several studies have been conducted to investigate cellular and chloroplast ultrastructural changes that occur in adult leaves of poikilochlorophyllous and homoiochlorophyllous plants as they desiccate and rehydrate (Table 2.1). The most common desiccation-induced cellular ultrastructural changes reported in these plants include the relocation of chloroplasts from the periphery to the centre of the cell, fragmentation of the large central vacuole into numerous smaller vacuoles, and a change in the shape of chloroplasts from oval to spherical (Cooper & Farrant, 2002; Schneider et al., 1993; Vecchia et al., 1998). Within the chloroplasts, starch

granules decrease, the number of plastoglobules increases, and thylakoid membranes are dismantled in poikilochlorophyllous plants, in response to desiccation (Charuvi et al., 2019; Cooper & Farrant, 2002; Oung et al., 2022). These alterations are thought to play a pivotal role in ensuring plant adaptation during desiccation.

As presented in Table 2.1, these studies investigated ultrastructural changes in adult leaf tissues. One of the limitations of working on adult plants is that the water content is variable along the length of the leaf. The average %RWC is reported for a leaf, but TEM samples are usually taken from a small section of the leaf. In addition to the limited sampling as leaves desiccate, the correlation between average %RWC and actual %RWC of the section may be weak. Further, most of the ultrastructural studies in the literature were done to compare three end points, namely, hydrated, dehydrated, and rehydrated leaf states (Charuvi et al., 2019; Cooper & Farrant, 2002; Moore et al., 2005; Oung et al., 2022; Quartacci et al., 1997; Schneider et al., 1993; Sherwin & Farrant, 1996, 1998; Vecchia et al., 1998). Although these provide insights about the overall ultrastructural changes, this strategy does not effectively capture the series of changes at different %RWC and how fast they occur.

Previous study on *X. viscosa* demonstrated that this species is DT at different stages of seedling development even when dried rapidly in the laminar flow hood (Lyall et al., 2014). Therefore, using seedlings serves as an excellent model for investigating the changes in both cells and chloroplasts as leaves undergo desiccation and subsequent rehydration. The small seedling leaves offer the advantage of more uniform drying and a reproducible rate under well-defined conditions.

2.1.2 Aim and Objectives of the Study

The objective of this chapter was to use transmission electron microscopy to characterize whether similar ultrastructure changes occur in the cells and chloroplasts of 14-day old two-leaf seedlings as reported in adult plants. Additionally, the study aimed to provide a detailed record of ultrastructural changes at various time points during desiccation and rehydration processes in homoiochlorophyllous *X. elegans* and poikilochlorophyllous *X. schlechteri.*

Table 2.1. Ultrastructural Studies Conducted in Several Resurrection Plants

Species	Poikilochlorophyllous/ Homoiochlorophyllous	Tissue type measured	Stages of desiccation	Stages of rehydration	References
Xerophyta elegans	Homoiochlorophyllous	Adult leaf tissue	(i) None (ii) 59, 50, 38 & 8% RWC	(i) 1, 2, 4, 8, 12, 24 & 48 h (ii) None	(i) Hallam & Luff. 1978 (ii) Hallam & Gaff. 1980
Xerophyta humilis	Poikilochlorophyllous	Adult leaf tissue	None	3, 6, 9, 12, 15, 18 & 24 h	Ingle et al 2008
Sporobolous stapfianas	Poikilochlorophyllous	Adult leaf tissue	(i) 3.4% RWC (ii) 78 & 4% RWC	(i) 96.5% RWC (ii) 90% RWC	(i) Quartacci et al, 1997 (ii) Vecchia et al, 1998
Myrothamnus flabellifolius	Homoiochlorophyllous	Adult leaf tissue	(i) <5% RWC (ii) 86% & 12% RWC	(i) 12 h (ii) None	(i) Sherwin & Farrant. 1996 (ii) Moore et al. 2005
Craterostigma wilmsii	Homoiochlorophyllous	Adult leaf tissue	(i) <5% RWC (ii) <5% RWC (iii) 85-70, 65-50 & 40-25% RWC	(i) 12 & 48 h (ii) None (iii) 100% RWC	(i) Sherwin & Farrant. 1996 (ii) Sherwin & Farrant. 1998 (iii) Cooper & Farrant. 2002
Xerophyta schlechteri	Poikilochlorophyllous	Adult leaf tissue	60, 35, 20 & <5% RWC	12, 24, 48, 72 & 168 h	Radermacher et al. 2019
Craterostigma pumilum	Homoiochlorophyllous	Adult leaf tissue	(i) 15% RWC (ii) 40% RWC	(i) None (ii) 48 h	(i) Charuvi et al. 2019 (ii) Oung et al. 2022
Xerophyta viscosa	Poikilochlorophyllous	Adult leaf tissue	(i) <5% RWC (ii) <5% RWC	(i) 24 & 48 h (iI) None	(i) Sherwin & Farrant 1996 (ii) Cooper & Farrant. 2002

2.2 Methods and Materials

2.2.1 Seed Germination and Drying Down Experiments

X. elegans and *X. schlechteri* seeds were aseptically plated on half strength MS media [2.165 g/L Murashige and Skoog (MS) Basal medium with Gamborg's vitamins, 7 g/L bacteriological agar], and incubated at 23 °C under 16-hour light and 8-hour dark cycles in a plant growth chamber (Percival Scientific, Iowa, USA) to germinate and grow until they reached two-leaf developmental stage. Next, a time point series experiment, involving two biological replicates of samples undergoing dehydration and rehydration was conducted for ultrastructural analysis. Prior to inducing desiccation, two-leaf seedlings were pre-plated on a damp 90 mm Whatman grade 2 filter paper (GE Healthcare, Amersham Place Little Chalfont, UK) with 2 mL distilled water for 24 hours so that they could adjust from MS agar media. Subsequently, 20 two-leaf seedlings were transferred onto a petri dish lid with a single wet (1 mL dH_2O) Whatman grade 5 filter qualitative paper and placed in a transparent 15 L plastic storage box (41.5 cm (L) x 17 cm (H) x 29 cm (W)). In total, each storage box contained 8 petri dish lids (uncovered), each with 20 seedlings, and these were left to dry down in the Percival over a period of 72 hours and sampled at different time points (0, 3, 6, 9, 12, 24, and 72 hours) for cellular ultrastructure analysis. For rehydration, seedlings were dried down for 72 hours as described above, and re-watered by adding 2 mL of distilled water. Petri dish lids with rehydrated seedlings were capped with the bottom part of the plate and sealed with parafilm to minimize evaporation. Rehydrating seedlings were sampled at 1, 2, 4, 8, 12 and 48 hours post re-watering. The RWC estimations of these seedlings were determined by taking weight measurements of 20 seedlings at each time point, and calculated using the following formula:

$$\%\text{RWC} = \frac{Fresh\ weight - dry\ weight}{Turgid\ weight - dry\ weight} \text{ x } 100$$

2.2.2 Sample Preparation for Cellular Ultrastructure

Xerophyta tissues were processed for TEM ultrastructure using a protocol described by (Farrant et al., 1999), with minor modifications. Two-leaf seedlings were transferred into a microfuge tube containing 500 µL of fixative 1 [2.5% glutaraldehyde, 0.1 M phosphate buffer, 0.5% caffeine, pH 7.4], and incubated at 4 °C for 24 hours. After fixation, the fixative was removed from the tube, and replaced with 0.1 M phosphate buffer, pH 7.4, and incubated for 5 minutes. This wash step was repeated 3 times. Following the removal of the final buffer wash, 250 µL

of 2% (w/v) osmium tetraoxide and 250 μL of 0.2 M phosphate buffer were added into the tubes and allowed to fix for 1 hour at room temperature. Afterwards, samples were washed as described above, and dehydrated for 5 minutes in a graded ethanol series (30% (v/v), 50%, 70%, 85%, and 95% ethanol) at room temperature. After removing 95% ethanol, 100% ethanol was added and left for 10 minutes before adding 100% acetone for another 10 minutes. *Xerophyta* tissues were infiltrated with epoxy resin (Spurr, 1969) by adding one-part acetone and one-part room temperature Spurr's resin (50% resin) and left overnight at 4 °C. This was repeated to obtain 75%, 87.5% and 100% resin over a period of 4 days. Finally, samples were embedded in pure Spurr's resin, and hardened at 60 °C oven for at least 16 hours.

2.2.3 Trimming and Sectioning

Resin blocks with fixed seedling leaf tissues were appropriately trimmed into a pyramid shape using a sharp and sterile razor blade, and the surface of the block was smoothened with a histo diamond knife. This was followed by producing 90 nm thick gold interference-coloured ultrathin sections using a microtome (Ultracut-S, Reichert, Germany), and then carefully placing them on 200 nm mash copper grids.

2.2.4 Staining

The specimen on the grids were stained with 2% (w/v) uranyl acetate and 1% (w/v) lead citrate (Reynolds, 1963). Briefly, sample grids were placed on a few drops of uranyl acetate for 15 minutes, rinsed by immersing them three times with pre-boiled distilled water, and then blotting on a clean piece of filter paper before applying the second stain. Lead citrate staining was performed in a CO_2 free environment to prevent precipitation caused by long exposure to air. This was done by placing a few sodium hydroxide pellets onto a glass petri dish plate and immediately closing it with the lid to absorb the CO_2 inside the dish. After 10 minutes of lead citrate staining, the grids were washed with distilled water as described above, and then allowed to dry on filter paper before transferring them onto a grid holder.

2.2.5 Imaging and Quantification

Stained sections were examined using TEM (Talos F200C, Thermo Scientific) at both low (2000x) and high (11 000x) magnifications. The examination covered the general cell structure at low magnification and individual chloroplasts in various leaf sections at high magnification. A total of 25 images were taken in each biological repeat, comprising 5 images depicting the overall cell structure and 20 images displaying individual chloroplasts from different leaf regions. To assess the reproducibility of the two biological replicates, the quantification of starch granules and plastoglobules was conducted on 10 chloroplasts from *X. elegans* for each experiment at each time point. ImageJ software (version 2.9.0/1.53t) was used for this analysis. Next, 15 high-quality images were chosen from these two sets of replicates for the examination and quantification of ultrastructural changes at each time point. The selection was made based on the image quality within each replicate.

Ultrastructural quantification encompassed measurements of chloroplast length/width ratio, grana stack width, and counts of plastoglobules, starch granules, and vesicles. Prior to taking measurements, the image scale was established in the 'set scale' window on ImageJ, and the same scale was consistently applied to all images. Chloroplast length measurements were made using a straight-line selection tool. This approach was also used to measure chloroplast and grana widths. The quantification of plastoglobules, starch granules, and vesicles within each chloroplast was performed by tallying them using a point tool. Vesicle size was measured by determining the diameter of each vesicle using ImageJ. Vesicles were classified into 'big', ‘medium’, 'small' categories based on size thresholds defined in our study: with vesicles larger than 200 μm were classified as 'big', those between 100 μm and 200 μm as ‘medium’, and those smaller than 100 μm as 'small.'

2.3 Results

2.3.1 Similar Ultrastructural Changes Observed in two Independent Experiments

Two independent experiments were conducted, and seedlings were sampled at different time points for ultrastructure analysis using TEM. To assess reproducibility, the number of starch granules and plastoglobules was quantified across two biological replicates in *X. elegans*. The quantification of starch granules and plastoglobules in chloroplasts from two-leaf seedlings showed consistent results between the two experiments (Fig. 2.1). During dehydration, the number of plastoglobules in both experiments gradually declined in tandem with the decreasing water content in the seedlings. However, a dramatic increase in plastoglobule numbers happened 24 hours after drying. Interestingly, these numbers decreased again at the 72-hour mark post dehydration. Notably, starch granule quantities remained relatively consistent at all time points, except when in the desiccated state where none were detected (Fig. 2.1). Both biological replicates showed similar trends during the rehydration series, with a gradual decline in plastoglobule numbers and an emergence of starch grains, increasing from complete absence at the desiccated state to approximately 4 per chloroplast at 48 hours post rehydration. These results underscore the reproducibility of the two independent experiments.

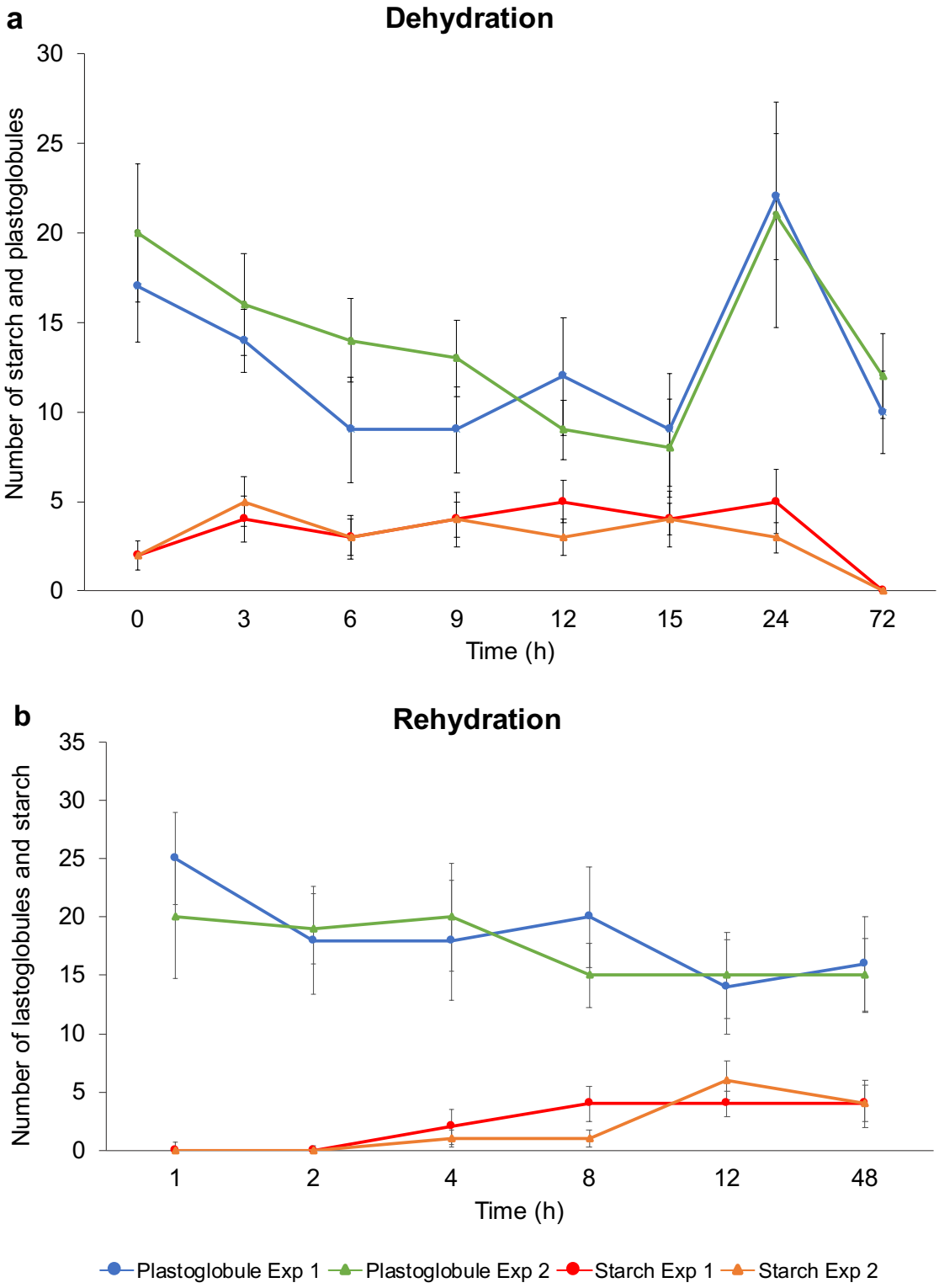

Figure 2.1. Changes in the number of starch granules and plastoglobules in *Xerophyta elegans* chloroplasts observed in two independent experiments. Starch grains and plastoglobules were quantified from 10 chloroplasts in different cells across two biological replicates. The quantification was done in each replicate per time point using ImageJ software. Average number of starch and plastoglobules are displayed. Values shown are means ± SD.

2.3.2 Changes in the Ultrastructure of *X. elegans* and *X. schlechteri* Leaf Cells in Response to Desiccation and Rehydration

Cell modifications and changes in chloroplast ultrastructure are some of the key desiccation-induced responses that occur in resurrection plants. In *X. elegans* and *X. schlechteri* seedlings, fully hydrated leaves were characterised by a large vacuole which occupied most of the cell volume, while the cytoplasmic material, including chloroplasts, was located at the periphery of the cells (Fig. 2.2a-b). During the first 12 hours of drying, no obvious cellular changes were observed in either species (Fig. 2c-j). The most marked changes were apparent at 24 and 72 hours post desiccation (Fig. 2m-p). Of these changes, fragmentation of the central vacuole into smaller vacuoles and centralization of chloroplasts were common in *X. elegans* and *X. schlechteri* cells. At fully desiccated state, both seedlings were dry, with *X. schlechteri* leaves turning yellow (Fig. 2.2 o-p). In addition, all cells in the two species appeared dry and contracted. Notably, the cell wall remained intact throughout the desiccation series. It is worth mentioning that all changes that occurred at the cellular level were similar across these species.

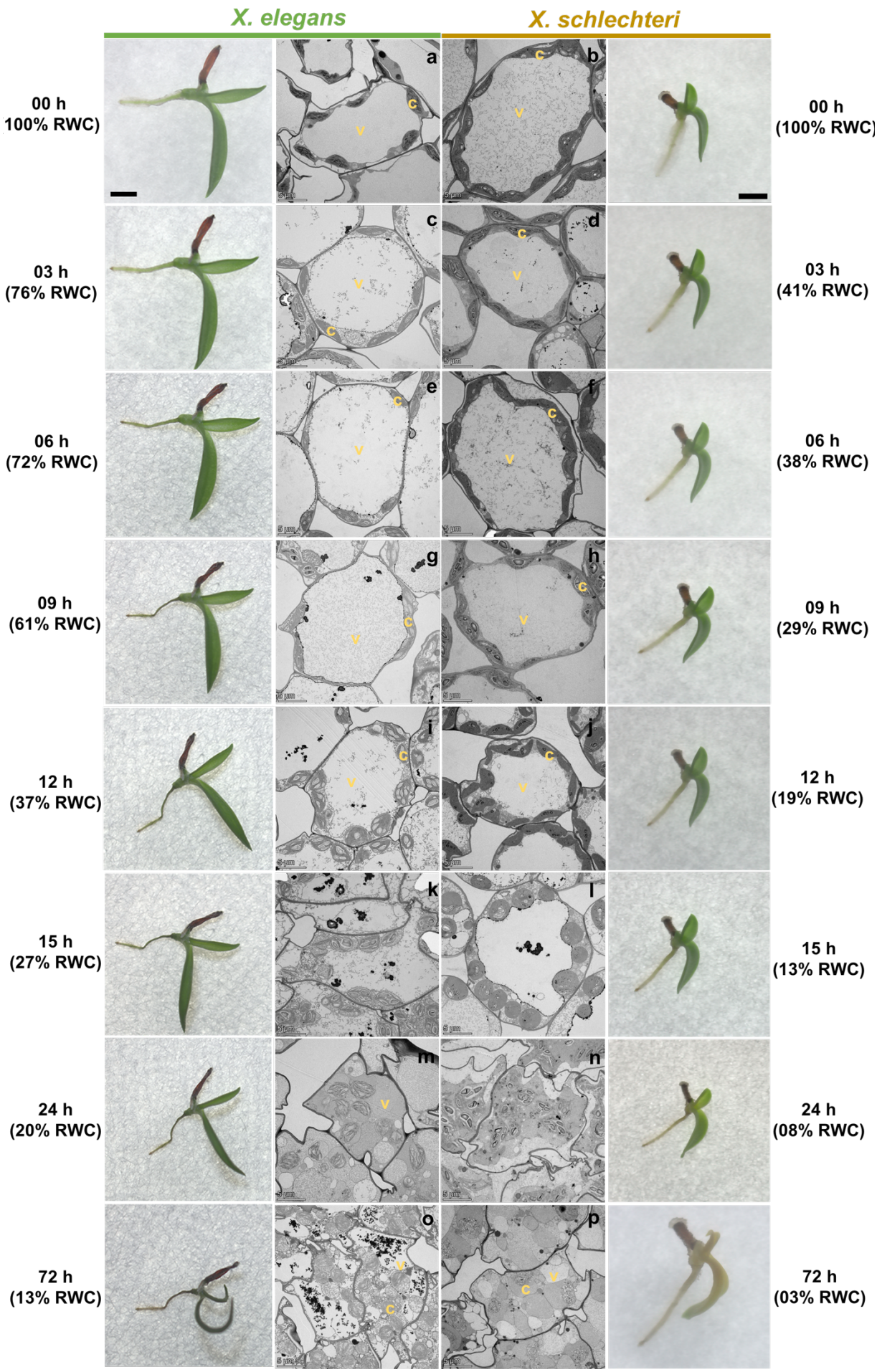
X. elegans
X. schlechteri
00 h (100% RWC)
03 h (76% RWC)
06 h (72% RWC)
09 h (61% RWC)
12 h (37% RWC)
15 h (27% RWC)
24 h (20% RWC)
72 h (13% RWC)
00 h (100% RWC)
03 h (41% RWC)
06 h (38% RWC)
09 h (29% RWC)
12 h (19% RWC)
15 h (13% RWC)
24 h (08% RWC)
72 h (03% RWC)
a
b
c
d
e
f
g
h
i
j
k
l
m
n
o
p
C
V

Figure 2.2. Transmission electron micrographs displaying dehydrating leaf cells of *X. elegans* and *X. schlechteri* over a 72-hour period. Scale bars = 5 μm, c-chloroplast, v-vacuole.

Upon rehydration, rapid ultrastructural changes occurred within the cells. An interesting observation was the presence of condensed compounds particularly within the small vacuoles of *X. elegans* cells 1 hour after the addition of water (Fig. 2.3a). These compounds had a black core, surrounded by a darker grey layer. By the 2-hour time point, these compounds had exited the small vacuoles and had reduced in size. As the water content increased, the number of small vacuoles gradually diminished, ultimately resulting in the enlargement of a single vacuole (Fig. 2.3g-h). Two days post rehydration, the chloroplasts had re-located to the periphery of the cell, and the vacuole had enlarged and assumed a central position (Fig. 2.3i-j). This was observed in both species, although a few small vacuoles were still visible in the *X. schlechteri* cells (Fig. 2.3j), possibly indicating that the cells had not fully recovered.

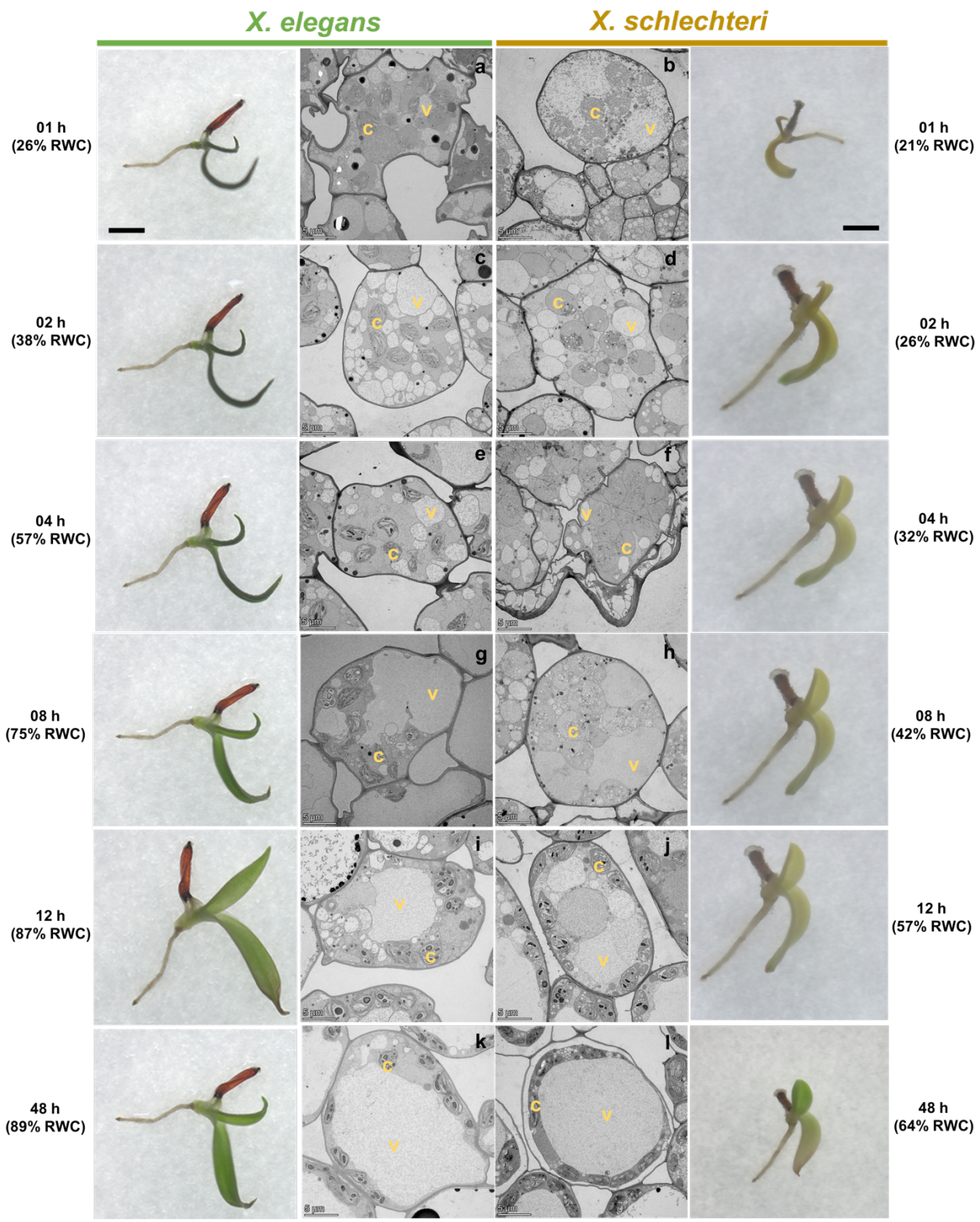

Figure 2.3. Transmission electron micrographs showing changes in rehydrating leaf cells of *X. elegans* and *X. schlechteri* seedlings over a 48-hour period. Scale bars = 5 µm, c-chloroplast, v-vacuole.

2.3.3 Chloroplast Ultrastructural Changes in the Two-Leaf Tissues of *X. elegans* and *X. schlechteri* during Desiccation and Rehydration

Similar to findings in other ultrastructural studies in adult plant leaf tissues, the well-hydrated two-leaf seedlings of *Xerophyta* exhibited characteristics such as intact grana stacks and oval-shaped chloroplasts (Fig. 2.4a). The average length and width ratios of chloroplasts were 0.78 x 0.3 µm and 0.85 x 0.3 µm for *X. elegans* and *X. schlechteri*, respectively. Additionally, the chloroplasts in fresh tissue samples were rich in plastoglobules, with an average of 18 and 15 in each chloroplast for *X. elegans* and *X. schlechteri*, respectively (Fig. 2.5).

During the desiccation process, minimal changes in the appearance of chloroplasts were evident in tissues sampled between 3 and 15 hours for both *Xerophyta* species (Fig. 2.4k-l). However, a gradual change in chloroplast shape, transitioning from oval to spherical, became noticeable at the 15-hour mark, particularly in *X. schlechteri*. Furthermore, 15 hours post drying, an indication of starch degradation, marked by the presence of a visible split in the middle of the starch granule, was observed in *X. elegans* chloroplasts. This phenomenon was also observed in ten additional chloroplasts of the same species (data not displayed), but it was not evident in *X. schlechteri* chloroplasts. Nevertheless, most starch granules within the same chloroplast still appeared intact.

Further ultrastructural changes included considerable withdrawal of thylakoid structures from the inner membrane of the chloroplast, which was observed at the 24 and 72-hour time points. This resulted in an extra open space around the chloroplast, as indicated by the red arrows in Figure 2.4 (m-p). At the desiccated state, i.e. 13% RWC in *X. elegans* and 3% RWC in *X. schlechteri*, chloroplasts were totally devoid of starch granules, and the number of plastoglobules were lower in *X. elegans* and slightly higher in *X. schlechteri* than at fully hydrated state, with an average of 12 and 19, respectively (Fig. 2.5). Notably, thylakoid membranes were still visible at fully desiccated state in *X. elegans* but rather disordered (Fig. 2.4o). In contrast, *X. schlechteri* had completely dismantled its thylakoid membranes, resulting in the development of vesicles with different sizes. On average, each chloroplast had 25 small, 15 medium, and 4 big sized vesicles (Fig. 2.4p and 2.5). The retention of thylakoid membranes by *X. elegans* and their degradation in *X. schlechteri* seem to be one important factor distinguishing these two *Xerophyta* species.

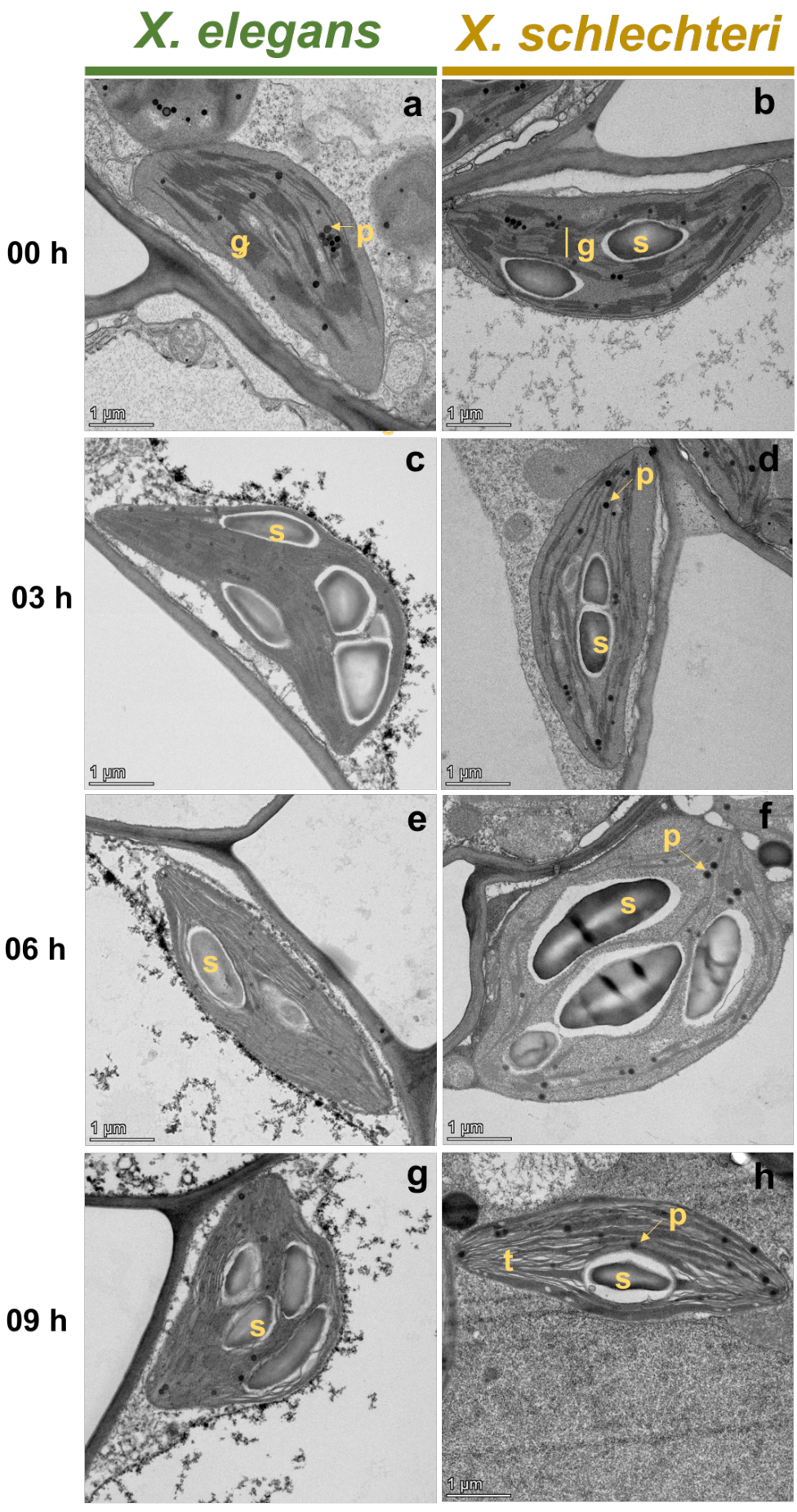
X. elegans
X. schlechteri
00 h
03 h
06 h
09 h
a
b
c
d
e
f
g
h
g
p
s
t
1 µm

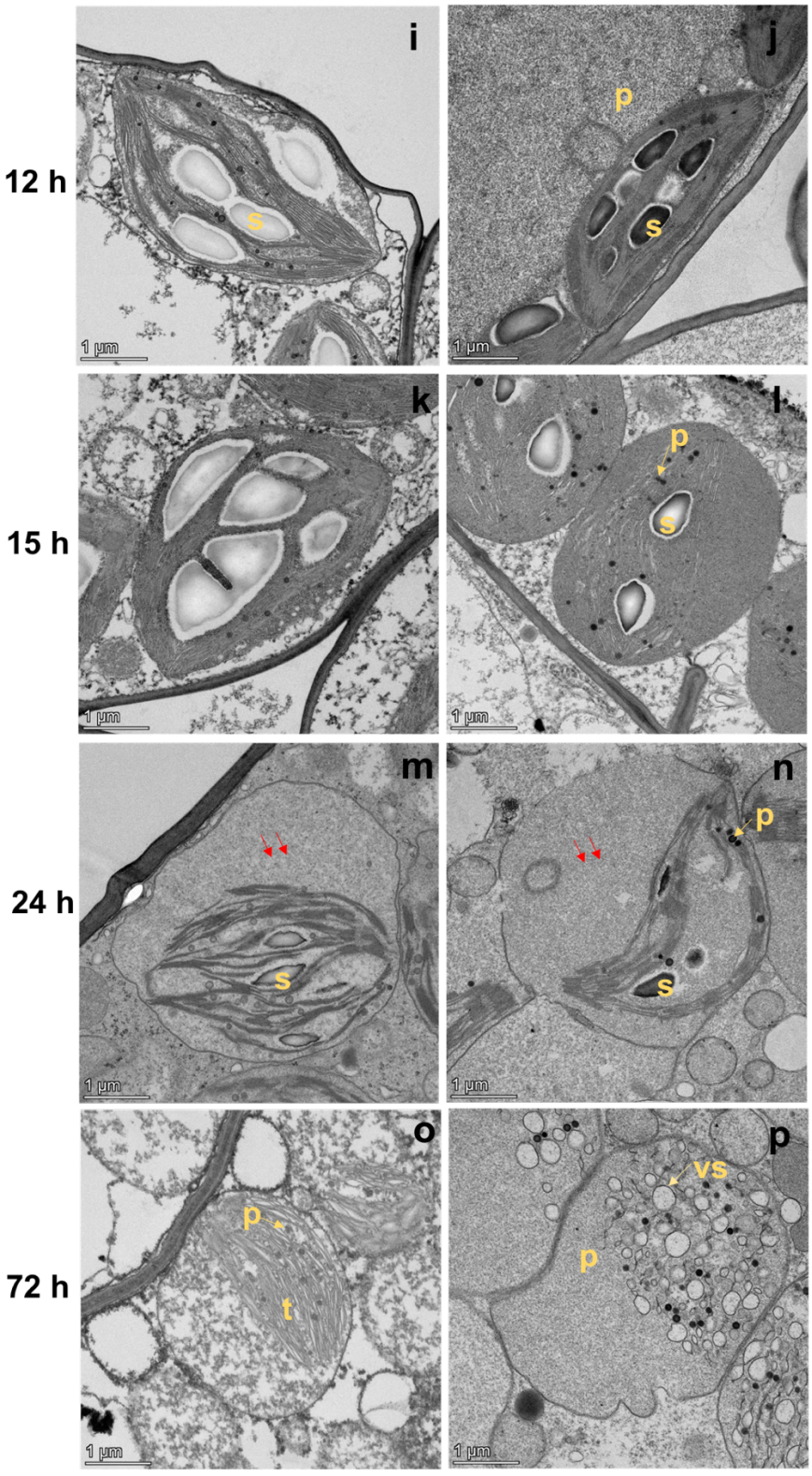

Figure 2.4. Transmission electron micrographs displaying chloroplasts ultrastructural changes in desiccating leaves of *Xerophyta elegans* and *X. schlechteri* seedlings over a 72-hour period. Scale bars = 1µm, p-plastoglobule, vs-vesicle, t-thylakoid membrane, g-grana, s-starch granule, red arrows-open space within the chloroplast. The time points from 0 to 72 hours correspond to respective relative water content for *X. elegans* and *X. schlechteri* shown in Figure 2.2.

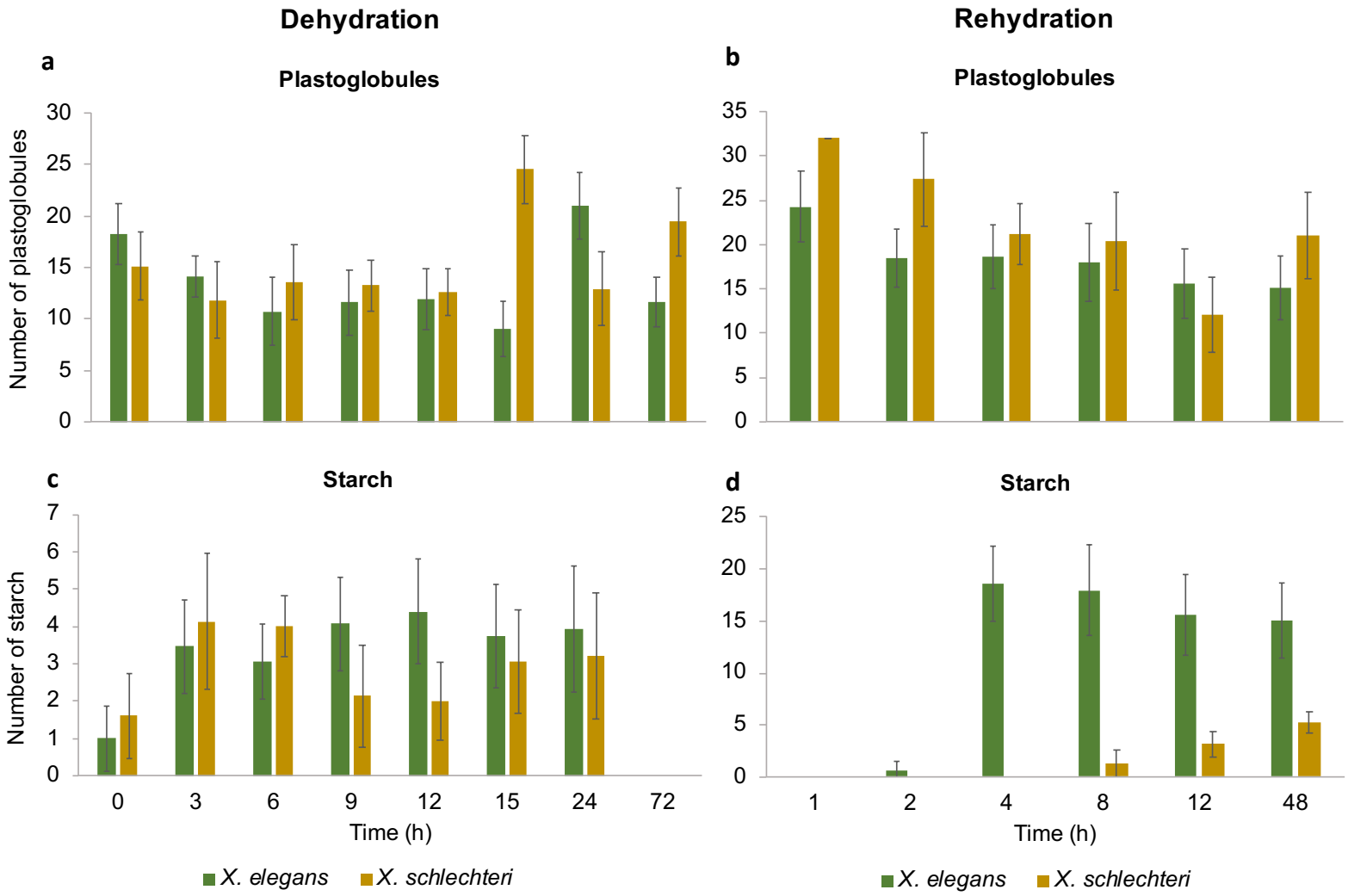

Figure 2.5. The number of plastoglobules and starch granules in desiccating and rehydrating chloroplasts of *Xerophyta elegans* and *X. schlechteri* leaf tissues. Measurements were quantified from 15 chloroplasts per time point (n=15) using ImageJ. Values shown are means ± SD.

Following rehydration, ultrastructural rearrangements in the chloroplasts quickly took place, leading to full recovery after two days. Among the first changes that occurred in *X. elegans* were an increased number of plastoglobules (Fig. 2.5b), and an expansion in the size of the chloroplasts, with a length-to-width (L/W) ratio of 0.77 x 0.68 μm (Fig. 2.6a). Notably, the width of these chloroplasts was twice the size of those in the hydrated tissues (0.78 x 0.32 μm). The rapid reconstitution of thylakoid structures in *X. elegans* chloroplasts was particularly remarkable, with intact grana stacks becoming clearly visible within the first hour of rehydration (Fig. 2.6a).

Conversely, the reassembly of thylakoid membranes in *X. schlechteri* chloroplasts occurred more slowly, with their initial appearance becoming noticeable only after 12 hours of rehydration, although still not very distinct (Fig. 2.6b-j). By 48 hours, the thylakoid membranes had reassembled, however, they had not yet been organized into grana stacks. Interestingly, the appearance of thylakoid membranes and disappearance of vesicles in *X. schlechteri* coincided (Fig. 2.6l and 2.7), suggesting that the re-synthesis of thylakoids from membrane vesicles. Notably, starch was first detected in *X. schlechteri* at 8 hours post rehydration. What is particularly intriguing about this observation is that, at this time, thylakoid membranes were not yet visible, only vesicles remained, though in reduced numbers compared to the 4-hour time point. It is possible that thylakoid membranes were already beginning to form as the vesicle count decreased, but their presence was not detectable in the TEM images, potentially due to fixation artifacts.

Overall, the rate at which ultrastructural changes took place in the chloroplasts following the addition of water was notably faster in *X. elegans* compared to *X. schlechteri* seedlings. This difference aligns with their respective characteristics as homoiochlorophyllous and poikilochlorophyllous species.

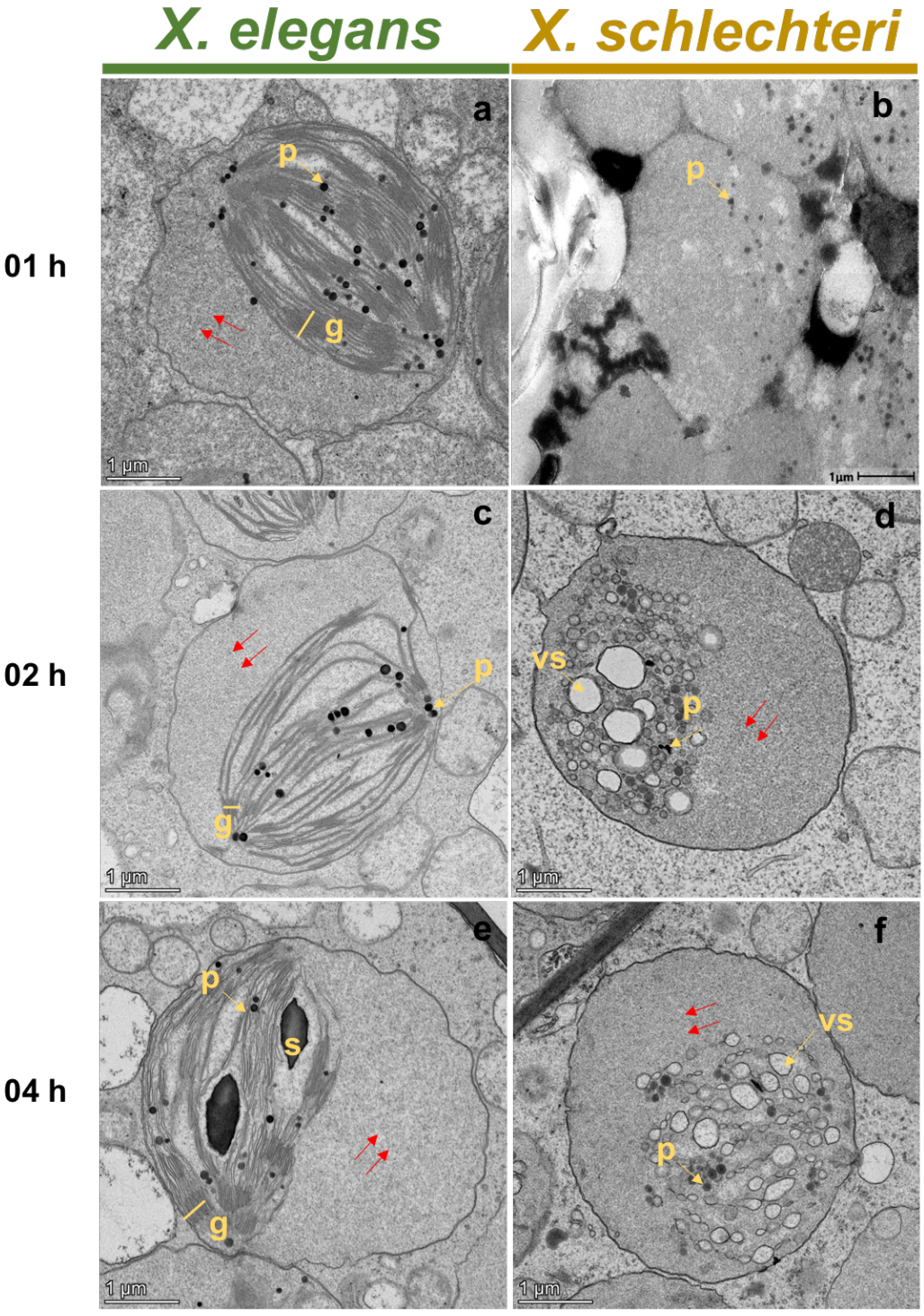
X. elegans
X. schlechteri
01 h
02 h
04 h
a
b
c
d
e
f
p
g
vs
s
1 µm
1µm

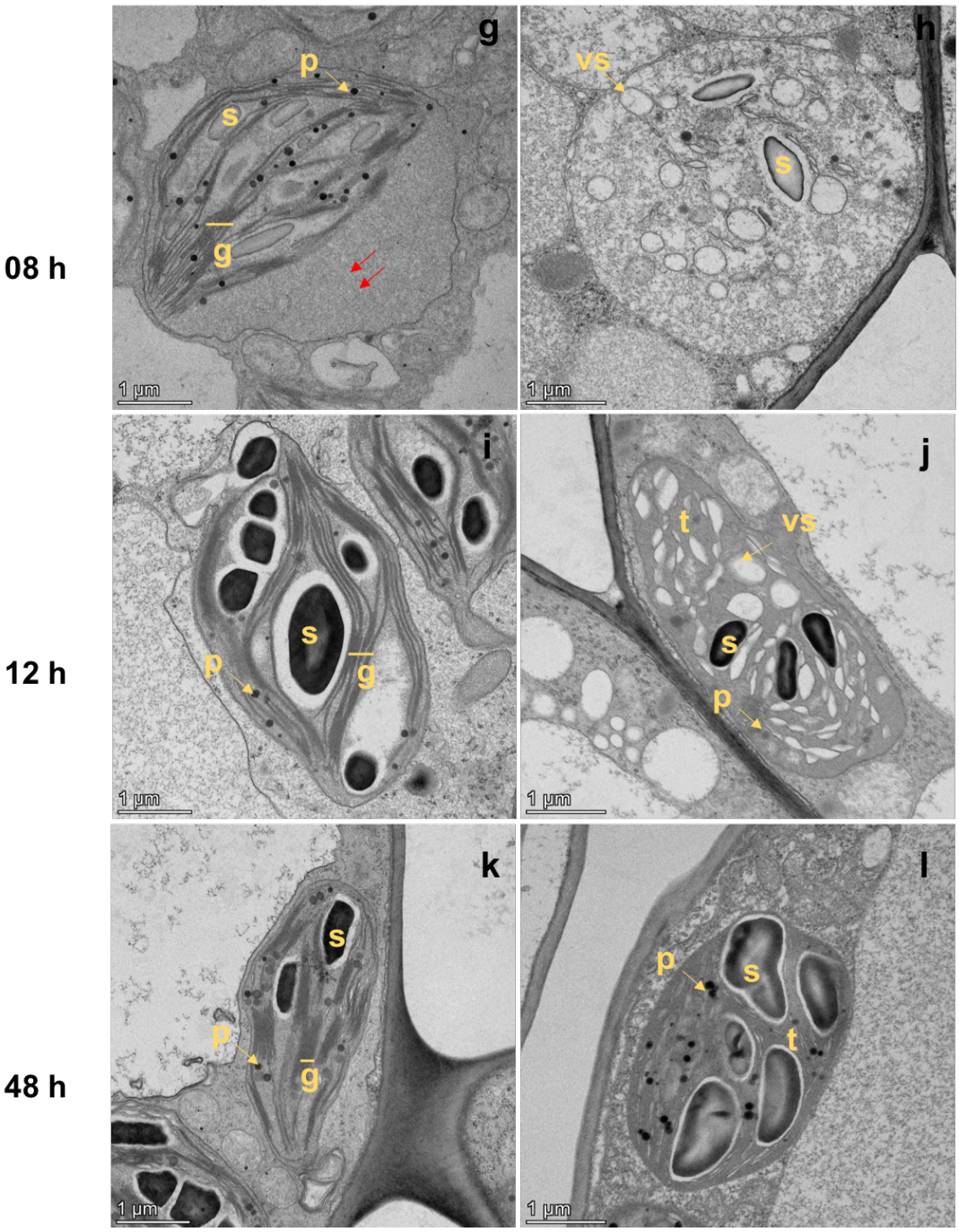

Figure 2.6. Chloroplast ultrastructural changes in rehydrating leaves of *Xerophyta elegans* and *X. schlechteri* seedlings. Scale bars = 1µm, p-plastoglobule, vs-vesicle, t-thylakoid membrane, g-grana, s-starch granule, red arrows-open space within the chloroplast. The time points from 1 to 48 hours correspond to respective relative water content for *X. elegans* and *X. schlechteri* shown in Figure 2.3.

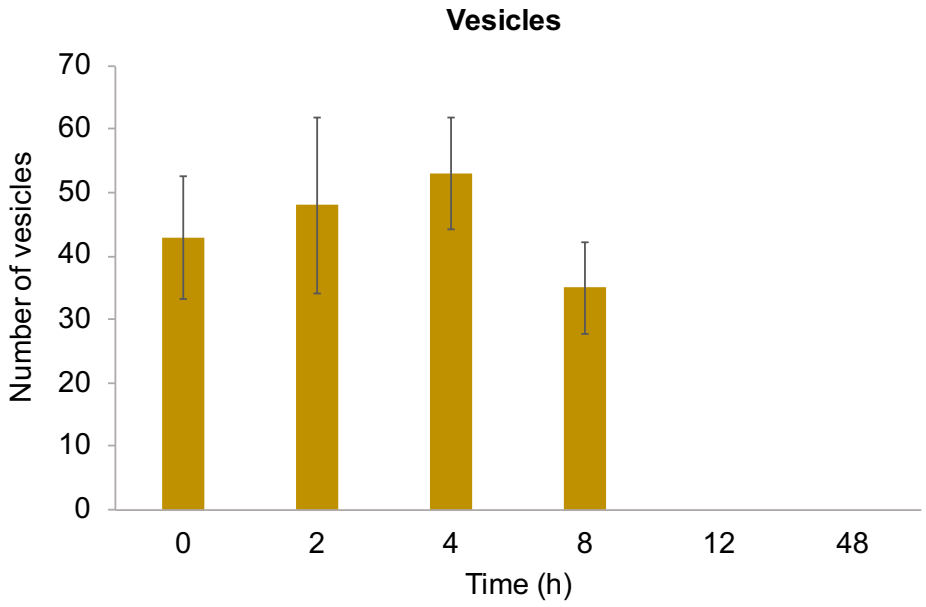

Figure 2.7. Changes in the number of vesicles in *Xerophyta schlechteri* chloroplasts during the rehydration series. The number of vesicles was determined by quantifying their presence in 15 chloroplasts per time point (n =15) using ImageJ software, and the values shown are means ± SD. The initial time point, labelled as 0 h, corresponds to the desiccated state (3% RWC) prior to rehydration.

2.4 Discussion

X. elegans and *X. schlechteri* species employ two different strategies to attain VDT. During desiccation, *X. elegans* retains most of its thylakoid structures while its counterpart completely dismantles them. In this study, a detailed time-course analysis of ultrastructural changes in leaf cells and chloroplasts of two-leaf seedlings of *X. elegans* and *X. schlechteri* was performed following desiccation and rehydration using TEM. The aim was to enhance our understanding of desiccation responses employed by these two species to survive dry conditions. This was also to characterize whether similar ultrastructure changes typically observed in mature leaf tissues of resurrection plants, occur in cells and chloroplasts of young *Xerophyta* seedlings.

Prior to dehydration, the central vacuole occupied a major portion of the cell volume and the cytoplasmic material was pushed to the periphery of the cell, as is commonly observed in hydrated cells. Upon desiccation, the central vacuole in both *X. elegans* and *X. schlechteri* cells fragmented into smaller vacuole bodies (Fig. 2.2m-p). Vacuole fragmentation is thought to play a critical role in protecting cells against potential membrane rupture and ultimate cell death (Charuvi et al., 2019). This phenomenon has also been observed in several resurrection plants including *S. stafianus* (Vecchia et al., 1998), *C. wilsmii* (Cooper & Farrant, 2002), and

C. pumilum (Charuvi et al., 2019), and has been linked to adaptation to water loss (Markovska et al., 1994).

Dehydration was further accompanied by a change in the arrangement of thylakoids in the chloroplast. In the case of *X. elegans*, grana stacks remained intact, although some partial loosening of the grana and swelling of the thylakoids were noted in other chloroplasts, particularly at fully desiccated state. Thylakoid dilation is linked to substantial changes in the chemical composition of the chloroplast stroma during dehydration (Venzhik et al., 2019). This could be due to biochemical changes in the chloroplast occurring during desiccation. For example, alterations in the concentration of metabolites and osmolytes could influence the stroma environment, which in turn affects the structural integrity of thylakoids and grana stacks, leading to observed changes like grana loosening and thylakoid swelling.

Unlike *X. elegans*, the rearrangement of thylakoid membranes was quite dramatic in desiccated *X. schlechteri* chloroplasts as they were completely dismantled at fully desiccated state, resulting in the development of vesicles. This is typical of poikilochlorophyllous plants as they lose their chlorophyll during water loss. Interestingly, considerable withdrawal of thylakoids from the chloroplast membrane observed in *Xerophyta* species (Fig. 2.4m-p) was also evident in *S. sporabolous* homoiochlorophyllous adult plant leaves (Vecchia *et al*. 1998). The significance of this is not fully understood, but it may play a role in stress adaptation.

Plastoglobules, which are thylakoid-associated lipid bodies functioning in lipid storage and metabolism (Charuvi, *et al*., 2019), were present in both hydrated and desiccating conditions of the two *Xerophyta* species as illustrated in Figures 2.3 and 2.4. This contrasts with the findings of most ultrastructural studies on adult plant tissues where increased levels of plastoglobules are only detected in desiccated tissues, not in the hydrated ones (Charuvi et al., 2019; Sherwin & Farrant, 1998). The reason for their accumulation in dry states lies in their role in repair and recycling processes (Besagni & Kessler, 2013). Moreover, the material stored within plastoglobules during water-deficient conditions may be used to restore the thylakoid membranes when water becomes available (Charuvi et al., 2019). In addition to this role, plastoglobules also function in the development of thylakoids. Given that the *Xerophyta* leaves used in this study were from young developing seedlings less than three weeks old, it is logical that these lipid bodies were also abundant in hydrated leaf cells. Notably, there was a dramatic increase of plastoglobule numbers at 24 hours of drying, followed by a subsequent decline at

72-hour time point (Fig. 2.1). This is unusual, as plastoglobule numbers typically remain elevated in the desiccated tissues of mature resurrection plant leaves. It is possible that the total number of plastoglobules remained high at 72 hours but were not clearly visible due to fixation artifacts. The challenges associated with staining desiccated tissues may have hindered proper staining and visualisation, resulting in an underestimation of these lipid bodies at this time point.

Another distinctive feature of dry chloroplasts was the absence of starch granules. According to Venzhik et al. (2019), alpha amylase hydrolyses starch granules into monosaccharides. These monosaccharides, together with other soluble osmolytes such as proline and glycine betaine that accumulate in the plastid stroma, play a protective role during water loss. These monosaccharides can be used in sucrose synthesis, which is an essential component of DT. Moreover, they help prevent protein inactivation and membrane peroxidation (Venzhik et al., 2019), thereby ensuring the integrity of the membrane. The membrane integrity may indicate that some of the metabolic processes responsible for producing membrane proteins and lipids remain active, thus safeguarding the cell from leakage and ensuring its protection.

After a desiccation period of 72 hours, seedlings were re-watered and changes that occurred within cells and chloroplasts were observed over a period of 48 hours. At the 1-hour mark post rehydration, distinct dark structures were observed within fragmented vacuoles in *X. elegans* cells (Fig. 2.3a). These dark structures are believed to be polyphenols, which are secondary metabolites that function in protecting membranes against desiccation and damage induced by ROS (Moore et al., 2005). The occurrence of these compounds is not exclusive to seedlings, as they have been previously observed in adult leaves of *X. elegans* (Hallam & Luff, 1980). As seen in Figure 2.3, these compounds are more prevalent in *X. elegans* compared to *X. schlechteri* cells, which precisely aligns with the homoiochlorophyllous nature of *X. elegans,* which relies on other protective mechanisms against photo-oxidative stress. It is noteworthy that these polyphenolic compounds are clustered together and look like small black balls rather than being dispersed. This clustering is primarily attributed to the presence of caffeine in the fixative, which condenses plant produced-phenolics inside vacuoles. This prevents the leaching of these compounds into the cytoplasm, which would result in the darkening of the cytoplasmic space (Mueller & Greenwood, 1978). Notably, after 2-4 hour (38-57% RWC) of rehydration, most polyphenol structures were no longer detected inside the vacuoles of *X. elegans* cells. It is possible that they had dissolved as the water content increased, or they relocated to the

cytoplasmic area as seen in Figure 2.3c-e. Cells were completely devoid of polyphenols from 8-hour time point, suggesting that recovery was in process. This could also imply that normal metabolic processes had resumed, and therefore there was decreased dependence on stress responsive secondary metabolites.

Rehydration-induced ultrastructural changes in chloroplasts included rapid re-assembly of thylakoid membranes and appearance of grana stacks in *X. elegans* tissues within the 1st hour after adding water. This fast recovery upon rehydration resembles *S. stapfianus,* another resurrection plant that retains its thylakoid membranes during drying (Vecchia et al., 1998). In contrast, chloroplasts in *X. schlechteri* seedlings were predominantly filled with vesicles, which persisted for 12 hours post-rehydration before being replaced by thylakoid membranes. This observation suggests a correlation between the appearance of thylakoid membranes and the disappearance of vesicles. Similar results were noted in a study on chloroplast biogenesis during rehydration in *X. humilis* (Ingle et al., 2008).

2.5 Conclusion

This study has demonstrated that the seedling model is a good model for studying the ultrastructural changes in cells and chloroplasts as leaves undergo desiccation and rehydration. The ultrastructural results obtained here suggest that *Xerophyta* seedlings employ mechanisms similar to those observed in the leaves of adult resurrection plants in response to desiccation. Furthermore, the detailed characterization of chloroplast ultrastructure in *X. elegans* and *X. schlechteri* seedlings was highly informative as it allowed us to observe both the rate and nature of these changes. An excellent example is the rapid accumulation of polyphenols and development of intact grana stacks in *X. elegans,* which happened within just one hour of rehydration. Overall, *X. elegans* retains thylakoid membranes in its chloroplasts during desiccation, allowing for rapid reassembly and resumption of photosynthesis upon rehydration. In contrast, *X. schlechteri* undergoes complete dismantling of thylakoid membranes during desiccation, resulting in a slower process of thylakoid reassembly upon rehydration.

CHAPTER 3

Comparison of the Transcriptome Response to Desiccation in Three *Xerophyta* Species at Two Stages of Seedling Development

3.1 Introduction

It has been noted that a number of genes involved in seed maturation are also up-regulated in desiccated leaf tissues of resurrection plants (Illing et al., 2005; Vanburen et al., 2015). This observation led to the hypothesis that there might be a common regulatory mechanism between orthodox seeds and vegetative tissues of resurrection plants (Illing et al., 2005; Oliver et al., 2000; VanBuren et al., 2017). Illing et al (2005) identified seed-specific LEA proteins and antioxidant enzymes as evidence to support this hypothesis. ABI3 and ABI5 were proposed to be involved in conferring DT in desiccating leaves of resurrection plants but there was little direct evidence to support this (Costa et al., 2017a; VanBuren et al., 2017). A study on *X. humilis* revealed that members of the LAFL network are indeed highly expressed during seed maturation stages but remain absent in the desiccating leaves of this species (Lyall et al., 2020). The absence of *ABI3* and *ABI5* in desiccating adult *X. humilis* leaves suggests that VDT in this plant did not result from the reactivation of the downstream effectors of the canonical LAFL regulatory network associated with seed development (Lyall et al., 2020). Instead of ABI3, ABFs were identified as candidate regulators of the ABI3 regulon in adult *X. humilis* leaves. This was due to the enrichment for ABRE motif in DE genes and protoplast assays that showed ABF1 can drive expression of several *X. humilis* desiccation responsive genes (Lyall et al., 2020).

It is well documented that DT is gradually lost as orthodox seeds germinate, reaching a critical 'point of no return' beyond which seedlings cannot withstand the effects of dehydration (Bewley et al., 2013). Notably, exposure to mild osmotic stress such as polyethylene glycol (PEG), can briefly extend the window in which germinating seedlings are DT (Buitink et al., 2003; Lyall et al., 2014). This exposure induces several physiological and molecular responses that help the seedlings cope with stress. The extent to which seedlings survive desiccation following PEG application does vary depending on the developmental stage. For example, in *A. thaliana*, DT was completely lost during early stages of seed germination, at radicle emergence, but could be fully restored to 100% post incubation in PEG (Maia et al., 2011). In another study, the re-induction of DT in PEG-treated *M. truncatula* seedlings with radicle

lengths of 2 and 3 mm was successful in all the former and in 72% of the latter. However, seeds with radicles measuring 4 mm or longer were unable to regain DT (Buitink et al., 2003).

The question is: are similar patterns observed in the seedlings of resurrection plants? It has been reported that early-stage *X. schlechteri* seedlings, which were incubated in the dark for 3 days prior to rapid drying, are sensitive to rapid desiccation, and only acquire DT at a later stage of development. However, their tolerance ability is improved when pre-treated with ABA (Costa et al., 2017b). In contrast, another study found that *X. viscosa* seedlings remain DT at all stages of seedling development (Lyall et al., 2014). *X. viscosa* seedlings at different developmental stages were subjected to rapid drying conditions in a laminar flow hood, in the presence and absence of PEG. Under these conditions, *X. viscosa* seedlings were fully DT at early seedling stages (cotyledon length < 0.1 mm). However, the survival rate decreased to 6% as the seedlings increased in size (cotyledon lengths of 1.6-2 mm) but rose again in larger seedlings (cotyledon length 3.4-5 mm). This dip in survival could be fully rescued by the pre-treatment of seedlings with PEG (Lyall et al., 2014). Similar observations were made in *X. humilis* seedlings at various developmental stages (Lyall, 2016). Unlike *A. thaliana* and *M. trancatula* seedlings, *Xerophyta* seedlings pre-treated with PEG remain DT under rapid drying conditions at all stages of seedling development. However, the variations in survival of untreated seedlings across developmental stages suggests potential differences in the regulation of desiccation response as *Xerophyta* seedlings transition from the early to later stages. These results indicate the possibility of a genetic switch in the regulation of DT as seedlings progress from an early to a late stage of development.

The switch from seed maturation to germination involves the suppression of *LAFL* genes and activation of genes related to vegetative growth (Tsukagoshi et al., 2007). An important regulatory mechanism in this process is histone 3 trimethylation at K27 (H3K27me3), which controls genes involved in plant development (Mozgova & Hennig, 2015). This epigenetic modification is mediated by the Polycomb Responsive Complex (PRC) 2, a crucial chromatin regulatory complex possessing histone 3 lysine 27 trymethylase activity that leads to the silencing of many maturation genes including the *LAFL* genes (Lepiniec et al., 2018; Mozgova & Hennig, 2015). In addition, PRC1-mediated ubiquitination at K119 of histone H2A contributes to the repression of the *LAFL* network seed genes during germination (Lepiniec et al., 2018), leading to the loss of DT ability during seedling development. To counteract these repressive mechanisms, ABI5 acts in concert with ABI3 to regulate post-germinative growth

arrest in *A. thaliana* and *Medicago trancatula* seedlings, enabling DT re-acquisition during early stages of seedling development. The significance of these TFs is underscored by the desiccation-sensitive phenotype observed in abi3 and abi5 mutants of *A. thaliana* and *M. trancatula* (Lopez-Molina et al., 2001; Terrasson et al., 2013).

This leads to the question of whether early-stage *Xerophyta* seedlings use the LAFL network to activate the desiccation protection programme, similar to *A. thaliana* and *M. trancatula*, and whether later in development, there is a switch over to a different set of TFs that activate the desiccation protection programme.

3.1.1 Aim and Objectives

The aims of the work presented in this chapter were to confirm that *Xerophyta* seedlings are desiccation tolerant, and to test the hypothesis that the desiccation response in the early (pre-leaf) stages of seedling development is under different transcriptional control compared to later (two-leaf) stage seedlings. Further, we aimed to identify the core conserved transcriptional regulators of desiccation, by using a three-way comparison of *X. elegans*, *X. schlechteri* and *X. humilis* seedlings at the early pre-leaf and late two-leaf stages of development.

The objectives were:

i. to perform genome size estimations of *Xerophyta* species including *X. elegans*, *X. schlechteri* and *X. humilis* using flow cytometry,
ii. to confirm that *Xerophyta* seedlings at the pre-leaf stage and two-leaf stage of development are fully desiccation tolerant,
iii. to perform comparative gene expression analysis of hydrated and desiccated seedlings of *X. elegans*, *X. schlechteri* and *X. humilis* species at the pre-leaf and two-leaf developmental stages using DESeq2,
iv. to compare the expression levels of seed maturation TFs in four tissues of *X. humilis* (seeds, pre-leaf and two-leaf seedlings, and adult leaves), and across the pre-leaf and two-leaf seedling stages of *X. elegans*, *X. schlechteri* and *X. humilis*, under both hydrated and desiccated conditions,
v. to identify gene orthogroups conserved among the three *Xerophyta* species, and
vi. to identify motifs enriched in protomer regions of differentially expressed genes in both early and late-stage seedlings across the three *Xerophyta* species.

3.2 Materials and Methods

3.2.1 Genome size estimation

3.2.1.1 Plant material

Adult *Xerophyta* plant leaves were used for nuclei extraction and estimate of genome size. *X. schlechteri* and *X. purpurascens* plants were collected from Buffelskloof Nature Reserve, Mpumalanga Province, South Africa (Permit MPB. 1394). *X. elegans* and *X. viscosa* from Drakensburg, KwaZulu Natal Province (Permit OP 3925/2019), and *X. humilis* from Borakalalo Nature Reserve, North West Province (Permit 062 NW-12). *Raphanus sativus* and *Solanum lycopersicum* seeds for the size standards in flow cytometry were obtained from Jaroslav Dolezel (Institute of Experimental Botany, Czech Republic). Plants were grown at a temperature of 25 °C under a 16-hour light and 8-hour dark cycle in the plant growth rooms of the Department of Molecular and Cell Biology (MCB), University of Cape Town.

3.2.1.2 Preparation of Nuclear Suspension Samples

Young, rapidly growing leaves from adult plants were harvested on the day of the experiment. Fresh plant leaf tissues (400-600 mg) were chopped up to a fine state with a sharp sterile razor blade in 1 mL of ice-cold Otto I [0.1 M citric acid, 0.5% (v/v) cell culture Tween 20] solution in a plastic petri dish. The homogenate was mixed and filtered through a Falcon 40 μm nylon cell strainer (Corning, Durham, USA) into a clean 1.5 mL microfuge tube. Isolated nuclei were then pelleted by centrifuging at 100 x g for 6 minutes. The supernatant was removed, leaving approximately 100 μL of the liquid above the pellet. An equivalent volume of fresh ice-cold Otto I solution was added, and samples were kept at 4 °C. Six biological replicates were prepared for each species.

3.2.1.3 Analysis of Nuclear DNA Content

Prior to the analysis, 800 μL of Otto II [0.2 M Na_2HPO_4 .$12H_2O$] solution was added to the resuspended nuclei, along with 50 μg mL^{-1} RNase A and 50 μg mL^{-1} of propidium iodide. The fluorescent intensity of the stained nuclei was measured on a flow cytometer (BD LRFortessa™, Becton, Dickinson and Company, USA). Samples were run at 400 V excitation voltage and viewed on a linear scale. A gate was used to filter out low signal strength noise and the position of the gate varied between samples. A histogram was plotted, and gates were drawn on G2 peaks. The mean values, obtained from the peaks, were used to calculate the average 2C nuclear DNA content of *Xerophyta* plants through the following formula:

$$\text{Sample 2C value (DNA pg)} = Reference\ 2C\ value\ x\ \frac{\text{sample 2C mean peak position}}{\text{reference 2C mean peak position}}$$

The DNA mass was converted from picograms to the number of base pairs as follows: 1 pg DNA = 0.978 x 10^9 bp.

3.2.2 Transcriptomic Analysis

3.2.2.1 Plant Material

This part of the study utilized *Xerophyta* seeds either collected from locations detailed in section 3.2.1.1, or from seeds sourced from mature plants grown in a greenhouse.

3.2.2.2 Seed Sterilization

Wild-collected *Xerophyta* seeds are highly contaminated with bacteria/fungi, and common sterilization techniques were insufficient to prevent the spread of contaminants after plating. The following sterilization procedure was employed. Firstly, seeds were placed into PCR tubes and heat treated at 65 °C for 2 hours on a GeneAmp PCR System (Applied Biosystems, Foster City, USA). Post heat treatment, *Xerophyta* seeds were transferred into 2 mL microfuge tubes and surface sterilized. The first sterilization step involved adding 500 µL of absolute ethanol to the seeds and vortexing for 10 seconds. Solution A [1 mL of 70% (v/v) ethanol + 1 µL/mL triton-x100] was added and vortexed for 20 seconds. This was then followed by washing the seeds for 1 minute with 1 mL distilled sterile water, alternating with solution C [water and triton-x100] 3 times. Post washing, solution B [15% hydrogen peroxide (H_2O_2) + Triton-x100] was added and the seeds were vortexed for 1 minute. Lastly, the seeds were washed 3 times with distilled sterile water for 1 minute and then transferred onto sterile filter paper on petri dish plates.

3.2.2.3 Seed Germination

Using sterile forceps, sterilized *Xerophyta* seeds were aseptically plated out onto half-strength MS plates [2.165 g/L Murashige and Skoog (MS) Basal medium with Gamborg's vitamins, 7 g/L bacteriological agar]. The plates were then sealed with parafilm and incubated at 23 °C under 16-hour light and 8-hour dark cycles in a plant growth chamber (Percival Scientific, Iowa, USA) to germinate and grow until seedlings reached either the pre-leaf (4-5 days post germination) or two-leaf stage of development (14-30 days post germination).

3.2.2.4 Seedling Survival Experiments

Xerophyta seedlings at early pre-leaf and late two-leaf stages of development were desiccated for 48 hours. Prior to inducing desiccation, 60 pre-leaf and 20 two-leaf seedlings were carefully transferred from MS agar media to a damp 90 mm Whatman grade 2 filter paper (GE Healthcare, Amersham Place Little Chalfont, UK) for 24 hours. Subsequently, desiccation was induced by transferring these seedlings onto a petri dish lid with a single wet (1 mL distilled water) 90 mm Whatman grade 5 filter qualitative paper. The wet filter paper and seedlings were placed into a transparent 15 L plastic storage box (41.5 cm (L) x 17 cm (H) x 29 cm (W)) fitted with a lid. In total, each storage box contained uncovered 8 petri dishes, each with either 60 pre-leaf stage or 20 two-leaf stage seedlings, and these were left to dry down in the Percival for 48 hours (Fig. 3.1b).

The viability of *Xerophyta* seedlings to recover from desiccation was assessed by rehydrating them and checking for re-initiation of growth. Rehydration was conducted as described in Section 2.2.1, except that here the seedlings rehydrated for 4 days before assessing seedling viability. Given the distinct morphologies and early development characteristics of the three *Xerophyta* species, seedling survival criteria were established based on unique germination stages for each species. For early-stage seedlings, survival was determined by specific features such as cotyledon elongation and root development in *X. humilis*, and the emergence of the first leaf in *X. elegans* and *X. schlechteri*. In late-stage seedlings, recovery was marked by changes in leaf colour from yellow (*X. schlechteri* and *X. humilis*) or dark purple (*X. elegans*) to green, leaf opening, root elongation, and sustained growth.

3.2.2.5 Comparative Transcriptomics

Matched datasets for RNA-Seq and lipid/metabolite in fully hydrated and desiccated seedlings (pre-leaf and two-leaf stage) were generated (Fig. 3.1), however, the lipid/metabolite data are presented in Chapter 4. Seedlings were pre-plated on a damp filter paper overnight as described above before sampling the hydrated state and starting the desiccation cycle. After the drying down period of 48 hours, seedlings were flash frozen in liquid nitrogen and stored at -80 °C until use for RNA and lipid/metabolite extractions. For RNA-Seq analysis, three biological repeats per hydration/developmental stage combination were generated for each of the three *Xerophyta* species.

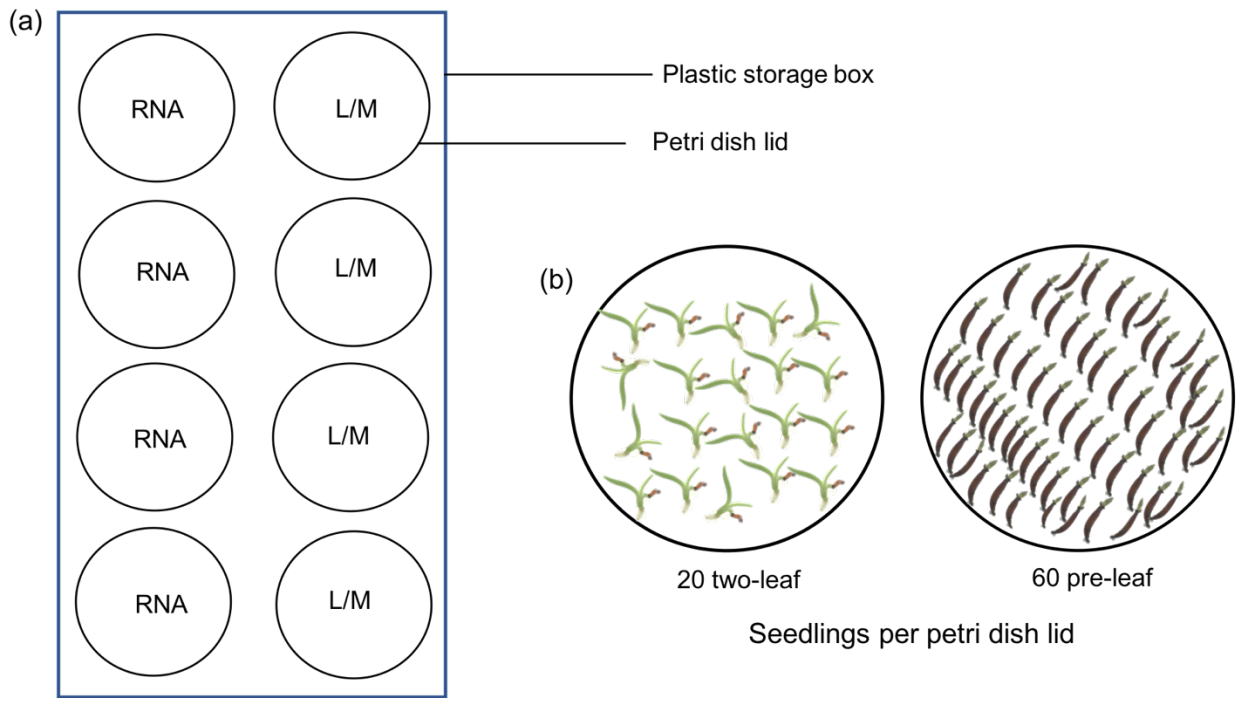

Figure 3.1. Experimental setup illustrating how the seedlings were dried down to generate matched datasets for RNA-Seq and lipid/metabolite analyses. Each plate contained 20 two-leaf seedlings and 60 pre-leaf seedlings for both RNA and lipid/metabolite (L/M) samples.

3.2.2.6 RNA Extraction from *Xerophyta* Seedlings

Two different protocols were used to extract RNA from early and late-stage seedlings, namely, Footitt and TRIzol/Zymo-Spin methods. The TRIzol/Zymo-Spin extraction method worked well for two-leaf seedlings, however, it produced extremely low RNA yields from pre-leaf seedlings. This is presumably due to the high polyphenols and polysaccharides content found in seeds, which interferes with the quality of RNA yielded. For this reason, a method adapted from Footitt et al. (2018) was used for extracting RNA in early seedlings.

3.2.2.7 RNA Extraction from Two-leaf Seedlings using a Modified TRIzol/Zymo-Spin Method

A total volume of 400 µL RNA extraction buffer [50 mM TRIS pH8, 150 mM LiCl, 5 mM EDTA pH 8, 1% (w/v) SDS] was added to each tube, and frozen two-leaf samples were crushed with autoclaved plastic pestles until a homogenized mixture was formed, and then vortexed for 2 minutes. This was followed by adding 400 µL phenol (pH4): chloroform:isoamyl alcohol (25:24:1) mixture, vortexing for 5 seconds and incubating on ice for 5 minutes before centrifuging for 12 minutes at 12, 000 x g at 4 °C. Thereafter, 400 µL of the supernatant was

transferred into a new microfuge tube containing 500 µL of TRIzol (Zymo research). Samples were vortexed and incubated at room temperature for 5 minutes, before purifying on Zymo-Spin columns (Zymo research, California, USA). The purification, DNase treatment, wash steps and elution steps were performed according to the manufacturer's instructions. The concentration of total RNA extracted was determined using a Nano-Drop ND 1000 spectrophotometer.

3.2.2.8 RNA Extraction from Pre-leaf Seedlings using the Footitt Method

RNA from early-stage seedlings was extracted using the protocol outlined in Footitt et al. (2018), with the following modifications. Contaminating DNA was removed by adding 80 µL of DNase I cocktail (Zymo Research) [5 L DNase I (6 U/µL) and 75 µL DNA digestion buffer] to the RNA pellet and incubated at room temperature for 15 minutes. Post incubation, centrifugation at 12 000 x g was carried out and the supernatant was discarded before washing the pellet in 75% ethanol and centrifuging for 10 minutes. The pellet was air dried for 10 minutes and re-dissolved in 50 µL nuclease-free water.

3.2.2.9 RNA Agarose Gel Electrophoresis

RNA integrity was determined by gel electrophoresis. A 1.2% (w/v) RNA agarose gel was prepared in 1x MOPS buffer pH7 [0.2 M MOPS, 0.05 M sodium acetate, 0.001 M EDTA] and 18.3% (v/v) formaldehyde. RNA samples were prepared by adding 2x volume of RNA sample loading buffer [63.7% (v/v) formamide, 22.3% (v/v) formaldehyde, 12.7% (v/v) MOPS, 10 mg/mL ethidium bromide] to 2 µg of RNA and heating at 55 °C for 5 minutes. The mixture was then loaded onto the RNA agarose gel and electrophoresed in 1x MOPS running buffer before visualisation.

3.2.2.10 Library Construction, Sequencing, and Quality Checks

RNA samples were sent to the Beijing Genomic Institution (BGI) group in China for library sequencing. Prior to shipment, the samples were applied to GenTegra-RNA stable tubes according to the manufacturer's instructions. The sequencing library was prepared by BGI using the DNBSEQ^{TM} Eukaryotic Strand-specific mRNA kit. The resulting raw 150 bp paired-end reads were filtered by removing adaptor sequences, contamination, and low-quality reads from raw reads. This yielded clean RNA reads which were then uploaded on the BGI FTP server. Sequencing quality was checked by FastQC and visualized with MultiQC.

3.2.2.11 RNA Read Mapping and Read Counts

The STAR alignment tool was used to align RNA-Seq reads for all three species to their respective genomes; *X. elegans* v1*, X. schlechteri* v2, and *X. humilis* v13B (assembled and annotated by Eugene Kabwe, University of Cape Town). Read counts per gene were determined using featureCounts which counted against annotated gene regions in the reference genome. Genome annotation files, generated via BREAKER2, included all gene features such as introns, exons, and coding sequences. Previously generated RNA-Seq datasets (SRA, NCBI BioProject ID PRJNA505754) derived from *X. humilis* seed maturation stages (early, mid, dry) and *X. humilis* desiccating leaf series (100, 80, 60, 40, 5% RWC; Lyall et al., 2020), along with *X. humilis* early and late seedlings under hydrated and dehydrated conditions, were all mapped to version 13B (Eugene Kabwe, University of Cape Town) of the assembled *X. humilis* genome for comparative analysis.

3.2.2.12 Differential Gene Expression Analysis

The differential gene expression analysis was performed using the DESeq2 package for R (version 1.38.3; Love et al., 2014). Genes with low expression, <10 counts across 3 replicates, were removed from the analysis. DE genes were defined as those with an absolute log fold change (LFC) > 1 between the tested conditions (dehydrated vs hydrated), i.e. s-value < 0.005 as defined by DESeq2 lfcThreshold.

3.2.2.13 Orthogroup Analysis

To allow cross species comparison of gene expression, a 'master file' encompassing orthologous gene groups (orthogroups) shared between *X. elegans*, *X. schlechteri*, *X. humilis*, *A. thaliana*, and other angiosperms was generated using OrthoFinder (Emms & Kelly, 2019), adjusting the predicted protein sequences of each species. Given the focus on *X. elegans*, *X. schlechteri*, and *X. humilis* species, a filtering step was applied to the master orthogroup (OG) file, retaining OGs that contain genes present in any of the three *Xerophyta* species (Fig. 3.2).

Starting with the master OG file, orthogroups were filtered based on the following process:

1. OGs not found in all three *Xerophyta* species were discarded
2. Similarly, shared OGs that did not contain a DE gene in all three species were discarded
3. OGs were divided into three groups, based on the expression of DE genes in that group:
   (a) all DE genes in the three species that were up-regulated
   (b) all DE genes in the three species that were down-regulated

(c) OGs that contained both up- and down-regulated DE genes (for this purpose, non-DE genes are discarded)

4. Only OGs with shared DE gene expression profiles (all up- or all down-regulated) were retained for the final analysis.

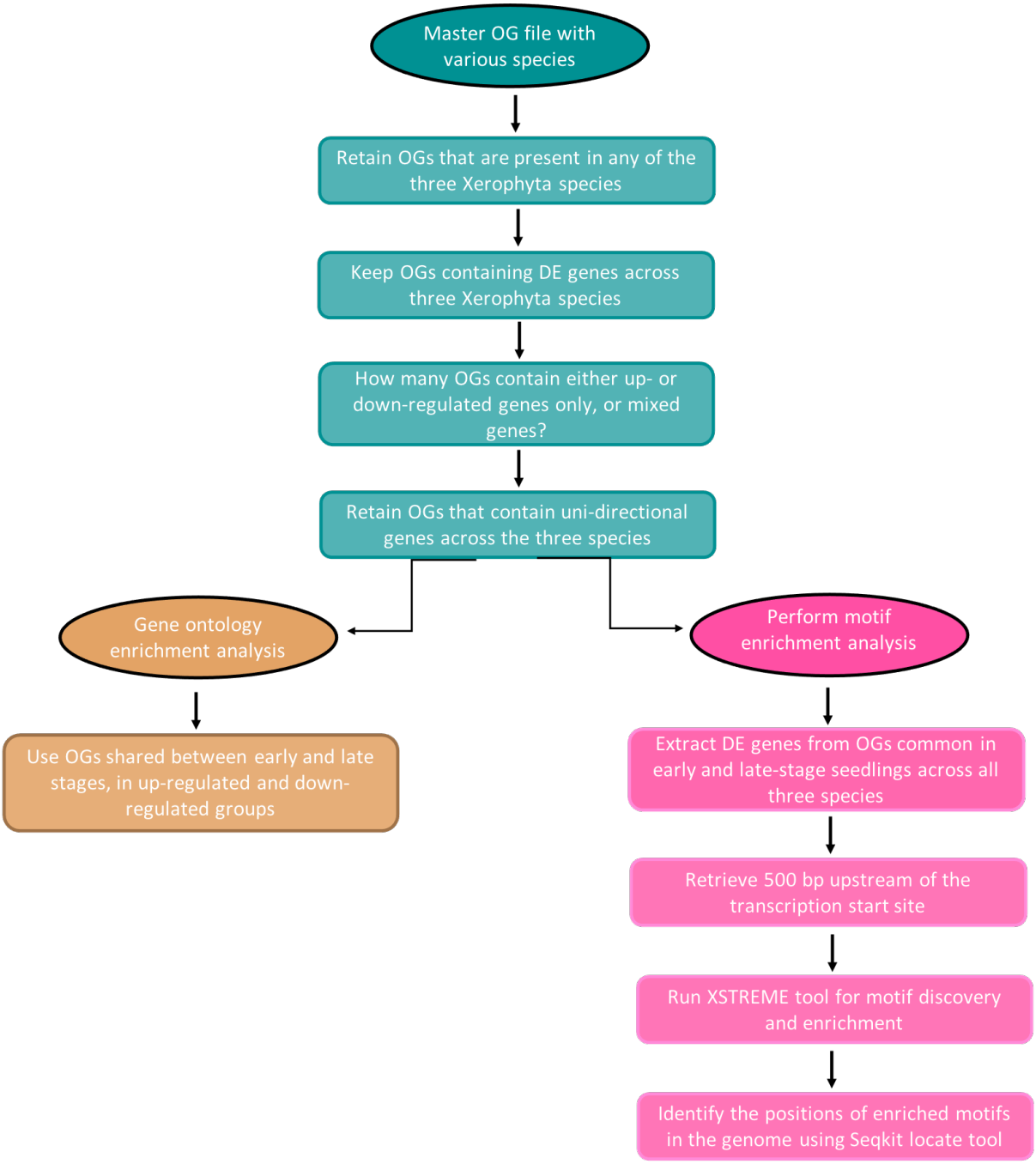

Figure 3.2. Orthogroup analysis workflow. Gene ontology and motif enrichment analyses were conducted using ViSEAGO and XSTREME tools, respectively.

3.2.2.14 Gene Ontology Enrichment

Gene Ontology (GO) enrichment analysis was performed using the wordcloud, treemap, and Visualization, Semantic Similarity, and Enrichment Analysis of Gene Ontology (ViSEAGO) for R (version 1.38.3). The analysis aimed to identify enriched GO terms associated with both up-regulated and down-regulated genes, as well as OGs at early and late-stage seedlings across all three *Xerophyta* species, specifically focusing on the Biological Process category. For OG level analysis, all gene members of an orthogroup for each species were taken, and their corresponding GO terms were retrieved from the annotation files. The Fisher's exact test with the weight01 algorithm was employed. Additionally, GO terms were clustered based on their semantic similarity to provide a more comprehensive understanding of functional relationships. This means that terms describing similar biological functions, processes, or components are clustered together, providing a clearer view of the functional relationships between genes. To define the gene background, all expressed genes were considered, excluding those with low expression counts <10 across three replicates.

3.2.2.15 Promoter Motif Enrichment Analysis

To explore the regulation of desiccation response during early and late seedling stages, motif enrichment analysis was performed (Fig. 3.2). Firstly, up-regulated and down-regulated genes for *X. elegans*, *X. schlechteri* and *X. humilis* were extracted from the OGs shared between the early and late seedling stages. Next, 500 bp regions upstream of the known transcriptional start sites were retrieved for both up- and down-regulated genes. For the background, all expressed genes were used, excluding those with low expression counts <10 across three replicates. Subsequently, sequence motifs were identified using the XSTREME tool (version 5.5.5), which employs the Multiple EM for Motif Elicitation (MEME) and Sensitive, Thorough, Rapid Enriched Motif Elicitation (STREME) algorithms to discover novel sequence motifs in the input sequences of interest (Grant & Bailey, 2021). This was followed by employing a motif enrichment analysis algorithm called Simple Enrichment Analysis (SEA) to detect the enrichment of previously characterized functional motifs, and to rank the enrichment of discovered and known motifs, from the JASPAR core 2024 plants database, on the same scale. Motifs with an e-value cut-off of 0.05 ($e \leq 0.05$) were considered enriched. In the final step of XSTREME, enriched motifs were grouped based on their similarity using a clustering algorithm. XSTREME performed this clustering at the level of each overlap (species and expression direction), which limited the ability to compare clusters between groups. To address

this, the same hierarchical clustering algorithm used by XSTREME was used to cluster the motifs identified across species.

Finally, the positions of enriched motifs in the genome were identified using the Seqkit locate tool and the motif consensus sequence. To speed up the Seqkit locate search process, the genomes of each *Xerophyta* species were hard masked, replacing all nucleotides with "N", except for the regions containing promoters of interest. Gene IDs, and motif clusters were included in the final BED file output to enable easy access to more information about the enriched motifs of interest.

3.3 Results

3.3.1 Estimation of Genome Sizes for Five *Xerophyta* Species

Several genome size estimates have been previously documented for *Xerophyta* species in the literature. For instance, *X. humilis,* with a genome size of 523 Mbp (Hanson et al., 2001), and *X. schlechteri* (incorrectly referred to as *X. viscosa*) by the authors, which has a genome size of 295.5 Mb (Costa et al., 2017b). Despite the reported genome size of *X. schlechteri* being 295.5 Mb, as identified through k-mer analysis of PacBio data, the authors stated that the genome is octoploid. However, if this was indeed the case, the predicted 1C genome size of 295.5 Mb would be ~1.2 Gb (4 x 295.5 Mb), which contradicts the observed size. In light of this discrepancy and recognizing the importance of a good assembly of plant genomes for RNA-Seq, we used FACS analysis to measure the genome size (1C value) of five *Xerophyta* species as a first step towards this direction.

In the flow cytometry experiments performed here, *X. schlechteri* had the smallest estimate genome size of 191.30 Mbp, followed by *X. viscosa* at 277.80 Mbp, and *X. elegans* at 395.50 Mbp (Fig. 3.3). Notably, the genome size of *X. humilis* was estimated at 883.10 Mbp through FACS analysis and at 745.25 Mb via k-mer prediction (Eugene Kabwe, University of Cape Town), exceeding the previously reported genome size (1C) of 523 Mbp for *X. humilis* by more than 200 Mbp (Hanson et al., 2001). The variation in the predicted genome sizes could be attributed to the geographical location of the *X. humilis* plants used in these two studies. Samples used in the current study were collected from Borakalalo Nature Reserve, North West Province, South Africa, while those from the previously reported *X. humilis* genome were obtained from the central District of Botswana (22°00'S 26°00'E). The observed difference

suggests the possibility of a duplication event in the population from South Africa. Finally, *X. purpurascens* had the largest genome, measuring 1234 Mbp.

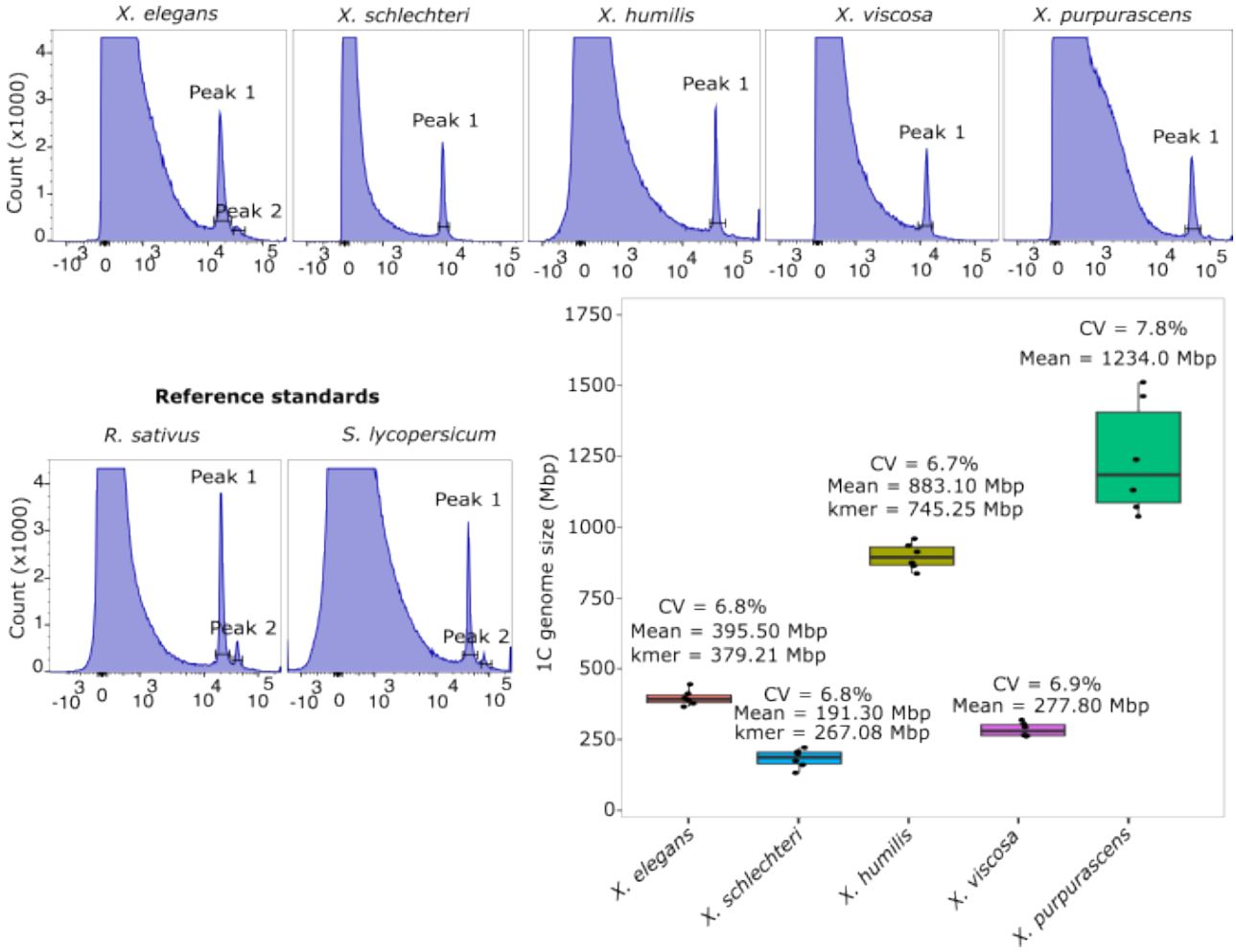

Figure 3.3. Genome size estimates for *Xerophyta* species using flow cytometry. *Raphanus sativus* was used as the reference standard for the smaller genome size species: *Xerophyta elegans*, *Xerophyta schlechteri* and *Xerophyta viscosa*, while *Solanum lycopersicum* served as a reference standard for the larger genome species *Xerophyta humilis* and *Xerophyta purpurascens*. Peaks 1 and 2 in the plots represent G1 and G2 phases of the cell cycle, respectively. The box plots show a summary of means and coefficient of variations (CV) for all *Xerophyta* leaves from six biological repeats (n = 6).

3.3.2 Survival of Early and Late-stage Seedlings to Desiccation

Seedling survival experiments were conducted to confirm that *Xerophyta* seedlings are indeed desiccation tolerant, at early and late seedling stages. Contrary to previous reports stating that *X. schlechteri* seedlings are not DT, both early-stage *X. schlechteri* seedlings and late-stage seedlings, survived desiccation under slow drying conditions in the growth chamber (Fig. 3.4). The study was extended to two other *Xerophyta* species, *X. elegans* which has similar

developmental processes, but is homoiochlorophyllous, and *X. humilis*, which is more similar to *X. viscosa* (Lyall et al., 2014) in its stages of germination. Early-stage seedlings were consistently more tolerant (95-100% survival rate) than later stage seedlings (80% survival rate; Fig. 3.4b). Poikilochlorophyllous *X. schlechteri* and *X. humilis* seedlings were similar to adult plants, and broke down their chlorophyll during desiccation, while *X. elegans* seedlings retained their chlorophyll. Upon rewatering, the seedling leaves and roots returned to full stage of turgor and resumed growth (Fig. 3.4a). These results are congruent with the survival of *X. viscosa* seedlings in response to drying, which despite having a dip in the survival rate, their window of DT remained open (Lyall et al., 2014), suggesting their DT ability across various developmental stages.

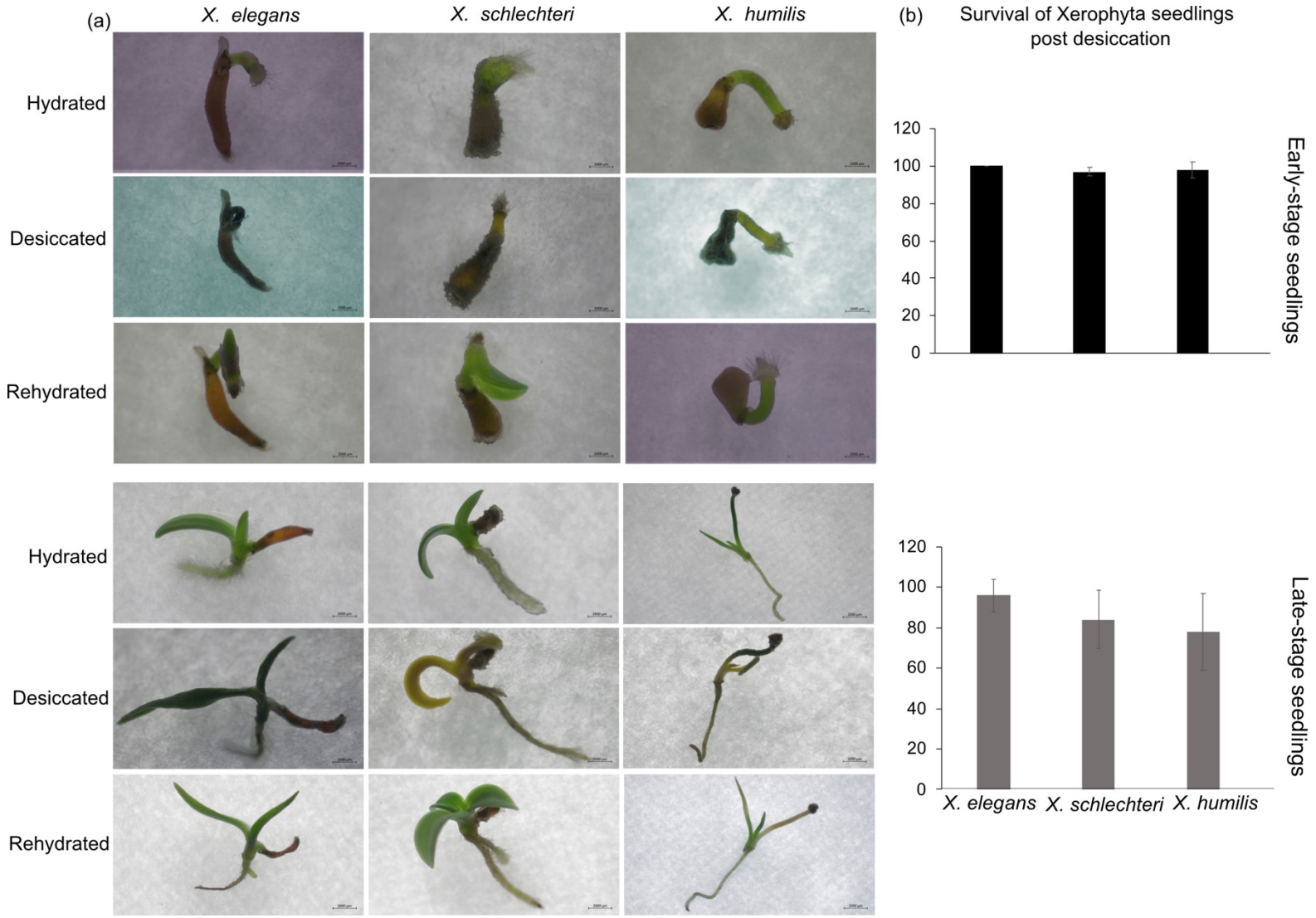

Figure 3.4. The recovery of early and late-stage *Xerophyta* seedlings from desiccation (a) Panels show seedlings prior to dehydration, after 48 hours of dehydration, and after 4-days of rehydration. (b) Graphs depicting the survival of *Xerophyta* seeds at early and late stages (n = 3).

3.3.3 Gene Expression Analysis in *X. humilis* Tissues

Previous work had identified that the LAFL network of TFs was expressed during seed maturation in *X. humilis*, but not during desiccation of adult leaves (Lyall et al., 2020). This previous study made use of a TRINITY *de novo* assembly of RNA-Seq data to quantify read counts as an assembled genome was not available (Lyall et al., 2020). We mapped these RNA-Seq reads to the newly assembled *X. humilis* genome (v13B) so that the maturing seeds, early and late seedlings, and adult leaves could be directly compared in a single analysis. It has been hypothesized by several authors (Costa et al., 2017a; Illing et al., 2005; Oliver et al., 2000; VanBuren et al., 2017) that adult VDT evolved from a reactivation of the seedling desiccation programme. It was thus of interest to use a PCA analysis to directly compare how similar the transcriptomes of maturing seed, developing seedlings and adult leaves undergoing desiccation are.

Figure 3.5 shows a clear distinction between hydrated and desiccated tissues across all samples. In PC1, there is a trend by which samples are separated by tissue type, with seed samples on the right, adjacent to the seedlings, and leaf samples on the left (Fig. 3.5). Further separation by the state of desiccation is observed in PC2, with desiccated leaves, seedlings, and mature seeds in the top half of the PCA plot, and hydrated samples in the bottom. Essentially, maturating seeds are more similar to seedlings at early developmental stages, while late-stage seedlings are more like adult leaves.

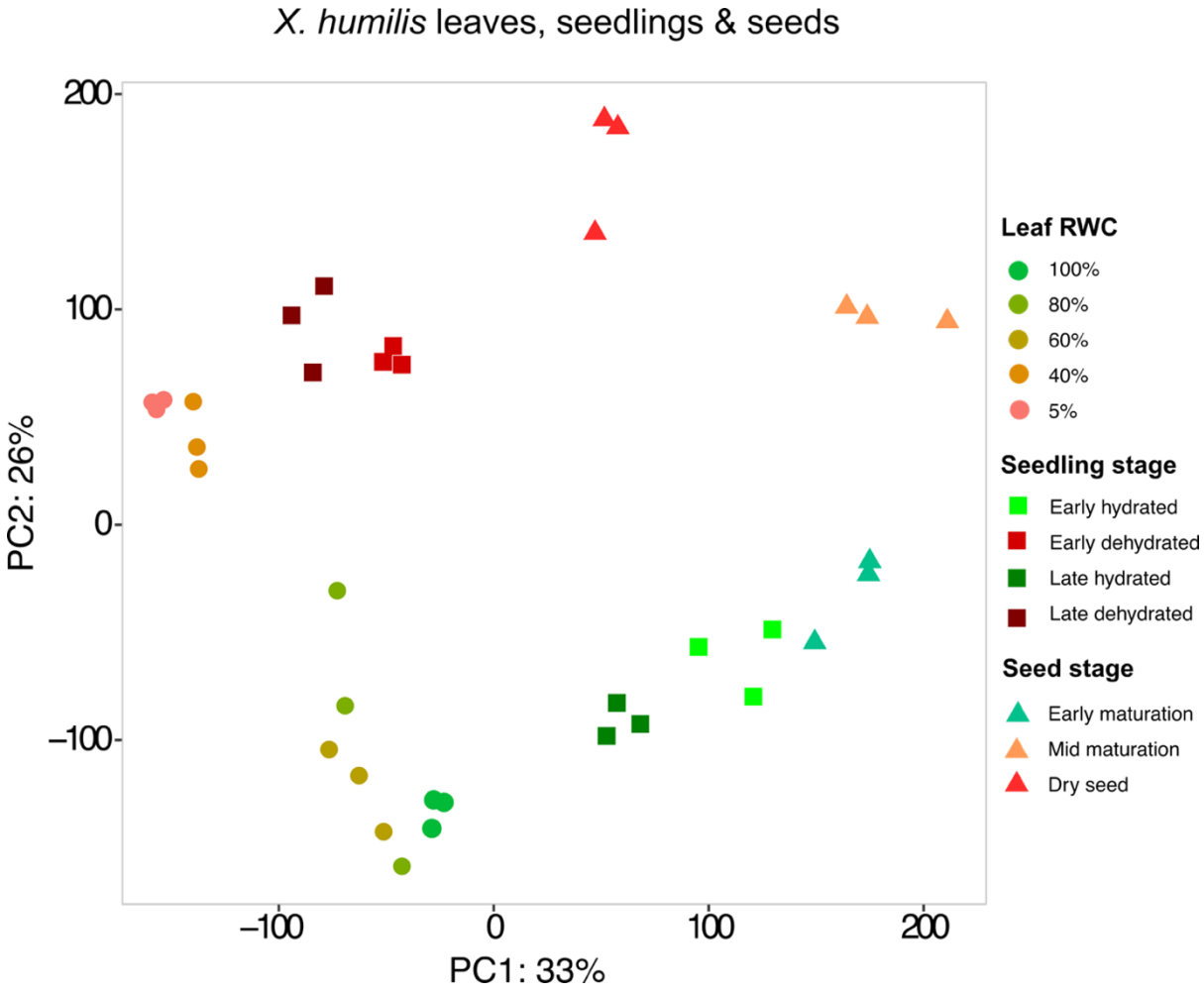

Figure 3.5. PCA score plots showing gene counts from *Xerophyta humilis* tissues transformed by DESeq2 variance-stabilizing transformation at different developmental stages and conditions. Triangles, squares and circles represent three biological repeats for maturing seeds, hydrated and dehydrated seedlings, and desiccating *Xerophyta humilis* leaves, respectively. Hydrated tissues are shown by different shades of green and the orange-maroon colour gradient indicates dehydrating/desiccated samples. The PCA plot was generated from all gene counts in each tissue type.

3.3.4 The Expression of the *LAFL* network genes, *ABI5* and *ABFs* in *X. humilis*

A key question is whether *Xerophyta* seedlings at early stages of development activate the desiccation protection program via the LAFL network, and whether there is a switch in the transcriptional regulatory activators as seedlings mature. Because we have a comprehensive transcriptomic data for *X. humilis*, encompassing seeds, pre-leaf seedlings, two-leaf seedlings, and adult leaves, we directly compared the expression of the LAFL network genes, and two members of the bZIP genes family: *ABI5* and *ABF* in all these tissues. Before performing this analysis, it was imperative to examine the relationship between orthologous genes from the B3 and bZIP families across the three *Xerophyta* species, as well in other model species such as

A. thaliana, *Oryza sativa* and *Sellaginella moellendorfii.* This examination was crucial to understand the evolutionary conservation and functional diversification of these gene families.

The majority of the LAFL network members, including ABI3, FUS3 and LEC2, are part of the B3 TF family, which is characterised by the B3 DNA binding domain, except for LEC1, which belongs to the NFY family (Fig. 3.7). Unlike *A. thaliana*, *O. sativa* and *S. moellendorfii*, which possess a single copy of ABI3, all three *Xerophyta* species have four copies of ABI3 (Fig. 3.6); *ABI3A*, *ABI3B*, *ABI3C* and *ABI3D,* indicating an expansion of this gene family in *Xerophyta*. However*, ABI3A* is the only paralogue containing full-length B3 DNA-binding domain, and the other three completely lack the B3 domain due to the presence of a premature stop codon (Lyall et al., 2020). As such, only *XhABI3A* could be considered analogous to the canonical LAFL *ABI3* gene found in other plants. Additionally, the bZIP members consist of 2 copies of ABI5, and 4 copies of ABF (*ABFA* - *ABFD*), orthologous to *AtABF1* - *ABF4,* respectively (Fig. 3.8).

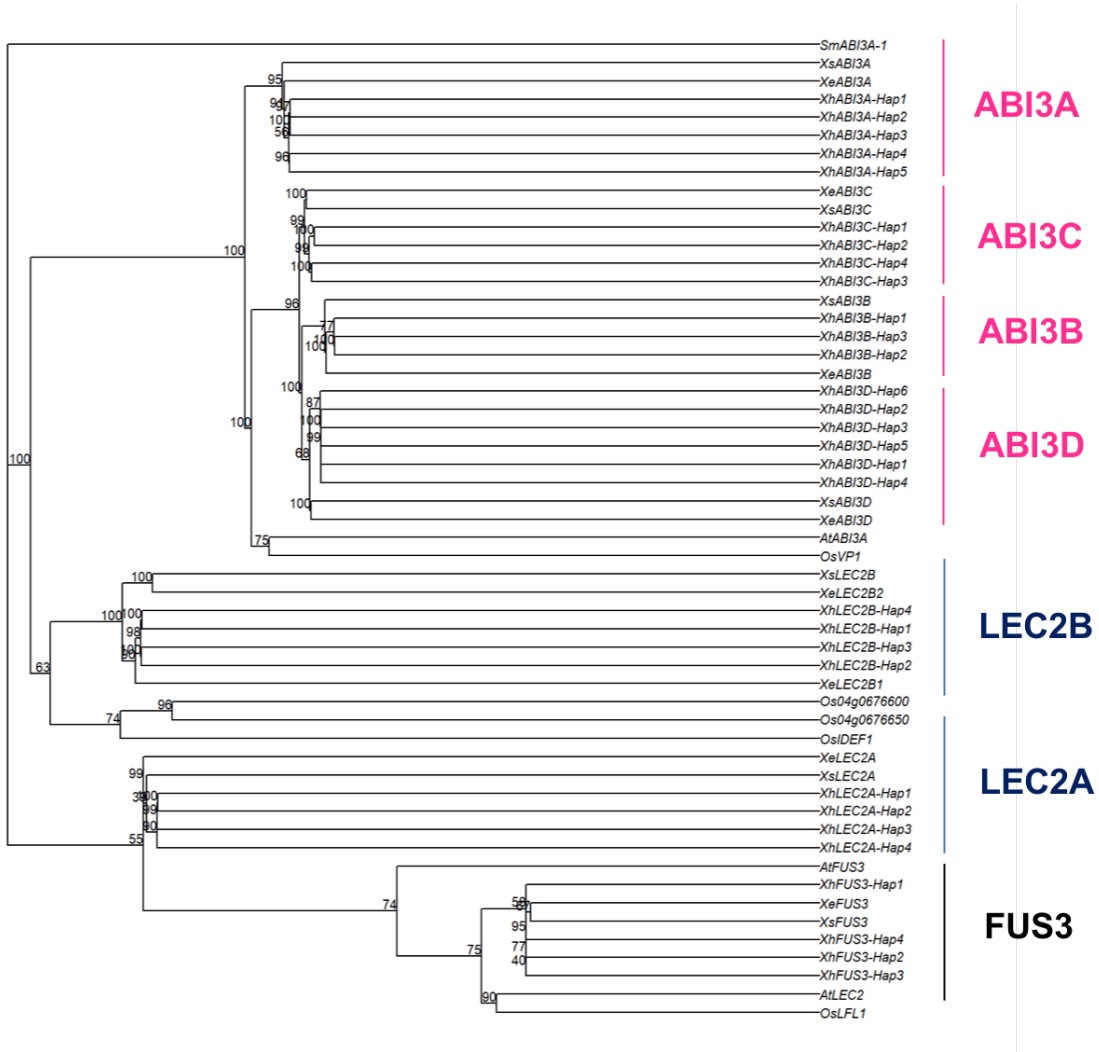

Figure 3.6. A phylogenetic tree depicting members of the B3 transcription factor family. Three members of the LAFL network; ABI3, LEC2 and FUS3 from *X. humilis*, *X. elegans*, *X. schlechteri*, *A. thaliana*, *O. sativa* and *S. moellendorfii* are displayed. The iqtree2 tool was used to generate trees using maximum likelihood and a bootstrap of 1000. The Hap in *X. humilis* stands for haploid.

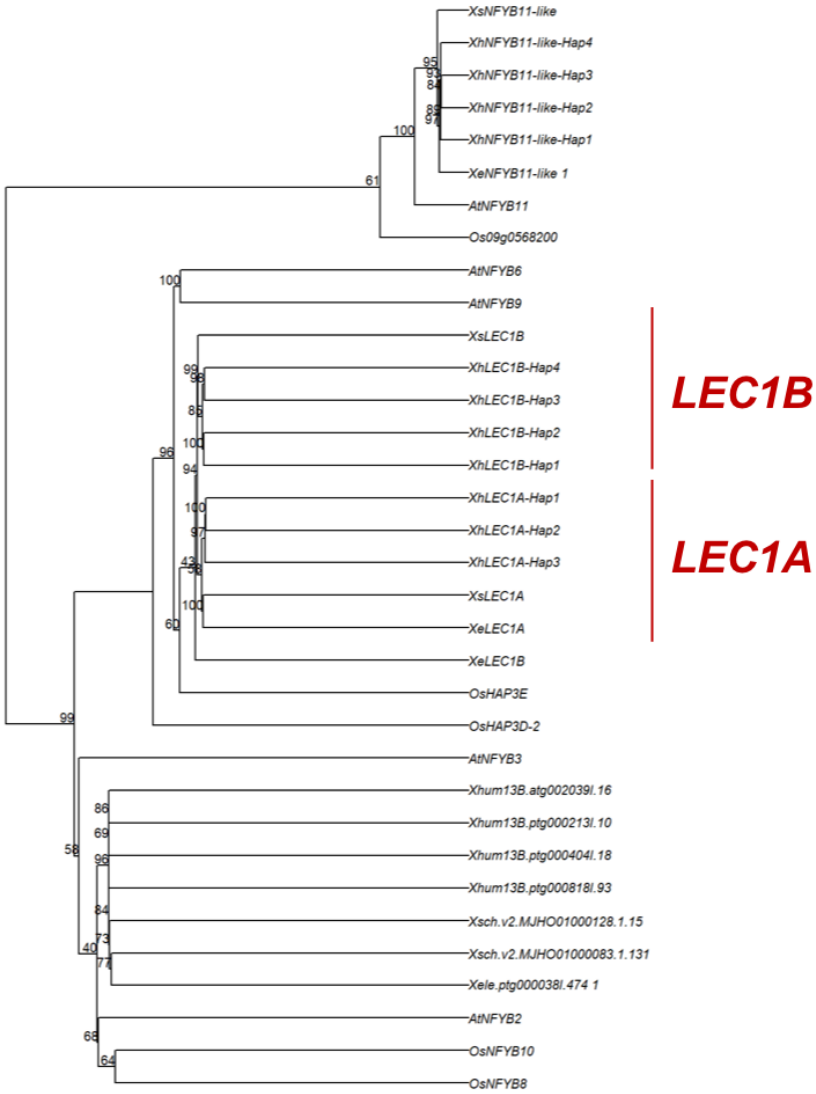

Figure 3.7 A phylogenetic tree showing LEC1 from the NFY family. The iqtree2 tool was used to generate trees using maximum likelihood and a bootstrap of 1000.

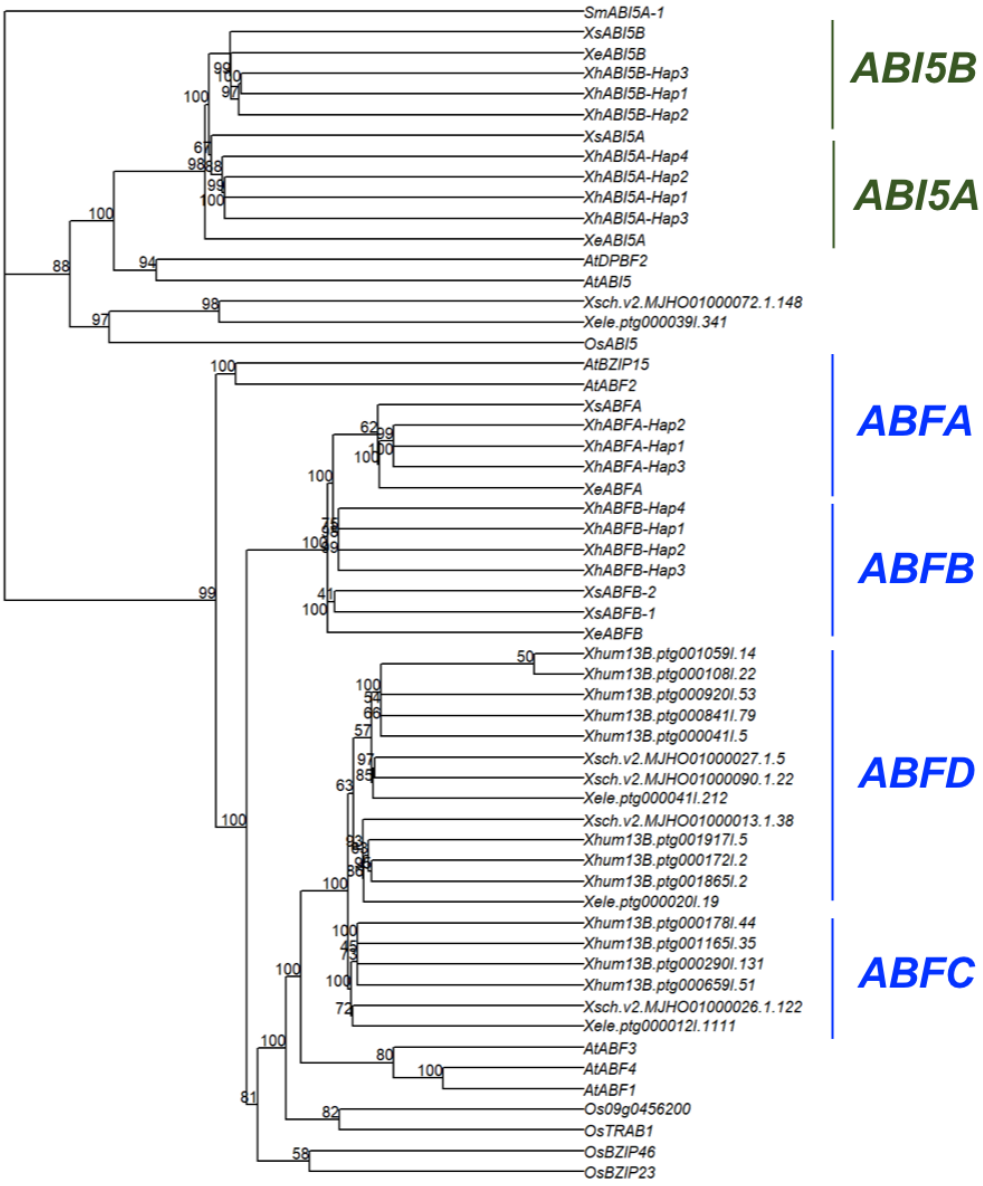

Figure 3.8. A phylogenetic tree showing ABI5 and ABF group A members from the bZIP family. The relationship between orthologous genes from two members of the group A bZIP family from various species is shown. The iqtree2 tool was used to generate trees using maximum likelihood and a bootstrap of 1000.

As previously reported, both genes of *XhLEC1* and *XhLEC2* are expressed during the early and mid-maturation stages of seed development in *X. humilis*, but not during the late seed maturation nor during any stage of adult leaf dehydration (Lyall et al., 2020). The expression of LEC1, LEC2 and FUS3 during the growth phase of embryonic development have been shown to play an important role in the regulation of growth arrest, which precedes seed maturation (Raz et al., 2001). It is therefore not surprising that neither *XhLEC1* or *XhLEC2*

were detectable in hydrated or dehydrated early or late seedlings (Fig. 3.9a-d). The expression of *XhFUS3* was also high during the mid-maturation stage of seed development but was expressed at low levels in mature seed. Expression in hydrated and dry early-stage *X. humilis* seedlings was negligible (Fig. 3.9e).

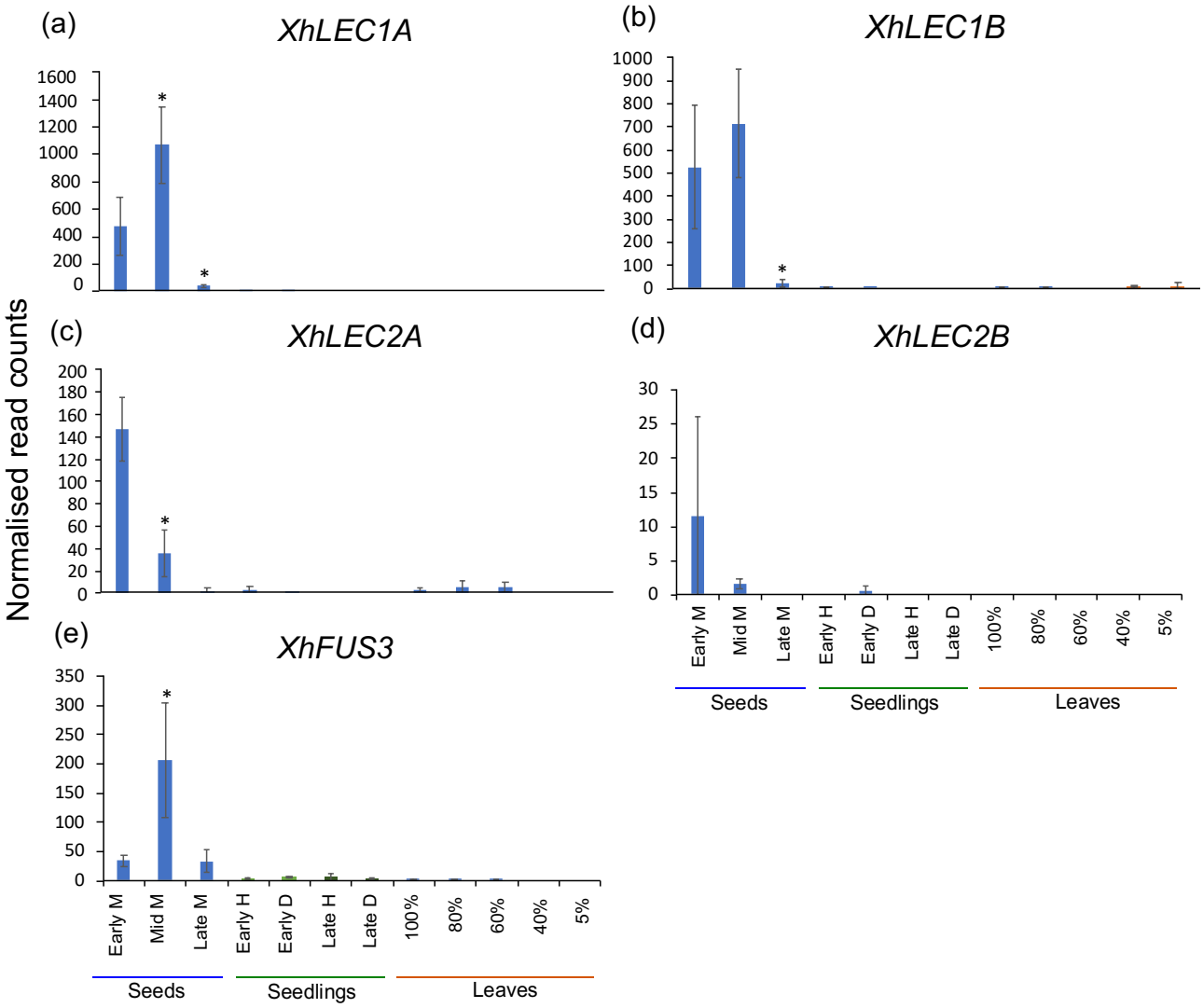

Figure 3.9. Expression of *LEC1, LEC2* and *FUS3* genes in *Xerophyta humilis* tissues. DESeq2-normalised counts of *X. humilis* seed regulators during seed maturation (blue), seedling development (light/dark green) and vegetative desiccation tolerance (orange). The M, H and D symbols denote maturation, hydrated, and dehydrated, respectively. Percentages (%) in leaf samples represent RWC values. Error bars are standard deviation (n = 3). Significance was tested against the hydrated sample in each condition (early seed, hydrated seedling, 100% RWC leaf) using DESeq2 at LFC > 1, s-value < 0.005. Asterisks (*) indicate significant differences at s < 0.005.

XhABI3 is up-regulated in dry seeds and dry pre-leaf seedlings (Fig. 3.10a). Interestingly, the truncated *XhABI3B* transcript is expressed at all developmental stages and is induced in response to dehydration (Fig. 3.10b). *XhABI3D* is also expressed in hydrated tissues at all developmental stages but is repressed in response to dehydration. Notably, the expression levels of *XhABI3C* and *XhABI3D* are 10x lower than for *XhABI3A* and *XhABI3B*.

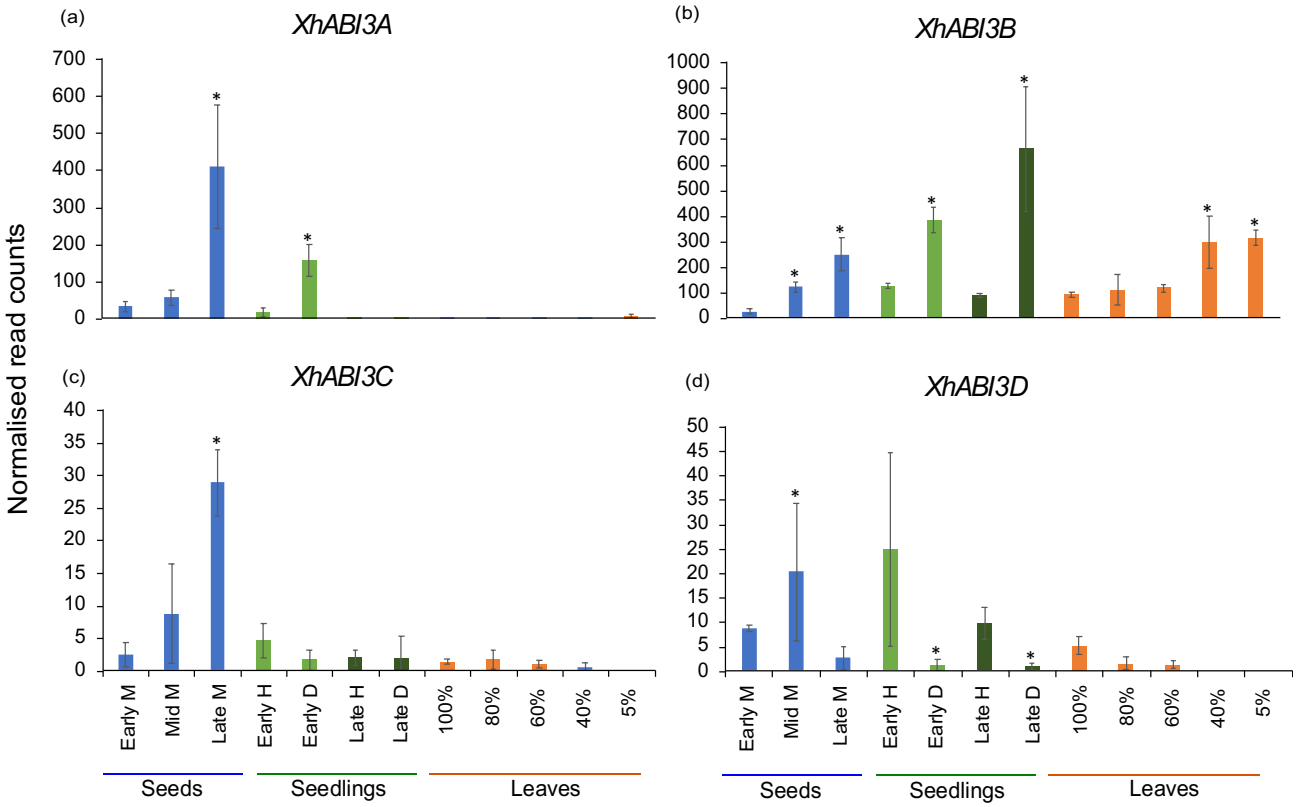

Figure 3.10. Expression of *XhABI3* genes in *Xerophyta humilis* tissues. DESeq2-normalised counts of *X. humilis* seed regulators during seed maturation (blue), seedling development (light/dark green) and vegetative desiccation tolerance (orange). The M, H and D symbols denote maturation, hydrated, and dehydrated, respectively. Percentages (%) in leaf samples represent RWC values. Error bars are standard deviation (n = 3). Significance was tested against the hydrated sample in each condition (early seed, hydrated seedling, 100% RWC leaf) using DESeq2 at LFC > 1, s-value < 0.005. Asterisks (*) indicate significant differences at s < 0.005.

The ABI5 TF often acts in concert with ABI3 to regulate post-germinative growth arrest in *Arabidopsis* and *Medicago* seedlings, facilitating the acquisition of DT during early stages of seedling development (Lopez-Molina et al., 2001; Terrasson et al., 2013). *XhABI5A* was constitutively expressed at elevated levels in early-stage seedlings, and there was no significant difference between hydrated and desiccated seedlings. However, it was barely expressed in

late-stage seedlings or adult leaves (Fig. 3.11a). *XhABI5B*, was expressed across all conditions but only responsive to desiccation (down-regulated) in early and late-stage seedlings (Fig. 3.11b). However, the transcript counts were much lower than *XhABI5A*. Another member of the group A bZIP TFs, *XhABFA*, had increased expression patterns in dry seeds, and was significantly induced by desiccation in early- and late-stage seedlings and leaves (Fig. 3.11c). Two other transcripts, *XhABFB* and *XhABFC* showed similar expressions but were not induced by desiccation in leaves (Fig. 3.11d-e). In addition, *XhABFD* and *XhABFE* were desiccation induced at all developmental stages (Fig. 3.11 f-g). However, in adult leaf tissues, their expression levels were the highest when RWC was 40%. Although their expression declined at 5% RWC, it remained higher compared to the hydrated state (Fig. 3.11 g).

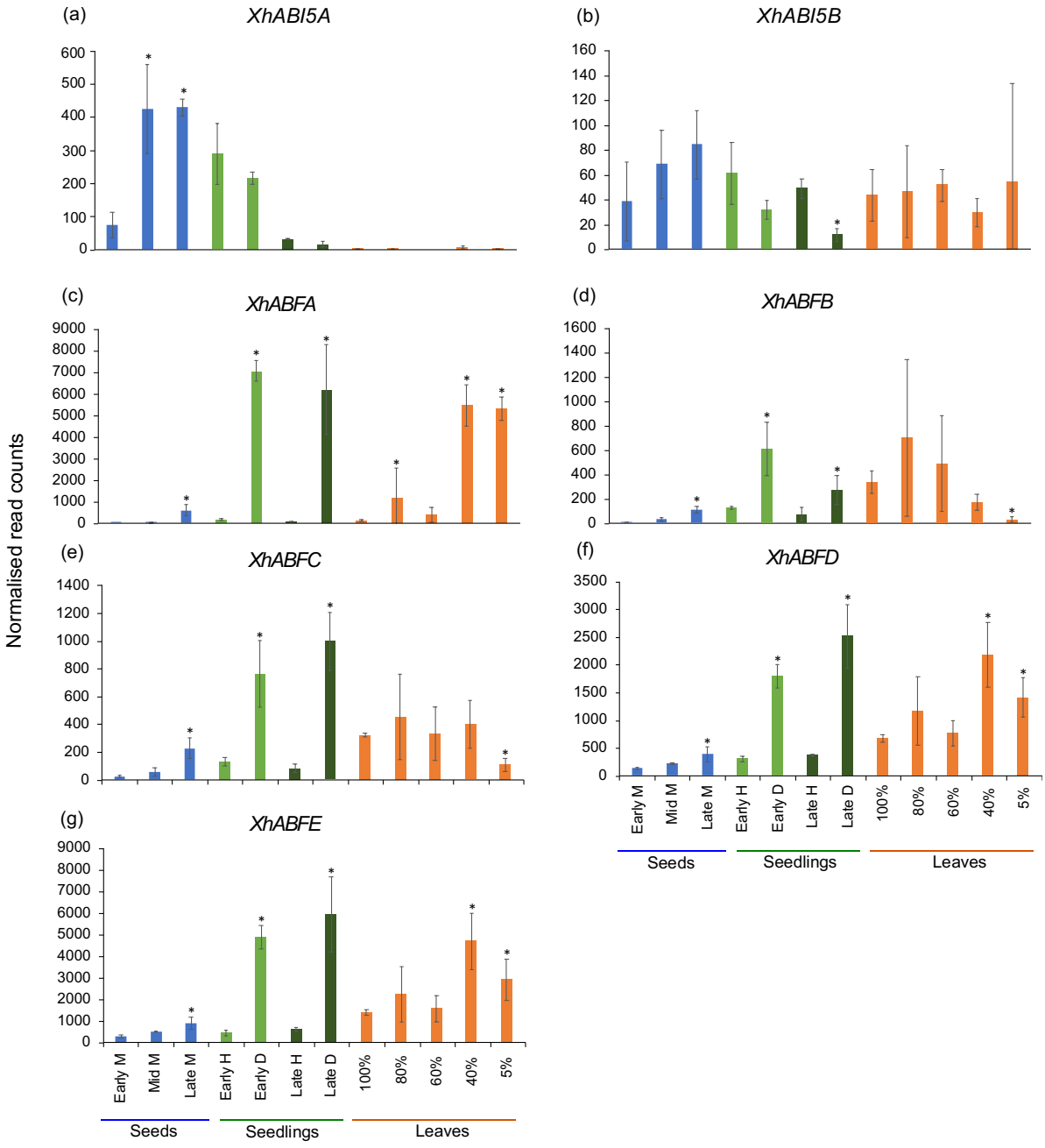

Figure 3.11. Expression of *XhABI5* and *XhABF* genes in *Xerophyta humilis*. DESeq2-normalised counts of *X. humilis* seed regulators during seed maturation (blue), seedling development (light/dark green) and vegetative desiccation tolerance (orange). The M, H and D symbols denote maturation, hydrated, and dehydrated, respectively. Percentages (%) in leaf samples represent RWC values. Error bars are standard deviation (n = 3). Significance was tested against the hydrated sample in each condition (early seed, hydrated seedling, 100% RWC leaf) using DESeq2 at LFC > 1, s-value < 0.005. Asterisks (*) indicate significant differences at s < 0.005.

3.3.5 Cross-species Expression of the LAFL, ABI5 and ABF Genes in Early- and Late-stage *Xerophyta* Seedlings

Having observed the expression patterns of members of the *LAFL* network, *ABI5* and *ABF* in maturing seeds, hydrated and dry seedlings, and desiccating leaves in *X. humilis*, it would be good to know if the observations are consistent in the other two *Xerophyta* species. For this, we did a comparative analysis of the expression of the aforementioned seed maturation regulators in the early and late-stage seedlings of *X. elegans*, *X. schlechteri* and *X. humilis*. One limitation of the cross-species comparison conducted is that only the early and late-stage seedling data was available, as there were no data for maturing seed and desiccating leaves. Nonetheless, the early and late-stage seedlings will give us insights on what the general expression patterns of the LAFL members are and whether they are conserved in various *Xerophyta* species.

Prior to examining the LAFL network genes, PCA plots were generated to analyse the clustering of raw reads from three independent biological repeats of early and late-stage seedlings at hydrated and dehydrated conditions. The separation observed in PC1, for all three *Xerophyta* species, is clearly based on condition, with hydrated samples positioned on the left and the dehydrated samples on the right across both developmental stages (Fig. 3.12). PC2 separated samples for all three *Xerophyta* species based on stage of development, with early and late seedlings occupying lower-negative and upper-positive components, respectively. Interestingly, the hydrated samples for early and late-stage *X. elegans* and *X. humilis* seedlings were more closely grouped on PC2 in comparison to the dried samples.

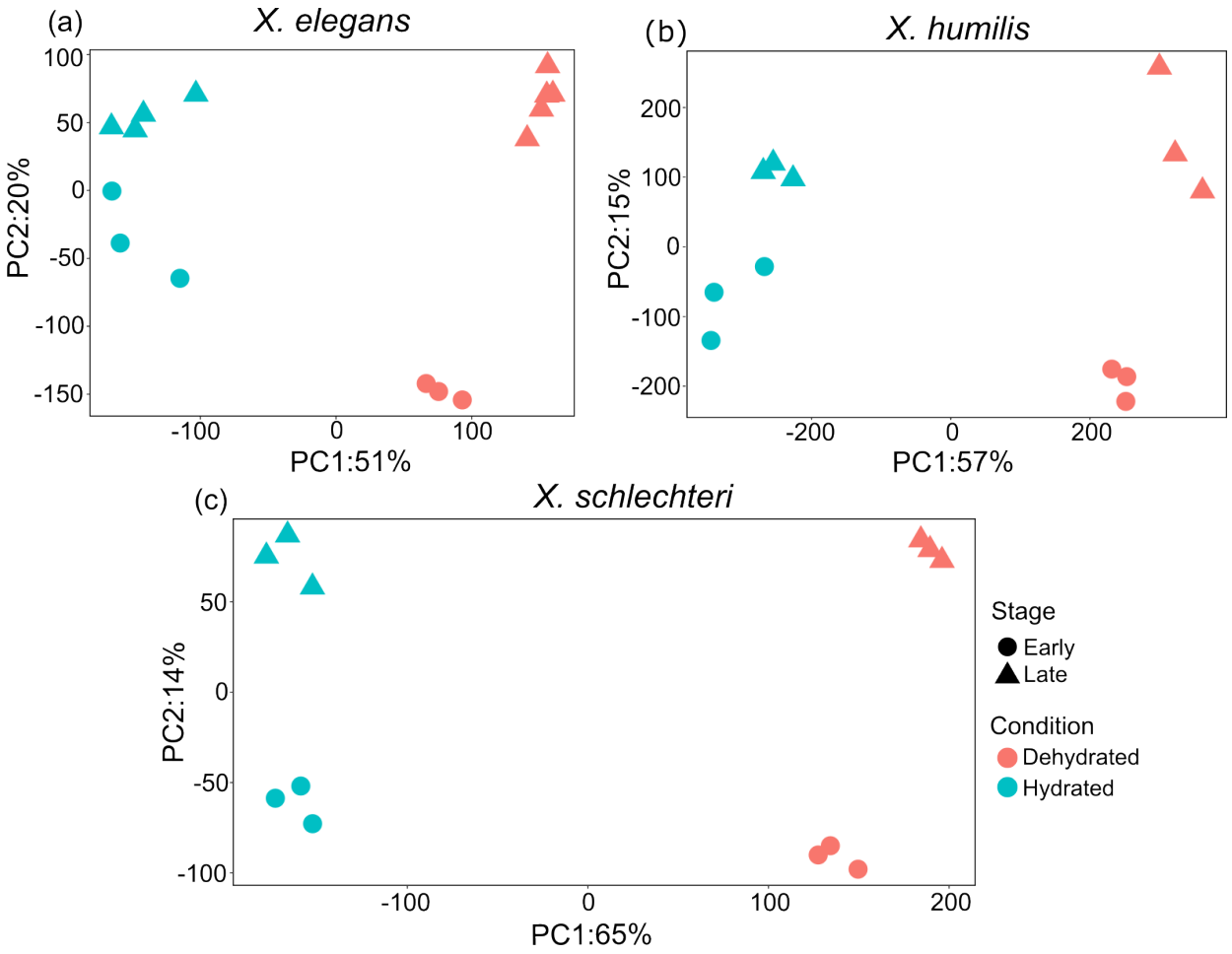

Figure 3.12. PCA score plots of gene counts transformed by DESeq2 variance-stabilizing transformation in hydrated and dehydrated *Xerophyta* seedlings at two developmental stages. As specified in the key on the right, the blue points on the plots represent hydrated samples and the red ones show dehydrated samples. The differentiation between early and late stages is denoted by circle and triangle shapes.

Based on the data from *X. humilis* seeds and seedlings, our prediction is that the ABI3/ABI5 response should be specific to early-stage seedlings across all *Xerophyta* species and absent in older seedlings. This aligns precisely with the observations; *ABI3A* is absent from hydrated tissues in all three species but is induced by desiccation only in early-stage seedlings (Fig. 3.13a), whereas *ABI5A* and *ABI5B* are expressed throughout germination and maintained in desiccated tissues (Fig. 3.13c-d). However, the truncated ABI3, *ABI3B,* and *ABFB* are up-regulated by desiccation in both early-stage seedlings and, to a lesser extent, in late-stage seedlings for all three *Xerophyta* species (Fig. 3.13b, f). *ABFA* is barely expressed in hydrated tissues but is significantly induced by desiccation during both developmental stages (Fig. 3.13e).

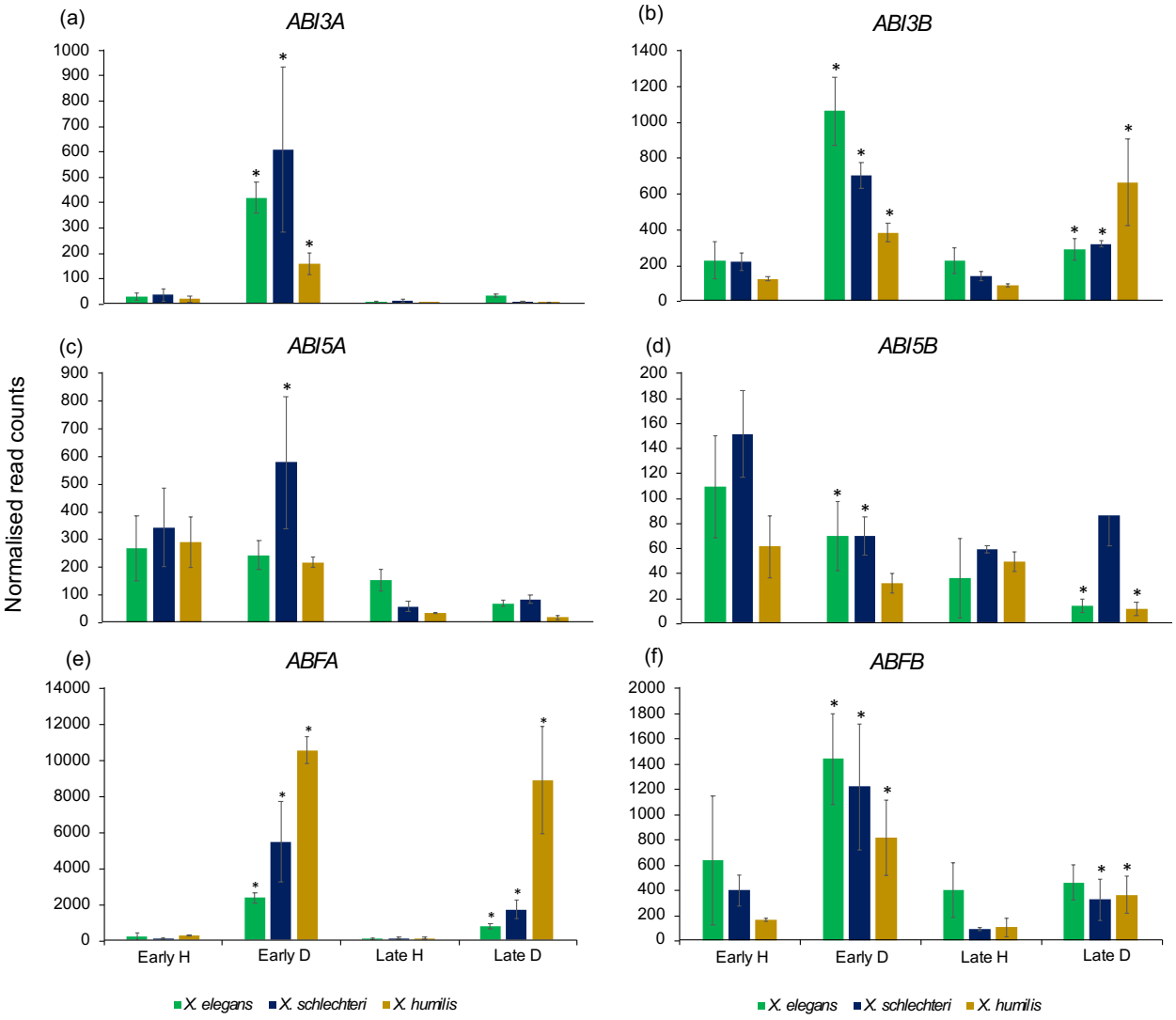

Figure 3.13. Expression of *ABI3, ABI5* and *ABF genes* in *Xerophyta* seedlings. DESeq2-normalised counts of *Xerophyta elegans* (green), *X. schlechteri* (blue) and *X. humilis* (gold) *ABI3*, and two gene members of the bZIP family. H and D denote hydrated and dehydrated, respectively. Error bars are standard deviation (n = 3). Significance was tested against the hydrated seedlings in each stage using DESeq2 at LFC > 1, s-value < 0.005. Asterisks (*) indicate significant differences at s < 0.005.

3.3.6 Analysis of Differential Gene Expression in Desiccated Tissues of *Xerophyta* Seedlings

The comparison of LAFL gene expressions in the four *X. humilis* tissues and seedling data from the three *Xerophyta* species revealed that the TFs important in seed DT during maturation are not involved in the regulation of DT acquisition in two-leaf seedlings and adult leaves. Now, the question is, which genes are involved? Are these similar across all *Xerophyta* species

and developmental stages? To find out, DE genes in seeds, early and late seedlings, and desiccating *X. humilis* leaves were examined, followed by performing GO analysis of these gene sets.

Genes with significant differences in read counts were identified between four X. humilis tissues (seeds, early and late-stage seedlings, and adult leaf tissues), and between the two developmental stages across all three species. This was done as a first step to quantify how many transcripts showed a conserved pattern of regulation across all tissue types and how many were unique to each tissue type and *Xerophyta* species. When comparing DEGs across four *X. humilis* tissues, a core set of 1174 up-regulated and 936 down-regulated transcripts shared between these tissues were identified (Fig. 3.14). Similarly, in the cross-species comparison, gene sets of 1513 (32.93%), 2488 (50.20%), and 5797 (38.01%) up-regulated, and 1494 (28.32%), 1892 (38.88%) and 5351 (35.55%) down-regulated transcripts, were shared between early and late-stage seedlings of *X. elegans*, *X. schlechteri* and *X. humilis*, respectively (Fig. 3.14). These observations raise the question on what the functions of these core set of transcripts shared between four *X. humilis* tissues, and early and late seedling stages are. Our hypothesis is that these shared gene sets might contain the core, essential desiccation-responsive genes. To confirm this, we explored the enriched GO terms associated with these genes.

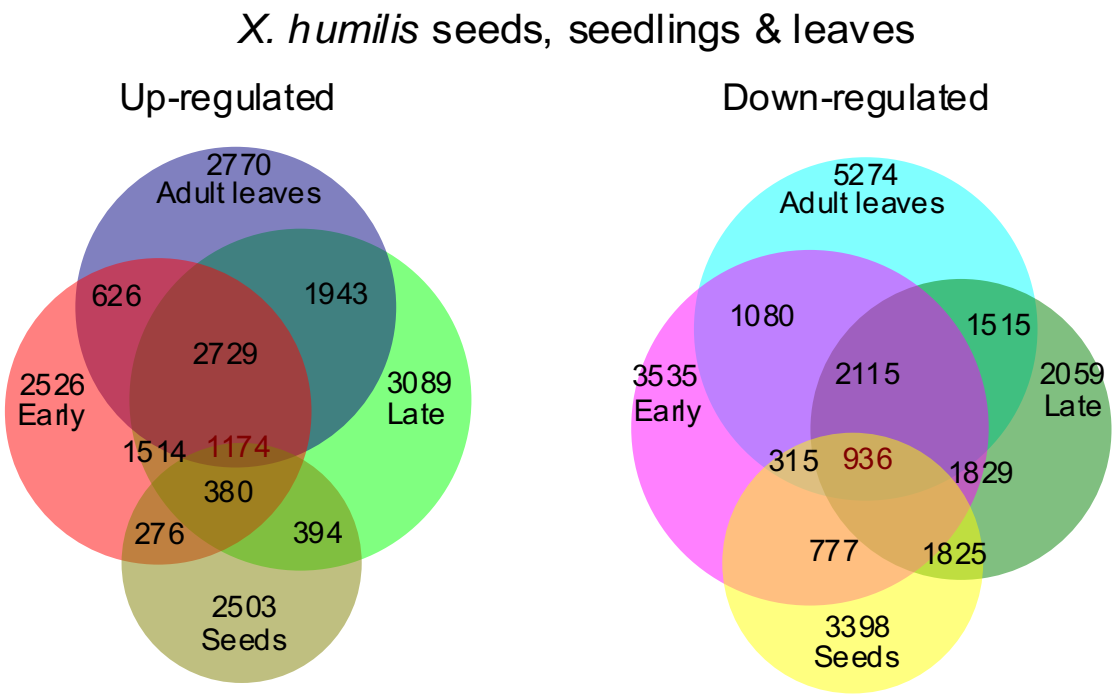

Figure 3.14. Number of DEGs shared between mature *X. humilis* seeds, early-stage, late-stage, and desiccated adult leaves. Mature seeds are depicted using olive/yellow. Early- and late-stage seedlings are represented with orange/purple and light/dark green colours, respectively. The Light/dark blue colours represent desiccated adult leaf tissues. Seedlings in the early stage are depicted using orange/purple colours, while those in the late stage are represented with light/dark green colours. The Venn diagrams were generated using DeepVenn (Hulsen, 2022).

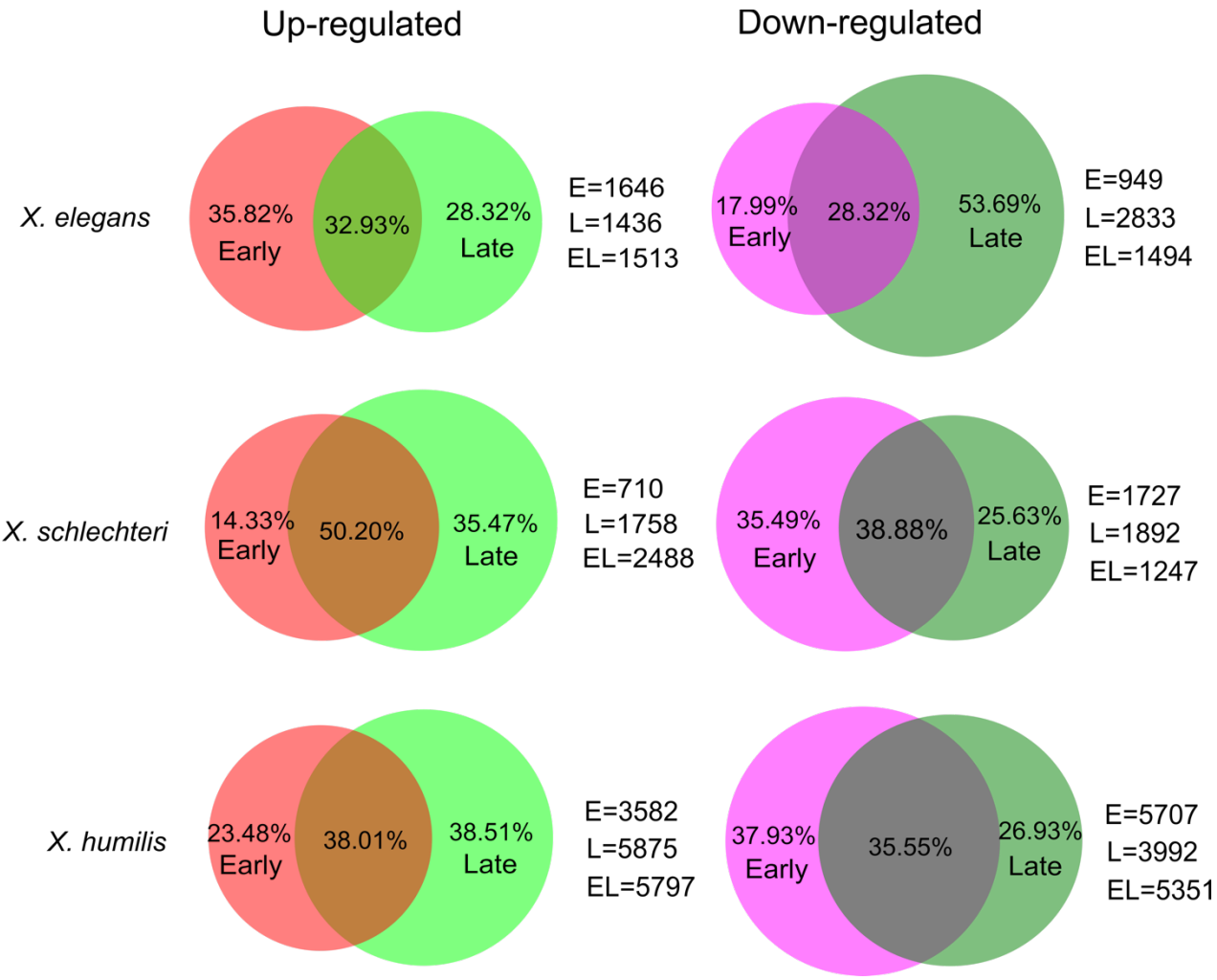

Figure 3.15. Number of differentially expressed genes shared between early-and late-stage *Xerophyta* seedlings. The E, L and EL letters on the right side of the Venn diagrams represent the actual number of genes in the Early, Late and Early-Late seedlings, respectively. The Venn diagrams were generated using DeepVenn (Hulsen, 2022).

3.3.7 GO term Enrichment Analysis

The GO enrichment term analysis for the biological process was conducted on the up- and down-regulated genes shared between *X. humilis* mature seeds, early and late-stage seedlings, and adult leaf tissues. It is not surprising that "cellular response to desiccation", "response to

water deprivation", "negative regulation of chlorophyll catabolic process", and "response to cold" were among the significantly enriched GO terms in the up-regulated gene category (Fig. 3.16). Furthermore, there was noticeable accumulation of genes associated with heat stress, including heat shock factors, heat shock proteins, and LEA proteins, indicated by the enrichment of the "response to heat" GO terms. Similar stress-related GO terms were also enriched for DE genes shared between early and late-stage seedlings across the three *Xerophyta* species (Table 3.1). Notably, the GO term "negative regulation of chlorophyll catabolic process" was enriched in the two poikilochlorophyllous species; *X. schlechteri* and *X. humilis*, and not in *X. elegans.*

Photosynthesis is one of the processes that is shutdown during desiccation, and it thus makes sense that "photosynthesis, light harvesting in photosystem I", light harvesting in photosystem I", "photosynthesis" and "photosystem II stabilization" GO terms were among the most enriched across all four *X. humilis* tissues among the down-regulated genes (Fig. 3.17). Additionally, some of the GO terms common in *X. elegans*, *X. schlechteri* and *X. humilis* included "regulation of floral meristem growth", "lateral root morphogenesis", and "leaf abscission" (Table 3.1), all indicative of growth and developmental processes.

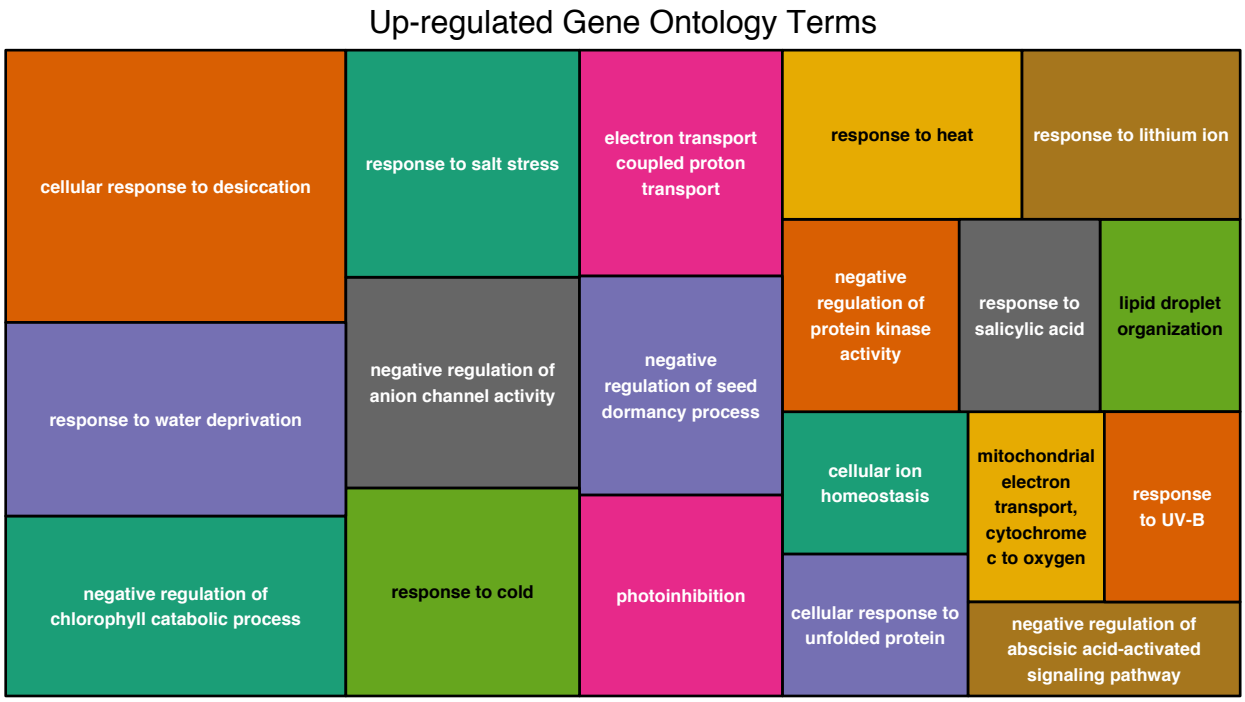

Figure 3.16. Gene ontology terms enriched for the core set of up-regulated *Xerophyta humilis* genes in maturing seeds, desiccated early and late-stage seedlings, and leaves. Only top 20 GO terms, ranked by the adjusted p-value after a Fisher's exact test, are displayed. The treemap package in

R was used to generate the diagram. The sizes of the boxes correspond to the log10 values of the GO terms.

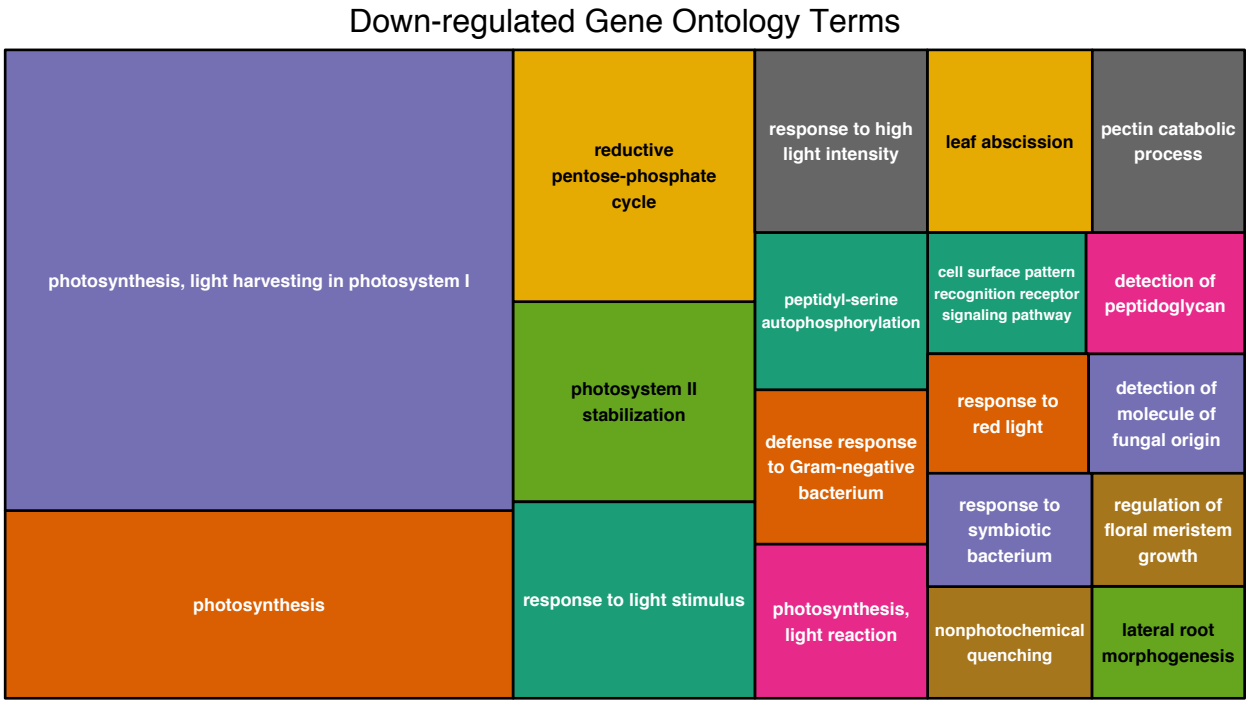

Figure 3.17. Gene ontology terms enriched for the core set of *Xerophyta humilis* genes that are down-regulated in maturing seeds, desiccated early, and late-stage seedlings and leaves. Only top 20 GO terms, ranked by the adjusted p-value after a Fisher's exact test, are displayed. The treemap package in R was used to generate the diagram. The sizes of the boxes correspond to the log10 values of the GO terms.

Table 3.1. Common GO terms enriched for up and down-regulated genes across *Xerophyta elegans*, *X. schlechteri* and *X. humilis* at the early and late seedling stages.

Up-regulated DEGs		
Stage	**GO:ID**	**GO terms common in 3 *Xerophyta* species**
Early and late	GO:0009414	Response to water deprivation
	GO:0071465	Cellular response to desiccation
	GO:0009409	Response to cold
	GO:0006970	Response to osmotic stress
	GO:0006979	Response to oxidative stress
	GO:0009737	Response to abscisic acid
	GO:0009651	Response to salt stress
	GO:0009408	Response to heat
	GO:0034389	Lipid droplet organization
	GO:1902039	Negative regulation of seed dormancy process
Down-regulated DEGs		
Early and late	GO:0009934	Regulation of meristem structural organization
	GO:0031540	Regulation of anthocyanin biosynthetic process
	GO:0010067	Procambium histogenesis
	GO:0009739	Response to gibberellin
	GO:0010089	Xylem development
	GO:2000280	Regulation of root development
	GO:0010223	Secondary shoot formation
	GO:0009768	Photosynthesis
	GO:0010227	Floral organ abscission
	GO:0010102	Lateral root morphogenesis

***** GO terms are ranked by the adjusted p-value after a Fisher's exact test.

3.3.8 Orthogroup and Gene Ontology Analyses

The GO terms associated with up- and down-regulated DEGs are similar across the three *Xerophyta* species and overlap with GO terms enriched for the core transcripts that are differentially expressed across four tissue types in *X. humilis*. This prompts two key questions: firstly, are there genes from orthologous genes that show the same expression patterns across all three species? Identifying such genes is crucial as they could reveal conserved VDT mechanisms and essential functions maintained across different *Xerophyta* species. Secondly, is there evidence of common regulation of these orthologs in both early and late seedling

stages? To delve into these questions, we identified a common set of orthologs in early and late-stage seedlings in *X. elegans*, *X. schlechteri* and *X. humilis* species using orthogroup analysis (Section 3.3.2.13), followed by performing GO term enrichment to understand their biological roles, and motif enrichment analysis to identify promoter elements that are conserved across all three species.

The conventional method for identifying orthologous genes across species involves a one-to-one approach, where OGs containing a single gene in each species are selected for analysis (Vanburen et al., 2015). However, despite its simplicity, this method presents several challenges. Notably, many genes are omitted during the filtering process, often leaving only core housekeeping genes that are of limited interest. Furthermore, applying this approach to the three *Xerophyta* species under study posed complications due to differences in genome assemblies: while *X. elegans* and *X. schlechteri* have haploid assemblies, the genome of *X. humilis* is tetraploid, resulting in a 1:1:4 gene copy relationship. Consequently, the traditional one-to-one approach was deemed unsuitable. Instead, we pursued an alternative strategy by identifying sets of OGs that contained DE genes showing consistent expression patterns; either all up- or all down-regulated, across the three species. Despite the absence of a direct one-to-one correspondence between species, the DE genes within these OGs are functionally analogous, performing similar functions across each species.

A total of 18,066 OGs were identified across the three *Xerophyta* species. Among these, 7,787 in early-stage and 8,579 in late-stage seedlings contained at least 1 DE gene in each species (Fig. 3.18a). Most OGs (84%) contained DE genes going in opposite directions, i.e. up-regulated and down-regulated genes (Fig. 3.18b), and so were discarded from the analysis. Only the profiles of DE members from these OGs that showed unidirectional expression patterns, either up-regulated or down-regulated, were used for further analysis (Fig. 3.18b).

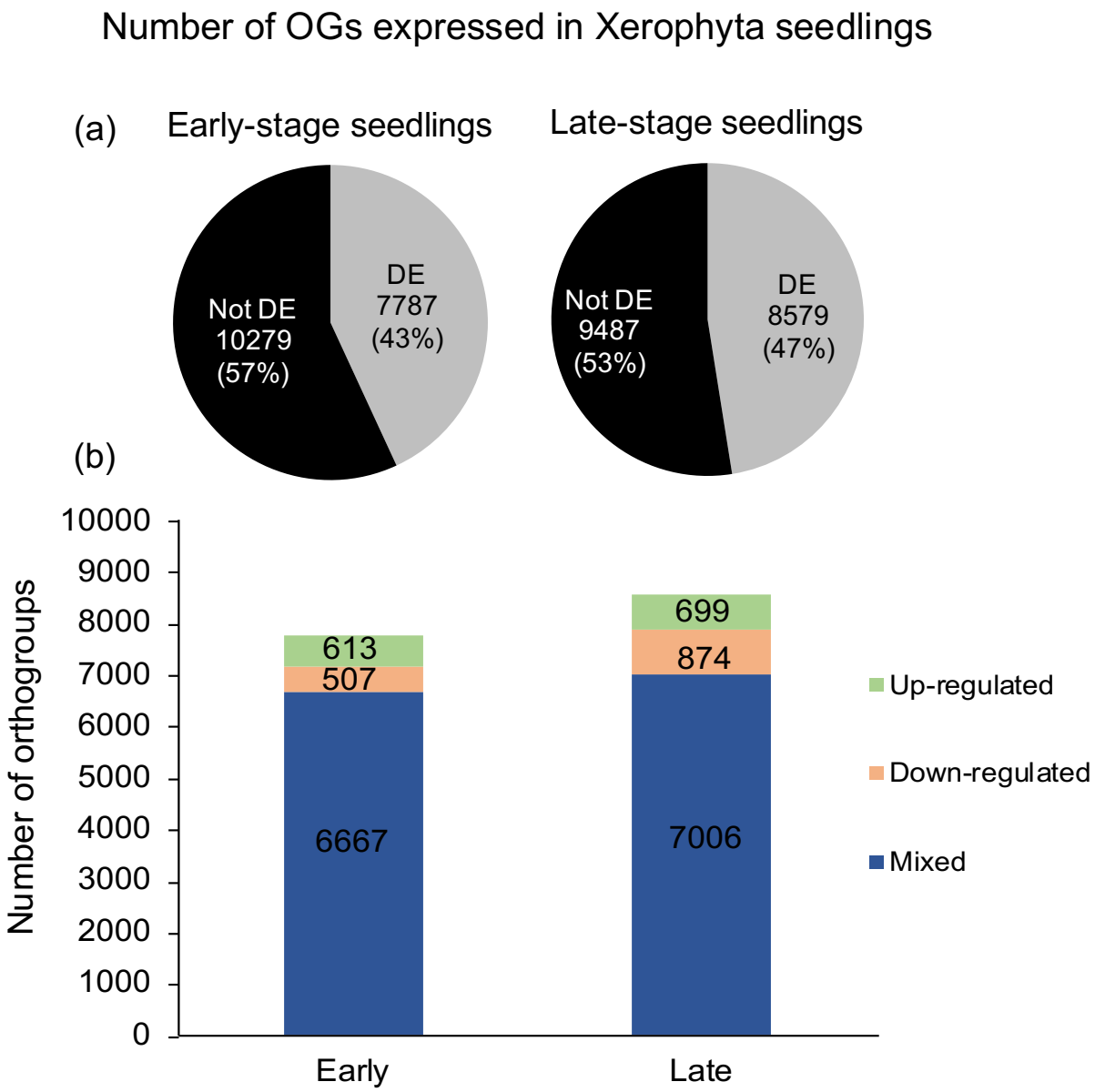

Figure 3.18. Total number of orthogroups expressed in *Xerophyta* species during early and late-stage seedlings. (a) shows the proportions of OGs that contain differentially and non-differentially expressed genes. OGs containing DE genes expressed exclusively in one direction are classified into up- and down-regulated categories. The mixed OG category comprises DE genes that exhibit both up- and down-regulation (b).

As a first step towards identifying gene sets for functional analysis, we examined the distribution of OGs containing the unidirectional DE genes in Venn diagrams to get an idea of how many are shared between species and how many are specific to each species. Within the up-regulated and down-regulated classifications of early-stage seedlings, a shared group of 613 and 507 OGs in the up-regulated and down-regulated categories, respectively, were observed in *X. elegans*, *X. schlechteri*, and *X. humilis* (Fig. 3.19). Notably, the late-stage seedlings

exhibited a greater number of OGs containing down-regulated genes, with 874 of these being common among the three *Xerophyta* species (Fig. 3.19).

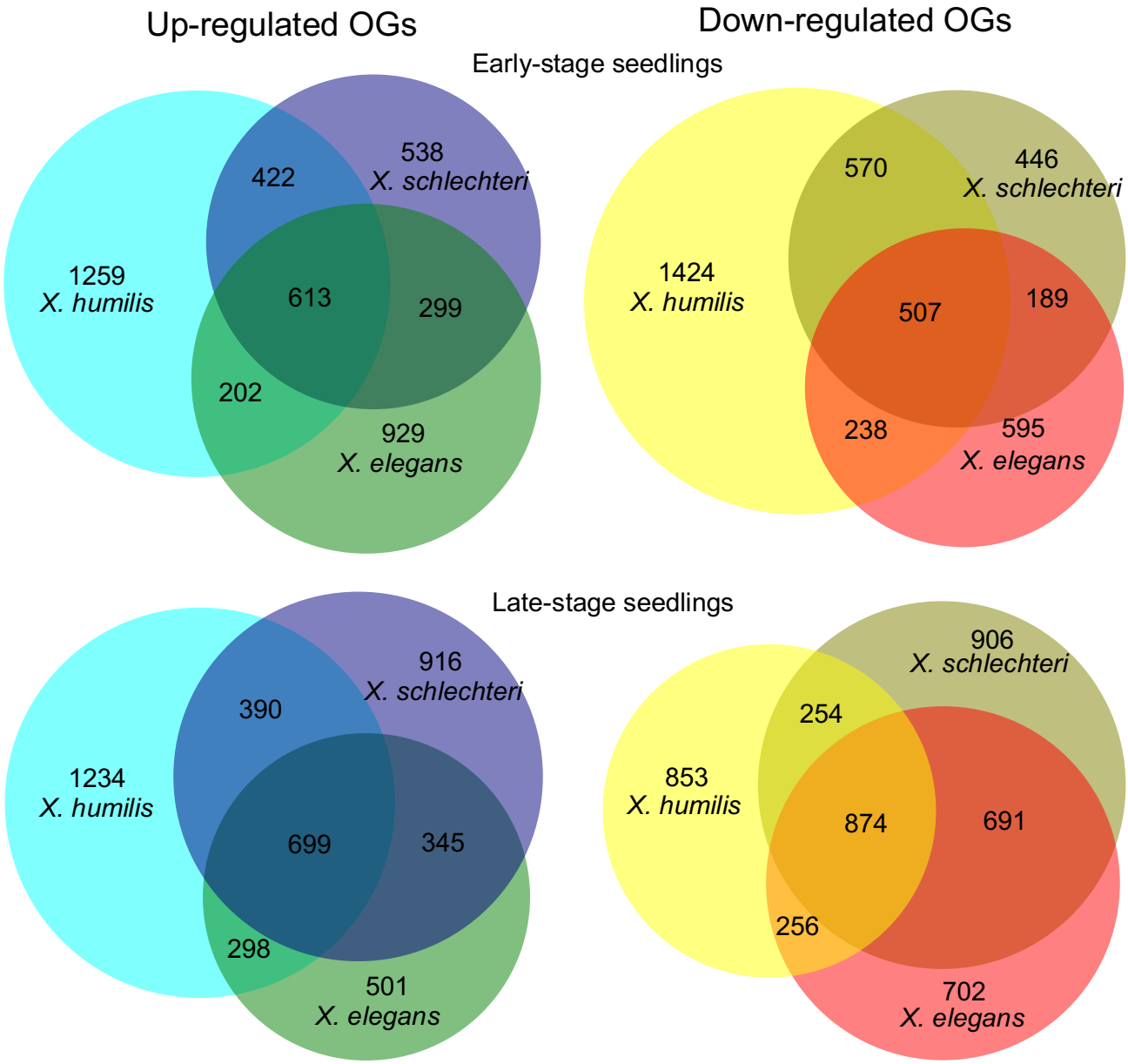

Figure 3.19. The overlap of orthogroups containing up-regulated and down-regulated genes in *Xerophyta elegans*, *X. schlechteri* and *X. humilis* at early and late-stages. OGs only consisting of unidirectional differentially expressed genes, either up-regulated or down-regulated, were used to make these diagrams. Venn diagrams were generated using DeepVenn (Hulsen 2022).

X. elegans, *X. schlechteri* and *X. humilis* share common OGs that contain DE genes in both early and late-stage seedlings. The question is, how many of these show a conserved pattern of up or down-regulation across all three species, regardless of the developmental stage? This is important because it can reveal core regulatory mechanisms that are critical for the adaptation and stress tolerance of *Xerophyta* species. Differentially expressed OGs common across these species were examined, and a total of 705 OGs were found to be conserved, with 370 displaying up-regulation and 335 showing down-regulation in response to desiccation (Fig. 3.20). These OGs shared between early and late-stage seedlings contain core desiccation response genes. Those that do not fall within this shared group are specific to their respective developmental stages.

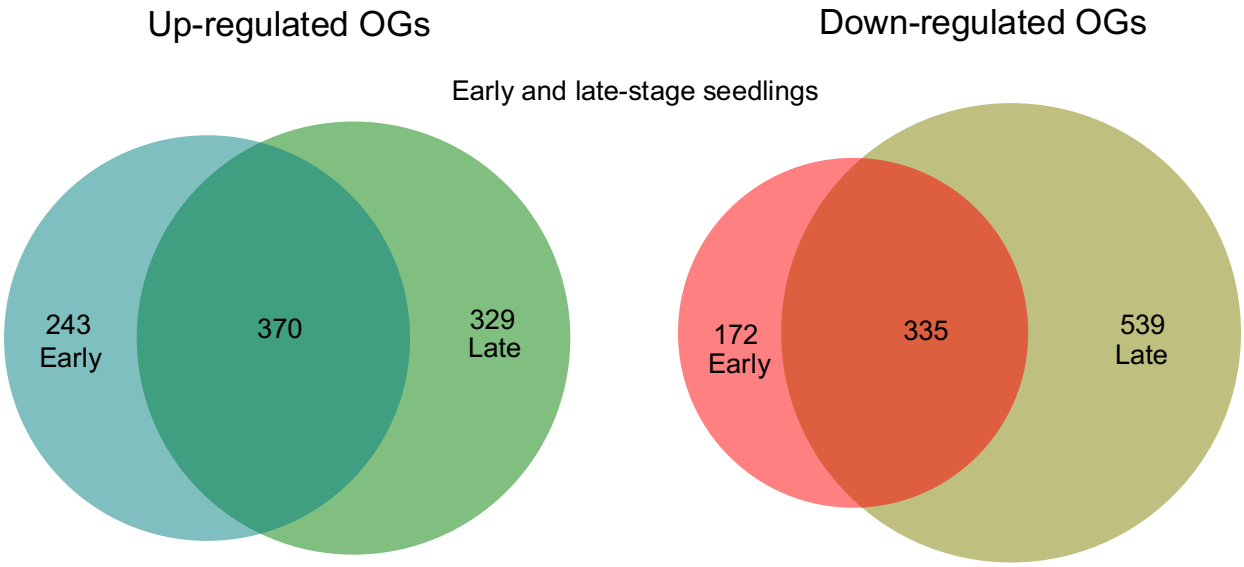

Figure 3.20. The number of conserved and stage-specific orthogroups in *Xerophyta* seedlings. The Venn diagrams were generated using DeepVenn (Hulsen 2022).

GO enrichment analysis, for both early-specific and late-specific OGs, along with the conserved OGs, in both up-regulated and down-regulated categories, was performed to understand their biological functions. Given the degree of overlap between the early and late seedlings, we expected a substantial enrichment of stress-related GO terms. However, contrary to expectations, only 10 GO terms were significant in the shared group, with "starch catabolic process" being the most enriched (Fig. 3.21). Interestingly, three upregulated GO terms common to both early and late seedlings are related to ion sulfur cluster assembly, cellular ion homeostasis, and stress responses to metal ions. Water loss in plants often disrupts cellular ion balance and induces oxidative stress, which could help explain the enrichment of these specific

GO terms. Significantly enriched terms in the early-specific OGs comprised “secretion”, “chaperone cofactor-dependent protein refolding” and “response to stress”, whereas “proton transmembrane transport”, “regulation of stomatal movement” and “protein targeting to vacuole” emerged as the most enriched in the late-specific group (Fig. 3.21).

Unsurprisingly, a large portion of the down-regulated OGs shared between early, and older seedlings were “regulation of root meristem growth”, “regulation of meristem structural organization” and “gametophyte development.” Notably, the term “photosynthesis” was enriched in the older seedlings and not in the younger ones (Fig. 3.21). This is not surprising as the early-stage seedlings are likely not yet photosynthetic.

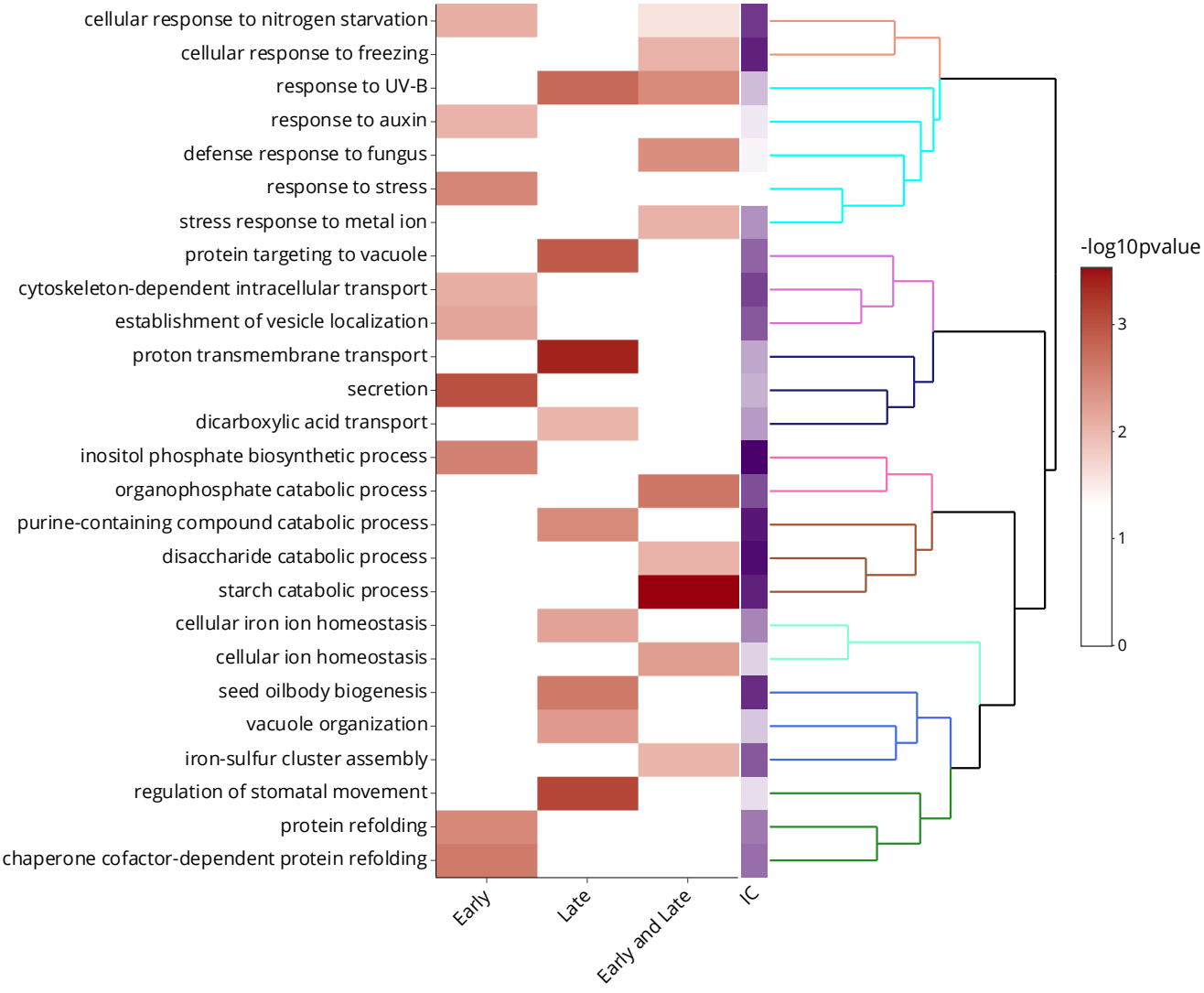

Figure 3.21. Gene ontology terms enriched for orthogroups containing genes that are up-regulated in the early only, late only, and both early and late-stage seedlings. GO terms are ranked by the adjusted p-value from a Fisher’s exact test, with all expressed OGs were used as the reference

set. “IC” refers to Information Content, which indicates the specificity of the enriched GO terms relative to the dataset. The dendrogram illustrates the hierarchical clustering of GO terms based on their similarities. Different colours in the dendrogram represent groups of GO terms that share related biological functions or processes.

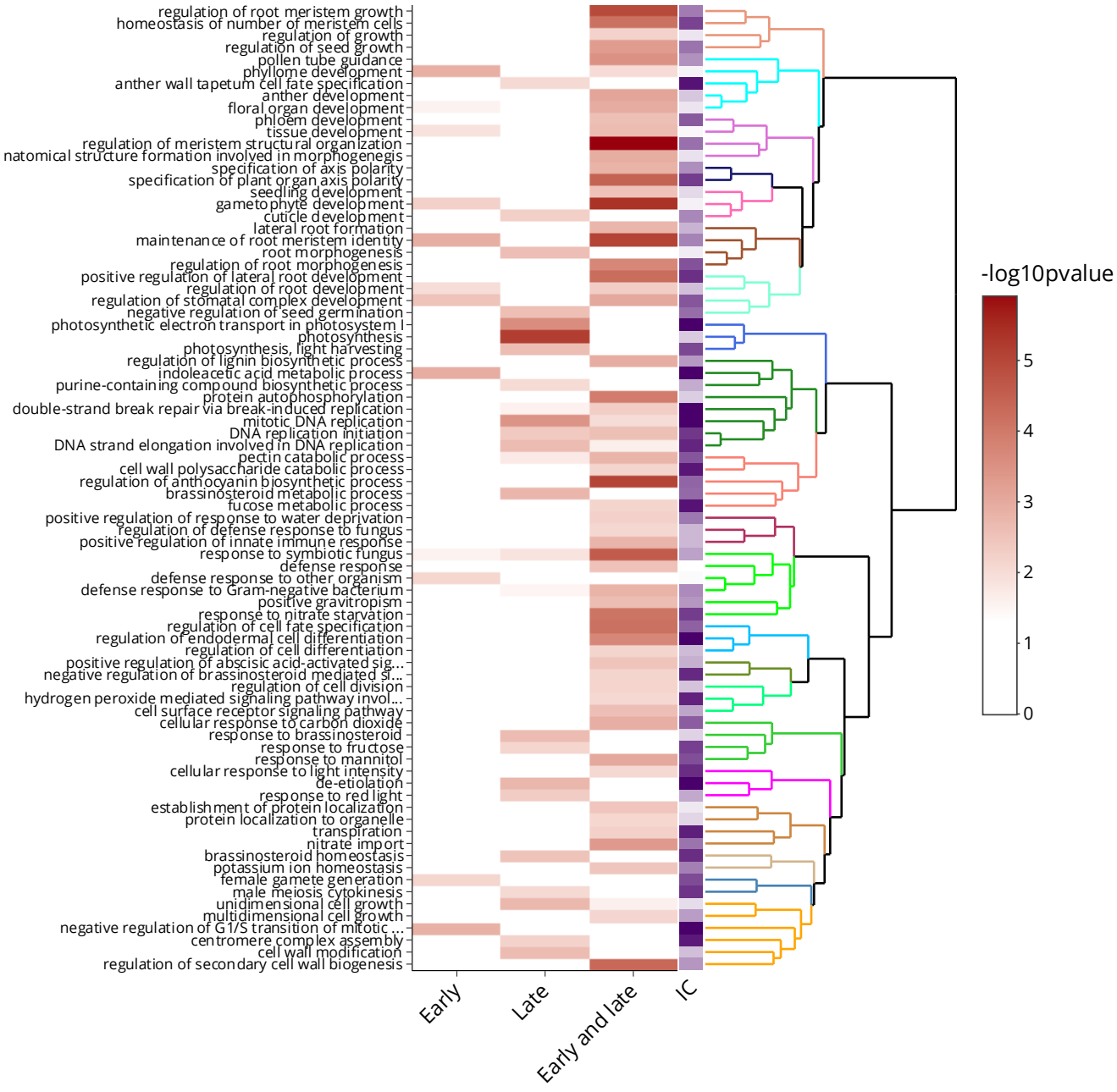

Figure 3.22 Gene ontology terms enriched for orthogroups containing genes that are down-regulated in early only, late only, and both early and late-stage *Xerophyta* seedlings. GO terms are ranked by the adjusted p-value from a Fisher’s exact test, with all expressed OGs were used as the reference set. “IC” refers to Information Content, which indicates the specificity of the enriched GO terms relative to the dataset. The dendrogram illustrates the hierarchical clustering of GO terms based

on their similarities. Different colours in the dendrogram represent groups of GO terms that share related biological functions or processes.

3.3.9 Motif Enrichment Analysis

Now that we have gleaned insights into the functional roles of orthologous gene groups through GO enrichment analysis, and showed that the LAFL network remains inactive in older seedlings and desiccating leaves of *X. humilis*, the pivotal questions arise: what mechanisms govern the regulation of the desiccation responsive genes? Is there evidence of common regulation of these orthologs in *Xerophyta* seedlings? Motif enrichment analysis was undertaken to identify conserved motifs across the three *Xerophyta* species. We focused on the 370 up-regulated and 335 down-regulated OGs common between early and late-stage seedlings (Fig. 3.20) as these contain core desiccation response genes. These two sets of OGs were analysed separately. The 370 and 335 common OGs have different number of DE members across the three species, and these are shown in the white boxes in Figure 3.23 below. Regions 500 bp upstream of the transcription start site of these DE target genes were used as input for motif discovery and enrichment with XSTREME (Grant & Bailey, 2021).

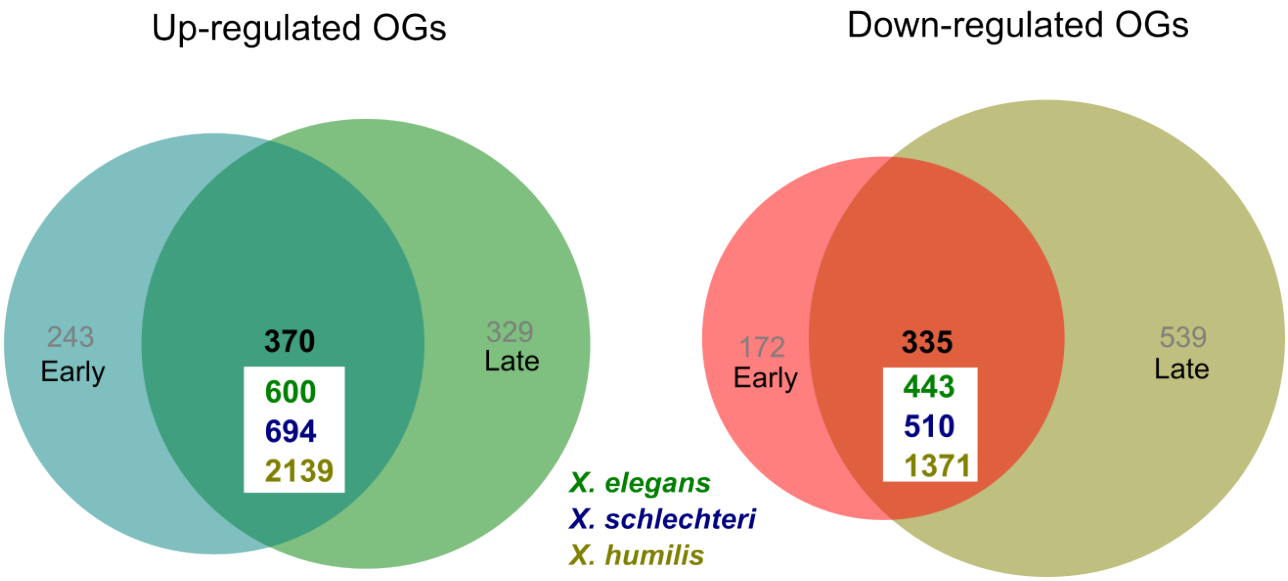

Figure 3.23. Number of differentially expressed genes from core orthogroups shared among the three *Xerophyta* species. *X. elegans*, *X. schlechteri* and *X. humilis* gene numbers are written in green, blue and gold colours, respectively.

X. elegans, *X. schlechteri* and *X. humilis* had a total of 473, 435 and 768 enriched motifs in the promoters of up-regulated genes, respectively, and 391, 374, 667 motifs enriched in the promoters of down-regulated target genes, respectively. These motifs known include binding

sites for various TF families such as Myeloblastosis viral oncogene homolog (MYB), cysteine-rich Polycomb-like Proteins (CPP), WRKY, GATA-binding factors, Heat Shock Factors (HSF), AT-Hook Motif Nuclear Localised Protein (AHL) and C_2H_2 Zink Finger Protein (ZAT). Comparative genome analysis has revealed *Xerophyta* specific expansion of three of these TF families, namely, HSFs, AHLs, and C_2H_2 ZATs. This means that these families have significantly higher number of gene copies due to duplication events or other evolutionary mechanisms. Our subsequent analysis specifically focused on these families that are exclusively expanded in *Xerophyta* species.

3.3.9.1 Enrichment of HSF motifs in *Xerophyta* genes

Several HSF motifs were enriched within the promoter regions of target genes shared among *Xerophyta* species, and these were grouped into two clusters through hierarchical clustering (Fig. 3.24). Cluster AC0091 consisted of four members: HSFA1B, HSFB2A, HSFB2B and HSFB4. Cluster AC0092 comprised six members: HSFA1E, HSFA4A, HSFA6A, HSFA6B, HSFB3 and HSFC1. It is worth noting that one of the HSF members, HSFC-1 (TTCYAGAA), was among the expanded gene groups in *Xerophyta* species.

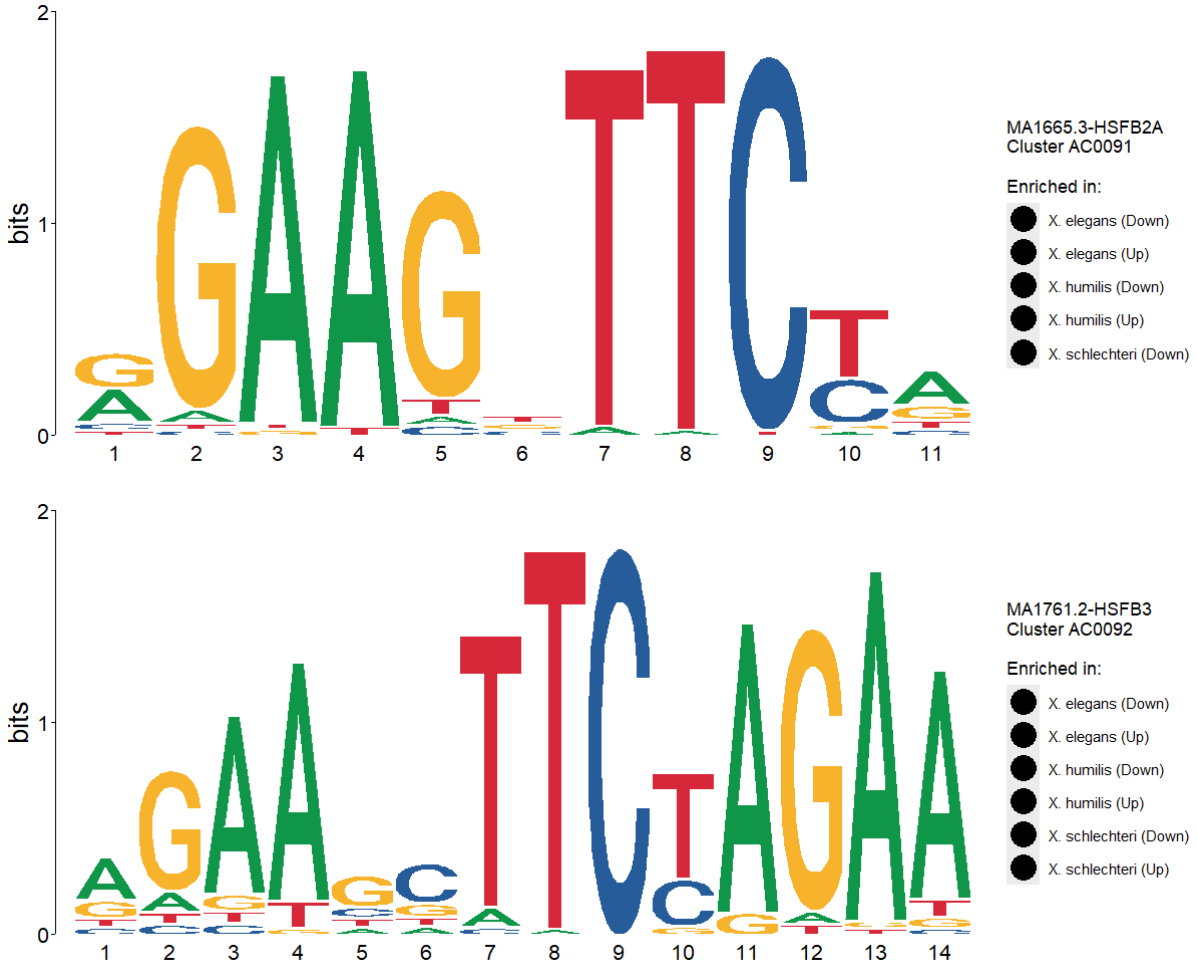

Figure 3.24. Sequence logos of HSF motifs in the promoters of *Xerophyta* genes. Motif clusters were generated through aligning motif sequences by TOMTOM and hierarchical clustering based on e-values.

The subsequent task was to determine whether these motifs are conserved across *Xerophyta* species. This was accomplished by examining common OGs that contain HSF motifs in *X. elegans*, *X. schlechteri* and *X. humilis* genes. Our results reveal that nine up-regulated and three down-regulated HSF motif-containing OGs are shared among the three species (Table 3.2, Fig. 3.25). Examples of the HSF-motif containing OGs that are up-regulated include stachyose synthase, WRKY TF, solanesyl-diphosphate synthase, DOMON domain-containing protein, and respiratory burst oxidase homolog protein C. The remaining four OGs are proteins of unknown functions. All these proteins regulate various stress-related processes such as "response to water deprivation", "response to wounding", "response to oxidative stress" and "response to heat" (Fig. 3.26c). On the other hand, the three down-regulated OGs; B3 domain-containing protein, rhamnogalacturonan I rhamnosyltransferase 1, and endoglucanase 23 are involved in plant growth and development processes (Fig. 3.25). For instance, "lateral root

development", "leaf shaping", "regulation of seed growth" and "shoot system development" (Fig. 3.25d).

Table 3.2. Up-regulated and down-regulated HSF containing-motif orthogroups conserved in the three *Xerophyta* species.

Orthogroup ID	Orthogroup name	Direction	Number of genes
OG0000322	Uncharacterised protein	↑	26
OG0000837	Stachyose synthase	↑	23
OG0001962	WRKY transcription factor	↑	16
OG0002120	Respiratory burst oxidase homolog protein C	↑	6
OG0004185	Solanesyl-diphosphate synthase 2	↑	5
OG0004958	Uncharacterised protein	↑	8
OG0007096	Uncharacterised protein	↑	11
OG0022255	Cytochrome b561 and DOMON domain-containing protein	↑	7
OG0024644	Uncharacterised protein	↑	6
OG0000275	B3 domain-containing protein Os02g0683500	↓	12
OG0000493	Rhamnogalacturonan I rhamnosyltransferase 1	↓	11
OG0001379	Endoglucanase 23	↓	35

*The upward and downward arrows indicate up-regulated and down-regulated genes, respectively

*The number of genes is the cumulative count of DE genes from *X. elegans*, *X. schlechteri* and *X. humilis*

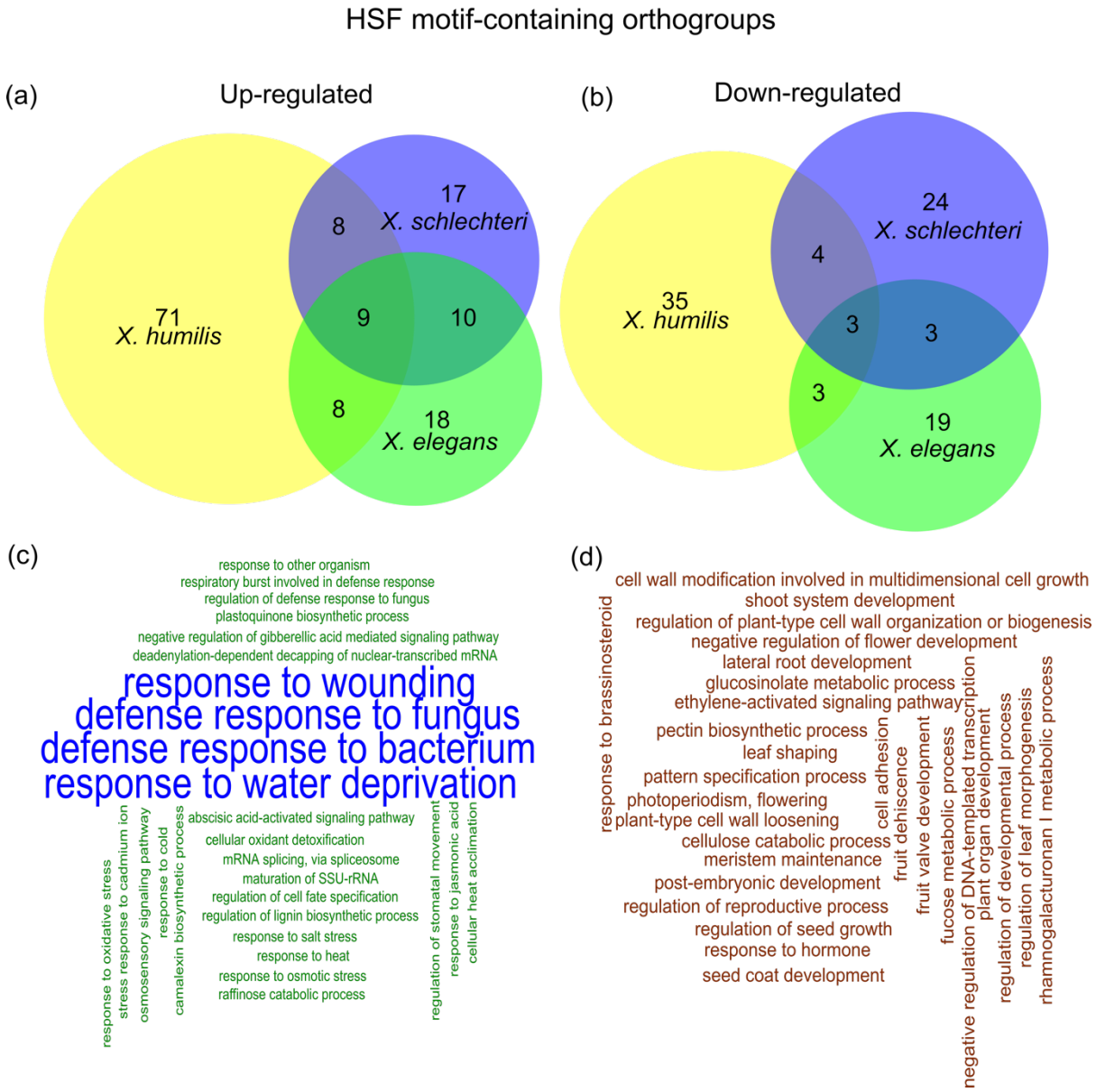

Figure 3.25. HSF-containing orthogroups and their gene ontology terms in three *Xerophyta* species. A GO database in GO.db R package was used to search for GO terms associated with the specified OGs. The GO terms were filtered to biological processes. The size of words in the wordcloud diagrams corresponds to the frequency of the GO term

One other interesting overlap in Figure 3.25a is between the two poikilochlorphyllous species; *X. schlechteri* and *X. humilis,* which have 8 common up-regulated OGs. Having the knowledge that the two species break down their chlorophyll during desiccation, we wanted to know if the shared HSF-containing OGs have GO terms that are related to chlorophyll/chloroplast. Contrary to our expectations, most of the GO terms associated with these OGs are stress related, and do not seem to be specific to poikilochlorophyllous species (Fig. 3.26a). We also looked another overlap between *X. elegans* and *X. schlechteri*, both of which employ similar

developmental processes during germination. These species had 10 common up-regulated OGs (Fig. 3.25a), and the GO terms present were related to both stress and developmental processes. For example, among the stress related terms were "positive regulation of response to water deprivation", "response to hydrogen peroxide" and "positive regulation of cellular response to heat" (Fig. 3.26a). GO terms related to growth and development included "regulation of seed germination", "lateral root formation" and "positive regulation of growth" (Fig. 3.26b).

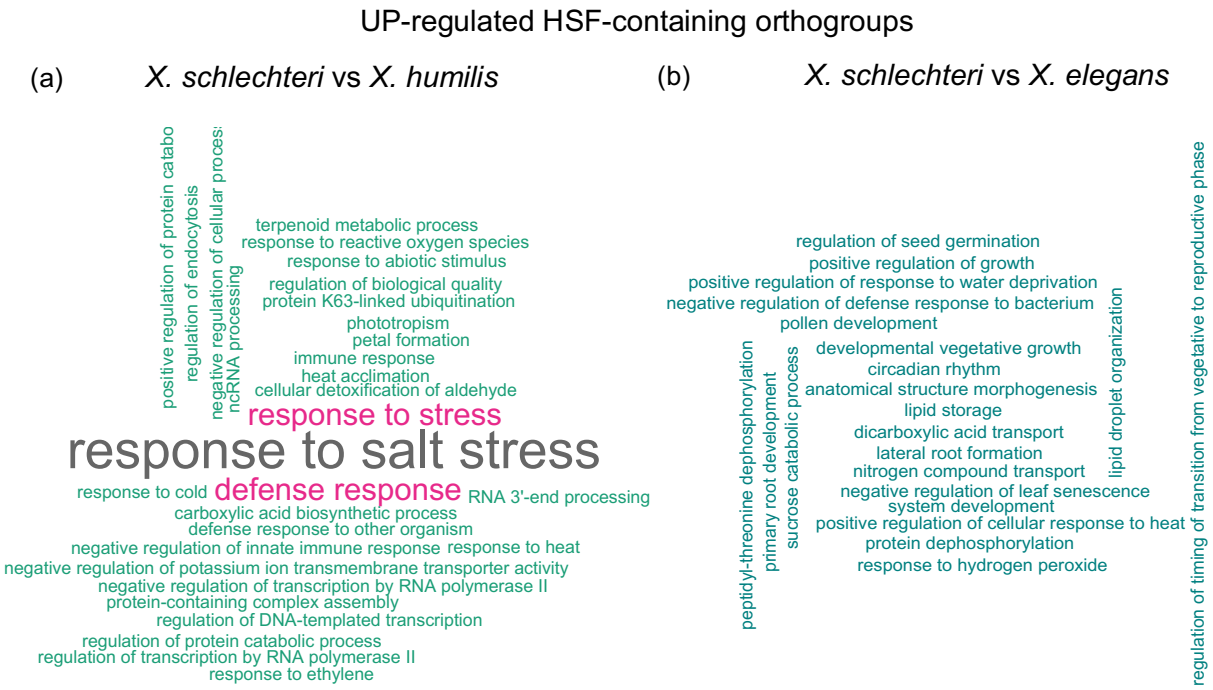

Figure 3.26. Gene ontology terms associated with HSF motif-containing orthogroups shared among poikilochlorophyllous species (a) and *X. schlechteri* vs *X. elegans* (b). The size of the words corresponds to the frequency of the GO term. GO.db database was used to search for GO terms in R. The GO terms were filtered to biological processes.

3.3.9.2 Enrichment of AHL motifs in *Xerophyta* genes

AHLs are highly conserved TFs in land plants that have been shown to regulate a variety of biological processes in plants (Zhang et al., 2022). In this study, four types of AHL motifs were enriched in the promoter regions of up-regulated and down-regulated target genes in three *Xerophyta* species. These were grouped into clusters AC0076 and AC0077 (Fig. 3.27), with the former containing one member, AHL13, and the latter comprising AHL12, AHL20 and AHL25 members.

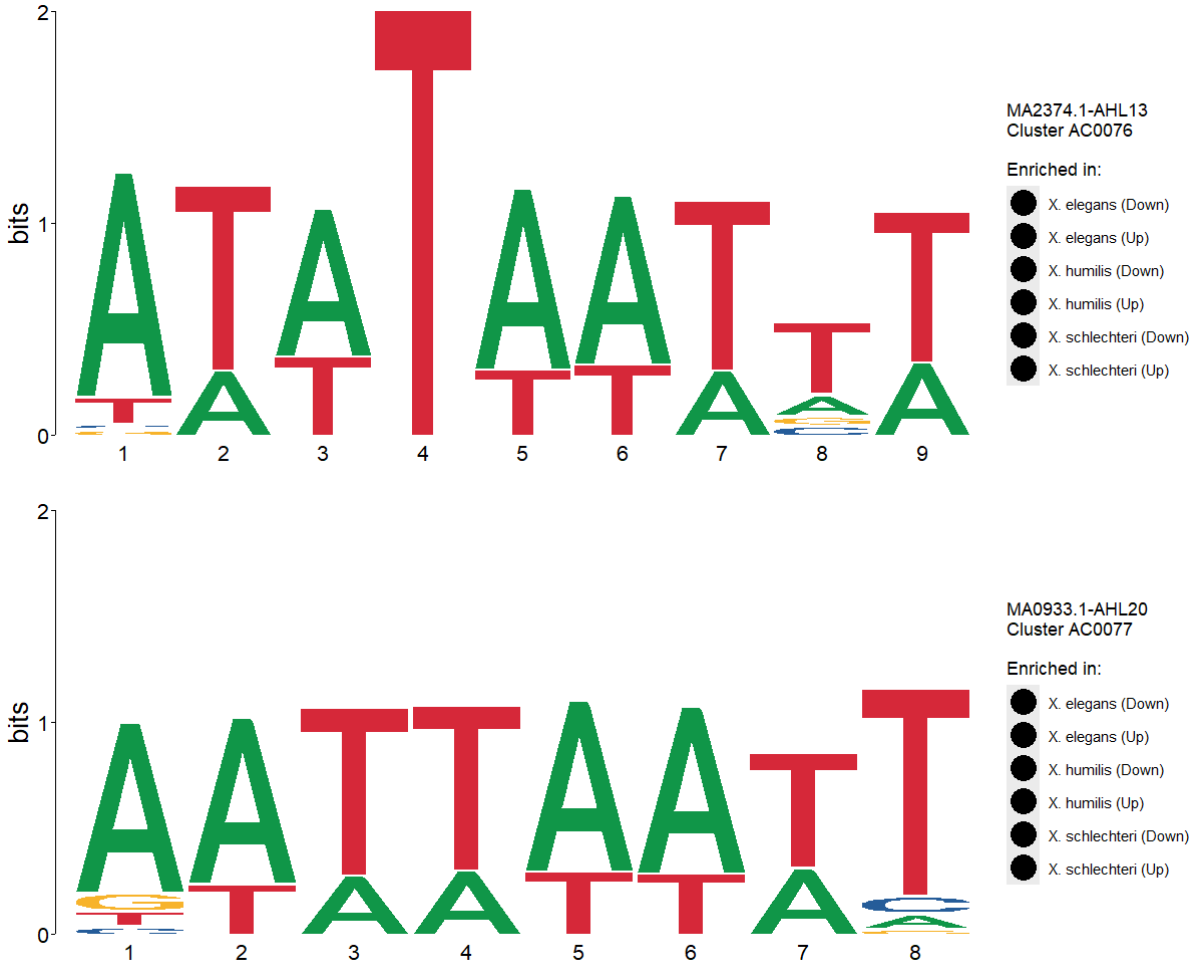

Figure 3.27. Sequence logos of AHL motifs in the promoters of *Xerophyta* genes Motif clusters were generated through aligning motif sequences enriched in *Xerophyta elegans*, *Xerophyta schlechteri* and *Xerophyta humilis* genes with TOMTOM and hierarchical clustering based on e-values.

The central question is whether these AHL motifs found in the three *Xerophyta* species are regulated by the same group of TFs. We found that the AHL-motif containing OGs had a significant overlap between the three species, which was larger than the OGs specific to each species. The overlaps were 295 and 272 in the up-regulated and down-regulated OGs, respectively, indicating their conservation in the *Xerophyta* species. The GO terms in the up-regulated OGs were largely associated with desiccation stress, such as "response to water deprivation," "response to salt stress," "response to abscisic acid," and "response to oxidative stress." In contrast, the down-regulated OGs were involved in a range of biological processes, including stress-related and growth and development processes (Fig. 3.28d). Some of the growth-related terms were "xylem development," "plant-type cell wall organization," and "root development." In addition to the aforementioned stress-related GO terms associated with the up-regulated OGs (Fig. 3.28c), there were also terms related to “defense response”, “response

to wounding", and "response to heat". We also checked the overlap between *X. schlechteri* and *X. humilis* (poikilochlorophyllous) to see if there are any chlorophyll related GO terms, however, none were detected (results not shown).

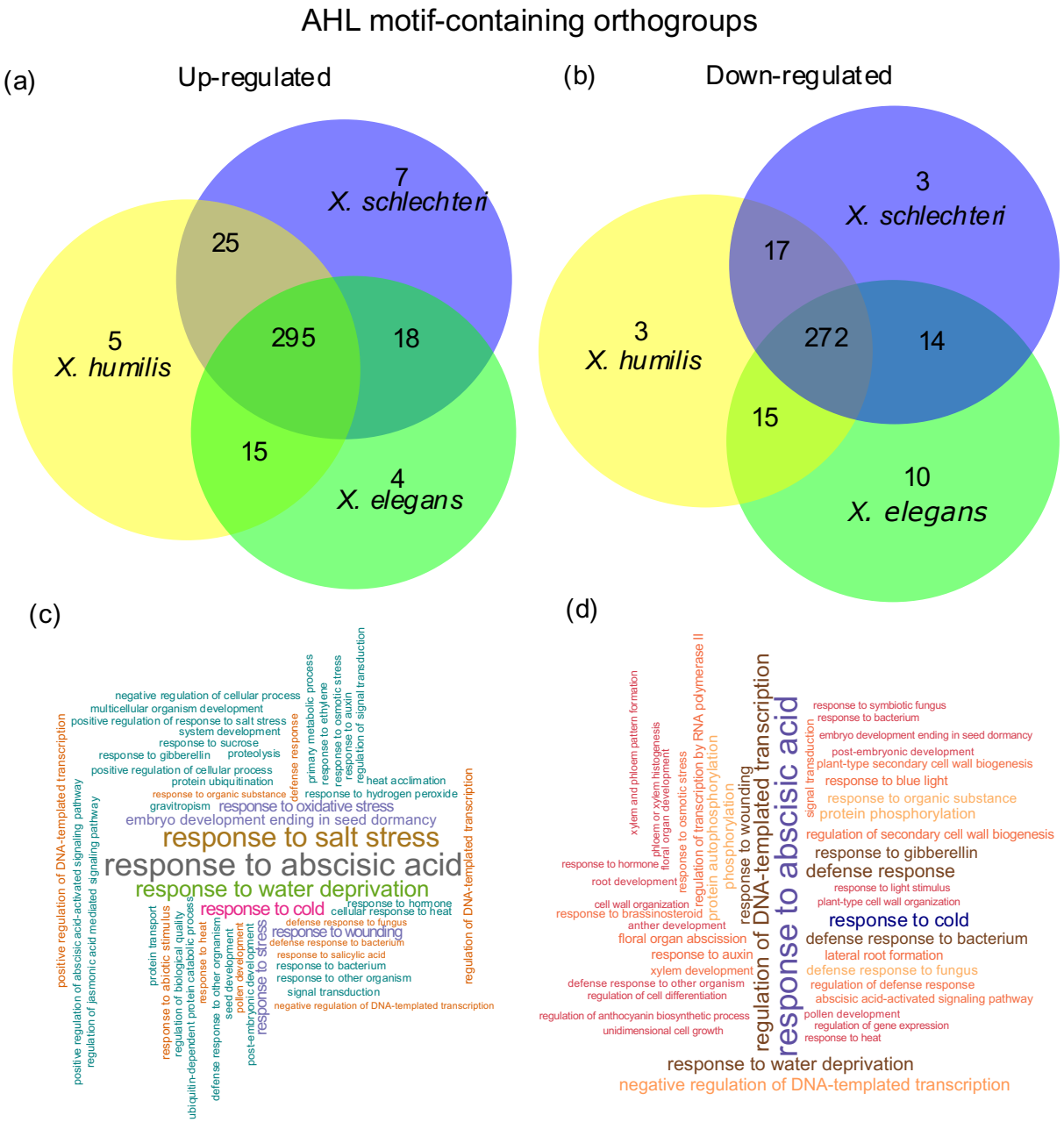

Figure 3.28. Gene ontology terms associated with AHL motif-containing orthogroups common in three *Xerophyta* species. A GO database in GO.db R package was used to search for GO terms associated with the specified orthogroups. The GO terms were filtered to biological processes. The size of words in the wordcloud diagrams corresponds to the frequency of the GO term.

3.3.9.3 Enrichment of ZAT motifs in *Xerophyta* Promoter Genes

Two ZAT motifs, namely ZAT6 and ZAT10, were enriched in the promoter regions of target genes in *X. elegans*, *X. schlechteri* and *X. humilis*. The motif hierarchical clustering resulted in two distinct ZAT clusters, with ZAT6 falling under cluster AC0039 and ZAT10 under cluster AC0114. Notably, both of these motif clusters were enriched in the promoter regions of both up-regulated and down-regulated genes (Fig. 3.29). The main focus now shifts towards determining the OGs containing genes with ZAT motifs and identifying which of these are shared among the three species.

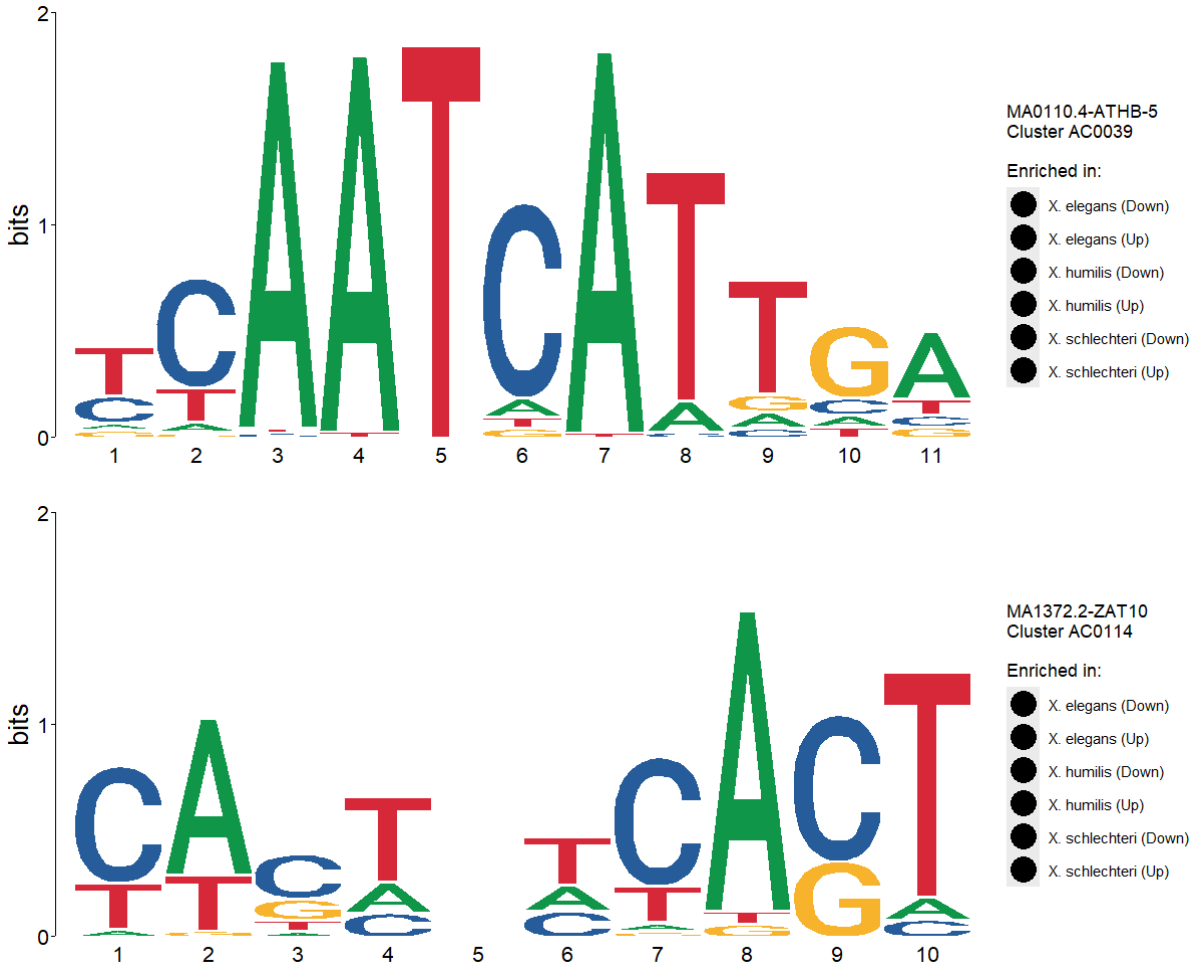

Figure 3.29. Sequence logos of ZAT motifs in the promoters of *Xerophyta* genes. Motif clusters were generated through aligning motif sequences by TOMTOM and hierarchical clustering based on e-values.

Among the up-regulated OGs in *X. elegans*, *X. schlechteri* and *X. humilis,* 61 contained the ZAT motif. Only one OG, protein NRT1/ PTR FAMILY 2.13 (NFP) was common across the three species (Fig 3.30a). NFP 2.13, a low-affinity proton-dependent nitrate transporter

expressed in phloem, has been shown in *Arabidopsis* mutants to cause growth retardation under nitrogen-deficient conditions (Fan et al., 2009). Therefore, it is expected that the majority of GO term biological processes linked to NFP 2.13 involve phloem, transport, and stress. Examples include “phloem tube growth”, “phloem nitrate loading”, “phloem glucosinolate loading stress”, “di-/tri-peptide transport”, “cellular response to nitrogen levels”, and “response to stress” (Fig. 3.30c).

In the down-regulated category, 51 OGs containing the ZAT motif were identified, with two being common to the three *Xerophyta* species (Fig. 3.30b). One is the transcription factor TCP15, while the other remains uncharacterized. TCP15 plays a role in regulating plant growth and development (S. Li, 2015). Along with the unknown protein (At2G17290.1), these proteins are implicated in various developmental processes, including “stamen filament development”, “regulation of seed germination”, “root development”, and “regulation of timing of transition from vegetative to reproductive phase” (Fig. 3.30d).

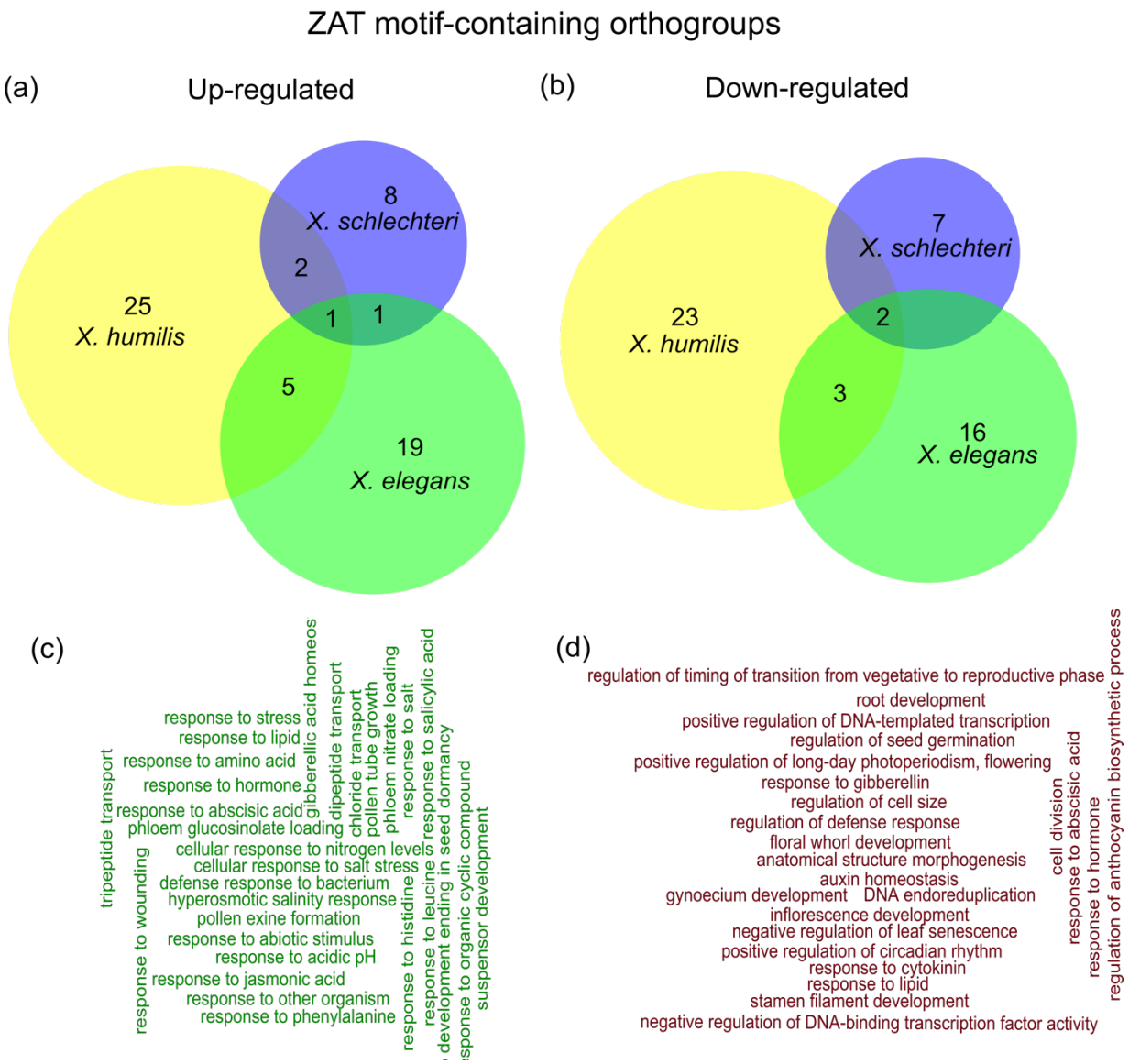

Figure 3.30. Gene ontology terms associated with ZAT motif-containing orthogroups common in three *Xerophyta* species. A GO database in GO.db R package was used to search for GO terms associated with the specified orthogroups. The GO terms were filtered to biological processes. The size of words in the wordcloud diagrams corresponds to the frequency of the GO term.

Results presented earlier in this chapter (sections 3.36-3.37) demonstrated that *ABI3A* and *ABI5A* are only expressed in early-stage seedlings during desiccation and are absent in older dry seedlings. Conversely, *ABF* genes are active in both early and late-stage seedlings of all three *Xerophyta* species, as well as in desiccated *X. humilis* leaf tissues, suggesting their role in regulating DT in these species. The B3 domain of ABI3 recognizes the RY motif (CATGCA), while the basic region of ABFs binds to the ABRE motif (ACGTG[G/T][C/A]) to regulate their respective target genes. We examined the enrichment of these motifs in the promoters of genes common to all *Xerophyta* species. As expected, the ABRE motif was

enriched in the promoters of *Xerophyta* genes, recognized by five bZIP TFs, including ABF1-4 and ABI5. These were grouped into two hierarchical clusters: cluster AC0003 (ABF1, ABF2, and ABI5) and cluster AC0006 (ABF3 and ABF4; Fig. 3.31). Notably, the RY motif was only found in up-regulated genes in *X. humilis* and *X. schlechteri*, but not in *X. elegans* (Fig. 3.31). This could be due to the absence of ABI3 and other B3 TFs in the late-stage seedlings.

ABRE motif

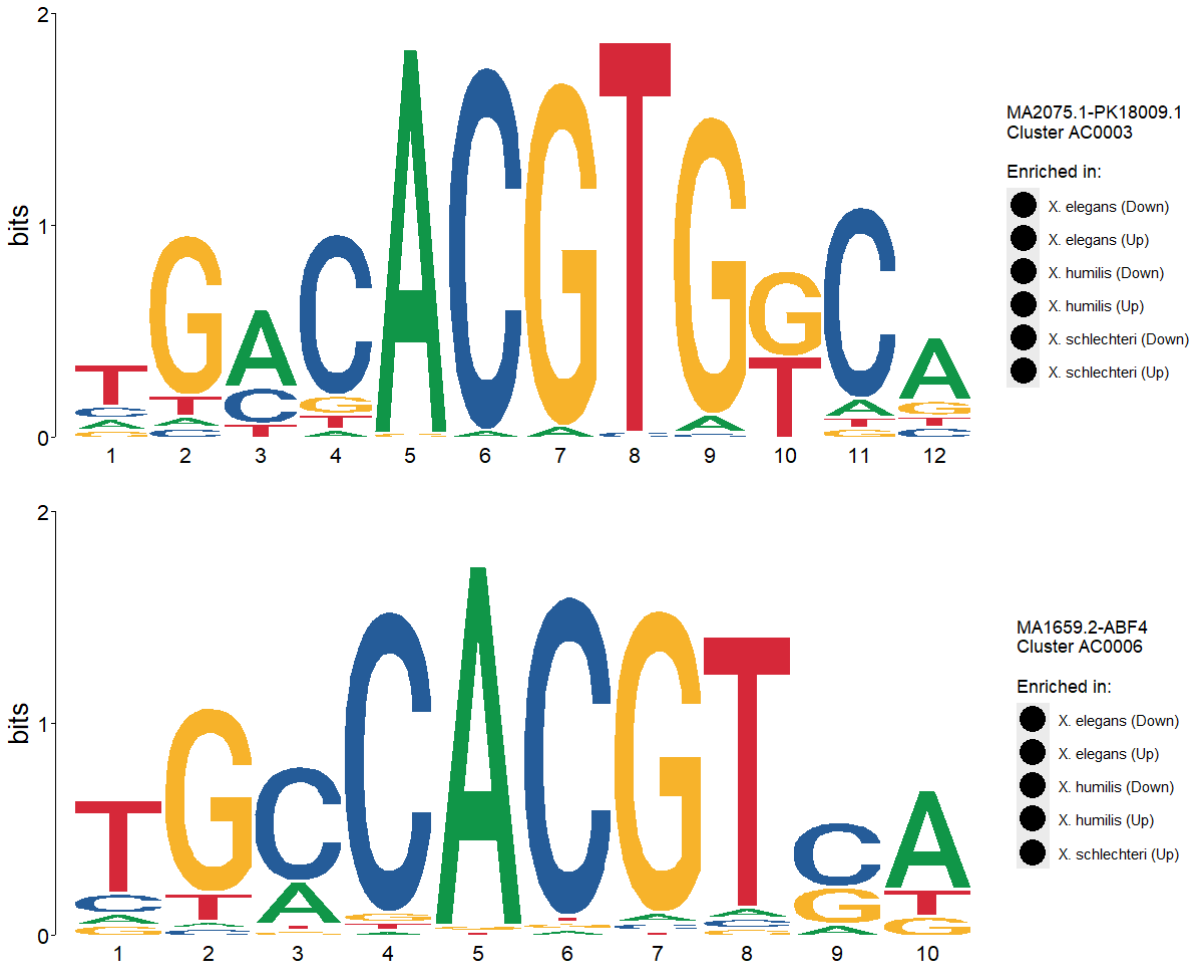

RY motif

Figure 3.31. ABRE and RY motifs enriched within the promoter regions of *Xerophyta* genes. Motif clusters were generated through aligning motif sequences by TOMTOM and hierarchical clustering based on e-values.

3.4 Discussion

Understanding the molecular mechanisms underlying VDT is crucial to unravel the adaptive strategies of resurrection plants under water-limited conditions. Previous research indicates a potential overlap in the regulatory mechanisms between seed maturation and VDT, as seen in the expression of seed maturation genes in desiccated leaf tissues (Costa et al., 2017a; Illing et al., 2005, VanBuren et al., 2017a). While Lyall et al. (2020) showed that members of the *LAFL* network and *ABI5* are silent in the desiccating leaves of *X. humilis*, it remains unclear whether they are expressed in *Xerophyta* seedlings. The work on this chapter focused on the desiccation response mechanisms employed by *Xerophyta* seedlings at the early pre-leaf and late two-leaf stages to investigate the potential differences in transcriptional control between the two developmental stages, and also identify core desiccation tolerance mechanisms conserved across the three *Xerophyta* species.

Comparing the full set of *X. humilis* transcriptomic data revealed that maturating seeds exhibit greater similarity to dry seedlings in early and late developmental stages, and desiccated adult leaves as seen by the clustering of samples on the PCA plot (Fig. 3.5). Similar expression patterns were observed in a microRNA study where desiccated *X. humilis* seed transcriptome showed similarities to desiccated roots and leaves, compared to hydrated roots and leaves (Walford, 2008). In comparison, *A. thaliana* seeds clustered completely separately from leaves and roots on a PCA plot (Walford, 2008) These results confirm the hypothesis that the

transcriptome that is active in *Xerophyta* vegetative tissues is similar to that of mature seeds, rather than a modified abiotic stress response (Illing et al., 2005).

The subsequent analysis involved directly comparing the expression of the *LAFL* network genes, and two group A bZIP family members, *ABI5* and *ABF* in *X. humilis* seeds, early-stage and late-stage seedlings, and adult leaf tissues. None of the *LAFL* network genes were expressed in the late-stage seedlings of any *Xerophyta* species, nor in the desiccating leaves of *X. humilis*. This is not surprising considering that LEC1, LEC2 and FUS3 are typically activated during the earlier stages of seed development (Fatihi et al., 2016). Specifically, LEC1 has been shown to pay an important role in the initial stages of seed maturation in *A. thaliana* but diminishes as maturation progresses (Raz et al., 2001). Our results align precisely with this pattern, as *XhLEC* and *XhFUS3* genes were barely detectable in the final stages of seed maturation in *X. humilis* (Fig. 3.9).

Elevated levels of *XhABI3A* gene in dry seeds and its up-regulation in dry early-stage seedlings is consistent with its known role in seed maturation and the acquisition of seedling DT in sensitive species (Suzuki et al., 2001). Moreover, *XhABI5A* expression levels were elevated during seed maturation and displayed constitutive expression in early-stage seedlings (Fig. 3.11). ABI5 often acts in concert with ABI3 to regulate growth arrest and confer DT re-acquisition in early-stage seedlings of *A. thaliana* and *M. trancatula* (Lopez-Molina et al., 2001). The high expression levels of *XhABI3* and *XhABI5* in dry pre-leaf seedlings of *X. humilis*, along with their absence in late-stage seedlings, implies that early-stage *Xerophyta* seedlings may utilize ABI3/ABI5 to activate the desiccation protection program, analogous to the reacquisition of DT exhibited by germinating *A. thaliana* and *M. trancatula* seedlings.

Previous research revealed that among the four group A bZIP TFs differentially expressed in *X. humilis*, only *XhABFA*, was up-regulated during desiccation in maturating seeds and desiccating adult leaves (Lyall et al., 2020). Our findings are consistent with this observation as *ABFA* was strongly induced by desiccation across all *Xerophyta* species at all developmental stages (Fig. 3.1), underscoring its role in regulating vegetative abiotic stress response (Yoshida et al., 2015).

Members of the bZIP family, such as ABF and ABI5 TFs, are known to bind to the ABRE motif. This motif is a crucial cis-regulatory element that plays a vital role in the regulation of

gene expression in response to ABA. Promoter regions of DE genes common between *X. elegans*, *X. schlechteri* and *X. humilis* species were enriched for ABRE motifs (Fig. 3.31). This suggests a conserved mechanism for ABA-mediated stress response across different *Xerophyta* species, highlighting the importance of these motifs in the regulation of genes involved in desiccation tolerance.

Further investigation into DT mechanisms in *Xerophyta* seedlings entailed GO enrichment analysis. We had hypothesised that the DE genes shared between all four *X. humilis* tissues contain core desiccation-responsive genes. This hypothesis was validated as evidenced by the GO terms associated with stress response among the up-regulated genes, while terms enriched in the down-regulated group were predominantly associated with growth and developmental processes. The results obtained from cross-species seedling comparisons echoed those observed in *X. humilis*. Interestingly, *X. elegans* and *X. schlechteri* share a significant number of GO terms that are down-regulated in response to desiccation. This observation is interesting given that the former is homoiochlorophyllous, while the latter is poikilochlorophyllous. Taking a closer look into their morphology could potentially provide insight into this phenomenon. During germination, both species typically develop radicles, roots, and first leaf tissues at the same time. Additionally, they have similar root sizes, leaf shapes, and reach the two-leaf stage in 15 days. This distinguishes them from *X. humilis*, which is characterised by thinner leaves, longer roots, and a more extended developmental period of over 30 days to reach the two-leaf stage.

To further understand regulatory mechanisms employed by the three *Xerophyta* species, we focused on the enriched motifs from three gene families that were exclusively expanded in *Xerophyta* species, namely, HSFs, AHLs and ZATs. HSFs are a family of TFs that bind to heat shock elements and regulate the expression of heat shock proteins, which act as molecular chaperones during stress conditions (Becker & Craig, 1994). HSFs have been identified in a wide range of plants including tomato (Scharf et al., 1990), *Arabidopsis* (Liu et al., 2011; Swindell et al., 2007), maize (Lin et al., 2011), and *B. hygrometrica* (Zhu et al., 2009). The high evolutionary cross-species conservation of HSFs reflects their importance as regulators of the heat shock response and other abiotic stresses (Pirkkala et al., 2001). Therefore, it is unsurprising that the promoters of the target genes of the three *Xerophyta* species under study were enriched for HSF motifs. This was evident in both up-regulated and down-regulated target genes. Among the nine HSF motif-containing OGs conserved across *Xerophyta* species was a

WRKY transcription factor. WRKY TFs are a large family of proteins in plants that are characterized by the WRKY domain, that binds to W-box motifs in the promoters of target genes (Chen et al., 2019). They play key roles in regulating plant responses to biotic and abiotic stresses, development, and metabolism (Li et al., 2023).

Apart from WRKY TFs, another HSF motif-containing OG that was up-regulated in response to desiccation in *Xerophyta* seedlings was stachyose synthase, an enzyme which contributes to the raffinose family oligosaccharide (RFO) accumulation in seeds (Gangl & Tenhaken, 2016). This enzyme is particularly pivotal for the synthesis of stachyose, which, along with other RFO members, accumulates during desiccation. Increased expression levels of stachyose were observed in desiccated leaves of three *Craterostigma* species; *C. plantagineum*, *C. agnewi* and *C. pumilum* (Egert et al., 2015). Interestingly, stachyose appeared as the dominant RFO accounting for approximately 50% of total RFOs in these three species (Egert et al., 2015). This dominance highlights its crucial role in protecting cells against stresses associated with desiccation, suggesting its importance in DT mechanisms.

In addition, other OGs containing HSF motif that were up-regulated in dry tissues include solanesyl-diphosphate synthase 2 which is involved in the synthesis of isoprenoids, organic compounds that can have protective roles against pathogens and environmental stresses (Lai et al., 2014); respiratory burst oxidase homolog protein C, which is a calcium-dependent NADPH oxidase that generates superoxide (Foreman et al., 2003); and cytochrome b561 and DOMON domain-containing protein, which may function as a trans-membrane electron transporter, possibly regulated by catecholamines (Verelst & Asard, 2004). Catecholamines are compounds whose synthesis is regulated by stress conditions, however, their roles are poorly understood. Additionally, several desiccation-induced OGs were annotated as gene families of unknown function. Their conserved response in the three *Xerophyta* species points towards their function in survival of desiccation conditions.

Although HSFs are well known for their stress response functions, it has been noted that they may also be involved in non-stress roles such as embryonic development, cellular differentiation and roles during cell cycle (Pirkkala et al., 2001). We have also identified three conserved HSF motif-containing OGs in the down-regulated target genes of *X. elegans*, *X. schlechteri* and *X. humilis* during desiccation. These include Rhamnogalacturonan I (RG-I) rhamnosyltransferase 1, B3 domain-containing protein Os02g0683500, and Endoglucanase 23.

Rhamnosyltransferase is a member of the glycosyltransferase family involved in the formation of RG- I, which is a major plant cell wall pectic polysaccharide (Wachananawat et al., 2020). The B3 domain-containing protein is associated with RAV6 and was found to regulate cell wall bound invertases in Sugarcane (Banerjee et al., 2022). The GO term analysis showed that these proteins are involved in a lot of developmental processes such as shoot system development, lateral root development, regulation of leaf morphogenesis, and post embryonic development (Fig. 3.25). This signifies that HSFs play a role in the regulation of some developmental processes under normal cellular conditions, which are shutdown during desiccation stress.

The analysis of AHL motif-containing OGs revealed a significant overlap of more than 250 OGs shared among the three *Xerophyta* species, in both up-regulated and down-regulated groups (Fig. 3.28). Within these OGs, the JASPAR database identified four different types of AHLs: AHL12, AHL13, AHL20 and AHL25. Homologs of these AHLs have been previously identified in *Arabidopsis*, which contains a total of 29 AHLs in its genome (Lu et al., 2010). All AHL proteins are characterised by an AT-hook motif and a highly conserved PPC (plants and prokaryotes conserved) domain. Furthermore, it has been shown that AHLs are involved in chromatin remodelling through their ability to bind to AT-rich regions of DNA (Lim et al., 2007), influencing the structure and accessibility of chromatin to regulate gene expression.

AHLs participate in a wide range of functions, including the regulation of plant growth and development, as well as stress responses. This is evidenced by the high number of stress-related GO terms such as response to water deprivation, response to oxidative stress and response to salt stress, present in the up-regulated AHL motif-containing OGs identified in this study. Interestingly, the down-regulated group exhibited a mixture of both developmental processes and stress-related GO terms (Fig. 3.28). This suggests that AHLs may exhibit bifunctional regulatory roles. Similar patterns have been observed in pathogen stress responses, where some members, such as AHL13, positively regulate the immune response against pathogens, while others, including AHL20 and AHL27, act as negative regulators of plant innate immunity (Lu et al., 2010).

While AHLs have been studied in various plant species, research specifically focusing on their role in resurrection plants remains relatively limited. Further investigation into the function of

AHLs in these species could provide valuable insights into the mechanisms underlying their VDT ability.

The last expanded gene family in *Xerophyta* species was the ZATs, which only had 3 conserved ZAT-motif containing OGs (Fig. 3.30). The only up-regulated protein which was conserved across *X. elegans*, *X. schlechteri* and *X. humils*, was the NRT1/ PTR FAMILY 2.13 (NFP). Members of the NFP family generally function in the transportation of a large variety of substrates, including dipeptides, nitrate, nitrite, chloride, glucosinolates, and amino acids, as well as several plant hormones including auxin, abscisic acid, jasmonates and/or gibberellins (Corratgé-Faillie & Lacombe, 2017). In particular, NFP2.13 is expressed in the phloem in *Arabidopsis* and is involved in the distribution of nitrate and peptides throughout the plant (Fan et al., 2009). GO terms, associated with NFP2.13 identified in *Xerophyta* species, are related to the transportation of most of the abovementioned substrates, signifying the conservation of NFP functions across various plant species, including the desiccation sensitive ones.

3.5 Conclusion

In summary, *Xerophyta* seedlings are desiccation tolerant at different stages of development when subjected to slow drying conditions under more physiological, controlled conditions in a plant growth chamber. The up-regulation of *ABIA* and *ABI5A* genes in the dry tissues of early-stage seedlings suggests that *Xerophyta* seedlings at this developmental stage employ *ABI3/ABI5* genes to activate the desiccation protection programme similar to *A. thaliana s* and *M. trancatula* seedlings. Neither *ABI3A* nor *ABI5A* were expressed in the dry two-leaf seedlings of *Xerophyta* species as well as the adult leaf tissues of *X. humilis*, suggesting that the older seedlings may rely on a different set of TFs for DT acquisition. Notably, the *ABFA* bZIP member was significantly induced by desiccation at all developmental stages across the three species, suggesting a potential role in VDT. The three-way comparison revealed 370 up-regulated and 335 down-regulated OGs in *Xerophyta* species, and these potentially represented a core set of desiccation-responsive genes. These core genes were enriched with binding sites for HSF, AHL and C_2H_2 ZAT TF families. Members of these families are conserved across all three *Xerophyta* species and are involved in desiccation responses believed to enhance their VDT ability. Of particular note are HSF motif-containing OGs including WRKY transcription factor, stachyose synthase and solanesyl-diphosphate synthase 2 which were up-regulated in

dry tissues and have been shown to play important roles in various desiccation response processes.

CHAPTER 4

The Analysis of Metabolites and Lipids in Hydrated and Desiccated Seedlings of three *Xerophyta* Species

4.1 Introduction

Plants synthesize a wide array of metabolites which are typically classified into two main groups: primary metabolites, highly conserved in most organisms, and secondary, also known as specialized metabolites, which vary from plant to plant. Primary metabolites such as carbohydrates, amino acids and organic acids play direct roles in supporting plant growth and development (Fernie & Pichersky, 2015).

While primary metabolites primarily support plant growth, previous research indicates the significant involvement of a subset in the desiccation response (Dace et al., 2023b; Oliver et al., 2011; Sun et al., 2018). Sugars, a key component of primary metabolites, have been shown to play a crucial role in this regard (Liu et al., 2024). During dehydration, the hydroxyl groups of sugars replace water molecules, aiding in the formation of glassy fluids within the cytoplasm in conjunction with proteins (Zhang & Bartels, 2018). This mechanism helps in adjusting cellular osmotic potential and stabilizing essential macromolecules and cellular structural components (Liu et al., 2024).

Of particular note is the accumulation of sucrose and raffinose family oligosaccharides (RFOs) observed during water deficit conditions in various resurrection plants, including *X. viscosa* (Peters et al., 2007), *C. plantagineum* (Egert et al., 2015), and *X. schlechteri* (Radermacher et al., 2019). Interestingly, the accumulation of RFO members such as raffinose, stachyose and verbascose can vary across species during desiccation. For example, while stachyose predominates in dry *C. plantagineum* leaves, *X. viscosa* exhibits increased levels of raffinose (Egert et al., 2015; Peters et al., 2007). But despite these differences in RFO proportions, it appears that the acquisition of DT remains unaffected. This could imply that the function performed by RFO sugars is generic and is not specific to a single member of this group.

Plants also produce a wide array of secondary metabolites to help them overcome various biotic and abiotic stresses imposed to them. These can be grouped into four major classes, terpenoids,

alkaloids, phenolic compounds and flavonoids (Hartmann, 2007). Many of these compounds have been observed to increase in abundance in response to desiccation in different resurrection plants including *B. hygrometrica* (Sun et al., 2018) and *H. rhodopensis* (Gechev et al., 2013; Moyankova et al., 2014) and *Selaginella lepidophylla* (Yobi et al., 2012). For instance, α-tocopherol, the lipid soluble antioxidant known for safeguarding plant cells against oxidative stresses, showed increased levels in the desiccated tissues of both *H. rhodopensis* and *B. hygrometrica*, mirroring findings in other resurrection plants such as *S. stapfianus* (Oliver et al., 2011).

In addition to the modulation of secondary metabolites, lipids also play an important role in DT, particularly in safeguarding the integrity of cellular membranes, which are the primary targets of damage during dehydration stress. Maintaining membrane integrity is vital for the survival of plants under such conditions. During desiccation, lipid composition undergoes alterations aimed at enhancing membrane stabilization (Torres-Franklin et al., 2007). Monogalactosyldiacylglycerol (MGDG) and digalactosyldiacylglycerol (DGDG) are two predominant lipids found in thylakoid membranes and are among lipids that undergo significant changes under severe conditions (Kelly & Dörmann, 2004). For example, in *C. plantagineum*, profound changes occurred in membrane lipid composition, while the total lipid content remained constant during desiccation and rehydration, indicating the plant's ability to maintain membrane stability (Gasulla et al., 2013). Among these changes, a notable shift included a decrease in MGDG, accompanied by an increase in DGDG and oligogalactolipids (Torres-Franklin et al., 2007). The conversion of MGDG into DGDG and oligogalactolipids contributes to membrane stabilization during dehydration (Gasulla et al., 2013).

Previous metabolic studies have offered valuable insights into some of the mechanisms underlying VDT in various resurrection plants (Table 4.1). However, our understanding of metabolic changes in plants still lags behind that of RNA, and to a lesser extent, protein. This could be due to the inherent complexity of metabolic pathways and the challenges associated with studying metabolites comprehensively. Unlike RNA, which can be analysed using global approaches such as microarrays and RNA-Seq, metabolites present unique analytical challenges due to their diverse chemical properties and dynamic nature. The comprehensive analysis of metabolites requires advanced analytical techniques capable of detecting and quantifying thousands of metabolites simultaneously. Several analytical techniques have been used, with nuclear magnetic resonance (NMR) spectroscopy and mass spectrometry (MS)

emerging as the predominant methods in metabolomics research. Although NMR is highly reproducible and quantitative, one of the disadvantages is that it has low sensitivity and resolution for complex mixtures (Emwas, 2015). On the other hand, MS stands out for its exceptional sensitivity, allowing for the simultaneous analysis of numerous metabolites, ranging from hundreds to thousands, in a single measurement and with regularity (Bedair & Sumner, 2008). In contrast to NMR, MS is superior in enabling the analysis of secondary metabolites at detection levels ranging from picomoles to femtomoles (Bedair & Sumner, 2008).

In recent years, advancements in MS and chromatography have revolutionized metabolomics research by enabling high-throughput and comprehensive analysis of metabolites. Typically, in MS analysis, metabolites undergo chromatographic separation through liquid chromatography, gas chromatography or electrophoresis before detection, and various MS techniques are often employed to analyse different classes of metabolites, facilitating a broader coverage of the metabolome. Gas chromatography-mass spectrometry (GC-MS) and liquid chromatography-mass spectrometry (LC-MS) are two widely used platforms for metabolite analysis, each offering unique advantages and capabilities. GC-MS is well-suited for volatile and semi-volatile metabolites, offering high resolution and sensitivity for compounds amenable to gas-phase separation (Kanani et al., 2008). On the other hand, LC-MS excels in the analysis of polar and non-volatile metabolites, providing excellent separation and detection capabilities for a wide range of compounds (Emwas, 2015).

A combined GC-MS and LC-MS approach is best in overcoming the limitations of individual analytical platforms and achieving comprehensive coverage of the metabolome. This integrative approach allows for a deeper exploration of the dynamic changes in metabolites and lipids, which are crucial for understanding the mechanisms that enable resurrection plants like *Xerophyta* species to acquire DT. By leveraging both GC-MS and LC-MS, we can gain a holistic view of the metabolomic and lipidomic changes that occur during desiccation.

4.1.1 Aim and Objectives

The aim of this chapter was to investigate desiccation-induced changes in the metabolite and lipid profiles of three *Xerophyta* species: *X. elegans, X. schlechteri* and *X. humilis,* at early pre-leaf and late two-leaf seedling stages.

The objectives were:

i. to perform GC-MS and LC-MS analyses to quantify changes in the levels of primary and secondary metabolites, along with lipids, between early and late-stage *Xerophyta* seedlings under hydrated and dehydrated conditions,

ii. to identify metabolites and lipids that change in abundance in desiccated versus hydrated seedlings across all three *Xerophyta* species at the early and late developmental stages,

iii. to identify metabolites and lipids that distinguish the two poikolochlorophyllous species (*X. schlechteri* and *X. humilis*) from the hoimoichlorophyllous species (*X. elegans*) in both seedling stages in response to desiccation.

Table 4.1. Summary of published papers on metabolomic and lipidomic studies from resurrection plants

Species	Treatments	Metabolites/Lipids identified	Detection methods	Reference(s)
Barbacenia purpurea	H: Control (day 0) D: 8, 16, 20, 24 days R: 12, 36, 84, 132 hours	Primary metabolites	GC-MS UPLC	Suguiyama et al., 2014
Haberlea rhodopensis	H: 90% RWC D: 35, 20, 6% RWC R: 75 and 90% RWC	Primary and secondary metabolites	GC-MS HPLC	Moyankova et al., 2014
Haberlea rhodopensis	H: Well-watered D: 42 and 4% RWC R: 4 days	Primary and secondary metabolites	GC-MS LC-MS	Getchev et al., 2013
Sporobolus stapfianus	H: Fully hydrated D: 60, 50, 40, 20% RWC and fully desiccated	Primary and secondary metabolites	GC-MS UHLC/MS/MS^2	Oliver et al., 2011
Selaginella lepidophylla	H:100% RWC D: 50% RWC	Primary and secondary metabolites	GC-MS UHLC/MS/MS^2	Yobi et al., 2012
Eragrostis nindensis, Myrothamnus flabellifolia, Craterostigma pumilum, Selaginella dregei, Xerophyta elegans, Xerophyta humilis, and *Xerophyta schlechteri*	H: Full hydration D: 30-50% RWC and desiccated	Primary metabolites	GC-MS	Dace et al., 2023
Craterostigma plantagineum	H: Control (day 0) D: 2 and 14 days R: 1 and 2 days	Lipids	Q-TOF MS/MS	Gasulla et al., 2013

Xerophyta humilis	H: 100% RWC D: <9% RWC R: 12, 24, 36 and 48 hours	Lipids	HPLC/MS, MRM	Tshabuse et al., 2018
Boea hygrometrica	H: Fully hydrated D: 14 days R: 3 days	Primary metabolites	GC-TOF/MS	Sun et al., 2018

H – hydrated, D- desiccated, R – rehydrated

GC-MS - Gas Chromatography-Mass Spectrometry

Q-TOF MS/MS - Quadrupole Time-of-Flight Mass Spectrometry

HPLC MS - High-Performance Liquid Chromatography Mass Spectrometry

UHLC/MS/MS - Ultra-High-Performance Liquid Chromatography/Tandem Mass Spectrometry

MRM - Multiple Reaction Monitoring.

4.2 Materials and Methods

4.2.1 Seed Sterilization, Seed Germination and Drying Down Experiments

Xerophyta seeds were sterilized prior to germination as described in Chapter 3, sections 3.2.2.2 and 3.2.2.4. As detailed in section 3.2.2.4 of the previous chapter, matched datasets for RNA-Seq and lipids/metabolites were generated by drying down seedlings at pre-leaf and two-leaf stages for 48 hours. Both hydrated and dehydrated seedlings were flash frozen in liquid nitrogen and stored at -80 ºC for subsequent use in metabolite and lipid extractions. Initially, only three biological replicates were prepared for these experiments. However, an additional set of triplicates was later prepared under the same conditions (increasing the number of biological replicates to six) in order to obtain better estimates of the mean levels of each metabolite.

4.2.2 Metabolite and Lipid Extractions

Primary metabolites, secondary metabolites, and lipids were extracted from hydrated and desiccated *X. elegans, X. schlechteri* and *X. humilis* pre-and two-leaf seedlings (Hummel et al., 2011). Frozen samples in 2 mL microfuge tubes were loaded onto pre-cooled Retsch ball mill (MM400) sample adaptors and pulverized at a frequency of 20 hertz for 1 minute. Pulverized tissues were immediately submerged into liquid nitrogen to avoid thawing before adding 1 mL of pre-cooled (-20 °C) extraction buffer [0.5 μg/mL corticosterone, 0.25 μg/mL (w/v) ampicillin, 0.5 μg/mL adonitol] and vortexed until fully resuspended. Samples were incubated on an orbital shaker at 4 °C for 10 minutes, followed by an additional 10-minute incubation in an ultrasonication bath at 100% amplitude. The sonication was performed using a pulse-on time of 20 seconds and a pulse-off time of 40 seconds. To prevent sample heating, ice was added to the bath, and the temperature was continuously monitored to maintain it below 8 °C. Next, 500 μL of water:methanol (3:1) ultraperformance liquid chromatography (UPLC) grade mixture was added and mixed by vortexing, and then centrifuged at 13 000 x g for 5 minutes at 4 °C. A total volume of 500 μL of the upper organic phase was transferred into a clean 1.5 mL microfuge tube, and of this, 300 μL was removed and spared for lipid analysis. Of the lower polar phase, 150 μL was used for GC-MS analysis of primary metabolites and 300 μL for LC-MS analysis of secondary metabolites. Extraction blank samples were also prepared and processed as described above except that they did not contain any plant material.

The lipid, polar GC, and LC extracts were concentrated in the SpeedVac (Savant SpeedVac Plus SC210A), overnight, and then sent to the Max Planck Institute (MPI) of Molecular Plant Physiology in Potsdam-Golm, Germany for GC-MS and LC-MS analyses.

4.2.3 GC-MS for Primary Metabolite Analysis

The primary metabolite samples were derivatized by adding 40 µL of methoxyamine hydrochloride (20 mg/mL in Pyridin) and shaking for 2 hours at 37 °C. Thereafter, they were briefly centrifuged at 14 000 x g before 70 µL of N-Methyl-N-trimethylsilyltrifluoroacetamide (MSTFA) was added for an additional agitation for 30 minutes at 37 °C. Following this, the samples were centrifuged for 1 minute at 14 000 x g and 70 µL of the supernatant was transferred to GC vials with inserts for GC-MS analysis.

To inject the samples into a gas chromatograph coupled to a time-of-flight mass spectrometer (Leco Pegasus HT TOF–MS; LECO Corporation, St. Joseph, MI, USA), an autosampler Gerstel Multi-Purpose system (Gerstel GmbH & Co.KG, Mülheim an der Ruhr, Germany) was used. Helium was used as carrier gas at a constant flow rate of 2 mL s−1, and GC was performed on a 30-m DB-35 column. The injection temperature was 230 °C, and the transfer line and ion source were set to 250 °C. The initial temperature of the oven (85 °C) increased at a rate of 15 °C/min up to a final temperature of 360 °C. After a solvent delay of 180 seconds, mass spectra were recorded at 20 scans s^{-1} with a mass-to-charge ratio (m/z) of 70 to 600 scanning range. Chromatograms and mass spectra were evaluated using Chroma TOF 4.5 (Leco) and TagFinder 4.2 software (Lisec et al., 2006).

4.2.4 LC-MS for Secondary Metabolite Analysis

The vacuum-dried polar phases were resuspended in 170 µL of 50% (v/v) methanol and incubated for 5 minutes at toom temperature before briefly vortexing and sonicating them for 3 minutes. All samples were then briefly vortexed and centrifuged at 14 000 x g for 4 minutes, followed by transferring 90 µL of the supernatant to LC vials with insert for analysis. Samples were analysed using a Waters Acquity UPLC system (Waters, Mildford, MA, USA) following the protocol outlined in (Giavalisco et al., 2009). This system had an HSS T3 C18 reverse phase column (100 × 2.1 mm i.d. 1.8 µm particle size, Waters) maintained at 40 °C. Mobile phases comprised 0.1% (v/v) formic acid in water (Solvent A) and 0.1% (v/v) formic acid in acetonitrile (Solvent B). The mobile phase flowed at a rate of 400 µL/min, and sample injection

was 2 µL per run. Gradient conditions were as follows: a hold at 1% solvent B for 0−1 minute, a linear gradient from 1% to 35% B for 1−13 minutes, a linear gradient from 35%−70% B for 13−14.5 minutes, a linear gradient from 70%−99% B for 14.5−15.5 minutes, a linear gradient to 1% B for 17-17.5 minutes, and a final hold at 1% B from 17.5-20 minutes.

This UPLC system was coupled to an Exactive Orbitrap-focus (Thermo Fisher Scientific) via a heated electrospray source. The spectra were recorded in full-scan positive and negative ion-detection mode, covering a mass range from m/z 100 to 1,500, with a resolution of 70 000 and a maximum scan time of 250 ms. The sheath gas was set to a value of 60 while the auxiliary gas was set to 35. The transfer capillary temperature was 150 °C, and the heater temperature was adjusted to 300 °C. The spray voltage was fixed at 3 kV, with a capillary voltage and skimmer voltage of 25 V and 15 V, respectively. MS spectra were recorded from minutes 0 to 19 of the UPLC gradient.

4.2.5 LC-MS for Lipid Analysis

The lipid pellets were resuspended by adding 150 µL 1:1 (v/v) acetonitrile:isopropanol mixture and vortexing gently. Sonication and centrifugation were performed as described in section 4.2.4, and then 90 µL was transferred into LC vials. Thereafter, the samples were analysed using UPLC (on a C8 reverse-phase column) coupled with Fourier transform mass spectrometry (Exactive mass spectrometer, Thermo Fisher) in positive and negative ionization modes as described in (Giavalisco et al., 2011).

4.2.6 Processing of Raw Chromatograms

The processing of chromatograms, peak detection, and integration of metabolites and lipids were performed using RefinerMS (version 5.3; GeneData). The two GeneData output files of each batch, each comprising three biological replicates across all species, were then aligned to one another so that only clusters with matching m/z's and retention times in both batches were retained. Here, an error of +- 0.15 min was allowed for the retention time and +- 0.005 was permitted for a m/z match. Next, peak picking was performed manually by examining the chromatograms of pooled samples in Thermo Scientific Xcalibur™ software (version 4.3) and selecting suitable features from the GeneData output. Some of the resulting features were identified by aligning the GeneData output to the MPI Golm metabolome database.

About 10 ppm mass error was allowed, and a dynamic retention-time shift of 0.1 relative to the MPI database. This also retrieved additional peaks that were not initially picked above. Of these, only those with an intensity less than 10^7 in all replicates within at least one sample group were retained in the final data matrix. The remaining unknown metabolites, particularly secondary metabolite peaks of interest, were annotated by inspecting the tandem MS (MS/MS) fragments and searching for masses or candidate compounds in MassBank, HMDB and the resurrection plant literature. The retention time, similarity of the spectra and correlation to known compounds was taken into consideration. The resulting annotated data matrix for primary metabolites, secondary metabolites, and lipids, was then log2 transformed and missing values were replaced by 1/10th of the minimum value across all samples for a given feature. In addition, a batch effect correction using the ComBat R function was applied to combine the two sample batches. The downstream statistical analysis was performed in R (version 1.3.1).

4.2.7 Statistical Analysis

Significance testing for all metabolites and lipids within each developmental stage of the three species was conducted using ANOVA. The analysis examined the interaction between water content (condition) and species to assess changes in metabolite levels. The model used was structured as: metabolite level = species | water content. The p-value for water content was used to assess significant differences in metabolite abundance between hydrated and dehydrated tissues. A significance criterion of Benjamini-Hochberg adjusted p-value of < 0.05 was applied. Further, compounds that increased in abundance were identified by fold change (FC) > 1 and BH adjusted p-value < 0.05, while those that decreased in abundance were determined by FC < 1 with BH adjusted p-value < 0.05.

4.3 Results

4.3.1 Metabolite and Lipid Profiles in the Early and Late-stage Seedlings

The analysis of primary metabolites, secondary metabolites, and lipids was performed on samples that were extracted from pre-leaf and two-leaf seedlings of *X. elegans*, *X. schlechteri* and *X. humilis,* under both hydrated and dehydrated conditions. Primary metabolites underwent GC-MS analysis, while secondary metabolites and lipids were analysed via LC-MS prior to GeneData processing for peak identification. The gene data output resulted in 159 raw primary metabolites, 236 secondary metabolites, and 212 lipids across the sample set. After applying peak picking and filtering methods described in section 4.2.6, the dataset was refined to 78

primary metabolites, with 69 annotated and 9 unidentified. Among secondary metabolites, 174 remained after filtering, comprising 131 annotated compounds and 43 unknowns. Additionally, 132 lipids were included in the final dataset, all of which were annotated.

To assess the clustering of primary and secondary metabolites and lipids across six independent biological replicates, PCA plots were employed. The first point of focus was to verify the reproducibility of the independent biological replicates and to observe patterns of each species' response to desiccation at the two stages of development.

Figure 4.1 shows that all the biological replicates in each species, seedling stage, and condition cluster together, confirming the reproducibility of the datasets. For both *X. elegans* and *X. schlechteri,* the separation of primary metabolite, secondary metabolite, and lipid datasets in PC1 is clearly based on the developmental stage, where the early-stage seedlings are segregated from the late-stage seedlings (Fig. 4.1a-f). Additionally, along PC2, the separation is on the basis of condition (water content), with hydrated samples clustering away from the dehydrated ones across all three datasets (Fig. 4.1a-f). In *X. humilis*, all three datasets; primary metabolites, secondary metabolites, and lipids are also separated based on developmental stage in PC1. However, unlike all the other datasets, the primary metabolite samples for hydrated and dry early-stage *X. humilis* seedlings cluster together on PC2 (Fig. 4.1g). This may be due to the developmental timing of *X. humilis* seedlings. For example, *X. humilis* germinates and grows rapidly during the early developmental stages compared to *X. elegans* and *X. schlechteri*. This fast growth might prioritize early biomass accumulation over the development of robust stress responses, which could lead to more similar metabolic profiles in the pre-leaf stage seedlings.

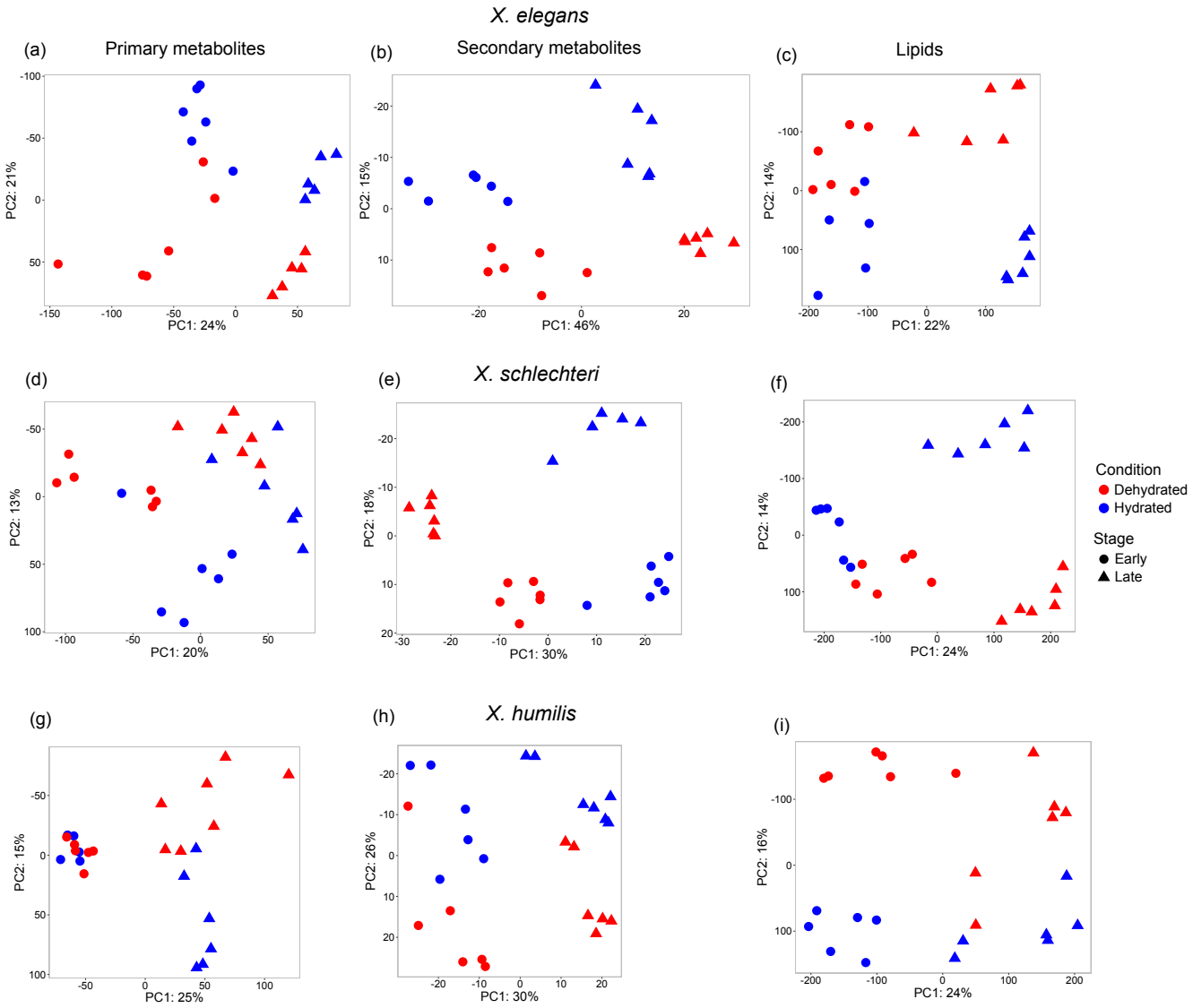

Figure 4.1. PCA analysis of primary and secondary metabolites and lipids in hydrated and dehydrated seedlings at early and late-stages for three *Xerophyta* species. As specified in the key on the right, the blue points in the plots represent hydrated samples, and the red ones show dehydrated samples. The differentiation between early and late seedling stages is denoted by circle and triangle shapes, respectively for *Xerophyta elegans* (a-c), *Xerophyta schlechteri* (d-f) and *Xerophyta humilis* (g-i).

The datasets were combined on a single PCA plot for all three species to investigate how similar the response of the primary and secondary metabolome and lipidome for the three *Xerophyta* species was to desiccation (Fig. 4.2).

The separation of the primary metabolites is not species-specific, and variation explained by PC1 is relatively low. However, there is a clear distinction of primary metabolites between the early-stage and late-stage seedlings (Fig. 4.2a). In contrast, secondary metabolites show clear

species-specific clustering, with sub-clustering by developmental stage within each species (Fig. 4.2b). *X. schlechteri* is positioned on the right side of the positive component of PC1, while *X. elegans* and *X. humilis* are located on the opposite sides of the plot and are separated from each other by PC2 (Fig. 4.2b). These patterns suggest that each species has a distinct complement of secondary metabolites. Similarly, the separation of lipid samples is not species-specific, as seen in primary metabolites. However, lipid profiles in *X. schlechteri* and *X. humilis* tend to cluster on the negative side of PC1, while *X. elegans* is predominately positioned on the positive side (Fig. 4.2c), indicating that *X. schlechteri* and *X. humilis* exhibit similar lipid patterns.

Although this analysis provides an overall view of metabolite and lipid patterns between hydrated and dehydrated seedlings of *Xerophyta* species (Fig. 4.2), it does not distinctly illustrate the effect of desiccation on specific metabolites and lipids in seedlings at early and late developmental stages. The next step was to analyse each of the species individually by heatmap to investigate the effects of water content on the changes in the levels of primary metabolites, secondary metabolites, and lipids in both developmental stages across all three *Xerophyta* species.

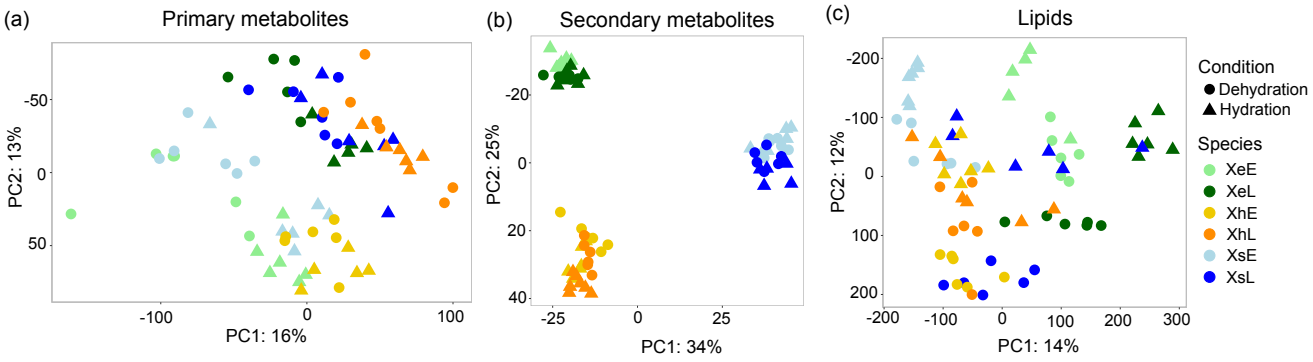

Figure 4.2. PCA analysis of metabolic and lipid profiles in three *Xerophyta* seedlings. As indicated in the key provided on the right, the two shades of the green points correspond to *Xerophyta elegans* (Xe), the light and dark blue coloured points correspond to *Xerophyta schlechteri* (Xs), and the yellow and orange points represent *Xerophyta humilis* (Xh). The E and L letters stand for early and late-stages, respectively. The distinction between hydrated and dehydrated is denoted by circle and triangle shapes, respectively.

4.3.2 Changes in the Abundance of Primary Metabolites during Desiccation

Primary metabolites are fundamental compounds involved in essential metabolic processes for plant growth. Understanding the dynamics of these metabolites can provide insights into how *Xerophyta* species at two stages of seedling development respond to changes in water content during desiccation. To examine changes in primary metabolites, we conducted a comprehensive analysis of sample means across all species and conditions using ANOVA with BH adjusted p-value threshold of less than 0.05. Among the 78 primary metabolites in the refined dataset, significant abundance changes were observed in 23 primary metabolites at early-stage seedlings, and 26 primary metabolites at late-stage seedlings in response to desiccation, across all the three *Xerophyta* species. The heatmaps illustrating the most variable metabolites in both seedling developmental stages are shown in Fig 4.3 below.

As expected, sucrose, a key sugar carbohydrate known for its vital role in DT, increased in abundance in the dry tissues of all *Xerophyta* species at both stages of development (Fig. 4.3a-b). Desiccation also led to the accumulation of glucose-6-phosphate in both early- and late-stage seedlings. Conversely, fructose, which is a subunit of sucrose, showed a decrease in abundance across all species at both seedling stages. Although glucose levels are typically expected to decrease during desiccation, our ANOVA results showed no statistically significant difference in glucose levels between hydrated and dehydrated conditions ($p > 0.05$). Beyond carbohydrate changes, certain amino acids, such as proline and tryptophan, also demonstrated increased abundance upon desiccation. Notably, these amino acids were consistently elevated in early-stage seedlings of *X. elegans*, whereas their levels remained relatively low in the other two species, particularly in *X. schlechteri* (Fig. 4.3a). Interestingly, in two-leaf seedlings, proline levels decreased in dehydrated tissues of *X. elegans*, but dramatically increased in response to desiccation in both *X. schlechteri* and *X. humilis* (Fig. 4.3b)

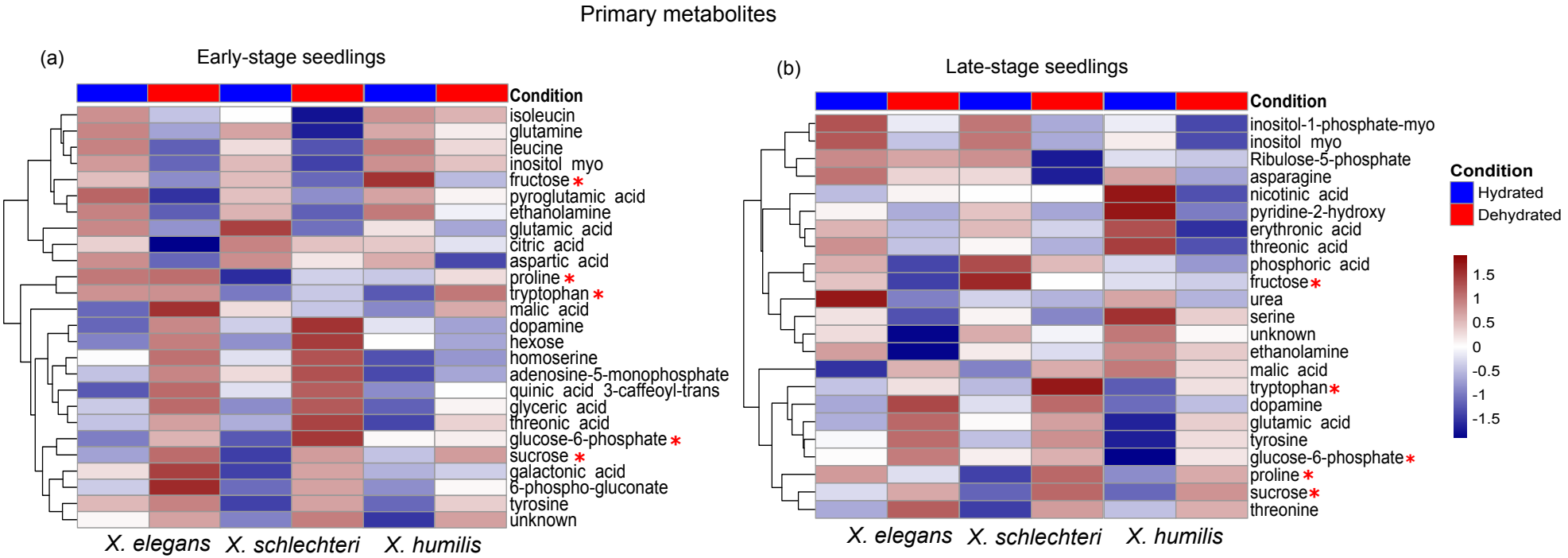

Figure 4.3. Significantly different primary metabolites between hydrated and desiccated *Xerophyta* seedlings. (a) presents a heatmap displaying compounds from the early-stage seedlings, while (b) showcases those found in late-stage seedlings across all three *Xerophyta* species. The distinction between hydrated and dehydrated states is represented by blue and red colours, respectively. The ANOVA analysis of sample means was performed with BH adjusted p-value threshold of less than 0.05.

4.3.3 Changes in the Abundance of Secondary Metabolites during Desiccation

The general trends in the changes of primary metabolites levels were largely consistent across species and developmental stages. However, while primary metabolites are important for basic physiological function of plant cells and are highly conserved, secondary metabolites are often induced in response to environmental stresses (Erb & Kliebenstein, 2020). They are found in specific tissues and vary between species. We anticipate an increased abundance of these compounds in response to dehydration as secondary metabolites are crucial for plant protection and adaptation. This analysis, along with the lipid analysis, is also expected to help us differentiate between the homoiochlorophyllous species (*X. elegans*) and the poikilochlorophyllous species (*X. schlechteri* and *X. humilis*), potentially revealing specific metabolic adaptations that contribute to their survival strategies.

A total of 164 secondary metabolites were identified in the younger seedlings, while 158 were identified in the older ones. Compounds that exhibited significant differences between hydrated and dehydrated samples were identified using ANOVA. Secondary metabolites were ranked based on the p-value for the water content term, which assesses whether metabolite levels differ between hydrated and dehydrated seedlings, regardless of species. This resulted in 68 and 69 secondary metabolites that changed in abundance in the early and late-stage seedlings, respectively. The top 40 of these metabolites, based on the p.adj < 0.05, are visualized in Fig. 4.4 on heatmaps, with clusters of interest highlighted in black rectangles.

Cluster 1 (A and B) denotes a group of metabolites in early and late-stage seedlings, that are constitutively high in abundance in both hydrated and dry tissues of *X. elegans* but behave in a desiccation responsive manner in *X. schlechteri* and *X. humilis* seedlings (Fig. 4.4 a-b). This group comprises several metabolites including “aspartyphenylalanine”, “kynurine free base” and “porphobilinogen” metabolites. The fact that these metabolites are present at high levels in dry seedlings of all three species suggests they play a key role in desiccation response. In *X. elegans,* the constitutively high levels of these metabolites in both hydrated and dehydrated tissues may indicate that this species accumulates them early as a preparatory response to stress conditions.

The second cluster (2A-B) highlights secondary metabolites induced by desiccation across all three species (Fig. 4.4a-b). Notable examples include “saponins” and “triterpenes”, which are

present in both the pre-leaf and two-leaf seedlings. In addition, some secondary metabolites that are well known for their protective role in DT were also noted. One such example is trehalose, which significantly accumulated across all three *Xerophyta* species in both developmental stages (Fig. 4.4a-b).

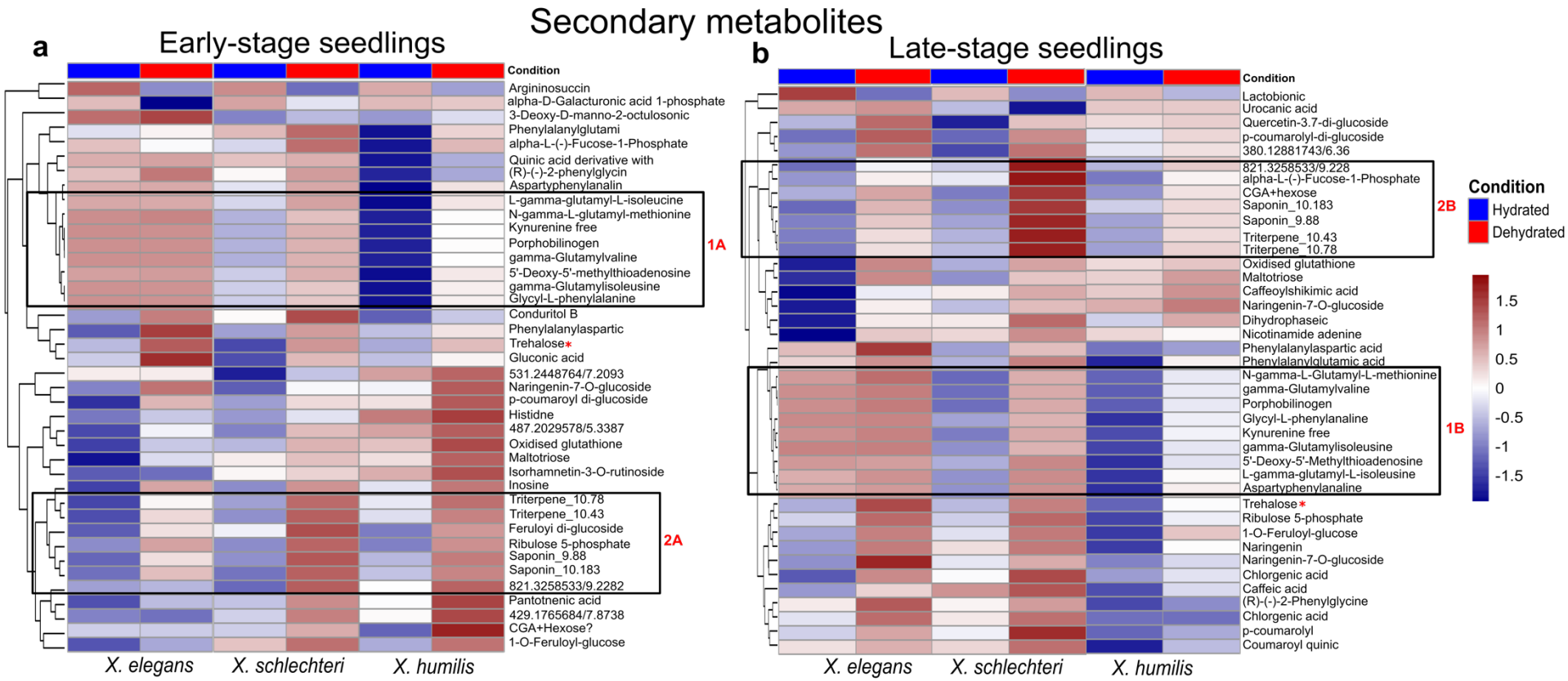

Figure 4.4. Top 40 most significantly different secondary metabolites between hydrated and desiccated *Xerophyta* seedlings. (a) presents a heatmap displaying secondary metabolites from the early-stage seedlings, while (b) showcases those found in late-stage seedlings across all three *Xerophyta* species. Clusters 1A-B and 2 A-B denote metabolites of particular interest at both stages. The distinction between hydrated and dehydrated states is represented by blue and red colours, respectively. The ANOVA analysis employed a BH adjusted p-value threshold of less than 0.05.

4.3.4 Changes in Lipid Profiles in *Xerophyta* Species during Desiccation

Building upon the analysis of primary and secondary metabolites, it is imperative to delve into the changes in lipid composition that *Xerophyta* species undergo during desiccation. Lipids play a crucial role in maintaining membrane stability and function, which are important for cellular survival under extreme water-deficient conditions. They are also integral part of the thylakoid membranes, which undergo several changes during desiccation. This section explores how lipid profiles in the early-stage and late-stage *Xerophyta* seedlings change in response to desiccation, providing a deeper understanding of the molecular mechanisms enabling these plants to withstand severe dehydration stress.

Of the 132 lipids within the refined dataset, 48 showed significant changes in abundance in both early and late-stage seedlings, as revealed by ANOVA results. Similar to primary and secondary metabolites, the p-value for the water content term was applied to assess changes in lipid profiles between hydrated and dehydrated tissues regardless of the species. These lipids were quite diverse, ranging from phospholipids and lysophospholipids, to galactolipids and glycerolipids. In the early-stage seedlings, phosphocholine (PC) lipids showed an increase in abundance in dry tissues across all three *Xerophyta* species (Fig. 4.5a). Notably, different members of Triacylglycerols (TAGs) exhibited decreased levels across all species during the early stage. TAGs were notably low in *X. schlechteri* compared to the other two species. Interestingly, changes in the abundance of lipid profiles in the late two-leaf stage seedlings was slightly different compared to the early stage. For example, TAGs accumulated in the two-leaf seedlings of all three *Xerophyta* seedlings, and particularly showed a marked increase in *X. schlechteri* tissues (Fig. 4.5b). Interestingly, MGDG and DGDG galactolipids showed a dramatic decline in dry *X. schlechteri* and *X. humilis* tissues but remained constitutively expressed in *X. elegans* (Fig. 4.5b).

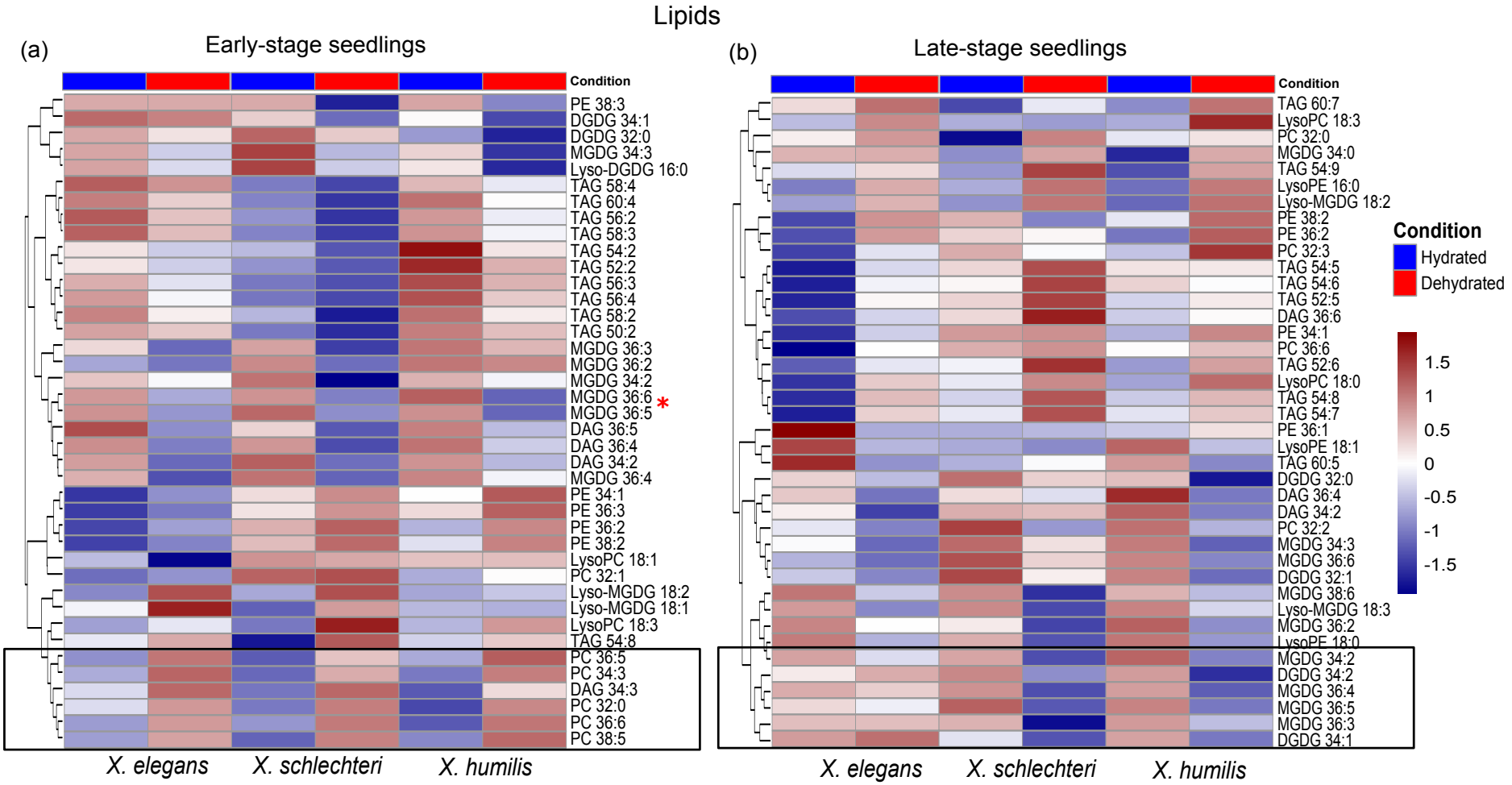

Figure 4.5. Top 40 most significantly different lipids between hydrated and desiccated *Xerophyta* seedling. (a) presents a heatmap displaying compounds from the early-stage seedlings, while (b) showcases lipids in the late-stage seedlings across all three *Xerophyta* species. The ANOVA analysis employed a BH adjusted p-value threshold of less than 0.05.

4.3.5 Differences between the Homoichlorophyllous and Poikilochlorophyllous *Xerophyta* Species

The three *Xerophyta* species examined in this study employ different strategies for protection against oxidative stress damage caused by desiccation. *X. schlechteri* and *X. humilis*, typical poikilochlorophyllous resurrection plants, lose their chlorophyll under desiccation conditions, while *X. elegans*, categorized as homoiochlorophyllous, retains its chlorophyll.

To gain insights into the metabolomic and lipidomic mechanisms that distinguish these species, we conducted a cross-species comparison across all *Xerophyta* species at both seedling stages. Our focus was specifically on analyzing changes in the up-regulation and down-regulation of secondary metabolites and lipids during both early and late stages of development. Primary metabolites were excluded from this analysis as most did not exhibit significant differences based on the volcano plot criteria (fold change > 1 and Benjamini-Hochberg adjusted p-value < 0.05) (Appendix C.1). Therefore, our attention was directed towards secondary metabolites and lipids. Secondary metabolites are typically induced in response to desiccation stress, offering species-specific adaptive advantages. Additionally, lipids, crucial components of cell membranes including thylakoid membranes, undergo notable changes during desiccation, influencing membrane integrity and function

4.3.5.1 Variations in the Abundance of Secondary Metabolites in *Xerophyta* Seedlings

To determine the differential abundance of secondary metabolites across all three *Xerophyta* species at the two developmental stages, volcano plots were generated (Appendix C.2). Subsequently, secondary metabolites that were significantly up-regulated during desiccation, as determined by a volcano plot criterion (FC > 1 and BH adjusted p-value < 0.05), were compared across the three species using a Venn diagram (Fig. 4.6). In early seedling samples, only *X. elegans* and *X. schlechteri* had metabolites that showed a statistically significant increase in abundance. However, in the *X. humilis* early-seedlings, the accumulation of all metabolites was not significant, failing to meet the predefined cut-off threshold of FC > 1 and p.adj < 0.05. Based on the clustering in PCA plot in Figure 4.1, it is not surprising that there was no significant difference between the hydrated and desiccated early-stage seedlings of *X. humilis*. A slightly lenient threshold of FC > 1 and p.adj < 0.1 was applied to all seedlings at the early stage, resulting in 19, 28 and 19 statistically significant metabolites in *X. elegans*, *X. schlechteri* and *X. humilis*, respectively. Of these, 11 were shared between *X. elegans* and *X.*

schlechteri while an overlap of 7 was present between *X. schlechteri* and *X. humilis*. Interestingly, no metabolites were common among all three *Xerophyta* species at the early-stage seedling development (Fig. 4.6a).

In late-stage seedlings, trehalose and terpenes were among secondary metabolites that were common between all three species in the late-stage seedlings. These were also present in the early seedlings, though their accumulation was statistically significant in *X. elegans* and *X. schlechteri* samples only. In addition, the metabolite "porphobilinogen" was significantly accumulated in both *X. schlechteri* and *X. humilis*, whereas its levels remained constant in *X. elegans*. It is worth noting that *X. elegans* uniquely employs flavonoids during dehydration while both poikilochlorophyllous species accumulate more dipeptides during desiccation in both pre-leaf and two-leaf seedlings (Fig. 4.6b).

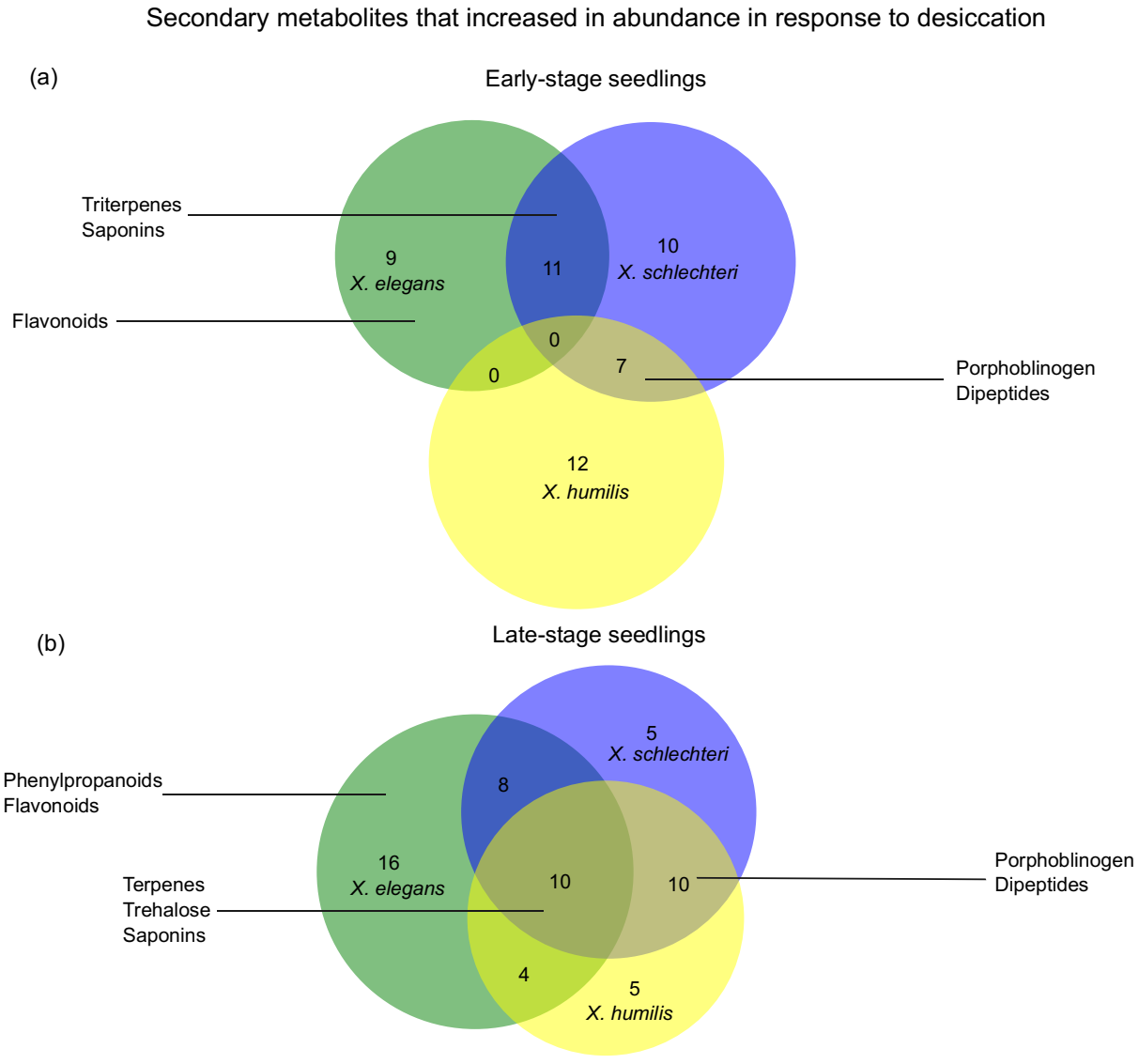

Figure 4.6. Accumulation of significantly different secondary metabolites in early and late-stage *Xerophyta* seedlings in response to desiccation. The Venn diagrams display the count of significant secondary metabolites that accumulated in response to desiccation. For early-stage seedlings, metabolites were considered significant if they had a fold change (FC) greater than 1 and an adjusted p-value (p.adj) < 0.1. For late-stage seedlings, a stricter criterion was used with an FC > 1 and a p.adj < 0.05.

4.3.5.2 Variations in the Abundance of Lipid Profiles in *Xerophyta* Seedlings

To elucidate the most significant lipid changes within each species, we employed volcano plots with a BH adj. p-value threshold of 0.05 and a FC greater than 1. Several lipid classes were notably up-regulated in response to dehydration in both the pre-leaf and two-leaf seedlings. TAGs emerged as the most prevalent lipid group, particularly TAG 54, which was consistently up-regulated across all *Xerophyta* species. TAGs demonstrated a significant increase in both early and late seedling stages (Fig. 4.7). In addition, lysophosphatidylethanolamine (LysoPE), another lipid group, was also shared among the three species and exhibited higher abundance predominantly in late-stage seedlings (Fig. 4.7b). However, it is noteworthy that LysoPE was not stage specific, as it also showed up-regulation in the early stage of *X. humilis* samples.

Moreover, two major phospholipids, phosphatidylethanolamine (PE) and PC, showed increased abundance across all species following desiccation (Fig. 4.7). Notably, some members of PE and PC also exhibited down-regulation in response to water loss. For example, PE members including PE 36:1 and PE 38:2-3, as well as PC members, such as PC 32:1-2 and PC 38:3, 5-6 (Fig. 4.7). This down-regulation was evident across all stages and species of *Xerophyta*. This dual regulation suggests a complex role for these phospholipids, possibly involving structural reorganization and signalling functions during the desiccation process.

In both seedling stages of *X. schlechteri* and *X. humilis*, we observed a diverse array of down-regulated galactolipid MGDGs, especially those containing 36 carbon atoms with double bonds ranging from 2 to 6 (MGDG 36:2-6), as well as MGDG 34. Among the down-regulated lipid groups, MGDG was the most prevalent (Fig. 4.7). Notably, MGDG did not show any significant changes in older *X. elegans* seedlings, showing down-regulation only in the younger ones (Fig. 4.7a, d). This observation is consistent with MGDG's role in chloroplast membranes, as its down-regulation in *X. schlechteri* and *X. humilis* during desiccation aligns with the dismantling of thylakoid membranes, a characteristic of the poikilochlorophyllous strategy.

Interestingly, another important galactolipid in the thylakoid membranes within chloroplasts, digalactosyldiacylglycerol (DGDG), also showed down-regulation in the two poikilochlorophyllous species but did not show significant changes in the homoiocholophyllous *X. elegans*.

These findings highlight the distinct lipidomic responses between poikilochlorophyllous and homoiochlorophyllous *Xerophyta* species during desiccation. The differential regulation of lipid classes, particularly the up-regulation of TAGs, lysoPE, PE and PC and the downregulation of MGDGs, underscores the adaptive mechanisms employed by these species to cope with dehydration stress.

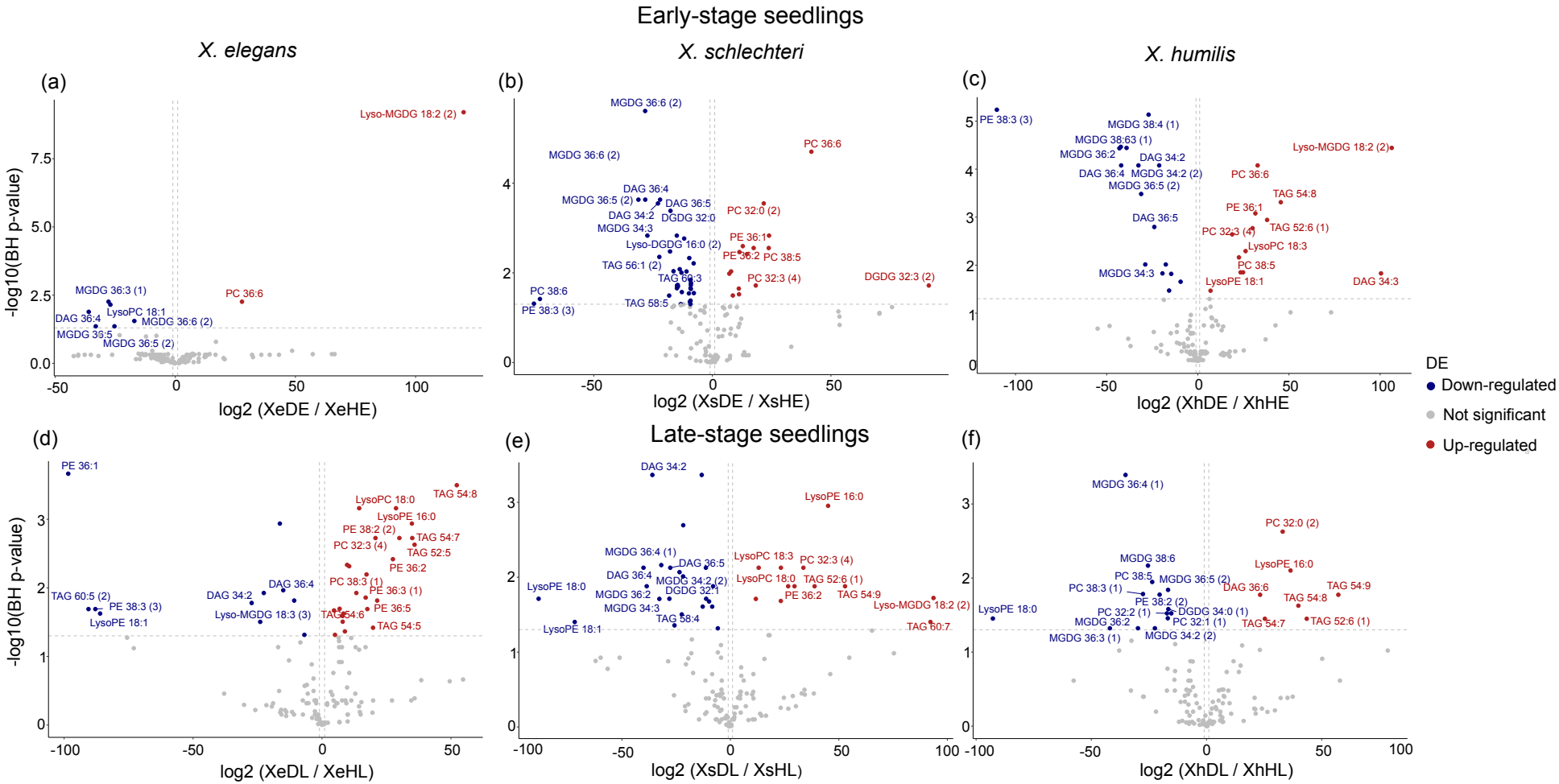

Figure 4.7. Volcano plots illustrating pairwise comparisons between hydrated and dehydrated seedlings of *Xerophyta* species. Each plot displays the log2 fold change in lipid abundance on the x-axis, comparing hydrated (H) versus dehydrated (D) samples. Lipids with the significance criteria of a Benjamini-Hochberg adjusted p-value of < 0.05 and a fold change > 1 are highlighted in colour red: indicates up-regulated lipids, blue denotes down-regulated lipids, and grey represents lipids that are not significantly different from the fully hydrated tissues.

4.4 Discussion

Primary metabolites, secondary metabolites, and lipids were examined across three *Xerophyta* species to uncover their roles in desiccation tolerance, and whether these are similar among the three species. Additionally, this part of the study aimed to identify changes in metabolite and lipid profiles that accumulate in early vs late-stage seedlings and compare homoichlorophyllous and poikilochlorophyllous species, which use different strategies for VDT acquisition.

The observation that hydrated tissues do not cluster with dehydrated samples, whether in early or late-stage seedlings, suggests that desiccation induces distinct metabolites and lipids in dry seedlings, potentially serving as a defence mechanism against desiccation stress.

Primary metabolites are generally conserved across different plant species and are known for their roles in the growth and development of plants. It comes as no surprise that there is no distinction between the three *Xerophyta* species in terms of the metabolites accumulated (Appendix C.1). Among the desiccation responsive sugar carbohydrates is sucrose, which is considered the most accumulated sugar in resurrection plants (Ingram & Bartels, 1996; Oliver et al., 2011). Sucrose acts as a water replacing molecule during desiccation, contributing to membrane and protein structure stabilization (Vicré et al., 2004). Both the pre-leaf and two-leaf stages of all the three *Xerophyta* seedlings accumulated high levels of sucrose during desiccation (Fig. 4.3). Sucrose accumulation is often accompanied by a decline in the levels of fructose and glucose, as seen in the dry leaf tissues of *X. viscosa, S. stapfianus, Eragrostis nindensis* and *H. rhodopensis* (Ghasempour et al., 1998; Moyankova et all., 2014; Whittaker et al., 2001). This was evident in both young and older *Xerophyta* seedlings under study, which showed a decrease, particularly in fructose, when dehydrated. However, glucose levels remained consistent between hydrated and dry samples, showing no significant difference between the two conditions. This observation deviates from a response seen in some resurrection plants including *B. hygroscopica* where glucose levels decreased during dehydration (Bianchi et al., 1991). The stability in glucose levels in *Xerophyta* seedlings suggests a potential role for glucose in maintaining basal metabolic functions and osmotic balance during desiccation. It highlights the possibility that the patterns of glucose change during desiccation can vary significantly among different species of resurrection plants. For instance, research on *S. stapfianus* leaf tissues revealed a different pattern of glucose response,

where glucose concentrations increased with decreasing RWC until a threshold of 50% RWC was reached (Ghasempour et al., 1998). The authors of this study postulate that this increase probably contributes to osmoregulation during moderate stress and confers general protective effects attributed to sugars under severe drought stress (Ghasempour et al., 1998). This contrasting response underscores the complexity of sugar metabolism and its regulation under desiccation stress across different plant species.

Notably, glucose-6-phosphate (G6P) accumulated in the dry tissues of all three *Xerophyta* species across both developmental stages. Glucose-6-phosphate plays a crucial role in various metabolic processes during desiccation. Firstly, G6P is a pivotal intermediate in the glycolytic pathway, providing a readily accessible source of energy through glycolysis. This is particularly important for maintaining ATP levels during periods of water deficit, where normal metabolic activity is disrupted. Additionally, the accumulation of G6P supports the pentose phosphate pathway, which is critical for generating NADPH (Xue et al., 2017) . NADPH plays a vital role in combating oxidative stress by maintaining the cellular redox state and supporting the synthesis of antioxidants. This function is crucial in desiccation-tolerant plants, where desiccation can lead to an increase in ROS and subsequent oxidative damage.

Apart from sugar carbohydrates, the accumulation of amino acids such as proline and tryptophan, which are associated with DT (Dinakar and Bartels 2013), were also noted in this study. These have been identified in other resurrection including *M. flabellifolia* and *S. dregai*, as well as a few other desiccation sensitive plants including *A. thaliana* and *Eragrostis tef* (Dace et al., 2023a). Both proline and tryptophan play crucial roles in conferring DT through several mechanisms. For example, proline acts as an osmoprotectant, accumulating in high concentrations within the cell to balance the osmotic pressure between the cell's internal and external environment. This helps maintain cell turgor and prevents cellular damage caused by osmotic stress (Kishor et al., 2015). Moreover, this osmolyte also functions in stabilizing proteins, membranes and cellular structures, thereby preserving their functionality during water deficient conditions (Verbruggen & Hermans, 2008). Tryptophan is involved in the biosynthesis of various secondary metabolites, including alkaloids and phytoalexins, which have protective roles against environmental stresses (Facchini et al., 2000).

The results obtained from the analysis of secondary metabolites highlight clear differences among the three *Xerophyta* seedlings, suggesting that changes in the abundance of these

compounds may vary between species. For instance, a number of secondary metabolites such as porpholinogen, kynurenine free and gamma-glutamylvaline, were constitutively elevated in both hydrated and dry seedlings of *X. elegans*, signifying metabolic readiness for desiccation. Such metabolic readiness has also been observed in *H. rhodopensis* (Gechev et al., 2013) and *S. stapfianus* (Oliver et al., 2011). It is thought to slow down water loss from tissues and protect cells from ROS generation because carbon fixation is prevented during the decrease in water potential (Oliver et al., 2011).

Further, flavonoids levels were high in *X. elegans* seedlings, and did not show an increase in *X. schlechteri* and *X. humilis* during dehydration. It is plausible that poikilochlorophyllous organisms do not accumulate significant levels of flavonoids. This can be attributed to their unique trait of chlorophyll breakdown, which reduces their reliance on the protective properties of flavonoids against ultraviolet (UV) radiation, primarily intended to safeguard chlorophyll.

Moreover, the observation that poikilochlorophyllous organisms tend to accumulate higher levels of dipeptides compared to *X. elegans* is not surprising. This accumulation may mirror the degradation of their most abundant protein, rubisco which is associated with their strategy of dismantling their photosynthetic machinery. Additionally, the increase in porphobilinogen levels in poikilochlorophyllous species, which is an essential intermediate in the synthesis of porphyrins including chlorophyll, could reflect the breakdown of chlorophyll into its precursor molecules as previously described for this strategy (Christ et al., 2014).

Among the secondary metabolites conserved across all species, particularly in the late-stage seedlings, are terpenes and trehalose. Terpenes are known for their role in plant defence against biotic and abiotic stresses (Singh & Sharma, 2015). Their accumulation in dry tissues of *Xerophyta* seedlings, at pre-leaf and two-leaf stages, is thus sensible. Elevated levels of the disaccharide trehalose have been noted under both hydrated and dehydrated conditions in tissues of *M. flabellifolia* and *S. dregai* (Dace et al., 2023a). Although previously thought to play a less significant role in the desiccation tolerance of resurrection plants (Gaff and Oliver, 2013), recent findings by Dace et al. (2023a) suggest a potential role for trehalose in desiccation response based on observed trends in *M. flabellifolia* and *S. dregai*. Moreover, *in vitro* studies have shown that trehalose is the most effective sugar in preserving enzyme activity during dry storage, especially concerning the length of storage time (Colaco et al., 1992). It is thus thought

to likely enhance the safeguarding effect of sucrose in drying tissue of most resurrection plants (Ghasempour et al., 1998).

MGDG is the most abundant lipid in thylakoid membranes, essential for photosynthesis and chloroplast development (Kalisch et al., 2016). Its fundamental role is evident given the substantial down-regulation observed in *X. schlechteri* and *X. humilis* early and late-stage seedlings, which undergo thylakoid membrane dismantling during desiccation. Similar reductions in MGDG levels have been documented in other DT plants such as *S. stafianus, C.* and *plantagineum* (Gasulla et al., 2013; Quartacci et al., 1997). This lipid breakdown highlights an effective adaptative strategy employed by poikilochlorophyllous plants to counteract dehydration stress.

MGDG serves as a precursor for the biosynthesis of DGDG (Dörmann et al., 1999), another critical galactolipid that maintains membrane stability during stress conditions. In *C. plantagineum*, for instance, desiccation induced MGDG reduction and DGDG elevation were attributed to the conversion of MGDG to DGDG (Gasulla et al., 2013). However, our results diverge from this pattern as we did not observe a clear inverse relationship between MGDG and DGDG levels. Instead, our analysis revealed that only a few DGDG species were detected, most of which were down-regulated, with a single exception showing up-regulation. Given this context, it is possible that MGDG in *Xerophyta* seedlings is hydrolysed by galactolipase enzymes, leading to the generation of various products, including lyso-MGDG (Gasulla et al., 2013). This hydrolysis process explains the presence of lyso-MGDG among the up-regulated lipids in *Xerophyta* seedlings, despite its small number (Fig. 4.5). It is not clear what the exact role of lyso-MGDG is, but it might be involved in membrane remodelling during the desiccation process. It is also possible that the accumulation of chloroplast vesicles, which occur as a result of the thylakoid membrane dismantling in the ultrastructure section (page 37), is linked to the hydrolysis of MGDG. However, this hypothesis remains speculative, as there is no direct evidence to support this.

The increase in TAG content, as observed in the three *Xerophyta* species, has also been linked to plant stress response (Lu et al., 2020). At the same time, some members of TAG decreased during desiccation, and this could be attributed to the synthesis and storage of TAGs. In higher plants, TAGs can either be synthesised and stored in the cytosol, within lipid droplets, or in the chloroplasts, within plastoglobules (Chapman et al., 2012). TAGs within plastoglobules are

involved in various functions including hormone metabolism, pathogen resistance, and stress response (Chapman et al., 2012). Additionally, increased accumulation in the levels of of two main phospholipids, PC and PE**,** as observed across all *Xerophyta* species, was also noted in dried tissues of *S. stapfianus* (Quartacci et al., 1997), indicating their role in DT.

4.5 Conclusion

GC-MS and LC-MS analyses were employed to investigate changes in primary metabolite, secondary metabolite, and lipid levels induced by desiccation in three *Xerophyta* species at two stages of seedling development. In summary, notable primary metabolites that accumulated in response to desiccation included sucrose, glucose-6-phosphate, proline, and tryptophan. Relative to the effect of desiccation on the secondary metabolites, the three species exhibit strong species-specific and to a lesser extent developmental stage effect. *X. elegans* accumulates flavonoids to protect its chlorophyll during desiccation in addition to accumulating other metabolites such as trehalose, oxidised glutathione and putative saponins. Conversely, *X. schlechteri* and *X. humilis* rely on dismantling their thylakoid membranes for protection against the effects of desiccation. This is also evident through the increased abundance of distinct secondary metabolites including dipeptides and porphobilinogen, as well as the degradation of the major galactolipid, MGDG, a non-bilayer-forming chloroplast lipid. The accumulation of lipids including TAGs, PCs and PEs observed across all three species during desiccation are thought to play an important role in DT acquisition. Moreover, the parallels drawn between our results and existing literature on adult tissues of resurrection plants underscore the conservation of underlying mechanisms throughout various developmental stages. Leveraging both GC-MS and LC-MS provided a holistic view of the metabolomic and lipidomic changes that occur during desiccation in different *Xerophyta* species.

CHAPTER 5

General Discussion and Conclusions

Resurrection plants are a remarkable group of plants known for their ability to withstand prolonged periods of extreme water deficit and recover upon rehydration. Previous studies have extensively explored the mechanisms enabling these plants to survive desiccation, focusing primarily on adult tissues. However, there are several drawbacks to working with adult plants, including the length of time they take to grow, spanning several months to years. This prolonged growth period may significantly limit the pace at which research can be conducted, thus impeding timely advancements in understanding desiccation responses. Another issue is that there is heterogeneity in water content across the plant, and even within a single leaf during drying. The dehydration rates of plants is further complicated by the size of the pot and the amount of soil the plants are grown in. To overcome these challenges, this study employed a seedling model to investigate desiccation responses in three *Xerophyta* species. The seedling model is particularly advantageous because it can be set up under controlled conditions which allows for reproducible rates of drying compared to adult plants. Because seedlings are tiny and of a similar size, rates of drying are more uniform. Seedlings are easy to germinate from seed, grow rapidly, and can be produced in larger numbers, facilitating quick experimental design and execution.

Several studies have previously reported on changes in transcripts, primary and secondary metabolites, and lipids in various resurrection plants (Table 4.1). However, to the best of our knowledge, none of these have generated matched datasets, both between the type of dataset (RNA transcripts, metabolites and lipids) and between species. Matched datasets are important as they allow for the direct comparison of biological data collected under the same controlled experimental conditions, thereby enabling a more integrated understanding of the underlying desiccation responses. To address this gap, the current study generated matched datasets for the analysis of changes in gene expression, primary and secondary metabolites, and lipid profiles in *Xerophyta* seedlings during early and late stages of seedling development.

It has been reported that *X. schlechteri* loses its DT during seedling development under rapid dehydration (Costa et al., 2017a). However, it is important to note that these experiments were performed on seedlings that had been kept in the dark for 3 days and so were not consistent with natural conditions. Under very rapid drying in a laminar flow hood, Lyall et al. (2014)

noted a transient decrease in survival rate as *X. viscosa* seedlings progress from early to late stages, particularly at 1.6 - 2 mm cotyledon length, followed by a recovery to over 40% at 4.4 – 5.9 mm cotyledon length. One potential explanation for this transient dip in survival rate is that there is a switch in the transcription factors regulating DT at this stage of gemination. We employed an experimental protocol where seedlings were dried more slowly, under more physiologically relevant, controlled conditions in a plant growth chamber. We demonstrated that *Xerophyta* seedlings maintain DT throughout all stages of development when subjected to drying under normal day-night cycle over 48 hours. We reasoned that the seedling model could be used to identify the core conserved transcriptional regulators of desiccation, as well as the core protective mechanisms and metabolic responses, by using a three-way comparison of *X. elegans*, *X. schlechteri* and *X. humilis* seedlings at the early pre-leaf and late two-leaf stages of development.

The central questions addressed using the seedling model for the three species of *Xerophyta* include:

- How do the desiccation-induced changes affect the ultrastructure of two-leaf *X. elegans* and *X. schlechteri* seedlings, and how do these compare to those observed in adult plants?
- Which transcription factors regulate DT in seedlings, and are these similar to those employed by adult maturing seeds or adult *Xerophyta* plants?
- How does the profile of primary metabolites, secondary metabolites, and lipids in these seedlings change in response to desiccation? Additionally, how do these changes differ between poikilochlorophyllous species (*X. schlechteri* and *X. humilis*) vs homoiochlorophyllous species (*X. elegans*)?

Conserved Core Metabolic Responses to Desiccation Identified in *Xerophyta* Seedlings

Resurrection plants undergo several changes during water deprivation to survive severe desiccation and oxidative stress. One of the most prominent responses widely observed across various species is the accumulation of sucrose in dry plant tissues (Illing et al., 2005; Farrant et al., 2007; Peters et al., 2007). This sugar plays a crucial role in cell protection by stabilizing membranes and forming a glassy state during desiccation (Peters et al., 2007). Our results for primary metabolites were consistent with these observations as sucrose levels were elevated in dehydrated tissues of both the early-stage and late-stage seedlings across all three *Xerophyta*

species. High levels of sucrose are often accompanied by a decrease in the accumulation of glucose and fructose (Farrant et al., 2009; Moyankova et al., 2014). Although fructose decreased in abundance across all *Xerophyta* seedlings and at both developmental stages, glucose levels remained unchanged between hydrated and dehydrated tissues, suggesting alternative carbon sources contribute to sucrose synthesis. Ultrastructural analysis of two-leaf *Xerophyta* seedlings revealed a complete disappearance of starch in dry *Xerophyta* chloroplasts, correlating with the up-regulation of starch catabolic process GO term, which mainly comprised of *DREB2H* genes. This implies that carbon skeletons from starch mobilization likely contributed to sucrose production, as also observed in other resurrection plants like *B. purpurea* (Suguiyama et al., 2014) and *H. rhodopensis* (Gechev et al., 2012; Moyankova et al., 2014).

Plants synthesize a diverse array of secondary metabolites, which often play crucial roles in responding to environmental stresses by protecting the plants against adverse effects. Saponins, triterpenes and trehalose are among secondary metabolites that accumulated in dehydrated tissues of *Xerophyta* seedlings across all species. Trehalose has been identified in several resurrection plants such as *S. stapfianus* and *M. flabellifolia*, and together with other sugars, this disaccharide sugar is crucial for protein stabilization and ensuring non-crystalline vitreous phases at very low water contents (Dace et al., 2023; Ghasempour et al., 1998). Although trehalose has previously been identified to play an important role in protecting cells, this is the first report of saponins being important for desiccation tolerance in resurrection plants. Saponins are an important group of plant secondary metabolites consisting of glycosylated triterpenes and steroids (Osbourn et al., 2003).

Conserved changes in lipid concentration were also identified in the three-way comparison of the response of *Xerophyta* seedlings to desiccation. Notably, triacylglycerides (TAGs) increased in abundance in response to desiccation across the three *Xerophyta* species. The observed increase in TAGs in the dry tissues is consistent with their function of providing energy during periods of low photosynthetic activity, highlighting their critical role in sustaining metabolic processes and ensuring cellular survival under adverse environmental conditions. The biosynthesis of TAG is associated with two enzymes, namely, Phetyl Ester Synthase 1 and 2 (PES1 and PES2), which are involved in fatty acid phytyl ester synthesis (Lippold et al., 2012). These enzymes have phytyl ester synthesis and diacylglycerol acyltransferase activities, exhibiting broad substrate specificities. One of the key substrates

they act on, DAG, serves as a precursor for TAG synthesis. Notably, the levels of DAG declined in dehydrated tissues of *Xerophyta* seedlings, indicating a shift in lipid metabolism under stress conditions. Once synthesized, TAGs are metabolized through β-oxidation of the fatty acids, a process which in plants, occurs in peroxisomes. Among the transcripts involved in this pathway, 3-Ketoacyl-CoA thiolase (KAT) 1 stands out as a key gene, being enriched in the cellular lipid metabolism process GO term. However, other genes crucial to peroxisomal β-oxidation, such as Acyl-CoA oxidase and Enoyl-CoA hydratase, were not significantly enriched in our RNA-Seq data.

TAGs are found within lipid-rich structures known as plastoglobules, which are associated with thylakoid membranes in chloroplasts. These lipid structures increased in numbers in desiccated two-leaf seedlings of *X. elegans* and *X. schlechteri* as revealed by the analysis of chloroplast ultrastructure. Plastoglobules are recognized for their accumulation during desiccation, where they play pivotal roles in repair and recycling processes, metabolism and lipid storage (Charuvi et al., 2019; Besagni and Kessler, 2013). Our RNA-Seq results further highlight "plastoglobule organization" as one of the enriched GO terms among the up-regulated genes in all three *Xerophyta* species. This term encompasses *Atypical Kinases 8 (ABC1K8)* and *sterol 4-alpha-methyl-oxidase (SMO2)* genes, both integral to the regulation of plastoglobule dynamics and lipid metabolism in response to desiccation. Changes in plastoglobules are consistent with previous observations in other studies on resurrection plants including *X. viscosa* and *C. wilmsii* (Sherwin & Farrant, 1998).

Homoiochlorophyllous versus Poikilochlorophyllous species

All resurrection plants have to protect themselves from oxidative stress caused by the accumulation of ROS in the photosynthetic complex as cells dry down. Most resurrection plants employ the poikilochlorophylly strategy, which involves completely dismantling thylakoid membranes during desiccation, resulting in the formation of vesicles. In contrast, plants employing the homoiochlorophylly strategy retain their thylakoid membranes during dry conditions and can quickly recover upon rehydration. Thylakoid degradation has been observed in adult leaf tissues of poikilochlorophyllous species such as *X. viscosa*, *X. humilis* and *X. schlechteri* (Ingle et al., 2008; Radermacher et al., 2019; Sherwin & Farrant, 1996). On the other hand, homoiochlorophyllous adult plants including *X. elegans* and *C. pumilum* retained their thylakoid membranes during dehydration conditions (Hallam & Gaff, 1980; Charuvi et al., 2019).

In our comparative ultrastructural analysis of *X. elegans* and *X. schlechteri* two-leaf seedlings, we observed changes similar to those previously documented in adult plant tissues. Through a detailed dehydration and rehydration time course series, we captured the progression of these changes. A notable distinction between the two *Xerophyta* species became evident after 72 hours, during the desiccated state (13% RWC). In *X. schlechteri*, thylakoid membranes were completely dismantled, leading to the formation of vesicles. In contrast, in *X. elegans*, thylakoid membranes remained visible but were not organized into grana stacks during this desiccated state. Upon rehydration, thylakoid reassembly and grana stack formation occurred rapidly within 1-hour (26% RWC) in *X. elegans*, whereas the first appearance of thylakoid membranes in *X. schlechteri* was observed only after 48 hours (89% RWC) post rehydration.

Thylakoid membranes are composed of a lipid bilayer incorporating several lipids, including DGDG and MGDG. Our lipid analysis showed a significant down-regulation of MGDGs in both early and late-stage seedlings of *X. schlechteri* and *X. humilis*. The breakdown of MGDG is primarily facilitated by MGDG galactolipase enzymes, with MGDG lipases playing a crucial role in hydrolysing this galactolipid into free fatty acids and glycerol derivatives. We observed an enrichment of the GO term "lipid droplet organization," in *Xerophyta* seedling genes. Lipid droplet organization is associated with processes related to the assembly, arrangement, or disassembly of lipid, and may be involved in the degradation of MGDG in the chloroplast structures of these species. A decrease in MGDG, a lipid essential for facilitating electron transfer between the light harvesting complexes and the reaction centres of photosystems I and II, may contribute to maintaining a reduced electron transport rate (Quartacci et al., 1997).

An analysis of GO terms enriched in the up-regulated genes of *X. schlechteri* and *X. humilis* highlighted enrichment in the term "chloroplast organization", potentially linked to changes in chloroplast ultrastructure. Key genes associated with this GO term include *HSP17*, *ETHYLENE RESPONSIVE TRANSCRIPTION FACTOR* (*ERF9*) and *STAY-GREEN* (*SGR2*). It has been reported that SGR proteins are involved in chlorophyll degradation process during leaf senescence and in response to stress. Two homologs of these proteins, SGR1 and SGR2, are present in Arabidopsis genome, each playing distinct roles in the chlorophyll degradation pathway (Sakuraba et al., 2014). SGR1 is primarily responsible for initiating and facilitating chlorophyll breakdown by destabilizing chlorophyll-protein complexes, a critical function during leaf senescence and abiotic stress responses. Both SGR1 and SGR2 encode magnesium

(Mg)-dechelatase, an enzyme that removes Mg from chlorophyll α and converts it to pheophytin α under stress conditions, marking a key step in chlorophyll breakdown (Jiao et al., 2020; Shimoda et al., 2016). In contrast, Sakuraba et al. (2014) reported that Arabidopsis SGR2 acts as a negative regulator of chlorophyll degradation during leaf senescence (Sakuraba et al., 2014). However, Shimoda et al. (2016) demonstrated an opposite effect. Given that chlorophyll breakdown occured in *X. schlechteri* and *X. humilis* seedlings, this phenomenon is not consistent with SGR2's role as a negative regulator.

Unlike *X. schlechteri* and *X. humilis*, *X. elegans* retains its chlorophyll during desiccation, and just like other homoiochlorophyllous plants, employs alternative mechanisms to combat oxidative stress. One key strategy is maintaining an antioxidant system that mitigates oxidative damage, thus enabling DT. Our secondary metabolites data analysis demonstrated the accumulation of antioxidants including flavonoids in dry *X. elegans* seedlings. Flavonoids are secondary metabolites that can scavenge ROS under biotic and abiotic stresses. These compounds not only neutralize ROS but also inhibit the activity of enzymes involved in ROS-generating pathways, thereby enhancing the plant's antioxidant defence system (Shomali et al., 2022).

Although *X. elegans* does not exhibit yellowing leaves, as is typical in other species undergoing desiccation and breaking down their chlorophyll, its leaves develop a dark purple hue as they dry out. It has been shown that this leaf pigmentation acts as a natural sunscreen, protecting the leaves from excessive light absorption and thereby minimizing photodamage during stress conditions. The ability of homoiochlorophyllous species to protect their thylakoid membranes during desiccation is achieved through the functions of antioxidant zeaxanthin, a-tocopherol and ELIPs (Oliver et al., 2020). ELIPs are chlorophyll binding proteins that protect photosynthetic machinery from damage induced by light (Liu et al., 2020). The ELIP2 genes were up-regulated in *X. elegans* seedlings at both pre-leaf and two-leaf stages and were associated with the "response to light intensity" GO term, enriched in both stages. In contrast, these genes were not up-regulated in *X. schlechteri* and *X. humilis* seedlings. A comparative study between the homoiochlorophyllous *Oropetium thomaeum* and the poikilochlorophyllous *Eragrostis nindensis* revealed that the former contained more ELIPs than the latter (St. Aubin et al., 2022). In *O. thomaeum.* all ELIPs were highly up-regulated in desiccated tissues, whereas only a few were present in the dry tissues of *E. nindensis,* and none of these were similar to those in the chlorophyll-containing species (St. Aubin et al., 2022). Interestingly, in *E.*

nindensis, ELIPs showed high expression during rehydration, suggesting they play a key role in protecting leaves as they resynthesize and repair their photosynthetic apparatus (Pardo et al., 2020). This indicates that ELIPs are expressed in both homoiochlorophyllous and poikilochlorophyllous species, although different ELIPs may be involved in distinct roles depending on the species and their unique stress responses.

Identification of Core Transcriptional Regulators in Dry *Xerophyta* Seedlings

Previous studies have all noted the activation of seed maturation genes in desiccated leaves of resurrection plants, suggesting a common transcriptional regulatory mechanism. It has been hypothesized that the ABI3 and ABI5 transcription factors, activate the seed maturation genes in the leaves of resurrection plants (Costa et al., 2017b; VanBuren et al., 2017). However, Lyall et al. (2020) reported that although these transcription factors are expressed in maturing *X. humilis* seeds, no evidence for the activation of full-length ABI3 or ABI5 transcription factors could be found in drying *X. humilis* or *X. schlechteri* leaves. This result suggests that VDT in *Xerophyta* species is not due to reactivation of the LAFL network. Instead, the ABRE binding factor, ABF, member of the bZIP family, was activated in both maturating seeds and desiccated adult leaves of *X. humilis* (Lyall et al., 2020).

We analyzed the expression of LAFL network members, ABI5, and ABF in early and late-stage seedlings of all three *Xerophyta* species, to investigate whether the transcriptional regulators activating the seed maturation genes change between these stages of development, and how this compares to adult leaves. Our results show *ABI3* and *ABI5* genes are highly expressed in pre-leaf seedlings of *Xerophyta* species, but they are not active in older seedlings. In contrast, *ABFA,* was significantly induced by desiccation across all species, and developmental stages, suggesting a potential role in VDT.

To identify core transcription regulators in desiccated seedlings, gene orthogroups that showed the same response to desiccation all three *Xerophyta* species at early and late developmental stages was performed. The three-way comparative analysis revealed a total of 370 up-regulated and 335 down-regulated orthogroups and these potentially represented a core set of desiccation-responsive genes in *Xerophyta* species. This is also evident from the enrichment of stress-related GO terms such as “response to water deprivation,” “response to oxidative stress,” “response to osmotic stress” and “response to abscisic acid”, in the up-regulated orthogroups. The down-regulation of orthogroups involved in plant growth and developmental processes

indicate that the energy normally used for plant growth is reallocated to support stress-related responses during desiccation. Furthermore, several desiccation-induced orthogroups were annotated as gene families of unknown function. Their conserved response in the three *Xerophyta* species points towards their function in survival of desiccation conditions.

An analysis of the promoter regions of these core orthogroups, across three *Xerophyta* species, showed that they were enriched with binding sites for various transcription factor families including MYB, CPP GATA-binding factors, HSF, AHL, and C_2H_2 ZAT transcription factors. HSF, AHL and C_2H_2 ZAT families were exclusively expanded in *Xerophyta* species, and were therefore analysed. The exclusive expansion of these transcription factor families in *Xerophyta* species suggests a potential adaptive mechanism to cope with desiccation, by regulating gene expression related to stress responses and metabolic adjustments.

We examined common orthogroups containing the ZAT, AHL and HSF motifs in the target genes of *X. elegans*, *X. schlechteri* and *X. humilis* to assess their conservation across *Xerophyta* species. Our results revealed 53 down-regulated and 1 up-regulated orthogroups containing ZAT motifs. For AHL motifs, 272 orthogroups were down-regulated and 295 were up-regulated. Finally, 3 HSF motif-containing orthogroups were down-regulated and 9 were up-regulated. Notably, WRKY transcription factor was among the nine up-regulated HSF-motif containing orthogroups. WRKY transcription factors play important roles in various biological processes, including responses to abiotic stresses. For example, they are involved in the regulation of genes like dihydroflavonol-4-reductase and chalcone synthase, which are key to anthocyanin and flavonoid biosynthesis, respectively. Proline biosynthesis, which accumulated in both early and late-stage *Xerophyta* seedlings during desiccation, is also activated by genes regulated by WRKY TFs. Proline is an important osmolyte that functions in osmoregulation and provides antioxidant protection during water-deficit conditions.

In addition, stachyose synthase is another example of conserved HSF-motif containing orthogroup that is highly expressed in all *Xerophyta* seedlings. This enzyme catalyzes the transfer of a galactosyl unit from galactinol to raffinose, forming stachyose. Like other Raffinose family oligosaccharides (RFOs), stachyose acts as an osmoprotectant, helping to maintain water in cells and providing protection against dehydration. Notably, none of the RFO members were detected in the metabolome analysis, suggesting that stachyose synthase could be involved in other functions important for DT in *Xerophyta* species.

In addition, three down-regulated HSF-motif containing orthogroups that were conserved across the three *Xerophyta* species were identified. These included Rhamnogalacturonan I (RG-I) rhamnosyltransferase 1, and B3 domain-containing protein Os02g0683500, and Endoglucanase 23, all of which are involved in growth related process. For example, rhamnosyltransferase plays a role in the formation a major plant cell wall pectic polysaccharide (RG- I) (Wachananawat et al., 2020). The B3 domain-containing protein is associated with the regulation of cell wall bound invertases enzymes catalyzing the hydrolysis of sucrose into its component monosaccharides. Lastly, Endoglucanase 23 is an enzyme that hydrolyses cellulose in the plant cell wall. The GO term enrichment analysis also showed that these proteins are involved in several developmental processes such as shoot system development, lateral root development, and regulation of leaf morphogenesis.

Together, members of the HSF, AHL and C_2H_2 ZAT families, all of which are conserved across the three *Xerophyta* species at both pre-leaf and two-leaf stage, may play pivotal roles in the regulation of desiccation response in these species.

5.1 Limitations of the Study and Future Work

Time-course analysis

The RNA-Seq and lipid/metabolite parts of this study exclusively focused on two endpoints: fully hydrated and the dehydrated states, to study DT mechanisms in three *Xerophyta* species. While we gained valuable insights into how these species achieve DT, this approach cannot capture the dynamic responses occurring during dehydration. By the time the water content drops below 40%, many early-response genes that were initially activated may have already been turned off. To address this, future research should employ a time-course analysis that monitors changes throughout the entire dehydration process. This approach would enable us to identify critical early-stage responses and regulatory mechanisms that are missed when only examining the end states. Furthermore, based on the TEM results, we would recommend including the 48-hour time point in the desiccation series, as the changes occurring between 24 and 72 hours are notably significant. Additionally, the rehydration series should incorporate a 24-hour time point to capture the early changes during rehydration, as well as a 72-hour time point to allow sufficient time for the seedlings to fully rehydrate.

Extending drying-down period for seedlings

Our observations of significant ultrastructural changes between 24 and 72 hours post dehydration indicate ongoing and potentially critical alterations during this period. The current protocol, which involves drying seedlings for 48 hours for the RNA-Seq and lipid/metabolite studies, may not adequately capture these late-stage changes. Therefore, extending the drying period to at least 72 hours will provide more comprehensive understanding of the desiccation process and the associated molecular and structural adaptations.

High-pressure fixation for ultrastructure analysis

In the ultrastructure component of the study, there is a risk of rehydration of desiccated leaf tissue during the chemical fixation process, which can alter the tissue's ultrastructure. To mitigate this, we recommend using the high-pressure freezing for fixation, especially when working with dry tissues. This method preserves the cellular structure in their native state, preventing the rehydration artifacts that can occur with chemical fixation. By employing high-pressure freezing, future studies will achieve more accurate and detailed ultrastructural data, enhancing our understanding of the cellular and molecular mechanisms underlying DT.

5.2 Concluding Remarks

In summary, this study has shown that *Xerophyta* seedlings are inherently DT at both pre-leaf and two-leaf stages of development, capable of surviving and recovering from severe dehydration. This resilience underscores the seedlings as an effective model for exploring DT mechanisms in resurrection plants.

The results presented in this study provide comprehensive insights into the VDT mechanisms of *Xerophyta* seedlings, highlighting their remarkable ability to withstand extreme dehydration at various stages of development. These findings demonstrate that at the two-leaf stage of seedling development, *Xerophyta* species exhibit DT mechanisms similar to those found in adult tissues of resurrection plants. The core mechanisms of protection against desiccation are deeply conserved between maturing seeds and early-stage seedlings of most flowering plants, two-leaf stage *Xerophyta* seedlings, and adult *Xerophyta* leaves. However, the transcription factor pathways regulating this conserved response differ. For example, two key seed master maturation transcription factors, ABI3A and ABI5A, are only active in desiccated early pre-leaf seedlings but are not expressed in the two-leaf seedings of *Xerophyta* species or adult plants.

This study further identified core orthogroups containing desiccation responsive genes through a three-way comparison of *Xerophyta* species. Promoter regions of these core orthogroups were enriched with binding sites for *Xerophyta* specific expanded transcription factor families including HSF, AHL, and C_2H_2 ZAT. These are potentially important for both activation of desiccation protection genes, and the suppression of growth-related genes.

The integration of ultrastructural, transcriptomic, and metabolomic data has provided a holistic understanding of the VDT mechanisms in *Xerophyta* seedlings. The consistency of VDT features across different levels of biological organization underscores the robustness of these mechanisms and their evolutionary significance in enabling resurrection plants to survive in extremely dry conditions.

REFERENCES

Adamska, I., Vii, V. I., Viii, I., Aro, E.-M., & Andersson, B. (2001). *The Elip Family of Stress Proteins in the Thylakoid Membranes of Pro-and Eukaryota*.

Alpert, P. (2005). *The Limits and Frontiers of Desiccation-Tolerant Life 1* (Vol. 45). https://academic.oup.com/icb/article/45/5/685/624353

Alscher, R. G., Erturk, N., & Heath, L. S. (2002). *Role of superoxide dismutases (SODs) in controlling oxidative stress in plants*.

Angelovici, R., Galili, G., Fernie, A. R., & Fait, A. (2010). Seed desiccation: a bridge between maturation and germination. In *Trends in Plant Science* (Vol. 15, Issue 4, pp. 211–218). https://doi.org/10.1016/j.tplants.2010.01.003

Armenta-Medina, A., Gillmor, C. S., Gao, P., Mora-Macias, J., Kochian, L. V., Xiang, D., & Datla, R. (2021). Developmental and genomic architecture of plant embryogenesis: from model plant to crops. In *Plant Communications* (Vol. 2, Issue 1). Cell Press. https://doi.org/10.1016/j.xplc.2020.100136

Artur, M. A. S., Rienstra, J., Dennis, T. J., Farrant, J. M., Ligterink, W., & Hilhorst, H. (2019). Structural Plasticity of Intrinsically Disordered LEA Proteins from Xerophyta schlechteri Provides Protection In Vitro and In Vivo. *Frontiers in Plant Science*, *10*. https://doi.org/10.3389/fpls.2019.01272

Banerjee, A., & Roychoudhury, A. (2016). Group II late embryogenesis abundant (LEA) proteins: structural and functional aspects in plant abiotic stress. In *Plant Growth Regulation* (Vol. 79, Issue 1, pp. 1–17). Springer Netherlands. https://doi.org/10.1007/s10725-015-0113-3

Banerjee, N., Kumar, S., Singh, A., Annadurai, A., & Thirugnanasambandam, P. P. (2022). Identification of microRNAs involved in sucrose accumulation in sugarcane (Saccharum species hybrid). *Plant Gene*, *29*. https://doi.org/10.1016/j.plgene.2022.100352

Bartels, D., Hanke, C., Schneider, K., Michel, D., & Salamini, F. (1992). A desiccation-related Elip-like gene from the resurrection plant Craterostigma plantagineum is regulated by light and ABA. *The EMBO Journal*, *11*(8), 2771–2778. https://doi.org/10.1002/j.1460-2075.1992.tb05344.x

Bartels, D., Phillips, J., & Chandler, J. (2008). Desiccation tolerance: gene expression, pathways, and regulation of gene expression. In *Plant Desiccation Tolerance* (Vol. 35, pp. 115–137). Blackwell Publishing Ltd. https://doi.org/10.1002/9780470376881.ch9

Basu, S., Ramegowda, V., Kumar, A., & Pereira, A. (2016). Plant adaptation to drought stress. In *F1000Research* (Vol. 5). Faculty of 1000 Ltd. https://doi.org/10.12688/F1000RESEARCH.7678.1

Battaglia, M., Olvera-Carrillo, Y., Garciarrubio, A., Campos, F., & Covarrubias, A. A. (2008). The enigmatic LEA proteins and other hydrophilins. In *Plant Physiology* (Vol. 148, Issue 1, pp. 6–24). American Society of Plant Biologists. https://doi.org/10.1104/pp.108.120725

Becker, J., & Craig, E. A. (1994). Heat-shock proteins as molecular chaperones. *European Journal of Biochemistry*, *219*(1–2), 11–23. https://doi.org/10.1111/j.1432-1033.1994.tb19910.x

Bedair, M., & Sumner, L. W. (2008). Current and emerging mass-spectrometry technologies for metabolomics. *TrAC - Trends in Analytical Chemistry*, *27*(3), 238–250. https://doi.org/10.1016/j.trac.2008.01.006

Behnke, H.-D., Hummel, E., Hillmer, S., Sauer-Gürth, H., Gonzalez, J., & Wink, M. (2013). *A revision of African Velloziaceae based on leaf anatomy characters and rbcL nucleotide sequences*. https://academic.oup.com/botlinnean/article/172/1/22/2416184

Besagni, C., & Kessler, F. (2013). A mechanism implicating plastoglobules in thylakoid disassembly during senescence and nitrogen starvation. In *Planta* (Vol. 237, Issue 2, pp. 463–470). Springer Verlag. https://doi.org/10.1007/s00425-012-1813-9

Bewley, J. D., Bradford, K. J., Hilhorst, H. W., Nonogaki, H., Bewley, J. D., Bradford, K. J., ... & Nonogaki, H. (2013). Germination. Seeds: Physiology of Development, Germination and Dormancy, 3rd Edition, 133-181.

Bianchi, G., Murelli, C., & Vazzana, C. (1991). Changes of low-molecular weight substances in Boea hygroscopica in response to desiccation and rehydration. *Phytochemistry*, 461–466.

Bohnert, H. J., Donald, ', Nelson, E., & Jensenayb, R. G. (1995). Adaptations to Environmental Stresses. In *The Plant Cell* (Vol. 7). American Society of Plant Physiologists.

Brand, A., Quimbaya, M., Tohme, J., & Chavarriaga-Aguirre, P. (2019). Arabidopsis LEC1 and LEC2 orthologous genes are key regulators of somatic embryogenesis in cassava. *Frontiers in Plant Science*, *10*. https://doi.org/10.3389/fpls.2019.00673

Braybrook, S. A., & Harada, J. J. (2008). LECs go crazy in embryo development. In *Trends in Plant Science* (Vol. 13, Issue 12, pp. 624–630). https://doi.org/10.1016/j.tplants.2008.09.008

Buitink, J., & Leprince, O. (2004). Glass formation in plant anhydrobiotes: Survival in the dry state. In *Cryobiology* (Vol. 48, Issue 3, pp. 215–228). https://doi.org/10.1016/j.cryobiol.2004.02.011

Buitink, J., Ly Vu, B., Satour, P., & Leprince, O. (2003). The re-establishment of desiccation tolerance in germinated radicles of Medicago truncatula Gaertn. seeds. *Seed Science Research*, *13*(4), 273–286. https://doi.org/10.1079/ssr2003145

Chapman, K. D., Dyer, J. M., & Mullen, R. T. (2012). Biogenesis and functions of lipid droplets in plants: Thematic review series: Lipid droplet synthesis and metabolism: From yeast to man. In *Journal of Lipid Research* (Vol. 53, Issue 2, pp. 215–226). https://doi.org/10.1194/jlr.R021436

Charuvi, D., Nevo, R., Aviv-Sharon, E., Gal, A., Kiss, V., Shimoni, E., Farrant, J. M., Kirchhoff, H., & Reich, Z. (2019). Chloroplast breakdown during dehydration of a homoiochlorophyllous resurrection plant proceeds via senescence-like processes. *Environmental and Experimental Botany*, *157*, 100–111. https://doi.org/10.1016/j.envexpbot.2018.09.027

Chen, X., Li, C., Wang, H., & Guo, Z. (2019). WRKY transcription factors: evolution, binding, and action. *Phytopathology Research*, *1*(1). https://doi.org/10.1186/s42483-019-0022-x

Christ, B., Egert, A., Süssenbacher, I., Kräutler, B., Bartels, D., Peters, S., & Hörtensteiner, S. (2014). Water deficit induces chlorophyll degradation via the "PAO/phyllobilin" pathway in leaves of homoio- (Craterostigma pumilum) and poikilochlorophyllous (Xerophyta

viscosa) resurrection plants. *Plant Cell and Environment*, *37*(11), 2521–2531. https://doi.org/10.1111/pce.12308

Collett, H., Shen, A., Gardner, M., Farrant, J. M., Denby, K. J., & Illing, N. (2004). Towards transcript profiling of desiccation tolerance in Xerophyta humilis: Construction of a normalized 11 k X. humilis cDNA set and microarray expression analysis of 424 cDNAs in response to dehydration. *Physiologia Plantarum*, *122*(1), 39–53. https://doi.org/10.1111/j.1399-3054.2004.00381.x

Cooper, K., & Farrant, J. M. (2002). Recovery of the resurrection plant Craterostigma wilmsii from desiccation: Protection versus repair. *Journal of Experimental Botany*, *53*(375), 1805–1813. https://doi.org/10.1093/jxb/erf028

Corratgé-Faillie, C., & Lacombe, B. (2017). Substrate (un)specificity of Arabidopsis NRT1/PTR FAMILY (NPF) proteins. In *Journal of Experimental Botany* (Vol. 68, Issue 12, pp. 3107–3113). Oxford University Press. https://doi.org/10.1093/jxb/erw499

[a]Costa, M.-C. D., Cooper, K., Hilhorst, H. W. M., & Farrant, J. M. (2017). Orthodox seeds and resurrection plants: two of a kind? *Plant Physiology*, pp.00760.2017. https://doi.org/10.1104/pp.17.00760

[b]Costa, M.-C. D., Hilhorst, H. W. M., & Farrant, J. M. (2017). A 'footprint' of desiccation tolerance in the genome of the resurrection plant Xerophyta viscosa. *South African Journal of Botany*, *109*, 336. https://doi.org/10.1016/j.sajb.2017.01.062

Cuming, A. C. (2019). Evolution of ABA signaling pathways. In Advances in botanical research (Vol. 92, pp. 281-313). Academic Press.

Dace, H. J. W., Reus, R., Ricco, C. R., Hall, R., Farrant, J. M., & Hilhorst, H. W. M. (2023). A horizontal view of primary metabolomes in vegetative desiccation tolerance. *Physiologia Plantarum*, *175*(6). https://doi.org/10.1111/ppl.14109

Dace, H., Sherwin, H. W., Illing, N., & Farrant, J. M. (1998). Use of metabolic inhibitors to elucidate mechanisms of recovery from desiccation stress in the resurrection plant Xerophyta humilis. In *Plant Growth Regulation* (Vol. 24).

Dure, L. (1993). A repeating 11-mer amino acid motif and plant desiccation. In *The Plant Journal* (Vol. 3, Issue 3, pp. 363–369). https://doi.org/10.1046/j.1365-313X.1993.t01-19-00999.x

Dure, L., Greenway, S. C., & Galau, G. A. (1981). Developmental Biochemistry of Cottonseed Embryogenesis and Germination: Changing Messenger Ribonucleic Acid Populations As Shown by in Vitro and in Vivo Protein Synthesis*. In *Biochemistry* (Vol. 20). https://pubs.acs.org/sharingguidelines

Egert, A., Eicher, B., Keller, F., & Peters, S. (2015). Evidence for water deficit-induced mass increases of raffinose family oligosaccharides (RFOs) in the leaves of three Craterostigma resurrection plant species. *Frontiers in Physiology*, *6*(JUL). https://doi.org/10.3389/fphys.2015.00206

Emms, D. M., & Kelly, S. (2019). OrthoFinder: Phylogenetic orthology inference for comparative genomics. *Genome Biology*, *20*(1). https://doi.org/10.1186/s13059-019-1832-y

Emwas, A.-H. (2015). *The Strengths and Weaknesses of NMR Spectroscopy and Mass Spectrometry with Particular Focus on Metabolomics Research*. http://www.springer.com/series/7651

Erb, M., & Kliebenstein, D. J. (2020). Plant Secondary Metabolites as Defenses, Regulators, and Primary Metabolites: The Blurred Functional Trichotomy1[OPEN]. In *Plant Physiology* (Vol. 184, Issue 1, pp. 39–52). American Society of Plant Biologists. https://doi.org/10.1104/PP.20.00433

Facchini, P. J., Huber-Allanach, K. L., & Tari, L. W. (2000). *Plant aromatic L-amino acid decarboxylases: evolution, biochemistry, regulation, and metabolic engineering applications*. www.elsevier.com/locate/phytochem

Fan, S. C., Lin, C. S., Hsu, P. K., Lin, S. H., & Tsay, Y. F. (2009). The Arabidopsis nitrate transporter NRT1.7, expressed in phloem, is responsible for source-to-sink remobilization of nitrate. *Plant Cell*, *21*(9), 2750–2761. https://doi.org/10.1105/tpc.109.067603

Farrant, J. M. (2000). A comparison of mechanisms of desiccation tolerance among three angiosperm resurrection plant species. In *Plant Ecology* (Vol. 151).

Farrant, J. M. (2007). *An Overview of Mechanisms of Desiccation Tolerance in Selected Angiosperm Resurrection Plants*. https://www.researchgate.net/publication/225285071

Farrant, J. M., Cooper, K., Kruger, L. A., & Sherwin, H. W. (1999). The Effect of Drying Rate on the Survival of Three Desiccation-tolerant Angiosperm Species. In *Annals of Botany* (Vol. 84).

Fatihi, A., Boulard, C., Bouyer, D., Baud, S., Dubreucq, B., & Lepiniec, L. (2016). Deciphering and modifying LAFL transcriptional regulatory network in seed for improving yield and quality of storage compounds. In *Plant Science* (Vol. 250, pp. 198–204). Elsevier Ireland Ltd. https://doi.org/10.1016/j.plantsci.2016.06.013

Fernie, A. R., & Pichersky, E. (2015). Focus issue on metabolism: Metabolites, metabolites everywhere. In *Plant Physiology* (Vol. 169, Issue 3, pp. 1421–1423). American Society of Plant Biologists. https://doi.org/10.1104/pp.15.01499

Footitt, S., Awan, S., & Finch-Savage, W. E. (2018). An improved method for the rapid isolation of RNA from Arabidopsis and seeds of other species high in polyphenols and polysaccharides. *Seed Science Research*, *28*(4), 360–364. https://doi.org/10.1017/S0960258518000296

Foreman, J., Demidchik, V., Bothwell, J. H. F., Mylona, P., Miedema, H., Torresk{, M. A., Linstead, P., Costa, S., Brownlee, C., Jonesk, J. D. G., Davies, J. M., & Dolan, L. (2003). *Reactive oxygen species produced by NADPH oxidase regulate plant cell growth*. www.nature.com/nature

Frydman, J. (2001). Folding of newly translated proteins in vivo: The role of molecular chaperones. In *Annual Review of Biochemistry* (Vol. 70, pp. 603–648). https://doi.org/10.1146/annurev.biochem.70.1.603

Gabier, H., Tabb, D. L., Farrant, J. M., Rafudeen, M. S., Marondedze, C., Chiapello, M., & Nikolovski, N. (2021). *A Label-Free Proteomic and Complementary Metabolomic Analysis of Leaves of the Resurrection Plant Xerophyta schlechteri during Dehydration*. https://doi.org/10.3390/life

Gaff, D. F., & Oliver, M. (2013). The evolution of desiccation tolerance in angiosperm plants: a rare yet common phenomenon. *Functional Plant Biology*. https://doi.org/10.1071/fp12321

Gangl, R., & Tenhaken, R. (2016). Raffinose family oligosaccharides act as galactose stores in seeds and are required for rapid germination of Arabidopsis in the dark. *Frontiers in Plant Science*, *7*(JULY2016). https://doi.org/10.3389/fpls.2016.01115

Gasulla, F., Vom Dorp, K., Dombrink, I., Zähringer, U., Gisch, N., Dörmann, P., & Bartels, D. (2013). The role of lipid metabolism in the acquisition of desiccation tolerance in Craterostigma plantagineum: A comparative approach. *Plant Journal*, *75*(5), 726–741. https://doi.org/10.1111/tpj.12241

Gechev, T. S., Benina, M., Obata, T., Tohge, T., Sujeeth, N., Minkov, I., Hille, J., Temanni, M. R., Marriott, A. S., Bergström, E., Thomas-Oates, J., Antonio, C., Mueller-Roeber, B., Schippers, J. H. M., Fernie, A. R., & Toneva, V. (2013). Molecular mechanisms of desiccation tolerance in the resurrection glacial relic Haberlea rhodopensis. *Cellular and Molecular Life Sciences*, *70*(4), 689–709. https://doi.org/10.1007/s00018-012-1155-6

Gechev, T. S., Dinakar, C., Benina, M., Toneva, V., & Bartels, D. (2012). Molecular mechanisms of desiccation tolerance in resurrection plants. In *Cellular and Molecular Life Sciences* (Vol. 69, Issue 19, pp. 3175–3186). https://doi.org/10.1007/s00018-012-1088-0

Georgieva, K., Dagnon, S., Gesheva, E., Bojilov, D., Mihailova, G., & Doncheva, S. (2017). Antioxidant defense during desiccation of the resurrection plant Haberlea rhodopensis. *Plant Physiology and Biochemistry*, *114*, 51–59. https://doi.org/10.1016/j.plaphy.2017.02.021

Ghasempour, H. R., Gaff, D. F., Williams, R. P. W., & Gianello, R. D. (1998). Contents of sugars in leaves of drying desiccation tolerant flowering plants, particularly grasses. In *Plant Growth Regulation* (Vol. 24).

Grant, C. E., & Bailey, T. L. (2021). *XSTREME: Comprehensive motif analysis of biological sequence datasets*. https://doi.org/10.1101/2021.09.02.458722

Hallam, N. D., & Gaff, D. F. (1918). REGENERATION OF CHLOROPLAST STRUCTURE IN TALBOTIA ELEGANS: A DESICCATION TOLERANT PLANT. In *New Phytol* (Vol. 81).

Hallam, N. D., & Luff, S. E. (1980). Fine Structural Changes in the Leaves of the Desiccation-Tolerant Plant Talbotia elegans during Extreme Water Stress. In *Gazette* (Vol. 141, Issue 2). https://about.jstor.org/terms

Hanson, L., McMahon, K. A., Johnson, M. A. T., & Bennett, M. D. (2001). First nuclear DNA C-values for 25 angiosperm families. *Annals of Botany*, *87*(2), 251–258. https://doi.org/10.1006/anbo.2000.1325

Harada, J. J. (2001). Role of Arabidopsis LEAFY COTYLEDON genes in seed development. In *J. Plant Physiol* (Vol. 158). http://www.urbanfischer.de/journals/jpp

Hartmann, T. (2007). From waste products to ecochemicals: Fifty years research of plant secondary metabolism. In *Phytochemistry* (Vol. 68, Issues 22–24, pp. 2831–2846). https://doi.org/10.1016/j.phytochem.2007.09.017

Hill, A., Nantel, A., Rock, C. D., & Quatrano, R. S. (1996). *A Conserved Domain of the viviparous-1 Gene Product Enhances the DNA Binding Activity of the bZIP Protein EmBP-1 and Other Transcription Factors**.

Huang, Y. C., Niu, C. Y., Yang, C. R., & Jinn, T. L. (2016). The heat stress factor HSFA6b connects ABA signaling and ABA-mediated heat responses. *Plant Physiology*, *172*(2), 1182–1199. https://doi.org/10.1104/pp.16.00860

Hulsen, T. (2022). *DeepVenn-a web application for the creation of area-proportional Venn diagrams using the deep learning framework Tensorflow.js*. https://www.deepvenn.com.

Illing, N., Denby, K. J., Collett, H., Shen, A., & Farrant, J. M. (2005). *The Signature of Seeds in Resurrection Plants: A Molecular and Physiological Comparison of Desiccation Tolerance in Seeds and Vegetative Tissues 1* (Vol. 45). www.genevestigator.ethz.ch

Ingle, R. A., Collett, H., Cooper, K., Takahashi, Y., Farrant, J. M., & Illing, N. (2008). Chloroplast biogenesis during rehydration of the resurrection plant Xerophyta humilis: Parallels to the etioplast-chloroplast transition. *Plant, Cell and Environment*, *31*(12), 1813–1824. https://doi.org/10.1111/j.1365-3040.2008.01887.x

Ingram, J., & Bartels, D. (1996). THE MOLECULAR BASIS OF DEHYDRATION TOLERANCE IN PLANTS. In *Annu. Rev. Plant Physiol. Plant Mol. Biol* (Vol. 47). www.annualreviews.org

Jaleel, C. A., Riadh, K., Gopi, R., Manivannan, P., Inès, J., Al-Juburi, H. J., Chang-Xing, Z., Hong-Bo, S., & Panneerselvam, R. (2009). Antioxidant defense responses: Physiological plasticity in higher plants under abiotic constraints. In *Acta Physiologiae Plantarum* (Vol. 31, Issue 3, pp. 427–436). https://doi.org/10.1007/s11738-009-0275-6

Jiao, B., Meng, Q., & Lv, W. (2020). Roles of stay-green (SGR) homologs during chlorophyll degradation in green plants. In *Botanical Studies* (Vol. 61, Issue 1). Springer Science and Business Media Deutschland GmbH. https://doi.org/10.1186/s40529-020-00302-5

Kalisch, B., Dörmann, P., & Hölzl, G. (2016). DGDG and glycolipids in plants and algae. *Subcellular Biochemistry*, *86*, 51–83. https://doi.org/10.1007/978-3-319-25979-6_3

Kanani, H., Chrysanthopoulos, P. K., & Klapa, M. I. (2008). Standardizing GC-MS metabolomics. *Journal of Chromatography B: Analytical Technologies in the Biomedical and Life Sciences*, *871*(2), 191–201. https://doi.org/10.1016/j.jchromb.2008.04.049

Kelly, A. A., & Dörmann, P. (2004). Green light for galactolipid trafficking. In *Current Opinion in Plant Biology* (Vol. 7, Issue 3, pp. 262–269). https://doi.org/10.1016/j.pbi.2004.03.009

Kishor, P. B. K., Hima Kumari, P., Sunita, M. S. L., & Sreenivasulu, N. (2015). Role of proline in cell wall synthesis and plant development and its implications in plant ontogeny. In *Frontiers in Plant Science* (Vol. 6, Issue JULY, pp. 1–17). Frontiers Research Foundation. https://doi.org/10.3389/fpls.2015.00544

Kranner, I., Beckett, R., Hochman, A., & Nash, T. H. (2008). Desiccation-Tolerance in Lichens: A Review. In *III Source: The Bryologist* (Vol. 111, Issue 4). Winter.

Kranner, I., Beckett, R. P., Wornik, S., Zorn, M., & Pfeifhofer, H. W. (2002). Revival of a resurrection plant correlates with its antioxidant status. *Plant Journal*, *31*(1), 13–24. https://doi.org/10.1046/j.1365-313X.2002.01329.x

Kwong, R. W., Bui, A. Q., Lee, H., Kwong, L. W., Fischer, R. L., Goldberg, R. B., & Harada, J. J. (2003). LEAFY COTYLEDON1-LIKE defines a class of regulators essential for embryo development. *Plant Cell*, *15*(1), 5–18. https://doi.org/10.1105/tpc.006973

Lai, D. H., Poropat, E., Pravia, C., Landoni, M., Couto, A. S., Pérez Rojo, F. G., Fuchs, A. G., Dubin, M., Elingold, I., Rodríguez, J. B., Ferella, M., Esteva, M. I., Bontempi, E. J., &

Lukeš, J. (2014). Solanesyl diphosphate synthase, an enzyme of the ubiquinone synthetic pathway, is required throughout the life cycle of Trypanosoma brucei. *Eukaryotic Cell*, *13*(2), 320–328. https://doi.org/10.1128/EC.00271-13

Lepiniec, L., Devic, M., Roscoe, T. J., Bouyer, D., Zhou, D. X., Boulard, C., Baud, S., & Dubreucq, B. (2018). Molecular and epigenetic regulations and functions of the LAFL transcriptional regulators that control seed development. In *Plant Reproduction* (Vol. 31, Issue 3, pp. 291–307). Springer Verlag. https://doi.org/10.1007/s00497-018-0337-2

Leprince, O., Pellizzaro, A., Berriri, S., & Buitink, J. (2017). Late seed maturation: Drying without dying. In *Journal of Experimental Botany* (Vol. 68, Issue 4, pp. 827–841). Oxford University Press. https://doi.org/10.1093/jxb/erw363

Li, J., Chen, Y., Zhang, R., Wu, B., & Xiao, G. (2023). Expression identification of three OsWRKY genes in response to abiotic stress and hormone treatments in rice. *Plant Signaling and Behavior*, *18*(1). https://doi.org/10.1080/15592324.2023.2292844

Li, S. (2015). The Arabidopsis thaliana TCP transcription factors: A broadening horizon beyond development. *Plant Signaling and Behavior*, *10*(7). https://doi.org/10.1080/15592324.2015.1044192

Ligterink, W., Dekkers, B. J. W., Hilhorst, H. W. M., Costa, M. C. D., Maia, J., & Bentsink, L. (2015). Acquisition and loss of desiccation tolerance in seeds: from experimental model to biological relevance. *Planta*. https://doi.org/10.1007/s00425-014-2240-x

Lim, P. O., Kim, Y., Breeze, E., Koo, J. C., Woo, H. R., Ryu, J. S., Park, D. H., Beynon, J., Tabrett, A., Buchanan-Wollaston, V., & Nam, H. G. (2007). Overexpression of a chromatin architecture-controlling AT-hook protein extends leaf longevity and increases the post-harvest storage life of plants. *Plant Journal*, *52*(6), 1140–1153. https://doi.org/10.1111/j.1365-313X.2007.03317.x

Lin, Y. X., Jiang, H. Y., Chu, Z. X., Tang, X. L., Zhu, S. W., & Cheng, B. J. (2011). Genome-wide identification, classification and analysis of heat shock transcription factor family in maize. *BMC Genomics*, *12*. https://doi.org/10.1186/1471-2164-12-76

Lippold, F., vom Dorp, K., Abraham, M., Hölzl, G., Wewer, V., Yilmaz, J. L., Lager, I., Montandon, C., Besagni, C., Kessler, F., Stymne, S., & Dörmann, P. (2012). Fatty acid phytyl ester synthesis in chloroplasts of Arabidopsis. *Plant Cell*, *24*(5), 2001–2014. https://doi.org/10.1105/tpc.112.095588

Liu, H. C., Liao, H. T., & Charng, Y. Y. (2011). The role of class A1 heat shock factors (HSFA1s) in response to heat and other stresses in Arabidopsis. *Plant, Cell and Environment*, *34*(5), 738–751. https://doi.org/10.1111/j.1365-3040.2011.02278.x

Liu, J., Moyankova, D., Djilianov, D., & Deng, X. (2019). Common and Specific Mechanisms of Desiccation Tolerance in Two Gesneriaceae Resurrection Plants. Multiomics Evidences. In *Frontiers in Plant Science* (Vol. 10). Frontiers Media S.A. https://doi.org/10.3389/fpls.2019.01067

Liu, J., Wang, Y., Chen, X., Tang, L., Yang, Y., Yang, Z., Sun, R., Mladenov, P., Wang, X., Liu, X., Jin, S., Li, H., Zhao, L., Wang, Y., Wang, W., & Deng, X. (2024). Specific metabolic and cellular mechanisms of the vegetative desiccation tolerance in resurrection plants for adaptation to extreme dryness. In *Planta* (Vol. 259, Issue 2). Springer Science and Business Media Deutschland GmbH. https://doi.org/10.1007/s00425-023-04323-9

Lopez-Molina, L., Bastien Mongrand, S., & Chua, N.-H. (2001). *A postgermination developmental arrest checkpoint is mediated by abscisic acid and requires the ABI5 transcription factor in Arabidopsis*. www.pnas.orgcgidoi10.1073pnas.081594298

Love, M. I., Huber, W., & Anders, S. (2014). Moderated estimation of fold change and dispersion for RNA-seq data with DESeq2. *Genome Biology*, *15*(12). https://doi.org/10.1186/s13059-014-0550-8

Lu, H., Zou, Y., & Feng, N. (2010). Overexpression of AHL20 negatively regulates defenses in arabidopsis. *Journal of Integrative Plant Biology*, *52*(9), 801–808. https://doi.org/10.1111/j.1744-7909.2010.00969.x

Lu, J., Xu, Y., Wang, J., Singer, S. D., & Chen, G. (2020). The role of triacylglycerol in plant stress response. In *Plants* (Vol. 9, Issue 4). MDPI AG. https://doi.org/10.3390/plants9040472

Lyall, R., Ingle, R. A., & Illing, N. (2014). The window of desiccation tolerance shown by early-stage germinating seedlings remains open in the resurrection plant, Xerophyta viscosa. *PLoS ONE*, *9*(3). https://doi.org/10.1371/journal.pone.0093093

Lyall, R., Schlebusch, S. A., Proctor, J., Prag, M., Hussey, S. G., Ingle, R. A., & Illing, N. (2020). Vegetative desiccation tolerance in the resurrection plant Xerophyta humilis has not evolved through reactivation of the seed canonical LAFL regulatory network. *Plant Journal*, *101*(6), 1349–1367. https://doi.org/10.1111/tpj.14596

Lyall Rafe. (2016). *Regulation of desiccation tolerance in Xerophyta seedlings and leaves*.

Maia, J., Dekkers, B. J. W., Provart, N. J., Ligterink, W., & Hilhorst, H. W. M. (2011). The re-establishment of desiccation tolerance in germinated arabidopsis thaliana seeds and its associated transcriptome. *PLoS ONE*, *6*(12). https://doi.org/10.1371/journal.pone.0029123

Markovska, Y. K., Tsonev, T. D., Kimenov, G. P., & Tutekova, A. A. (1994). Physiological Changes in Higher Poikilohydric Plants - Haberlea Rhodopensis Friv. and Ramonda Serbica Pan<c. during Drought and Rewatering at Different Light Regimes. *Journal of Plant Physiology*, *144*(1), 100–108. https://doi.org/10.1016/S0176-1617(11)81000-X

Marks, R. A., Farrant, J. M., Nicholas McLetchie, D., & VanBuren, R. (2021). Unexplored dimensions of variability in vegetative desiccation tolerance. *American Journal of Botany*, *108*(2), 346–358. https://doi.org/10.1002/ajb2.1588

Meyer, G., & Kloppstech, K. (1984). A rapidly light-induced chloroplast protein with a high turnover coded for by pea nuclear DNA. *European Journal of Biochemistry*, *138*(1), 201–207. https://doi.org/10.1111/j.1432-1033.1984.tb07900.x

Mihailova, G., Tchorbadjieva, M., Rakleova, G., & Georgieva, K. (2023). Differential Accumulation of sHSPs Isoforms during Desiccation of the Resurrection Plant Haberlea rhodopensis Friv. under Optimal and High Temperature. *Life*, *13*(1). https://doi.org/10.3390/life13010238

Mitra, J., Xu, G., Wang, B., Li, M., & Deng, X. (2013). Understanding desiccation tolerance using the resurrection plant Boea hygrometrica as a model system. In *Frontiers in Plant Science* (Vol. 4, Issue NOV). Frontiers Research Foundation. https://doi.org/10.3389/fpls.2013.00446

Moore, J. P., Farrant, J. M., & Driouich, A. (2008). A role for pectin-associated arabinans in maintaining the flexibility of the plant cell wall during water deficit stress. *Plant Signaling and Behavior*, *3*(2), 102–104. https://doi.org/10.4161/psb.3.2.4959

Moore, J. P., Nguema-Ona, E. E., Vicré-Gibouin, M., Sørensen, I., Willats, W. G. T., Driouich, A., & Farrant, J. M. (2013). Arabinose-rich polymers as an evolutionary strategy to plasticize resurrection plant cell walls against desiccation. *Planta*, *237*(3), 739–754. https://doi.org/10.1007/s00425-012-1785-9

Moore, J. P., Westall, K. L., Ravenscroft, N., Farrant, J. M., Lindsey, G. G., & Brandt, W. F. (2005). The predominant polyphenol in the leaves of the resurrection plant Myrothamnus flabellifolius, 3,4,5 tri-O-galloylquinic acid, protects membranes against desiccation and free radical-induced oxidation. In *Biochem. J* (Vol. 385). http://portlandpress.com/biochemj/article-pdf/385/1/301/717588/bj3850301.pdf

Moyankova, D., Mladenov, P., Berkov, S., Peshev, D., Georgieva, D., & Djilianov, D. (2014). Metabolic profiling of the resurrection plant Haberlea rhodopensis during desiccation and recovery. *Physiologia Plantarum*, *152*(4), 675–687. https://doi.org/10.1111/ppl.12212

Mozgova, I., & Hennig, L. (2015). The polycomb group protein regulatory network. *Annual Review of Plant Biology*, *66*, 269–296. https://doi.org/10.1146/annurev-arplant-043014-115627

Mueller, W. C., & Greenwood, A. D. (1978). The infrastructure of Phenolic-Storing Cells Fixed with Caffeine 1. In *Journal of Experimental Botany* (Vol. 29, Issue 110). https://academic.oup.com/jxb/article/29/3/757/435635

Müller, J., Sprenger, N., Bortlik, K., Boller, T., & Wiemken, A. (1997). Desiccation increases sucrose levels in Ramonda and Haberlea, two genera of resurrection plants in the Gesneriaceae . *Physiologia Plantarum*, *100*(1), 153–158. https://doi.org/10.1111/j.1399-3054.1997.tb03466.x

Mundree, S. G., Baker, B., Mowla, S., Peters, S., Marais, S., Willigen, C. Vander, Govender, K., Maredza, A., Muyanga, S., Farrant, J. M., & Thomson, J. A. (2002). Physiological and molecular insights into drought tolerance. *African Journal of Biotechnology*, *1*(2), 28–38. http://www.academicjournals.org/AJB

Nakamura, S., Lynch, T. J., & Finkelstein, R. R. (2001). Physical interactions between ABA response loci of Arabidopsis. *Plant Journal*, *26*(6), 627–635. https://doi.org/10.1046/j.1365-313X.2001.01069.x

Nakashima, K., & Yamaguchi-Shinozaki, K. (2013). ABA signaling in stress-response and seed development. In *Plant Cell Reports* (Vol. 32, Issue 7, pp. 959–970). https://doi.org/10.1007/s00299-013-1418-1

Ne Montané, M.-H., & Kloppstech, K. (2000). The family of light-harvesting-related proteins (LHCs, ELIPs, HLIPs): was the harvesting of light their primary function? In *Gene* (Vol. 258). www.elsevier.com/locate/gene

Oliver, M. J., Farrant, J. M., Hilhorst, H. W. M., Mundree, S., Williams, B., & Bewley, J. D. (2020). *Desiccation Tolerance: Avoiding Cellular Damage During Drying and Rehydration*. https://doi.org/10.1146/annurev-arplant-071219

Oliver, M. J., Guo, L., Alexander, D. C., Ryals, J. A., Wone, B. W. M., & Cushman, J. C. (2011). A sister group contrast using untargeted global metabolomic analysis delineates

the biochemical regulation underlying desiccation tolerance in Sporobolus stapfianus. *Plant Cell*, *23*(4), 1231–1248. https://doi.org/10.1105/tpc.110.082800

Oliver, M. J., Tuba, Z., & Mishler, B. D. (2000). The evolution of vegetative desiccation tolerance in land plants. In *Plant Ecology* (Vol. 151).

Oliver, M. J., Velten, J., & Mishler, B. D. (2005). *Desiccation Tolerance in Bryophytes: A Reflection of the Primitive Strategy for Plant Survival in Dehydrating Habitats? 1* (Vol. 45). https://academic.oup.com/icb/article/45/5/788/624442

Osbourn, A. E., Qi, X., Townsend, B., & Qin, B. (2003). Dissecting plant secondary metabolism - Constitutive chemical defences in cereals. In *New Phytologist* (Vol. 159, Issue 1, pp. 101–108). https://doi.org/10.1046/j.1469-8137.2003.00759.x

osefa Alamillo, J., artels, D. B., & Jordano, J. (1995). Constitutive expression of small heat shock proteins in vegetative tissues of the resurrection plant Craterostigma plantagineum. In *Plant Molecular Biology* (Vol. 29).

Oung, H. M. O., Mukhopadhyay, R., Svoboda, V., Charuvi, D., Reich, Z., & Kirchhoff, H. (2022). Differential response of the photosynthetic machinery to dehydration in older and younger resurrection plants. *Journal of Experimental Botany*, *73*(5), 1566–1580. https://doi.org/10.1093/jxb/erab485

Pardo, J., Man Wai, C., Chay, H., Madden, C. F., Hilhorst, H. W., Farrant, J. M., & VanBuren, R. (2020). Intertwined signatures of desiccation and drought tolerance in grasses. *Proceedings of the National Academy of Sciences*, 117(18), 10079-10088.

Peters, S., Mundree, S. G., Thomson, J. A., Farrant, J. M., & Keller, F. (2007). Protection mechanisms in the resurrection plant Xerophyta viscosa (Baker): Both sucrose and raffinose family oligosaccharides (RFOs) accumulate in leaves in response to water deficit. *Journal of Experimental Botany*, *58*(8), 1947–1956. https://doi.org/10.1093/jxb/erm056

Phillips, J. R., Fischer, E., Baron, M., Van Den Dries, N., Facchinelli, F., Kutzer, M., Rahmanzadeh, R., Remus, D., & Bartels, D. (2008). Lindernia brevidens: A novel desiccation-tolerant vascular plant, endemic to ancient tropical rainforests. *Plant Journal*, *54*(5), 938–948. https://doi.org/10.1111/j.1365-313X.2008.03478.x

Pirkkala, L., Nykanen, P., & Sistonen, L. (2001). Roles of the heat shock transcription factors in regulation of the heat shock response and beyond. *The FASEB Journal*, *15*(7), 1118–1131. https://doi.org/10.1096/fj00-0294rev

Porembski, S., & Barthlott, W. (2000). Granitic and gneissic outcrops (inselbergs) as centers of diversity for desiccation-tolerant vascular plants. In *Plant Ecology* (Vol. 151).

Quartacci, M. F., Forli, M., Rascio, N., Dalla Vecchia, F., Bochicchio, A., & Navari-Lzzo, F. (1997). Desiccation-tolerant Sporobolus stapfianus: lipid composition and cellular ultrastructure during dehydration and rehydration. In *Journal of Experimental Botany* (Vol. 48, Issue 311). https://academic.oup.com/jxb/article/48/6/1269/654733

Radermacher, A. L., du Toit, S. F., & Farrant, J. M. (2019). Desiccation-Driven Senescence in the Resurrection Plant Xerophyta schlechteri (Baker) N.L. Menezes: Comparison of Anatomical, Ultrastructural, and Metabolic Responses Between Senescent and Non-Senescent Tissues. *Frontiers in Plant Science*, *10*. https://doi.org/10.3389/fpls.2019.01396

Raz, V., Bergervoet, J. H. W., & Koornneef, M. (2001). *Sequential steps for developmental arrest in Arabidopsis seeds*.

Reynolds, E. S. (1963). *THE USE OF LEAD CITRATE AT HIGH pH AS AN ELECTRON-OPAQUE STAIN IN ELECTRON MICROSCOPY*.

Sakuraba, Y., Park, S. Y., Kim, Y. S., Wang, S. H., Yoo, S. C., Hörtensteiner, S., & Paek, N. C. (2014). Arabidopsis STAY-GREEN2 is a negative regulator of chlorophyll degradation during leaf senescence. *Molecular Plant*, *7*(8), 1288–1302. https://doi.org/10.1093/mp/ssu045

Scharf, K. D., Rose, S., Zott, W., Schöffl, F., Nover, L., & Schöff, F. (1990). Three tomato genes code for heat stress transcription factors with a region of remarkable homology to the DNA-binding domain of the yeast HSF. *The EMBO Journal*, *9*(13), 4495–4501. https://doi.org/10.1002/j.1460-2075.1990.tb07900.x

Schneider, K., Wells, B., Schmelzer, E., Salaminp, F., & Bartels, D. (1993). Desiccation leads to the rapid accumulation of both cytosolic and chloroplastic proteins in the resurrection plant Craterostigma plantagineum Hochst. In *Planta* (Vol. 189). Springer-Verlag.

Sherwin, H. W., & Farrant, J. M. (1996). Differences in Rehydration of Three Desiccation-tolerant Angiosperm Species. In *Source: Annals of Botany* (Vol. 78, Issue 6). https://about.jstor.org/terms

Sherwin, H. W., & Farrant, J. M. (1998). Protection mechanisms against excess light in the resurrection plants Craterostigma wilmsii and Xerophyta viscosa. In *Plant Growth Regulation* (Vol. 24).

Shimoda, Y., Ito, H., & Tanaka, A. (2016). Arabidopsis STAY-GREEN, mendel's green cotyledon gene, encodes magnesium-dechelatase. *Plant Cell*, *28*(9), 2147–2160. https://doi.org/10.1105/tpc.16.00428

Shrestha, A., Cudjoe, D. K., Kamruzzaman, M., Siddique, S., Fiorani, F., Léon, J., & Naz, A. A. (2021). Abscisic acid-responsive element binding transcription factors contribute to proline synthesis and stress adaptation in Arabidopsis. *Journal of Plant Physiology*, *261*. https://doi.org/10.1016/j.jplph.2021.153414

Singh, B., & Sharma, R. A. (2015). Plant terpenes: defense responses, phylogenetic analysis, regulation and clinical applications. *3 Biotech*, *5*(2), 129–151. https://doi.org/10.1007/s13205-014-0220-2

Smirnoff, N. (1993). Tansley Review No. 52. The Role of Active Oxygen in the Response of Plants to Water Deficit and Desiccation. In *Source: The New Phytologist* (Vol. 125, Issue 1). https://www.jstor.org/stable/2557905

Spurr, A. R. (1969). A Low-Viscosity Epoxy Resin Embedding Medium for Electron Microscopy. In *J. ULTRASTRUCTURE RESEARCH* (Vol. 26).

St. Aubin, B., Wai, C. M., Kenchanmane Raju, S. K., Niederhuth, C. E., & VanBuren, R. (2022). Regulatory dynamics distinguishing desiccation tolerance strategies within resurrection grasses. *Plant Direct*, 6(12), 457.

Suguiyama, V. F., Silva, E. A., Meirelles, S. T., Centeno, D. C., & Braga, M. R. (2014). Leaf metabolite profile of the Brazilian resurrection plant Barbacenia purpurea Hook. (Velloziaceae) shows two time-dependent responses during desiccation and recovering. In *Frontiers in Plant Science* (Vol. 5, Issue MAR). Frontiers Research Foundation. https://doi.org/10.3389/fpls.2014.00096

Sun, R. Z., Lin, C. T., Zhang, X. F., Duan, L. X., Qi, X. Q., Gong, Y. H., & Deng, X. (2018). Acclimation-induced metabolic reprogramming contributes to rapid desiccation tolerance acquisition in Boea hygrometrica. *Environmental and Experimental Botany*, *148*, 70–84. https://doi.org/10.1016/j.envexpbot.2018.01.008

Sun, Y., Pri-Tal, O., Michaeli, D., & Mosquna, A. (2020). Evolution of Abscisic Acid Signaling Module and Its Perception. In *Frontiers in Plant Science* (Vol. 11). Frontiers Media S.A. https://doi.org/10.3389/fpls.2020.00934

Suzuki, M., Kao, C. Y., Cocciolone, S., & McCarty, D. R. (2001). Maize VP1 complements Arabidopsis abi3 and confers a novel ABA/auxin interaction in roots. *Plant Journal*, *28*(4), 409–418. https://doi.org/10.1046/j.1365-313X.2001.01165.x

Suzuki, M., Yuan Kao, C., & McCartyl, D. R. (1997). The Conserved B3 Domain of VIVIPAROUSI Has a Cooperative DNA Binding Activity. In *The Plant Cell* (Vol. 9). American Society of Plant Physiologists. https://academic.oup.com/plcell/article/9/5/799/5986386

Swindell, W. R., Huebner, M., & Weber, A. P. (2007). Transcriptional profiling of Arabidopsis heat shock proteins and transcription factors reveals extensive overlap between heat and non-heat stress response pathways. *BMC Genomics*, *8*. https://doi.org/10.1186/1471-2164-8-125

Terrasson, E., Buitink, J., Righetti, K., Vu, B. L., Pelletier, S., Zinsmeister, J., Lalanne, D., & Leprince, O. (2013). An emerging picture of the seed desiccome: Confirmed regulators and newcomers identified using transcriptome comparison. *Frontiers in Plant Science*, *4*(DEC). https://doi.org/10.3389/fpls.2013.00497

Torres-Franklin, M. L., Gigon, A., De Melo, D. F., Zuily-Fodil, Y., & Pham-Thi, A. T. (2007). Drought stress and rehydration affect the balance between MGDG and DGDG synthesis in cowpea leaves. *Physiologia Plantarum*, *131*(2), 201–210. https://doi.org/10.1111/j.1399-3054.2007.00943.x

Tshabuse, F., Farrant, J. M., Humbert, L., Moura, D., Rainteau, D., Espinasse, C., Idrissi, A., Merlier, F., Acket, S., Rafudeen, M. S., Thomasset, B., & Ruelland, E. (2018). Glycerolipid analysis during desiccation and recovery of the resurrection plant Xerophyta humilis (Bak) Dur and Schinz. *Plant Cell and Environment*, *41*(3), 533–547. https://doi.org/10.1111/pce.13063

Tsukagoshi, H., Morikami, A., & Nakamura, K. (2007). *Two B3 domain transcriptional repressors prevent sugar-inducible expression of seed maturation genes in Arabidopsis seedlings*. www.pnas.org/cgi/content/full/

Tuba, Z., Protor, M. C. F., & Csintalan, Z. (1998). Ecophysiological responses of homoiochlorophyllous and poikilochlorophyllous desiccation tolerant plants: a comparison and an ecological perspective. In *Plant Growth Regulation* (Vol. 24).

Uno, Y., Furihata, T., Abe, H., Yoshida, R., Shinozaki, K., & Yamaguchi-Shinozaki, K. (2000). *Arabidopsis basic leucine zipper transcription factors involved in an abscisic acid-dependent signal transduction pathway under drought and high-salinity conditions*. www.pnas.org

Vanburen, R., Bryant, D., Edger, P. P., Tang, H., Burgess, D., Challabathula, D., Spittle, K., Hall, R., Gu, J., Lyons, E., Freeling, M., Bartels, D., Ten Hallers, B., Hastie, A., Michael, T. P., & Mockler, T. C. (2015). Single-molecule sequencing of the desiccation-tolerant

grass Oropetium thomaeum. *Nature*, *527*(7579), 508–511. https://doi.org/10.1038/nature15714

VanBuren, R., Wai, C. M., Zhang, Q., Song, X., Edger, P. P., Bryant, D., Michael, T. P., Mockler, T. C., & Bartels, D. (2017). Seed desiccation mechanisms co-opted for vegetative desiccation in the resurrection grass Oropetium thomaeum. *Plant Cell and Environment*, *40*(10), 2292–2306. https://doi.org/10.1111/pce.13027

Vecchia, F. D., El Asmar, T., Calamassi, R., Rascio, N., & Vazzana, C. (1998). *Morphological and ultrastructural aspects of dehydration and rehydration in leaves of Sporobolus stapfianus*.

Venzhik, Y. V., Shchyogolev, S. Y., & Dykman, L. A. (2019). Ultrastructural Reorganization of Chloroplasts during Plant Adaptation to Abiotic Stress Factors. In *Russian Journal of Plant Physiology* (Vol. 66, Issue 6, pp. 850–863). Pleiades Publishing. https://doi.org/10.1134/S102144371906013X

Verbruggen, N., & Hermans, C. (2008). Proline accumulation in plants: A review. In *Amino Acids* (Vol. 35, Issue 4, pp. 753–759). https://doi.org/10.1007/s00726-008-0061-6

Verelst, W., & Asard, H. (2004). Analysis of an Arabidopsis thaliana protein family, structurally related to cytochromes b561 and potentially involved in catecholamine biochemistry in plants. In *J. Plant Physiol* (Vol. 161). http://www.elsevier-deutschland.de/jplhp

Vicré, M., Farrant, J. M., & Driouich, A. (2004). Insights into the cellular mechanisms of desiccation tolerance among angiosperm resurrection plant species. In *Plant, Cell and Environment*. https://doi.org/10.1111/j.1365-3040.2004.01212.x

Vierling, E. (1991). The roles of heat shock proteins in plants. *Annual Review of Plant Physiology and Plant Molecular Biology*, *42*(1), 579–620. https://doi.org/10.1146/annurev.pp.42.060191.003051

Wachananawat, B., Kuroha, T., Takenaka, Y., Kajiura, H., Naramoto, S., Yokoyama, R., Ishizaki, K., Nishitani, K., & Ishimizu, T. (2020). Diversity of Pectin Rhamnogalacturonan I Rhamnosyltransferases in Glycosyltransferase Family 106. *Frontiers in Plant Science*, *11*. https://doi.org/10.3389/fpls.2020.00997

Walford, S.-A. (2008). *Activation of seed-specific genes in leaves and roots of the desiccation tolerant plant, Xerophyta humilis*.

Wang, W., Vinocur, B., Shoseyov, O., & Altman, A. (2004). Role of plant heat-shock proteins and molecular chaperones in the abiotic stress response. In *Trends in Plant Science* (Vol. 9, Issue 5, pp. 244–252). https://doi.org/10.1016/j.tplants.2004.03.006

Waters, E. R. (2013). The evolution, function, structure, and expression of the plant sHSPs. In *Journal of Experimental Botany* (Vol. 64, Issue 2, pp. 391–403). https://doi.org/10.1093/jxb/ers355

Waters, E. R., & Vierling, E. (2020). Plant small heat shock proteins – evolutionary and functional diversity. In *New Phytologist* (Vol. 227, Issue 1, pp. 24–37). Blackwell Publishing Ltd. https://doi.org/10.1111/nph.16536

Whittaker, A., Bochicchio, A., Vazzana, C., Lindsey, G., & Farrant, J. (2001). *Changes in leaf hexokinase activity and metabolite levels in response to drying in the desiccation-tolerant species Sporobolus stapfianus and Xerophyta viscosa*.

Xue, J., Balamurugan, S., Li, D. W., Liu, Y. H., Zeng, H., Wang, L., Yang, W. D., Liu, J. S., & Li, H. Y. (2017). Glucose-6-phosphate dehydrogenase as a target for highly efficient fatty acid biosynthesis in microalgae by enhancing NADPH supply. *Metabolic Engineering*, *41*, 212–221. https://doi.org/10.1016/j.ymben.2017.04.008

Yobi, A., Schlauch, K. A., Tillett, R. L., Yim, W. C., Espinoza, C., Wone, B. W. M., Cushman, J. C., & Oliver, M. J. (2017). Sporobolus stapfianus: Insights into desiccation tolerance in the resurrection grasses from linking transcriptomics to metabolomics. *BMC Plant Biology*, *17*(1). https://doi.org/10.1186/s12870-017-1013-7

Yobi, A., Wone, B. W. M., Xu, W., Alexander, D. C., Guo, L., Ryals, J. A., Oliver, M. J., & Cushman, J. C. (2012). Comparative metabolic profiling between desiccation-sensitive and desiccation-tolerant species of Selaginella reveals insights into the resurrection trait. *Plant Journal*, *72*(6), 983–999. https://doi.org/10.1111/tpj.12008

Yoshida, T., Fujita, Y., Maruyama, K., Mogami, J., Todaka, D., Shinozaki, K., & Yamaguchi-Shinozaki, K. (2015). Four Arabidopsis AREB/ABF transcription factors function predominantly in gene expression downstream of SnRK2 kinases in abscisic acid signalling in response to osmotic stress. *Plant, Cell and Environment*, *38*(1), 35–49. https://doi.org/10.1111/pce.12351

Yu, R., Song, Q., Wang, G., Wu, L., Ruan, J., Yang, C., Li, S., & Wang, J. (2024). Desiccation tolerance mechanisms of resurrection plant Selaginella pulvinata. *Environmental and Experimental Botany*, *218*. https://doi.org/10.1016/j.envexpbot.2023.105602

Yue Ma, Izabela Szostkiewicz, Arthur Korte, Danièle Moes, Yi Yang, Alexander Christmann, & Erwin Grill. (2009). Regulators of PP2C Phosphatase Activity Function as Abscisic Acid Sensors. *Science*, *324*(5930), 1061–1064. https://doi.org/10.1126/science.1171155

Zamora-Briseño, J. A., & de Jiménez, E. S. (2016). A LEA 4 protein up-regulated by ABA is involved in drought response in maize roots. *Molecular Biology Reports*, *43*(4), 221–228. https://doi.org/10.1007/s11033-016-3963-5

Zhang, Q., & Bartels, D. (2018). Molecular responses to dehydration and desiccation in desiccation-tolerant angiosperm plants. In *Journal of Experimental Botany*. https://doi.org/10.1093/jxb/erx489

Zhang, W. M., Cheng, X. Z., Fang, D., & Cao, J. (2022). AT-HOOK MOTIF NUCLEAR LOCALIZED (AHL) proteins of ancient origin radiate new functions. In *International Journal of Biological Macromolecules* (Vol. 214, pp. 290–300). Elsevier B.V. https://doi.org/10.1016/j.ijbiomac.2022.06.100

Zhang, Z., Wang, B., Sun, D., & Deng, X. (2013). Molecular cloning and differential expression of sHSP gene family members from the resurrection plant Boea hygrometrica in response to abiotic stresses. *Biologia (Poland)*, *68*(4), 651–661. https://doi.org/10.2478/s11756-013-0204-4

Zhu, Y., Wang, B., Phillips, J., Zhang, Z. N., Du, H., Xu, T., Huang, L. C., Zhang, X. F., Xu, G. H., Li, W. L., Wang, Z., Wang, L., Liu, Y. X., & Deng, X. (2015). Global transcriptome analysis reveals acclimation-primed processes involved in the acquisition of desiccation tolerance in Boea hygrometrica. *Plant and Cell Physiology*, *56*(7), 1429–1441. https://doi.org/10.1093/pcp/pcv059

Zhu, Y., Wang, Z., Jing, Y., Wang, L., Liu, X., Liu, Y., & Deng, X. (2009). Ectopic over-expression of BhHsf1, a heat shock factor from the resurrection plant Boea hygrometrica,

leads to increased thermotolerance and retarded growth in transgenic Arabidopsis and tobacco. *Plant Molecular Biology*, *71*(4–5), 451–467. https://doi.org/10.1007/s11103-009-9538-2

Zolkiewski, M., Zhang, T., & Nagy, M. (2012). Aggregate reactivation mediated by the Hsp100 chaperones. In *Archives of Biochemistry and Biophysics* (Vol. 520, Issue 1, pp. 1–6). https://doi.org/10.1016/j.abb.2012.01.012

APPENDICES

Appendix A. Sample scripts demonstrating the execution of programs used to generate the transcriptomic data in this study

Appendix A.1 Raw count normalization (DESeq2 v. 1.38.3)

```
library("DESeq2")
## X. elegans Late Seedlings DESeq2 normalization
setwd("/Users/SaSa/Desktop/UCT/PhD_Project/RNASeq/RNA-Seq
Results/Analysis/featureCounts/Xe/Late")
XeL_count <- read.csv(file = "XeL_combinedCounts.csv", row.names=1)
XeL_colData <- read.csv(file = "XeL_colData.csv", row.names = 1)

all(colnames(XeL_count) %in% row.names(XeL_colData))
all(colnames(XeL_count) == row.names(XeL_colData))

## Construct a DESeqDataSet object
XeL_dds <- DESeqDataSetFromMatrix(countData = XeL_count,
                          colData = XeL_colData,
                          design = ~ Condition)
##Set factor level and specify reference
XeL_dds <- relevel(XeL_ddsCondition, ref = "Late-hydrated")
is.atomic(XeL_dds)

## Run DESeq
XeL_dds1 <- DESeq(XeL_dds)
#Export DESeq2normalized counts
XeLdds_Normcounts <- counts(XeL_dds1, normalized=TRUE)

##First convert the count file to data.frame
XeLdds_Normcounts_df <- as.data.frame(XeLdds_Normcounts)
write.csv(XeLdds_Normcounts_df, XeLDESeq_NormCounts.csv", row.names = TRUE)
```

Appendix A.2 Identifying differentially expressed genes (DESeq2 v. 1.38.3)

```
##Read in count and metadata files
XeL_count <- read.csv(file = "XeL_combinedCounts.csv", row.names=1)
XeL_colData <- read.csv(file = "XeL_colData.csv", row.names = 1)

##Construct a DESeqDataSet object
XeL_dds <- DESeqDataSetFromMatrix(countData = XeL_count,
                          colData = XeL_colData,
                          design = ~ Condition)

##Pre-filtering step to remove rows with low gene counts and keep those with at least 10 reads
```

```
Xe_keepL <- rowSums(counts(XeL_dds) >= 10) >=3
XeL_dds <- XeL_dds [Xe_keepL,]

##Set factor level and specify the reference
XeL_dds$Condition <- relevel(XeL_dds$Condition, ref = "Hydrated")

##Run DESeq
XeL_dds1 <- DESeq(XeL_dds)
#save results
res_XeL <- results(XeL_dds1)
res_XeL = results(XeL_dds1, contrast=c("Condition","Dehydrated","Hydrated"))

XeL_reslfc1 <- lfcShrink(XeL_dds1, res=res_XeL, coef= "Condition_Dehydrated_vs_Hydrated",
lfcThreshold=1, type="apeglm")
XeL_reslfc1_df <- as.data.frame(XeL_reslfc1)
write.csv(XeL_reslfc1_df, "XeL_DESeq2_ALL_results.csv", row.names = TRUE”

#Keep deferentially expressed genes
XeL_reslfc1_df <- as.data.frame(XeL_reslfc1)
XeL_reslfc1_sig <- XeL_reslfc1_df %>% filter(svalue <0.005)
write.csv(XeL_reslfc1_sig, "XeL_DESeq2_DEG_results.csv", row.names = TRUE)
```

Appendix A.3 Preparing and filtering the "master” grthogroup file

```
library(tidyverse)
library(data.table)
library(dbplyr)

## Create separate dataframes for Xe, Xs and Xh
Original_MasterOGlistv2<- read.csv("MasterOGlist_Xerophyta_v2.csv", header=T)
Xe_df = Original_MasterOGlistv2 %>% select(OG, Xelegans) %>% filter(Xelegans != "") %>%
group_by(OG) %>% summarise(Xe=paste(Xelegans, collapse = ",")) %>% as.data.frame
write.csv(Xe_df, "Xe_OGlist_v2.csv")
Xs_df = Original_MasterOGlistv2 %>% select(OG,Xschlechteri) %>% filter(Xschlechteri != "") %>%
group_by(OG) %>% summarise(Xs=paste(Xschlechteri, collapse = ",")) %>% as.data.frame
write.csv(Xs_df, "Xs_OGlist.csv")
Xh_df = Original_MasterOGlistv2 %>% select(OG,Xhumilis) %>% filter(Xhumilis != "") %>%
group_by(OG) %>% summarise(Xh=paste(Xhumilis, collapse = ",")) %>% as.data.frame
write.csv(Xh_df, "Xh _OGlist.csv")

## merge the three dataframes into a single master file
Xero_masterOG_v2 = Xe_df %>% full_join(Xs_df,by="OG") %>% full_join(Xh_df,by="OG")
write.csv(Xero_masterOG_v2B, Xero_masterOG_v2B.csv")

## add total counts per species, and rearrange columns so that counts are first
Xero_masterOG_v2B_df = Xero_masterOG_v2B_df %>%
  mutate(Xe_genecount=sapply(strsplit(Xe,','), uniqueN)) %>%
  mutate(Xh_genecount=sapply(strsplit(Xh,','), uniqueN)) %>%
  mutate(Xs_genecount=sapply(strsplit(Xs,','), uniqueN)) %>%
```

```
  select(OG,Xe_genecount,Xh_genecount,Xs_genecount,Xe,Xh,Xs)
write.csv(Xero_masterOG2, Xero_masterOG2.csv")

##import the OG list and delete whitespace (important)
Xero_masterOG_v2B_df$Xe=str_replace_all(Xero_masterOG_v2B_df$Xe," ","")
Xero_masterOG_v2B_df$Xs=str_replace_all(Xero_masterOG_v2B_df$Xs," ","")
Xero_masterOG_v2B_df$Xh=str_replace_all(Xero_masterOG_v2B_df$Xh," ","")

## import all of the DEG lists
XeEarly_DOWN=read.csv(file="XeEarly_DEGs_DOWNREGULATED.csv",header=TRUE)  %>%
unlist %>% unname
XeEarly_UP=read.csv(file="XeEarly_DEGs_UPREGULATED.csv",header=TRUE)  %>%  unlist
%>% unname
XeLate_DOWN=read.csv(file="XeLate_DEGs_DOWNREGULATED.csv",header=TRUE)  %>%
unlist %>% unname
XeLate_UP=read.csv(file="XeLate_DEGs_UPREGULATED.csv",header=TRUE) %>% unlist %>%
unname

XsEarly_DOWN=read.csv(file="XsEarlyV2_DEGs_DOWNREGULATED.csv",header=TRUE)
%>% unlist %>% unname
XsEarly_UP=read.csv(file="XsEarlyV2_DEGs_UPREGULATED_24072023.csv",header=TRUE)
%>% unlist %>% unname
XsLate_DOWN=read.csv(file="XsLateV2_DEGs_DOWNREGULATED_24072023.csv",header=TR
UE) %>% unlist %>% unname
XsLate_UP=read.csv(file="XsLateV2_DEGs_UPREGULATED_24072023.csv",header=TRUE)
%>% unlist %>% unname

XhEarly_DOWN=read.csv(file="Xhv13B_DOWNREGULATED_Early.csv",header=TRUE)  %>%
unlist %>% unname
XhEarly_UP=read.csv(file="Xhv13B_UPREGULATED_Early.csv",header=TRUE)  %>%  unlist
%>% unname
XhLate_DOWN=read.csv(file="Xhv13B_DOWNREGULATED_Late.csv",header=TRUE)  %>%
unlist %>% unname
XhLate_UP=read.csv(file="Xhv13B_UPREGULATED_Late.csv",header=TRUE) %>% unlist %>%
unname
# add the gene lists for DEGs (this step is weird, sorry)
Xero_masterOG_v2B_df$XeEarly_DOWN=list(XeEarly_DOWN)
Xero_masterOG_v2B_df$XeEarly_UP=list(XeEarly_UP)
Xero_masterOG_v2B_df$XeLate_DOWN=list(XeLate_DOWN)
Xero_masterOG_v2B_df$XeLate_UP=list(XeLate_UP)

Xero_masterOG_v2B_df$XsEarly_DOWN=list(XsEarly_DOWN)
Xero_masterOG_v2B_df$XsEarly_UP=list(XsEarly_UP)
Xero_masterOG_v2B_df$XsLate_DOWN=list(XsLate_DOWN)
Xero_masterOG_v2B_df$XsLate_UP=list(XsLate_UP)

Xero_masterOG_v2B_df$XhEarly_DOWN=list(XhEarly_DOWN)
Xero_masterOG_v2B_df$XhEarly_UP=list(XhEarly_UP)
```

```
Xero_masterOG_v2B_df$XhLate_DOWN=list(XhLate_DOWN)
Xero_masterOG_v2B_df$XhLate_UP=list(XhLate_UP)

## convert the gene values to lists not char
Xero_masterOG_v2B_df=Xero_masterOG_v2B_df %>% mutate(Xe = strsplit(Xe,","),Xs = strsplit(Xs,","),Xh = strsplit(Xh,","))

## calculate the number of DEGs per group
Xero_masterOG_v2B_df=Xero_masterOG_v2B_df %>% rowwise() %>% mutate(num_XeEarly_DOWN = lengths(list(intersect(Xe,XeEarly_DOWN)))) %>% arrange(desc(num_XeEarly_DOWN))
Xero_masterOG_v2B_df=Xero_masterOG_v2B_df %>% rowwise() %>% mutate(num_XeEarly_UP = lengths(list(intersect(Xe,XeEarly_UP)))) %>% arrange(desc(num_XeEarly_UP))
Xero_masterOG_v2B_df=Xero_masterOG_v2B_df %>% rowwise() %>% mutate(num_XeLate_DOWN = lengths(list(intersect(Xe,XeLate_DOWN)))) %>% arrange(desc(num_XeLate_DOWN))
Xero_masterOG_v2B_df=Xero_masterOG_v2B_df %>% rowwise() %>% mutate(num_XeLate_UP = lengths(list(intersect(Xe,XeLate_UP)))) %>% arrange(desc(num_XeLate_UP))

Xero_masterOG_v2B_df=Xero_masterOG_v2B_df %>% rowwise() %>% mutate(num_XsEarly_DOWN = lengths(list(intersect(Xs,XsEarly_DOWN)))) %>% arrange(desc(num_XsEarly_DOWN))
Xero_masterOG_v2B_df=Xero_masterOG_v2B_df %>% rowwise() %>% mutate(num_XsEarly_UP = lengths(list(intersect(Xs,XsEarly_UP)))) %>% arrange(desc(num_XsEarly_UP))
Xero_masterOG_v2B_df=Xero_masterOG_v2B_df %>% rowwise() %>% mutate(num_XsLate_DOWN = lengths(list(intersect(Xs,XsLate_DOWN)))) %>% arrange(desc(num_XsLate_DOWN))
Xero_masterOG_v2B_df=Xero_masterOG_v2B_df %>% rowwise() %>% mutate(num_XsLate_UP = lengths(list(intersect(Xs,XsLate_UP)))) %>% arrange(desc(num_XsLate_UP))

Xero_masterOG_v2B_df=Xero_masterOG_v2B_df %>% rowwise() %>% mutate(num_XhEarly_DOWN = lengths(list(intersect(Xh,XhEarly_DOWN)))) %>% arrange(desc(num_XhEarly_DOWN))
Xero_masterOG_v2B_df=Xero_masterOG_v2B_df %>% rowwise() %>% mutate(num_XhEarly_UP = lengths(list(intersect(Xh,XhEarly_UP)))) %>% arrange(desc(num_XhEarly_UP))
Xero_masterOG_v2B_df=Xero_masterOG_v2B_df %>% rowwise() %>% mutate(num_XhLate_DOWN = lengths(list(intersect(Xh,XhLate_DOWN)))) %>% arrange(desc(num_XhLate_DOWN))
Xero_masterOG_v2B_df=Xero_masterOG_v2B_df %>% rowwise() %>% mutate(num_XhLate_UP = lengths(list(intersect(Xh,XhLate_UP)))) %>% arrange(desc(num_XhLate_UP))

## save count info
Xero_masterOG3counts_v2=Xero_masterOG_v2B_df %>% select("OG","Xe_genecount","Xs_genecount","Xh_genecount","num_XeEarly_DOWN","num_XeEarly_UP","num_XeLate_DOWN","num_XeLate_UP","num_XsEarly_DOWN","num_XsEarly_UP","num_XsLate_DOWN","num_XsLate_UP","num_XhEarly_DOWN","num_XhEarly_UP","num_XhLate_DOWN","num_XhLate_UP")
write.csv(Xero_masterOG3counts_v2, “Xero_masterOG3counts_v2.csv")
```

```
## DE OG count file
DEmasterOG_count_v2 = subset(Xero_masterOG3counts_v2, Xero_masterOG3counts_v2[, 5] > 0 |
Xero_masterOG3counts_v2[, 6] > 0 | Xero_masterOG3counts_v2[, 7] > 0 |
Xero_masterOG3counts_v2[, 8] > 0 | Xero_masterOG3counts_v2[, 9] > 0 |
Xero_masterOG3counts_v2[, 10] > 0 | Xero_masterOG3counts_v2[, 11] > 0 |
Xero_masterOG3counts_v2[, 12] > 0 | Xero_masterOG3counts_v2[, 13] > 0 |
Xero_masterOG3counts_v2[, 14] > 0 | Xero_masterOG3counts_v2[, 15] > 0 |
Xero_masterOG3counts_v2[, 16] > 0)
write.csv(DEmasterOG_count_v2, "DEmasterOG_counts_v2.csv")
```

Appendix A.4. Motif enrichment analysis (XSTREME v. 5.5.5)

```
## Extract gene IDs taken from OGs shared between early and late in csv from gff3 file
# Read gene IDs from the CSV file
Xe_fullbkg = read.csv("Xe_mergedBackground_05022024.csv", header = FALSE)
XeE_UP <- read.csv("XeE_UPlistfromOGvenn_DEonly_01022024.csv", header = FALSE)
XeE_DOWN <- read.csv("XeE_DOWNlistfromOGvenn_DEonly_01022024.csv", header = FALSE)
XeL_UP <- read.csv("XeL_UPlistfromOGvenn_DEonly_01022024.csv", header = FALSE)
XeL_DOWN <- read.csv("XeL_DOWNlistfromOGvenn_DEonly_01022024.csv", header = FALSE)
XeShared_UP <- read.csv("XeSHARED_UPlistfromOGvenn_DEonly_01022024.csv", header =
FALSE)
XeShared_DOWN <- read.csv("XeSHARED_DOWNlistfromOGvenn_DEonly_01022024.csv",
header = FALSE)
View(XeShared_DOWN)
## Extract the central part of the gene ID
XeE_UP_midgene <- gsub("^[^.]+\\.(.*)$", "\\1", XeE_UP$V1)
XeE_DOWN_midgene <- gsub("^[^.]+\\.(.*)$", "\\1", XeE_DOWN$V1)
XeL_UP_midgene <- gsub("^[^.]+\\.(.*)$", "\\1", XeL_UP$V1)
XeL_DOWN_midgene <- gsub("^[^.]+\\.(.*)$", "\\1", XeL_DOWN$V1)
XeShared_UP_midgene <- gsub("^[^.]+\\.(.*)$", "\\1", XeShared_UP$V1)
XeShared_DOWN_midgene <- gsub("^[^.]+\\.(.*)$", "\\1", XeShared_DOWN$V1)
View(XeE_UP_midgene)

## Filter GFF3 data for matched gene IDs
XeEUP_matched_gff3data <- gff3_gene_rows[gff3_gene_ids2 %in% XeEUP_matching_geneIDs, ]
XeEDOWN_matched_gff3data <- gff3_gene_rows[gff3_gene_ids2 %in%
XeEDOWN_matching_geneIDs, ]
XeLUP_matched_gff3data <- gff3_gene_rows[gff3_gene_ids2 %in% XeLUP_matching_geneIDs, ]
XeLDOWN_matched_gff3data <- gff3_gene_rows[gff3_gene_ids2 %in%
XeLDOWN_matching_geneIDs, ]
XeSharedUP_matched_gff3data <- gff3_gene_rows[gff3_gene_ids2 %in%
XeSharedUP_matching_geneIDs, ]
XeSharedDOWN_matched_gff3data <- gff3_gene_rows[gff3_gene_ids2 %in%
XeSharedDOWN_matching_geneIDs, ]
View(XeEDOWN_matched_gff3data)
```

```
## Extract the upstream region of the promoters
samtools faidx Xele_genome_v4_masked.fasta > Xele_genome_v4_masked.fai
bedtools flank -i Xe_extracted_genes.bed -g Xele_genome_v4_masked.fasta.fai -l 500 -r 0 -s > outputfile.bed

## Runing XSTREME
#!/bin/bash
for j in ./Promoters/*/
do
   basename -asz "$j"
   j="$(basename -asz "$j")"
   fasta-get-markov -m 2 ./Promoters/$j/*fasta ./Promoters/$j/2_order_markov
   mkdir ./xstreme/full_bkg/$j

for f in ./Promoters/$j/*/
do
    basename -asz "$f"
    f="$(basename -asz "$f")"
    xstreme --o ./xstreme/full_bkg/$j/$f --bfile ./Promoters/$j/2_order_markov --m ./Jaspar_core_plants_nonredundant_pfms.meme --align right --meme-p 8 --verbosity 1 --p ./Promoters/$j/$f/*_Promoter_Sequences.fasta --n ./Promoters/$j/$f/*_fullBackground.fasta
```

Appendix A.5. GO enrichment analysis

```
library("ViSEAGO")
library(orca)
library(readr)
library(data.table)
library(fgsea)
library(ggplot2)
library(plotly)
library(reticulate)

## Create a custom file
OGtoGO_customfile=read.csv(file="2024-01-24_filtered_OG_to_GO_list_RL_long.tsv",sep=",",header=TRUE)

## add new columns with set values, and relocate to reorder the columns
OGtoGO_customfile = OGtoGO_customfile %>% mutate(taxid="Xerophyta",evidence="NA",gene_symbol="NA") %>% relocate(taxid, gene_id, gene_symbol, GOID, evidence)
df_OGtoGO_customfile = as.data.frame(OGtoGO_customfile)

## Run custom2GO
Custom<- Custom2GO(file = "OGtoGO_customfile.tsv")

## 5 Read the background and differentially expressed OG files
background_OG <- read.csv(file = "merged_Early&Late_background_16012024.csv")
background_OG1 <- as.character(unlist(background_OG))
```

```
selectionUP_EarlyOG <- read.csv(file = "Early_uniqOGs_UP_26012024.csv") #row.names = "X")
selectionUP_EarlyOG1 <- as.character(unlist(selectionUP_EarlyOG))

selectionUP_LateOG <- read.csv(file = "Late_uniqOGs_UP_26012024.csv") #row.names = "X")
selectionUP_LateOG1 <- as.character(unlist(selectionUP_LateOG))

selectionUP_EL <- read.csv(file = "commonHSF_OGs_XeXs.csv") #row.names = "X")
selectionUP_EL1 <- as.character(unlist(selectionUP_EL))

## annotate by the entry in the taxid column
myGENE2GO<-ViSEAGO::annotate(
  "Xerophyta",
  Custom)

#Run topGO
topGO_object1<-ViSEAGO::create_topGOdata(
  geneSel=selectionUP_EarlyOG1,
  allGenes=background_OG1,
  gene2GO=myGENE2GO,
  ont="BP",
  nodeSize=10)

topGO_object2<-ViSEAGO::create_topGOdata(
  geneSel=selectionUP_LateOG1,
  allGenes=background_OG1,
  gene2GO=myGENE2GO,
  ont="BP",
  nodeSize=10)

topGO_object3<-ViSEAGO::create_topGOdata(
  geneSel=selectionUP_EL1,
  allGenes=background_OG1,
  gene2GO=myGENE2GO,
  ont="BP",
  nodeSize=10)

weight01_resE <- topGO::runTest(
  topGO_object1,
  algorithm ="weight01",
  statistic = "fisher")

weight01_resL <- topGO::runTest(
  topGO_object2,
  algorithm ="weight01",
  statistic = "fisher")

weight01_resEL <- topGO::runTest(
```

```
  topGO_object3,
  algorithm ="weight01",
  statistic = "fisher")

## viSEAGO allows you to compare multiple objects
BP_sResults<-ViSEAGO::merge_enrich_terms(
  Input=list(
    Early = c("topGO_object2", "weight01_resE"),
    Late = c("topGO_object5", "weight01_resL"),
    Early_Late = c("topGO_object6", "weight01_resEL")))

## display the merged table
ViSEAGO::show_table(BP_sResults)

## print the merged table in a file
ViSEAGO::show_table(
  BP_sResults,
  "BP_sResults_sharedUPregOGs_09022024.xls")

## count significant (or not) pvalues by condition (use this when doing multiple comparisons)
ViSEAGO::GOcount(BP_sResults)
# display interactions
ViSEAGO::Upset(
  BP_sResults,
  file="OLexport.xls")

myGOs<-ViSEAGO::build_GO_SS(
  gene2GO=myGENE2GO,
  enrich_GO_terms=BP_sResults)

## compute all available Semantic Similarity (SS) measures
myGOs<-ViSEAGO::compute_SS_distances(
  myGOs,
  distance="Wang")

## Assuming your 'myGOs' object contains the enriched GO terms data
## Sort the GO terms by their significance or enrichment score (adjust as needed)
enrich_GOs <- myGOs@enrich_GOs
enrich_data <- enrich_GOs@data

# Sort the data by 'Early_Late.pvalue'
sorted_enrich_data <- enrich_data[order(enrich_data$Early_Late.pvalue, decreasing = FALSE), ]
top_enrich_GOs <- head(sorted_enrich_data$term, 15)

## GOterms heatmap with the default parameters
Wang_clusters_wardD2<-ViSEAGO::GOterms_heatmap(
  top_enrich_GOs,
  showIC=TRUE,
```

```
showGOlabels=TRUE,
GO.tree=list(
  tree=list(
    distance="Wang",
    aggreg.method="ward.D2"),
  cut=list(
    dynamic=list(
      pamStage=TRUE,
      pamRespectsDendro=TRUE,
      deepSplit=2,
      minClusterSize =2))),
samples.tree=NULL,)
```

Appendix B. Enriched GO terms

Appendix B.1 List of 370 up-regulated GO terms from orthogroups shared among the three *Xerophyta* species. Enriched GO terms were identified using the ViSEAGO tool in R.

GO.ID	GO term	Early-stage specific p-value	Late-stage specific p-value	Early & Late stages p-value
GO:0030705	cytoskeleton-dependent intracellular transport	0.008570319	1	1
GO:0042026	protein refolding	0.003482902	1	0.4304127
GO:0006995	cellular response to nitrogen starvation	0.008570319	1	0.02632064
GO:0006950	response to stress	0.003253486	0.1598996	1
GO:0009733	response to auxin	0.00940714	0.7966662	0.6874548
GO:0032958	inositol phosphate biosynthetic process	0.002943526	0.1717331	1
GO:0046903	secretion	0.00098024	1	0.08683182
GO:0051650	establishment of vesicle localization	0.006687574	1	0.2036885
GO:0051085	chaperone cofactor-dependent protein refolding	0.002503643	0.4636514	0.3945777
GO:1902600	proton transmembrane transport	1	0.000414778	1
GO:0007033	vacuole organization	0.07686107	0.005279476	0.1263824
GO:0010344	seed oilbody biogenesis	1	0.00244166	1
GO:0006879	cellular iron ion homeostasis	1	0.006254935	0.4559045
GO:0006835	dicarboxylic acid transport	1	0.009615213	1
GO:0010119	regulation of stomatal movement	0.7316594	0.000797968	0.3405244
GO:0072523	purine-containing compound catabolic process	1	0.003551291	1
GO:0010224	response to UV-B	0.4408975	0.001700975	0.003646495
GO:0006623	protein targeting to vacuole	0.1961231	0.001250026	0.326422
GO:0050832	defense response to fungus	0.2807115	0.8517958	0.004020315
GO:0046352	disaccharide catabolic process	1	1	0.009323843
GO:0005983	starch catabolic process	1	0.3396171	0.000285774
GO:0046434	organophosphate catabolic process	1	0.2877884	0.002286461
GO:0071497	cellular response to freezing	1	0.1717331	0.009323843

GO:0097501	stress response to metal ion	1	0.3877048	0.009175241
GO:0016226	iron-sulfur cluster assembly	1	0.4323194	0.009988133
GO:0006873	cellular ion homeostasis	1	1	0.005774582

Appendix B.2 List of 335 down-regulated GO terms from orthogroups shared among the three *Xerophyta* species

GO.ID	GO term	Early-stage specific p-value	Late-stage specific p-value	Early & Late stages p-value
GO:0009683	indoleacetic acid metabolic process	0.001164401	1	1
GO:0007292	female gamete generation	0.007612762	0.5227439	1
GO:0010078	maintenance of root meristem identity	0.001271329	1	9.18E-06
GO:2000134	negative regulation of G1/S transition of mitotic cell cycle	0.001393174	1	1
GO:2000038	regulation of stomatal complex development	0.003173139	1	0.000913363
GO:0048827	phyllome development	0.00135424	1	0.009676978
GO:0098542	defense response to other organism	0.00788486	1	0.05676828
GO:0048229	gametophyte development	0.006051534	0.1509715	4.34E-06
GO:0009704	de-etiolation	1	0.00181226	1
GO:0015979	photosynthesis	1	7.00E-06	1
GO:0009826	unidimensional cell growth	0.7957281	0.001967314	0.02575723
GO:0010187	negative regulation of seed germination	1	0.002653854	0.2242919
GO:0007112	male meiosis cytokinesis	1	0.008984074	1
GO:0010114	response to red light	1	0.004758447	1
GO:0034508	centromere complex assembly	0.06893192	0.006244767	1
GO:0016131	brassinosteroid metabolic process	1	0.001794717	0.2660537
GO:0042335	cuticle development	0.1249422	0.005547599	1
GO:0010268	brassinosteroid homeostasis	1	0.003197548	1
GO:0010015	root morphogenesis	1	0.00256036	1
GO:0042545	cell wall modification	1	0.00234281	0.2881782
GO:0072522	purine-containing compound biosynthetic process	1	0.009298255	1
GO:0010234	anther wall tapetum cell fate specification	1	0.008984074	0.1710792
GO:0006270	DNA replication initiation	1	0.004217189	0.002733553
GO:0006271	DNA strand elongation involved in DNA replication	1	0.002237104	0.02374509
GO:0009765	photosynthesis, light harvesting	1	0.00241764	0.2496217
GO:1902969	mitotic DNA replication	1	0.000360106	0.009895336
GO:0009750	response to fructose	1	0.007540799	1
GO:0009773	photosynthetic electron transport in photosystem I	1	0.000262512	1
GO:0009741	response to brassinosteroid	0.2244509	0.002365542	0.104327
GO:0065001	specification of axis polarity	1	1	0.001544761
GO:0051302	regulation of cell division	0.4101571	0.8459671	0.006865424

GO:0010148	transpiration	1	1	0.006108754
GO:2000067	regulation of root morphogenesis	1	1	0.000191477
GO:0045490	pectin catabolic process	1	0.01850637	0.001670563
GO:1900150	regulation of defense response to fungus	1	0.5708627	0.008144385
GO:0042659	regulation of cell fate specification	1	0.425614	6.86E-05
GO:2000652	regulation of secondary cell wall biogenesis	0.1617976	0.6240113	4.52E-05
GO:0010555	response to mannitol	1	1	0.000913363
GO:0040008	regulation of growth	1	1	0.006366962
GO:0050829	defense response to Gram-negative bacterium	1	0.03086331	0.001522792
GO:0071244	cellular response to carbon dioxide	1	0.4102209	0.001256173
GO:0090708	specification of plant organ axis polarity	1	1	3.60E-05
GO:1903224	regulation of endodermal cell differentiation	1	1	0.000195124
GO:0009958	positive gravitropism	0.2199171	0.1524677	0.002405022
GO:1902584	positive regulation of response to water deprivation	0.1496822	0.2211166	0.005910721
GO:1901141	regulation of lignin biosynthetic process	0.1855303	0.3084584	0.001180341
GO:0010311	lateral root formation	0.05470098	0.3456493	0.00173481
GO:0048653	anther development	1	1	0.000799189
GO:0009934	regulation of meristem structural organization	0.1456063	0.05334386	1.21E-06
GO:0006952	defense response	0.0792734	0.1207628	0.003095605
GO:0010082	regulation of root meristem growth	1	0.3563782	1.18E-05
GO:0010088	phloem development	0.1165421	1	0.002733553
GO:0045184	establishment of protein localization	1	0.05266666	0.003577275
GO:0007639	homeostasis of number of meristem cells	1	0.425614	6.86E-05
GO:0009610	response to symbiotic fungus	0.02763921	0.01365961	2.63E-05
GO:0048646	anatomical structure formation involved in morphogenesis	0.08994669	0.6428916	0.001145202
GO:0009789	positive regulation of abscisic acid-activated signaling pathway	1	0.7789724	0.003368336
GO:0071484	cellular response to light intensity	1	1	0.008541777
GO:1901528	hydrogen peroxide mediated signaling pathway involved in stomatal movement	1	1	0.008541777
GO:0045595	regulation of cell differentiation	0.2633445	1	0.007319471
GO:0033365	protein localization to organelle	1	0.9887618	0.007865801
GO:1902025	nitrate import	0.1496822	0.5928845	0.000477627
GO:0006004	fucose metabolic process	1	1	0.007278879
GO:0055075	potassium ion homeostasis	1	1	0.00361595
GO:0044347	cell wall polysaccharide catabolic process	1	1	0.007278879

GO:0048437	floral organ development	0.0292178	1	0.001130901
GO:0090548	response to nitrate starvation	0.09950787	0.4406079	8.32E-05
GO:1900458	negative regulation of brassinosteroid mediated signaling pathway	1	1	0.007278879
GO:1901333	positive regulation of lateral root development	0.09087224	0.4102209	5.60E-05
GO:0009888	tissue development	0.01342715	0.05184245	0.002193918
GO:0007166	cell surface receptor signaling pathway	1	0.7541592	0.002580122
GO:0031540	regulation of anthocyanin biosynthetic process	0.1207518	0.5099387	9.12E-06
GO:0090351	seedling development	1	0.5034817	0.003073355
GO:0009825	multidimensional cell growth	0.1617976	1	0.007497733
GO:0080113	regulation of seed growth	0.1537393	0.0616564	0.000534836
GO:2000280	regulation of root development	0.01052909	1	0.005084305
GO:0046777	protein autophosphorylation	0.5306561	0.2242374	0.000116916
GO:0000727	double-strand break repair via break-induced replication	1	0.02638627	0.005033548
GO:0010183	pollen tube guidance	1	0.1714596	0.000309949
GO:0045089	positive regulation of innate immune response	1	0.1111856	0.001639723

Appendix B.3 List up-regulated AHL motif-containing orthogroups and their associated GO terms

OG ID	OG name	GO
OG0000106	kDa class I heat shock protein 2	"GO:0005634", "GO:0005737", "GO:0032991", "GO:0042802", "GO:0043621", "GO:0051082", "GO:0006457", "GO:0009651", "GO:0010286", "GO:0042542", "GO:0045471", "GO:0046685", "GO:0046686", "GO:0046688", "GO:0050821", "GO:0009408", "GO:0044183", "GO:0051259", "GO:0051260", "GO:0005515", "GO:0010035", "GO:0005622"
OG0000136	GlcAT14A	"GO:0005794", "GO:0015020", "GO:0046872", "GO:0006024", "GO:0009826", "GO:0048731", "GO:0016020", "GO:0006790", "GO:0007275", "GO:0000139"
OG0000180	protein phosphatase 2C 9	"GO:0019901", "GO:0010030", "GO:0010360", "GO:0010150", "GO:0006470", "GO:0006970", "GO:1902039", "GO:0043169", "GO:1902456", "GO:0048838", "GO:0009658", "GO:0006469", "GO:0009414", "GO:0009788", "GO:0048364", "GO:0004722", "GO:0005634", "GO:0009409", "GO:0009408", "GO:0009939", "GO:0051607", "GO:0005829", "GO:0010205", "GO:0033106", "GO:0046872", "GO:0017018", "GO:0035970", "GO:0010119", "GO:0031324", "GO:0009846"
OG0000263	transcription factor ABI4	"GO:2000082", "GO:0010286", "GO:0010182", "GO:1900036", "GO:0009611", "GO:0000976", "GO:0009555", "GO:0048316", "GO:0009873", "GO:0009736", "GO:0009409", "GO:0071472", "GO:0003700", "GO:0009749", "GO:0045595", "GO:0045893", "GO:0010119", "GO:0010896", "GO:0031930", "GO:0010353", "GO:2000070", "GO:0032880", "GO:0009620", "GO:0042542", "GO:0005983", "GO:0006952", "GO:0048527", "GO:0009744", "GO:0005634", "GO:0009738", "GO:0005515", "GO:0010449", "GO:0005737", "GO:0005886", "GO:0008219", "GO:0009414", "GO:0009753", "GO:0010224", "GO:0034605", "GO:0009737", "GO:0009743", "GO:0009416", "GO:0048731", "GO:0009658", "GO:0009751", "GO:0010928", "GO:0050832", "GO:0051301", "GO:0062211", "GO:0090357", "GO:0003677", "GO:0006355", "GO:0009651", "GO:0009834", "GO:0051707", "GO:0019760", "GO:0071497"

OG0000322	008801812.1uncharacterized protein LOC103715832	NA
OG0000371	F-box/kelch-repeat protein At1g15680	NA
OG0000392	receptor 1	"GO:0000139", "GO:0005768", "GO:0005802", "GO:0017119", "GO:0071944", "GO:0005509", "GO:0005515", "GO:0061630", "GO:0006511", "GO:0006623", "GO:0006896", "GO:0016567", "GO:0048522", "GO:0048856"
OG0000397	finger protein ZAT12	"GO:2000280", "GO:0042538", "GO:0007154", "GO:0009611", "GO:0000976", "GO:0009643", "GO:0009631", "GO:0009725", "GO:1901701", "GO:0009414", "GO:0005634", "GO:0006979", "GO:0003700", "GO:0009408", "GO:0005515", "GO:0045892", "GO:0071289", "GO:0033554", "GO:0033993", "GO:0010200", "GO:0043565", "GO:0003006", "GO:0006355", "GO:0007275", "GO:0009409", "GO:0009642", "GO:0009651", "GO:0009737", "GO:0032502", "GO:1902074", "GO:1902584", "GO:0042631", "GO:2000022", "GO:0055062", "GO:0009793", "GO:0010224", "GO:0046872", "GO:0006970", "GO:0045926"
OG0000425	039131974.1uncharacterized protein LOC120268763	"GO:0016020", "GO:0051015", "GO:0051764", "GO:0051014", "GO:0051693", "GO:0005737", "GO:0099636", "GO:0051592", "GO:0032432", "GO:0003729", "GO:0048767", "GO:0005884", "GO:0051017"
OG0000459	C2-DOMAIN ABA-RELATED 8	"GO:0008022", "GO:0009555", "GO:0005794", "GO:0009630", "GO:0006886", "GO:0043621", "GO:0043547", "GO:0006955", "GO:0005509", "GO:0005905", "GO:0005829", "GO:0060090", "GO:1900426", "GO:0005635", "GO:0009638", "GO:0032991", "GO:0045309", "GO:0009893", "GO:1901002", "GO:0005096", "GO:0009611", "GO:0000122", "GO:0031410", "GO:0042803", "GO:0005543", "GO:0005102", "GO:0009789", "GO:0006511", "GO:0004842", "GO:0070534", "GO:0005783", "GO:0005886", "GO:0005634", "GO:0045806", "GO:0005789", "GO:0043495", "GO:1902883", "GO:0055037", "GO:0005085", "GO:0030139", "GO:0009306", "GO:0061630", "GO:0042391", "GO:0019871", "GO:0016567"
OG0000482	metal-associated isoprenylated plant protein 3	"GO:0005634", "GO:0005515", "GO:0005730", "GO:0008270", "GO:0009910", "GO:0005622", "GO:0046914", "GO:0005737", "GO:0016020"
OG0000505	stress transcription factor A-2	"GO:0005634", "GO:0000976", "GO:0003700", "GO:0042802", "GO:0010286", "GO:0034605", "GO:0034620", "GO:0045893", "GO:0005737", "GO:0000978", "GO:0006357", "GO:1990841", "GO:0071456"
OG0000540	JINGUBANG	"GO:0015630", "GO:0007010", "GO:0009653", "GO:0007017", "GO:0051247", "GO:0003006", "GO:0031399", "GO:0016573", "GO:0051649", "GO:0016310", "GO:0006355", "GO:0048523", "GO:0048468", "GO:0009846", "GO:0009966", "GO:0006810", "GO:0006511", "GO:0005515", "GO:0005737", "GO:0016740", "GO:0031325", "GO:0043967", "GO:0051172", "GO:0031056", "GO:0051726", "GO:0030162", "GO:0000123", "GO:0010605", "GO:0036211", "GO:0007018", "GO:0044085", "GO:0048522", "GO:0016477", "GO:0051128", "GO:0048646", "GO:0000226", "GO:0006796", "GO:0031981", "GO:0008092", "GO:0009892", "GO:0009894", "GO:0006468", "GO:0050793", "GO:0070647", "GO:0065008", "GO:0043933", "GO:0004672", "GO:0009967", "GO:0005856", "GO:0000151", "GO:0048731", "GO:0016020", "GO:0006508", "GO:0097435", "GO:0030036", "GO:0071944", "GO:0019899", "GO:0010564", "GO:0006996", "GO:0030154", "GO:0016301", "GO:2000026", "GO:0061136", "GO:0008285", "GO:0033043", "GO:0042995", "GO:0009968", "GO:1903052", "GO:0046907", "GO:0031329", "GO:0031647", "GO:0010468", "GO:0012505", "GO:0016567"
OG0000551	NRT1/ PTR FAMILY 2.13	"GO:0005886", "GO:0009705", "GO:0097708", "GO:0010542", "GO:0015334", "GO:0042937", "GO:0071916", "GO:0080054", "GO:0090448", "GO:0009611", "GO:0009753", "GO:0009793", "GO:0009860", "GO:0010098", "GO:0010336", "GO:0010447", "GO:0010584", "GO:0014070", "GO:0042938", "GO:0042939", "GO:0043200", "GO:0043562", "GO:0090408", "GO:0090449",

		"GO:0006821", "GO:0006950", "GO:0009628", "GO:0009725", "GO:0033993", "GO:0009737", "GO:0009751", "GO:0042538", "GO:0042742", "GO:0043201", "GO:0080052", "GO:0080053", "GO:0035673", "GO:1902074", "GO:0051707", "GO:0071472"
OG0000630	dioxygenase NCED3, chloroplastic	"GO:0009535", "GO:0009570", "GO:0045549", "GO:0009414", "GO:0009555", "GO:0009688", "GO:0009733", "GO:0009737", "GO:0009739", "GO:0009751", "GO:0009835", "GO:0009856", "GO:0010114", "GO:0010162", "GO:0016121", "GO:0016123", "GO:0016124", "GO:0042538", "GO:0048653", "GO:1901177", "GO:0046872", "GO:0009738", "GO:1901811", "GO:0006950", "GO:0007275", "GO:0009628", "GO:0009725", "GO:0016114", "GO:0022414"
OG0000651	ubiquitin-protein ligase At1g12760	"GO:0016020", "GO:0004842", "GO:0009793", "GO:0005654", "GO:0005829", "GO:0005886", "GO:0012505", "GO:0042802", "GO:0061630", "GO:0140297", "GO:0000122", "GO:0000578", "GO:0010228", "GO:0016567", "GO:0043161", "GO:0043433", "GO:0005773", "GO:0005783", "GO:0016605", "GO:0017053", "GO:0031965", "GO:0003677", "GO:0003714", "GO:0046872", "GO:0006511", "GO:0045893", "GO:0005769", "GO:0005770", "GO:0005794", "GO:0051787", "GO:0000209", "GO:0007034", "GO:0009737", "GO:0042631", "GO:0051301", "GO:0051865", "GO:0061635", "GO:0071629", "GO:0010200", "GO:0050832", "GO:0005802", "GO:0017119", "GO:0005515", "GO:0006623", "GO:0006896", "GO:0009651", "GO:0009687", "GO:0009739", "GO:0010182", "GO:0006513", "GO:0071218", "GO:0043231", "GO:0005737"
OG0000724	exchanger 4	"GO:0000325", "GO:0005769", "GO:0005770", "GO:0005774", "GO:0005886", "GO:0010008", "GO:0005515", "GO:0015385", "GO:0015386", "GO:0007015", "GO:0009651", "GO:0030010", "GO:0035864", "GO:0048870", "GO:0051453", "GO:0055075", "GO:0090333", "GO:0098656", "GO:0098719", "GO:1902600", "GO:1990573", "GO:0098590", "GO:0005783", "GO:0005516", "GO:0051592", "GO:0055037", "GO:0008104", "GO:0005802", "GO:0055038", "GO:1901002", "GO:0006633", "GO:0042335", "GO:0000036", "GO:0009507", "GO:0009627", "GO:0031177", "GO:0012505"
OG0000764	OG0000764 Synaptotagmin-2	"GO:0000139", "GO:0005886", "GO:0010008", "GO:0005515", "GO:0005543", "GO:0046872", "GO:0006869", "GO:0006897", "GO:0009306", "GO:0016043", "GO:0005768", "GO:0005794", "GO:0042803", "GO:1901002", "GO:0009555", "GO:0009630", "GO:0043621", "GO:0009789", "GO:0009638", "GO:0005509", "GO:0005829", "GO:0008289", "GO:0050790", "GO:0031982", "GO:0033011"
OG0000837	synthase	"GO:0005737", "GO:0047268", "GO:0047274", "GO:0006979", "GO:0009312", "GO:0009414", "GO:0052692", "GO:0034484"
OG0000838	REVEILLE 6	"GO:0005634", "GO:0000976", "GO:0003700", "GO:0005515", "GO:0046872", "GO:0140492", "GO:0006508", "GO:0009409", "GO:0009734", "GO:0009739", "GO:0009744", "GO:0009845", "GO:0009909", "GO:0010243", "GO:0010597", "GO:0010600", "GO:0010628", "GO:0032922", "GO:0042753", "GO:0042754", "GO:0043254", "GO:0043433", "GO:0043966", "GO:0045892", "GO:0045944", "GO:0048574", "GO:0000987", "GO:0009408", "GO:0010378"
OG0000840	stress transcription factor B-2b	"GO:0005634", "GO:0005737", "GO:0000978", "GO:0003700", "GO:0042802", "GO:0006357", "GO:0034605", "GO:0005515", "GO:0008356", "GO:0009408", "GO:0042803", "GO:0000302", "GO:0045892", "GO:0045893"
OG0000860	29	"GO:0035251", "GO:0002238", "GO:0046246", "GO:0046283", "GO:0008194", "GO:0016758", "GO:0008299"
OG0000890	invertase 1, mitochondrial	"GO:0005739", "GO:0005829", "GO:0009507", "GO:0016020", "GO:0004575", "GO:0005987", "GO:0007623", "GO:0009555", "GO:0010029", "GO:0010311", "GO:0042542", "GO:0048510", "GO:0080022"
OG0000913	008788834.1uncharacterized protein LOC103706495	"GO:0010008", "GO:0005515", "GO:0015031", "GO:0043130"

OG0000918	DEHYDRATION-INDUCED 19 homolog 2	"GO:0005622", "GO:0005515", "GO:0007165", "GO:0005634", "GO:0003677", "GO:0009414", "GO:0009651", "GO:0009737", "GO:0045893", "GO:0009785", "GO:0010161", "GO:0006950", "GO:0009628", "GO:0010033", "GO:0071482", "GO:0005737", "GO:0048471"
OG0000932	protein homolog	"GO:0005634", "GO:0005829", "GO:0005886", "GO:0015630", "GO:0001664", "GO:0001671", "GO:0003729", "GO:0005524", "GO:0030544", "GO:0030957", "GO:0031625", "GO:0046872", "GO:0051082", "GO:0051087", "GO:0006626", "GO:0006952", "GO:0009408", "GO:0010628", "GO:0030433", "GO:0031048", "GO:0042026", "GO:0043065", "GO:0043462", "GO:0045047", "GO:0045892", "GO:0051223", "GO:0031324", "GO:0005788", "GO:0009507", "GO:0008092", "GO:0016491", "GO:0009553", "GO:0009651", "GO:0009737", "GO:0009860", "GO:0009911", "GO:0009958", "GO:0034605", "GO:0051085", "GO:0010033", "GO:0044794", "GO:0006997", "GO:0048284"
OG0000964	dehydrogenase TIC 32, chloroplastic	"GO:0005654", "GO:0005743", "GO:0005789", "GO:0005794", "GO:0005829", "GO:0005886", "GO:0009706", "GO:0005516", "GO:0019899", "GO:0033721", "GO:0042802", "GO:0006874", "GO:0015031", "GO:0045944", "GO:0048731", "GO:0110095", "GO:0010212", "GO:0050829", "GO:2000377", "GO:0005739", "GO:0016491", "GO:0048856", "GO:0006720", "GO:0005515", "GO:0070402", "GO:0010073", "GO:2000024"
OG0001015	nucleotide-binding protein subunit beta	"GO:0000123", "GO:0005737", "GO:0016020", "GO:0005515", "GO:0001934", "GO:0006352", "GO:0006355", "GO:0006366", "GO:0006810", "GO:0006996", "GO:0007186", "GO:0009967", "GO:0030154", "GO:0031056", "GO:0031328", "GO:0043085", "GO:0043967", "GO:0048731", "GO:0065003", "GO:0070647", "GO:0030162", "GO:0048646", "GO:0051173", "GO:0048523", "GO:0005730", "GO:0009966", "GO:0010604", "GO:0042273", "GO:0016043", "GO:0051726", "GO:0031325", "GO:0005815", "GO:0000226", "GO:0000398", "GO:0007049", "GO:0022607", "GO:0048522", "GO:0043933", "GO:0015630", "GO:0007275", "GO:0042995", "GO:0007017", "GO:0006357", "GO:0016071", "GO:0051179", "GO:0045893", "GO:0070461", "GO:0007165"
OG0001028	OG0001028 Serpin-ZXA	"GO:0005634", "GO:0005829", "GO:0048046", "GO:0004869", "GO:0005515", "GO:0005615", "GO:0006281", "GO:0005737", "GO:0006974", "GO:0010466", "GO:0005576", "GO:0004866", "GO:0006950"
OG0001065	reductase 1	"GO:0016616", "GO:0080110", "GO:0048316", "GO:0005783", "GO:0009813", "GO:0042754", "GO:0009409", "GO:0050661", "GO:0005515", "GO:0009809", "GO:0033729", "GO:0016621", "GO:0010597", "GO:0009964", "GO:0005829"
OG0001077	LIFEGUARD 2	"GO:0005773", "GO:0005783", "GO:0005795", "GO:0005886", "GO:0005515", "GO:0009742", "GO:0009826", "GO:0034620", "GO:0050832", "GO:0050848", "GO:1905421", "GO:0000323", "GO:0005774", "GO:0005794", "GO:0031410", "GO:0005739", "GO:0030659", "GO:0032469", "GO:0005764", "GO:0005768", "GO:0006952"
OG0001110	domain-containing protein CBSX5	"GO:0005737", "GO:0043231"
OG0001148	H3.3	"GO:0000786", "GO:0005576", "GO:0005654", "GO:0030875", "GO:0048555", "GO:0031492", "GO:0046982", "GO:0000122", "GO:0006334", "GO:0009567", "GO:0019827", "GO:0040029", "GO:0016020"
OG0001158	phosphatase PTPMT1	"GO:0000139", "GO:0005634", "GO:0004439", "GO:0004725", "GO:0005515", "GO:0008138", "GO:0008962", "GO:0017018", "GO:0006655", "GO:0035335", "GO:0046855", "GO:0048364", "GO:0046838", "GO:1901575", "GO:0005794", "GO:0006996", "GO:0031399", "GO:0051726", "GO:0015630", "GO:0031981", "GO:0080090", "GO:0005783", "GO:0004722", "GO:0030246", "GO:0006470", "GO:0009892", "GO:0042325", "GO:0050790", "GO:0004721", "GO:0006796", "GO:0044238", "GO:0071704", "GO:0008654", "GO:0016311"
OG0001166	embryogenesis abundant protein D-34	"GO:0005730", "GO:0005737", "GO:0005515", "GO:0006873", "GO:0009845", "GO:0010226"

OG0001177	domain-containing protein 48	"GO:1902890", "GO:1900150", "GO:0009793", "GO:1901002", "GO:0008361", "GO:0009611", "GO:0000976", "GO:0009555", "GO:1900057", "GO:0009751", "GO:0043424", "GO:0009409", "GO:0045892", "GO:1990841", "GO:0045893", "GO:0019760", "GO:0010099", "GO:0042803", "GO:1902584", "GO:0001216", "GO:0009867", "GO:0009788", "GO:0009744", "GO:0005634", "GO:0009831", "GO:0009835", "GO:0048653", "GO:0009825", "GO:0048317", "GO:0080060", "GO:0045995", "GO:0010628", "GO:1902265", "GO:0009646"
OG0001204	protein At2g27310	NA
OG0001221	E3 ubiquitin-protein ligase LOG2	"GO:0005769", "GO:0005783", "GO:0005886", "GO:0005515", "GO:0046872", "GO:0061630", "GO:0009968", "GO:0016567", "GO:0080144", "GO:1901527", "GO:0005654", "GO:0005829", "GO:0009941", "GO:0015629", "GO:0019899", "GO:0000209", "GO:0043066", "GO:0004842"
OG0001228	response regulator ORR21	"GO:0010492", "GO:0042802", "GO:0010082", "GO:2000031", "GO:0010150", "GO:0080022", "GO:0010380", "GO:0009787", "GO:0080036", "GO:0080113", "GO:0043565", "GO:0009873", "GO:0000156", "GO:0009414", "GO:1990110", "GO:0005634", "GO:0003700", "GO:0031537", "GO:0045893", "GO:0048576", "GO:0010119", "GO:0009723", "GO:0048367", "GO:0000160", "GO:0000976", "GO:2000022", "GO:0006355", "GO:0003677", "GO:0009793", "GO:0090506"
OG0001233	ROOT HAIR DEFECTIVE 3	"GO:0000139", "GO:0005634", "GO:0005789", "GO:0022625", "GO:0003729", "GO:0003735", "GO:0003924", "GO:0005515", "GO:0005525", "GO:0019843", "GO:0006412", "GO:0009832", "GO:0016320", "GO:0000166", "GO:0016020"
OG0001258	010923306.1uncharacterized protein LOC105046425 isoform X2	NA
OG0001264	complex component EXO70H1	"GO:0065008", "GO:0005634", "GO:0002237", "GO:0005515", "GO:0005829", "GO:0031982", "GO:0009620", "GO:0006887", "GO:0010089", "GO:0051179", "GO:0016020", "GO:1900426", "GO:0005576", "GO:0009628", "GO:0050793", "GO:0051239", "GO:0051128"
OG0001307	decarboxylase 2	"GO:0005829", "GO:0071944", "GO:0000287", "GO:0004737", "GO:0030976", "GO:0042802", "GO:0034059", "GO:0006091", "GO:0019752"
OG0001370	P450 reductase 3	"GO:0005739", "GO:0005789", "GO:0005829", "GO:0009507", "GO:0003958", "GO:0004128", "GO:0009055", "GO:0010181", "GO:0016787", "GO:0019899", "GO:0050660", "GO:0050661", "GO:0006723", "GO:0006979", "GO:0007584", "GO:0009410", "GO:0009698", "GO:0009812", "GO:0019395", "GO:0022900", "GO:0051762", "GO:0070988", "GO:0071548", "GO:0009534", "GO:0005515", "GO:0009579", "GO:0019438", "GO:0072686", "GO:0005525", "GO:0009733", "GO:0009911", "GO:0010228", "GO:2000280"
OG0001388	tolerance protein 5	"GO:0000139", "GO:0005770", "GO:0009705", "GO:0035618", "GO:0010486", "GO:0006826", "GO:0009787", "GO:0009845", "GO:0010042", "GO:0030026", "GO:0046688", "GO:0048316", "GO:0071421", "GO:0097577", "GO:1902600", "GO:2000022", "GO:2000031"
OG0001389	acid transporter AVT6A	"GO:0005774", "GO:0005789", "GO:0005886", "GO:0008324", "GO:0008514", "GO:0015175", "GO:0015179", "GO:0015804", "GO:0098655", "GO:0098656", "GO:0098590", "GO:0003333", "GO:0006812", "GO:0010628", "GO:0005829", "GO:0000166", "GO:0070524", "GO:0072582", "GO:0008202", "GO:0019438", "GO:0006865"
OG0001409	chloroplastic	"GO:0005739", "GO:0009507", "GO:0004322", "GO:0008198", "GO:0008199", "GO:0019904", "GO:0042802", "GO:0006826", "GO:0006880", "GO:0009409", "GO:0009617", "GO:0009737", "GO:0009908", "GO:0010039", "GO:0010043", "GO:0015979", "GO:0042542", "GO:0048366"
OG0001433	inactive poly [ADP-ribose] polymerase SRO2	"GO:0005739", "GO:0005515", "GO:0006979", "GO:0009651", "GO:0009725", "GO:0009791", "GO:0010035", "GO:0048731", "GO:0072593", "GO:0005737", "GO:0043231", "GO:0006970",

		"GO:0006950", "GO:0009628", "GO:0010033", "GO:0000303", "GO:0006809", "GO:0009414", "GO:0009793", "GO:0009867", "GO:0009873", "GO:0010102", "GO:0010193", "GO:0012501", "GO:0042742", "GO:2000377"
OG0001447	protein P58IPK homolog	"GO:0005654", "GO:0005788", "GO:0005829", "GO:0048471", "GO:0001671", "GO:0003677", "GO:0031072", "GO:0042802", "GO:0044183", "GO:0051082", "GO:0051087", "GO:0030036", "GO:0030198", "GO:0032880", "GO:0034504", "GO:0044794", "GO:0045892", "GO:0061077", "GO:0005730", "GO:0001664", "GO:0051223", "GO:0030544", "GO:0042026", "GO:0031625", "GO:0030957", "GO:0016020", "GO:0043065", "GO:0005789", "GO:0009507", "GO:0005506", "GO:0008092", "GO:0000740", "GO:0006950", "GO:0009737", "GO:0009958", "GO:0010198", "GO:0010322", "GO:0051085", "GO:1902395", "GO:0009651", "GO:0009911", "GO:0043462", "GO:0010598", "GO:0046872"
OG0001450	zinc finger protein 22	"GO:0008270", "GO:2000241", "GO:1905157", "GO:0090351", "GO:0000976", "GO:0006355", "GO:0009637", "GO:1900458", "GO:1902448", "GO:0048573", "GO:0005634", "GO:0003700", "GO:2000306", "GO:0005515", "GO:0003712", "GO:0010218", "GO:0010017", "GO:0010117", "GO:0010100", "GO:0071483", "GO:0070370", "GO:0046872", "GO:2000028", "GO:0048579", "GO:0045892", "GO:0009909", "GO:0048577", "GO:0048576", "GO:0009641", "GO:0010228", "GO:0140110"
OG0001483	006850890.2uncharacterized protein LOC18440689	NA
OG0001525	lumen protein-retaining receptor A	"GO:0000139", "GO:0005789", "GO:0005801", "GO:0030133", "GO:0005046", "GO:0005515", "GO:0006621", "GO:0006888", "GO:0006890", "GO:0038023", "GO:0046923", "GO:0015031", "GO:0016192"
OG0001533	DETOXIFICATION 27	"GO:0005773", "GO:0005886", "GO:0015297", "GO:0042910", "GO:0009813", "GO:0010252", "GO:0048767", "GO:1990961", "GO:0022857", "GO:0010023", "GO:0010231", "GO:0016020", "GO:0055085", "GO:0005774"
OG0001580	endo-1,3-beta-glucosidase	"GO:0042803", "GO:0042973", "GO:0006952", "GO:0007154", "GO:0007275", "GO:0045229", "GO:0098542", "GO:0050832"
OG0001600	413 plasma membrane protein 1	"GO:0005886", "GO:0009535", "GO:0009631", "GO:0009737", "GO:0009744", "GO:0009749", "GO:0009750", "GO:0009941", "GO:0070417", "GO:0042170", "GO:0009409", "GO:0042631", "GO:0043231", "GO:0004674", "GO:0005524", "GO:0016310", "GO:0042742", "GO:0016020"
OG0001609	STAY-GREEN homolog, chloroplastic	"GO:0009507", "GO:0005515", "GO:0055035", "GO:0009658", "GO:0009534", "GO:1903647", "GO:0016829", "GO:0009535", "GO:0009570", "GO:0031969", "GO:0010271", "GO:0015996"
OG0001629	methionine sulfoxide reductase	"GO:0005654", "GO:0005739", "GO:0005829", "GO:0005886", "GO:0009507", "GO:0015629", "GO:0005515", "GO:0008113", "GO:0036456", "GO:0007568", "GO:0009416", "GO:0009651", "GO:0034599", "GO:0009570", "GO:0006555", "GO:0030091", "GO:0000096"
OG0001633	TORNADO 2	"GO:0035265", "GO:0009506", "GO:0016020", "GO:0009554", "GO:0010305", "GO:0009956", "GO:0009934", "GO:0050829", "GO:0010015", "GO:2000280", "GO:0043434", "GO:0005515", "GO:2000377", "GO:0010078", "GO:0009734", "GO:0080022", "GO:0048527"
OG0001744	OG0001744 Peroxygenase	"GO:0009507", "GO:0012511", "GO:0004392", "GO:0005509", "GO:0020037", "GO:0042803", "GO:0071614", "GO:1990137", "GO:0006952", "GO:0009269", "GO:0009409", "GO:0009620", "GO:0009651", "GO:0009737", "GO:0009751", "GO:0009793", "GO:0009819", "GO:0010118", "GO:0010431", "GO:0010888", "GO:0031408", "GO:0034389", "GO:1902609", "GO:2000377", "GO:0005783", "GO:0102070", "GO:0016020", "GO:0016298", "GO:0031969", "GO:0043231", "GO:0016491", "GO:0009414", "GO:0019752"
OG0001766	kDa class II heat shock protein	"GO:0005737", "GO:0043621", "GO:0051082", "GO:0006457", "GO:0006972", "GO:0009408", "GO:0009651", "GO:0042542", "GO:0045471", "GO:0046685", "GO:0046686", "GO:0046688",

		"GO:0032991", "GO:0042802", "GO:0050821", "GO:0051259", "GO:0044183", "GO:0005829", "GO:0010286"
OG0001789	protein H5	"GO:0005634", "GO:0005737", "GO:0009737", "GO:0048700", "GO:0050821"
OG0001800	protein RABB1c	"GO:0000139", "GO:0005764", "GO:0005769", "GO:0005770", "GO:0005789", "GO:0005791", "GO:0005795", "GO:0005829", "GO:0016324", "GO:0030140", "GO:0048471", "GO:0055038", "GO:0003924", "GO:0005525", "GO:0019003", "GO:0006886", "GO:0006888", "GO:0006895", "GO:0007030", "GO:0008219", "GO:0030100", "GO:0032456", "GO:0032880", "GO:0045087", "GO:0045176", "GO:0045995", "GO:0047484", "GO:0051607", "GO:0005802", "GO:0031901", "GO:0042742", "GO:0005886", "GO:0045177", "GO:0090404", "GO:0009860", "GO:0042546", "GO:0009306", "GO:0070382", "GO:0006904", "GO:0019900", "GO:0080092", "GO:0043419", "GO:0009733", "GO:0016151", "GO:1905182", "GO:0015031"
OG0001814	protein	"GO:0005737", "GO:0005811", "GO:0005515", "GO:0019915", "GO:0034389", "GO:0045927", "GO:0080186", "GO:0043231", "GO:1902584"
OG0001925	c	"GO:0005758", "GO:0009055", "GO:0020037", "GO:0046872", "GO:0006122", "GO:0006123", "GO:0010336"
OG0001962	transcription factor WRKY24	"GO:0042659", "GO:0010120", "GO:0009651", "GO:0009611", "GO:0000976", "GO:0009555", "GO:0009753", "GO:1900057", "GO:0009414", "GO:0009832", "GO:0009409", "GO:0003700", "GO:0009627", "GO:0045893", "GO:0010214", "GO:0050832", "GO:0008270", "GO:0009863", "GO:0009961", "GO:0009960", "GO:0042742", "GO:0009788", "GO:0009942", "GO:0009938", "GO:0005634", "GO:0010508", "GO:0005515", "GO:0070370", "GO:0009957", "GO:0030010", "GO:0010228", "GO:0031347", "GO:0016740", "GO:1901141", "GO:0000978", "GO:1990170", "GO:1904369", "GO:0009846", "GO:0048316", "GO:1900150", "GO:1900425", "GO:0009723", "GO:0009751", "GO:0034605", "GO:0046872", "GO:0098542", "GO:0006970"
OG0001982	D zeta 1	"GO:0045727", "GO:0009395", "GO:0048364", "GO:0005789", "GO:0001666", "GO:0005080", "GO:0006970", "GO:0007265", "GO:0014070", "GO:0042542", "GO:0004630", "GO:0043434", "GO:0006654", "GO:0005634", "GO:0031941", "GO:0031985", "GO:0005773", "GO:0009733", "GO:0005768", "GO:0032266", "GO:0016036", "GO:0006995", "GO:0019375", "GO:0005938", "GO:0048367", "GO:0019827", "GO:0009408", "GO:0044183", "GO:0042162", "GO:1990879", "GO:0032211", "GO:0010521", "GO:0007264", "GO:0005783", "GO:0030659", "GO:0005794", "GO:0006979", "GO:0008654", "GO:0006650", "GO:0098542", "GO:0048870", "GO:0005515", "GO:0005886", "GO:0031410", "GO:0035556", "GO:0060627", "GO:0009628", "GO:0046473"
OG0001993	peptide chain release factor subunit 1-3	"GO:0005829", "GO:0010494", "GO:0018444", "GO:0005515", "GO:0016149", "GO:0043022", "GO:1990825", "GO:0000184", "GO:0002184", "GO:0006353", "GO:0006479", "GO:0005737", "GO:0003747", "GO:0006415"
OG0002017	stress transcription factor A-1	"GO:0005634", "GO:0000978", "GO:0003700", "GO:0042802", "GO:0006357", "GO:0010286", "GO:0034605", "GO:0034620", "GO:0045893", "GO:0042803", "GO:1990841", "GO:0000302", "GO:0071456", "GO:0005737", "GO:0009733", "GO:0009958", "GO:0048527", "GO:0048530"
OG0002021	peroxidase SPC4	"GO:0005576", "GO:0009505", "GO:0004601", "GO:0005509", "GO:0020037", "GO:0002215", "GO:0009827", "GO:0042744", "GO:0044347", "GO:0048658", "GO:0080001", "GO:0005773", "GO:0009269", "GO:0009409", "GO:0009908", "GO:0042538", "GO:0071456", "GO:0005737", "GO:0043231", "GO:0009809", "GO:0045730", "GO:0050832", "GO:0140825", "GO:0006979", "GO:0098869", "GO:1901430", "GO:0045926", "GO:0009808"
OG0002028	factor DIVARICATA	"GO:0090697", "GO:1901001", "GO:0000976", "GO:0009751", "GO:0009414", "GO:0009733", "GO:0000122", "GO:0030307", "GO:0003700", "GO:0045893", "GO:0009908", "GO:0010116", "GO:0016514", "GO:1901371", "GO:0042803", "GO:0010252", "GO:0010150", "GO:0009787", "GO:1905615", "GO:0008233",

		"GO:0009723", "GO:0009646", "GO:0048527", "GO:0009744", "GO:0009739", "GO:0046872", "GO:0005737", "GO:2000469", "GO:0009793", "GO:0009630", "GO:0010114", "GO:0005829", "GO:0010597", "GO:0005515", "GO:0008270"
OG0002032	020256829.1uncharacterized protein LOC109833529	"GO:0046872", "GO:0016020"
OG0002044	choline kinase 2	"GO:0005737", "GO:0016020", "GO:0043229", "GO:0004103", "GO:0004305", "GO:0005524", "GO:0042802", "GO:0006646", "GO:0006657", "GO:0009611", "GO:0009628", "GO:0009791", "GO:0016310", "GO:0035264", "GO:0009612", "GO:0005515", "GO:0000166", "GO:0006656", "GO:0005886"
OG0002131	protein At4g00755	"GO:0005515", "GO:0030246"
OG0002154	and GRAM domain-containing protein At1g03370	"GO:0008022", "GO:0005789", "GO:0005509", "GO:0065003", "GO:0019905", "GO:0045732", "GO:0005764", "GO:0043161", "GO:0023056", "GO:0000151", "GO:0019871", "GO:0061630", "GO:0009651", "GO:0005096", "GO:0005730", "GO:0005654", "GO:0000122", "GO:1901017", "GO:0005543", "GO:0006513", "GO:0031647", "GO:0010647", "GO:0051592", "GO:0005938", "GO:0070534", "GO:0042176", "GO:0022603", "GO:0009628", "GO:0006955", "GO:0005829", "GO:0030100", "GO:0042391", "GO:0032991", "GO:0045309", "GO:0000209", "GO:0005102", "GO:0006950", "GO:0009789", "GO:0006511", "GO:0004842", "GO:0005886", "GO:0030054", "GO:0031410", "GO:0005515", "GO:0032934", "GO:0006869", "GO:0065008", "GO:0048523", "GO:0005544", "GO:0070382", "GO:0005546", "GO:0048471", "GO:0046982", "GO:0055037", "GO:0030276", "GO:0006952", "GO:0042803", "GO:1901002", "GO:0009637", "GO:0043621", "GO:0009723", "GO:0098542", "GO:0009606", "GO:0050790", "GO:0009638", "GO:0009630", "GO:0005737", "GO:0016020", "GO:0043231", "GO:0008289", "GO:0046872","GO:0009506", "GO:0031982"
OG0002237	ACTIVITY OF BC1 COMPLEX KINASE 7, chloroplastic	"GO:0009507", "GO:0016301", "GO:0006979", "GO:0006996", "GO:0044238", "GO:0071704", "GO:0005739", "GO:0009536", "GO:0004672", "GO:0006950", "GO:0016020", "GO:0016740"
OG0002250	domain-containing protein 68	"GO:1902890", "GO:1900150", "GO:0009793", "GO:1901002", "GO:0008361", "GO:0009831", "GO:0009611", "GO:0000976", "GO:0009555", "GO:1900057", "GO:0009751", "GO:0043424", "GO:0009409", "GO:0045892", "GO:1990841", "GO:0045893", "GO:0019760", "GO:0010099", "GO:0042803", "GO:1902584", "GO:0001216", "GO:0009867", "GO:0009788", "GO:0009744", "GO:0005634", "GO:0048653", "GO:1902265", "GO:0009646", "GO:0048317", "GO:0080060", "GO:0045995", "GO:0010628", "GO:0009507", "GO:0001666"
OG0002255	010912583.2uncharacterized protein LOC105038478	character(0
OG0002287	membrane protein PPF-1, chloroplastic	"GO:0009535", "GO:0032991", "GO:0019904", "GO:0032977", "GO:0009658", "GO:0010027", "GO:0045038", "GO:0051205"
OG0002304	023873308.1uncharacterized protein LOC111985897	character(0
OG0002328	protein At5g19025	GO:0016020
OG0002335	protein At2g24330	"GO:0016020", "GO:0071782", "GO:0005515", "GO:0061630", "GO:0071784", "GO:0071786", "GO:0007275", "GO:0009344", "GO:0009534", "GO:0009654", "GO:0045156", "GO:0009767"
OG0002351	zinc metalloprotease FTSH 2, chloroplastic	"GO:0009535", "GO:0004176", "GO:0004222", "GO:0005524", "GO:0008270", "GO:0016887", "GO:0006508", "GO:0010206", "GO:0030163", "GO:0009534", "GO:0042170", "GO:0000166", "GO:0008237", "GO:0046872", "GO:0005743", "GO:0010073", "GO:0010304", "GO:0005745", "GO:0009941", "GO:0034982", "GO:0031966"
OG0002378	CLT3, chloroplastic	"GO:0009507", "GO:0031982", "GO:0002229", "GO:0034635", "GO:0031969", "GO:0046686", "GO:0016020"
OG0002392	7	"GO:0005794", "GO:0008194", "GO:0006004", "GO:0007155", "GO:0010214", "GO:0010395", "GO:0080157", "GO:0016020"
OG0002400	protein SKIP27	"GO:0005634", "GO:0005737", "GO:0005515", "GO:0009611", "GO:0009617", "GO:0009651", "GO:0009737", "GO:0009751",

		"GO:0009753", "GO:0006970", "GO:0009725", "GO:0033993", "GO:0006950", "GO:0009628", "GO:0010033", "GO:0009961"
OG0002405	010910245.1uncharacterized protein LOC105036183	NA
OG0002434	A1-Igamma2, chloroplastic	"GO:0005737", "GO:0043231", "GO:0004620", "GO:0052689", "GO:0044248", "GO:0016042", "GO:0009536", "GO:0009908", "GO:0006629"
OG0002444	p60 ATPase-containing subunit A1	"GO:0044877", "GO:0048487", "GO:0005829", "GO:0031117", "GO:0090148", "GO:0051260", "GO:0005886", "GO:0006888", "GO:0051013", "GO:0046872", "GO:0000070", "GO:0034214", "GO:0007032", "GO:0009611", "GO:0005694", "GO:0008568", "GO:0005654", "GO:0000166", "GO:0005768", "GO:0000281", "GO:0051228", "GO:0032467", "GO:0140570", "GO:0043014", "GO:0005741", "GO:0008017", "GO:0005778", "GO:0006626", "GO:0072593", "GO:0031965", "GO:0048471", "GO:0001578", "GO:0043066", "GO:0071782", "GO:0031122", "GO:0016787", "GO:0016887", "GO:0046034", "GO:0031468", "GO:0045787", "GO:0000287", "GO:0031410", "GO:0035266", "GO:0015630", "GO:0055075", "GO:0007033", "GO:0015031", "GO:0055078", "GO:0005771", "GO:0005730", "GO:0043248", "GO:0043622", "GO:0045128", "GO:0009579", "GO:0009408", "GO:0009507", "GO:0016192", "GO:0009825", "GO:0010078", "GO:0036503", "GO:0046907", "GO:0045732", "GO:0008233", "GO:0031648", "GO:0005516", "GO:0043161", "GO:0032991", "GO:0098771", "GO:0051641", "GO:0000502", "GO:0055080", "GO:0010073", "GO:0090436", "GO:0051211", "GO:0009536"
OG0002485	folate-biopterin transporter 7	"GO:0009507", "GO:0009526", "GO:0016020", "GO:0008514", "GO:0006835", "GO:0071705", "GO:0009941", "GO:0042170"
OG0002513	transporter 7	"GO:0005768", "GO:0005794", "GO:0005886", "GO:0009507", "GO:0009579", "GO:0005381", "GO:0005385", "GO:0005515", "GO:0006826", "GO:0010043", "GO:0015691", "GO:0051707", "GO:0071577", "GO:0005773", "GO:0005802", "GO:0005375", "GO:0009617", "GO:0015675", "GO:0009536"
OG0002526	protein phosphatase 2C 78	"GO:0005737", "GO:0005886", "GO:0005515", "GO:0017018", "GO:0046872", "GO:0006470", "GO:1900036", "GO:1900056", "GO:1900425", "GO:0035970", "GO:0004722", "GO:0043169"
OG0002528	multiplication protein 2A	"GO:0009705", "GO:0043621", "GO:0046786"
OG0002558	ubiquitin-protein ligase RING1-like	"GO:0000209", "GO:0006970", "GO:0009788", "GO:0004842", "GO:0005515", "GO:0046872", "GO:0043162", "GO:0019222", "GO:0005829", "GO:0051865", "GO:0005634", "GO:0016567", "GO:0006511", "GO:0061630", "GO:0009414", "GO:0031624", "GO:0051787", "GO:0008285", "GO:0009630", "GO:0009737", "GO:0009968", "GO:0046621", "GO:0048437", "GO:0061635", "GO:0071629", "GO:1900057", "GO:0009793", "GO:0006952", "GO:0016020", "GO:0098542"
OG0002617	repeat-containing protein 26 homolog	"GO:0043967", "GO:0043966", "GO:0010150", "GO:0006970", "GO:0006355", "GO:0009723", "GO:0009646", "GO:0009733", "GO:0000123", "GO:0051247", "GO:0031328", "GO:0009737", "GO:0042393", "GO:0005739", "GO:0016043", "GO:0005829", "GO:0051569", "GO:0034657", "GO:0005515", "GO:0006325", "GO:0031056", "GO:0031325", "GO:0045717", "GO:1901000", "GO:0009788", "GO:0006807", "GO:0032991", "GO:0043207", "GO:0009791", "GO:0051173", "GO:0006364", "GO:0050793", "GO:0048522", "GO:0010604", "GO:0042254", "GO:0006810", "GO:0031327", "GO:0005737", "GO:0051707", "GO:0048316", "GO:1990234", "GO:0006952", "GO:0044085", "GO:0010468"
OG0002618	043697250.1splicing regulatory glutamine/lysine-rich protein 1-like isoform X2	NA
OG0002632	carrier protein MTM1	"GO:0005743", "GO:0004784", "GO:0016530", "GO:0006828", "GO:0042592", "GO:0071705", "GO:0097501", "GO:1901562", "GO:1990542", "GO:0009536", "GO:0000295", "GO:0005310", "GO:0015698", "GO:0019430", "GO:0051503", "GO:1901679", "GO:1905039", "GO:0042170", "GO:0008514", "GO:0033554"

OG0002639	GTP diphosphokinase RSH2, chloroplastic	"GO:0009507", "GO:0008728", "GO:0016787", "GO:0009611", "GO:0009737", "GO:0010150", "GO:0015970", "GO:0015979", "GO:0005515", "GO:0008893", "GO:0005524", "GO:0005525", "GO:0016301", "GO:0016310"
OG0002644	proteinase 36	"GO:0005829", "GO:0005886", "GO:0043231", "GO:0090406", "GO:0004190", "GO:0006508", "GO:0009555", "GO:0009846", "GO:0009860", "GO:0010183", "GO:0030163", "GO:0098542", "GO:0010033", "GO:0006952"
OG0002647	H2	"GO:0012511", "GO:0016020", "GO:0009845", "GO:0010344", "GO:0010431", "GO:0019915", "GO:0034389", "GO:0050826"
OG0002717	protein phosphatase 2C 47	"GO:0005634", "GO:0005829", "GO:0004722", "GO:0005515", "GO:0043169", "GO:0006470", "GO:0009414", "GO:0009651", "GO:0009737", "GO:0042742", "GO:0050688", "GO:0016020", "GO:0046872", "GO:0017018"
OG0002792	protein RXW8	"GO:0005886", "GO:0009536", "GO:0005227", "GO:0008381", "GO:0015085", "GO:0071474", "GO:0098655", "GO:0006812", "GO:0034220", "GO:0016020"
OG0002856	isomerase 1	"GO:0005829", "GO:0004476", "GO:0005515", "GO:0006013", "GO:0009298", "GO:0009646", "GO:0009744", "GO:0009793", "GO:0010043", "GO:0019853", "GO:0032025", "GO:0033591", "GO:0046680", "GO:0046686"
OG0003024	synthase 1, chloroplastic	"GO:0009707", "GO:0046481", "GO:0009266", "GO:0009809", "GO:0009867", "GO:0016036", "GO:0019375", "GO:0031408", "GO:0042550"
OG0003043	010921707.1uncharacterized protein LOC105045215	"GO:0016020", "GO:0016798"
OG0003097	026401475.1uncharacterized protein LOC113297260	GO:0016020
OG0003127	boron transporter 5	"GO:0005768", "GO:0005773", "GO:0005886", "GO:0005515", "GO:0046715", "GO:0080139", "GO:0006950", "GO:0009628", "GO:0033036", "GO:0035445", "GO:0048364", "GO:0050801", "GO:0071702", "GO:0080029", "GO:0098590", "GO:0006812", "GO:0006873", "GO:0006885", "GO:0006820", "GO:0005737", "GO:0043231", "GO:0015297", "GO:0006811"
OG0003149	interactor EPSIN 2	"GO:0005634", "GO:0005905", "GO:0048471", "GO:0030276", "GO:0009790", "GO:0009966", "GO:0016197", "GO:0030036", "GO:0048522", "GO:0051128", "GO:0012505", "GO:0016020", "GO:0031410", "GO:0005515", "GO:0005737", "GO:0043231"
OG0003214	glycerol-3-phosphate dehydrogenase [NAD(+)] 1, cytosolic	"GO:0005829", "GO:0009331", "GO:0051287", "GO:0005975", "GO:0006116", "GO:0009627", "GO:0044255", "GO:0005515", "GO:0006629", "GO:0016616", "GO:0047952"
OG0003218	2	"GO:0002239", "GO:0005737", "GO:0043231", "GO:0051707", "GO:0009620", "GO:0043229"
OG0003237	phosphoglycerate mutase	"GO:0005740", "GO:0030145", "GO:0046537", "GO:0006007", "GO:0006096", "GO:0009409", "GO:0009555", "GO:0009637", "GO:0009737", "GO:0010037", "GO:0010118", "GO:0044262"
OG0003276	038980267.1uncharacterized protein LOC120110166 isoform X1	"GO:0009975", "GO:0016020"
OG0003280	nucleotide-binding protein 9	"GO:0005525", "GO:0034605", "GO:0030968", "GO:0003924", "GO:0005829", "GO:0042803", "GO:0005783", "GO:1900425", "GO:0005886", "GO:0005811", "GO:0043066", "GO:0005739", "GO:0065008", "GO:0042802", "GO:0000166", "GO:0048522", "GO:0019222", "GO:0005515", "GO:0030246"
OG0003305	protein SKIP14	"GO:0005634", "GO:0005829", "GO:0005515", "GO:0009788"
OG0003355	adenine nucleotide carrier 1	"GO:0005739", "GO:0009536", "GO:0005347", "GO:0015217", "GO:0015297", "GO:0006635", "GO:0007031", "GO:0015866", "GO:0015867", "GO:0080024", "GO:0090351", "GO:1901679", "GO:0009507", "GO:0098656", "GO:0005778", "GO:0055085", "GO:0006289", "GO:0010225", "GO:0043132", "GO:0044375"
OG0003472	E3 ubiquitin-protein ligase RHY1A	"GO:0008270", "GO:0061630", "GO:0009793", "GO:0000209", "GO:0006952", "GO:0009788", "GO:0005634", "GO:0009628", "GO:0043161", "GO:0005829", "GO:0031667", "GO:0010033", "GO:0005770", "GO:0009501", "GO:0005794", "GO:0005783", "GO:0009630", "GO:0005886", "GO:0098542", "GO:0005769",

		"GO:0033554", "GO:0070534", "GO:0010228", "GO:0005765", "GO:0031902", "GO:0012501", "GO:0051865", "GO:0043068", "GO:0006513", "GO:0006950", "GO:0009617", "GO:0002238", "GO:0005515", "GO:0009737", "GO:0009651", "GO:0010182", "GO:0009787", "GO:0009687", "GO:0004842", "GO:0009739", "GO:0016020", "GO:0016567", "GO:0042742", "GO:0009789", "GO:0047484", "GO:0000976", "GO:0051787", "GO:0061635", "GO:0071629", "GO:0005737", "GO:0012505", "GO:0043231"
OG0003493	Brevis radix-like 2	"GO:0048364", "GO:0065008", "GO:0005737", "GO:0043231", "GO:0006629", "GO:0009725", "GO:0009888", "GO:0052689", "GO:0004620", "GO:0043229", "GO:0016298"
OG0003510	lipoxygenase 6	"GO:0009507", "GO:0009579", "GO:0016165", "GO:0016166", "GO:0046872", "GO:1990136", "GO:0006633", "GO:0008299", "GO:0009555", "GO:0009611", "GO:0009617", "GO:0009620", "GO:0009644", "GO:0009695", "GO:0009737", "GO:0009751", "GO:0009753", "GO:0009901", "GO:0010193", "GO:0010311", "GO:0010597", "GO:0031408", "GO:0034440", "GO:0080086", "GO:1900366", "GO:0009534", "GO:0009570", "GO:0005506", "GO:0019395"
OG0003525	domain-containing protein 17	"GO:0043069", "GO:0009966", "GO:0098542", "GO:0005634", "GO:0004842", "GO:0009617", "GO:0005515", "GO:0048586", "GO:0016020", "GO:0071215", "GO:0005829", "GO:0031348", "GO:0016567", "GO:0061630", "GO:0009610", "GO:0043621", "GO:0005886", "GO:0031648", "GO:0002237", "GO:0009609", "GO:0070696", "GO:2000022", "GO:0051865", "GO:0090333", "GO:0005737", "GO:2000028", "GO:0043231"
OG0003537	ATPase HMA2	"GO:0005768", "GO:0005774", "GO:0005802", "GO:0009536", "GO:0030659", "GO:0045177", "GO:0098590", "GO:0005375", "GO:0005385", "GO:0005507", "GO:0005515", "GO:0005524", "GO:0008551", "GO:0016463", "GO:0016887", "GO:0007005", "GO:0009072", "GO:0009888", "GO:0010042", "GO:0010043", "GO:0010243", "GO:0010273", "GO:0030198", "GO:0032025", "GO:0033554", "GO:0035434", "GO:0042430", "GO:0046916", "GO:0048522", "GO:0048523", "GO:0055069", "GO:0055070", "GO:0070574", "GO:0071248", "GO:0071577", "GO:0071585", "GO:0097435", "GO:1901135", "GO:1901605", "GO:1901701", "GO:0010039", "GO:0010288", "GO:0046688", "GO:0071310", "GO:0005886", "GO:0009507", "GO:0009579", "GO:0046872", "GO:0006825", "GO:0009723", "GO:0006829"
OG0003551	specificity protein phosphatase PHS1	"GO:0043409", "GO:0043067", "GO:0080135", "GO:0009411", "GO:0043622", "GO:0006469", "GO:0006979", "GO:0048522", "GO:0071310", "GO:0010119", "GO:0035335", "GO:0050776", "GO:0005886", "GO:0007346", "GO:0008138", "GO:0004722", "GO:0005634", "GO:0005516", "GO:0033549", "GO:0009737", "GO:0005737", "GO:0010468", "GO:0012505", "GO:0030155", "GO:0009651", "GO:0043069", "GO:0010558", "GO:0010035", "GO:0019901", "GO:1902065", "GO:0042981", "GO:0014070", "GO:0000302", "GO:0045934", "GO:0031327", "GO:0016020", "GO:0010225", "GO:0032870", "GO:0010224", "GO:0017017", "GO:0006470", "GO:0005515", "GO:0009755", "GO:0016311", "GO:0048523", "GO:0007165"
OG0003557	transporter G family member 25	"GO:0010184", "GO:0051050", "GO:0051171", "GO:0005789", "GO:0051641", "GO:0140359", "GO:0048522", "GO:0140115", "GO:0010496", "GO:0010152", "GO:0015562", "GO:0014070", "GO:0042542", "GO:0008514", "GO:0042742", "GO:0030659", "GO:0010588", "GO:0042908", "GO:0010148", "GO:0010222", "GO:0016324", "GO:0009893", "GO:0080110", "GO:0009897", "GO:0009736", "GO:0009414", "GO:0006863", "GO:0000166", "GO:0009409", "GO:0009408", "GO:0005768", "GO:0048581", "GO:0070505", "GO:0015248", "GO:0042803", "GO:0055088", "GO:0080168", "GO:0005345", "GO:1901656", "GO:0009738", "GO:0030638", "GO:0010888", "GO:0010243", "GO:0019218", "GO:0044281", "GO:1905952", "GO:0005634", "GO:0071407", "GO:0042910", "GO:0032504", "GO:0098754", "GO:0043933", "GO:0051649", "GO:0005319", "GO:0006812", "GO:0015208", "GO:0080090", "GO:0015854", "GO:0005886", "GO:0042626", "GO:0009651", "GO:0033554", "GO:0015245", "GO:0009611",

		"GO:0010025", "GO:0010345", "GO:0042335", "GO:0051607", "GO:0080051", "GO:0080172", "GO:0006629"
OG0003573	1-phosphatidylinositol-3-phosphate 5-kinase FAB1D	"GO:0000139", "GO:0005829", "GO:0031901", "GO:0031902", "GO:0048471", "GO:0000285", "GO:0004674", "GO:0005515", "GO:0008270", "GO:0016308", "GO:0043813", "GO:0006612", "GO:0008333", "GO:0009555", "GO:0010256", "GO:0034504", "GO:0035556", "GO:0036289", "GO:0042147", "GO:0046854", "GO:0048523", "GO:0050829", "GO:0070647", "GO:0090332", "GO:0097352", "GO:1903426", "GO:2000785", "GO:0005797", "GO:0005801", "GO:0010008", "GO:0004888", "GO:0006796", "GO:0007033", "GO:0009624", "GO:0072657", "GO:0005886", "GO:0003779", "GO:0003006", "GO:0005975", "GO:0006520", "GO:0009791", "GO:0010015", "GO:0048468", "GO:0006897", "GO:0009856", "GO:0009932", "GO:0046488", "GO:0048588", "GO:0009958", "GO:0010118", "GO:0010311", "GO:0016043", "GO:0052742"
OG0003648	1, chloroplastic	"GO:0005634", "GO:0009570", "GO:0003700", "GO:0016161", "GO:0042802", "GO:0102229", "GO:0000024", "GO:0005983", "GO:0009409", "GO:0009414", "GO:0048831", "GO:0080027"
OG0003655	protein YKT61	"GO:0000139", "GO:0000421", "GO:0005576", "GO:0005739", "GO:0005789", "GO:0005829", "GO:0010008", "GO:0031201", "GO:0005484", "GO:0005515", "GO:0019706", "GO:0006886", "GO:0006888", "GO:0006891", "GO:0006895", "GO:0006903", "GO:0006904", "GO:0042144", "GO:0042147", "GO:0048280", "GO:0006906", "GO:0005886", "GO:0015031"
OG0003680	ENHANCED DISEASE RESISTANCE 2	"GO:0005737", "GO:0012505", "GO:0016020", "GO:0043231"
OG0003707	039136391.1uncharacterized protein LOC120273755	"GO:0005746", "GO:0016740", "GO:0033617"
OG0003710	protein At5g47470	"GO:0005737", "GO:0005886", "GO:0015179", "GO:0065008", "GO:0140115", "GO:0022857", "GO:0006865", "GO:0010817", "GO:0055085", "GO:0071554", "GO:0015171", "GO:0003333", "GO:0015186", "GO:0048316", "GO:0005774", "GO:0071944", "GO:0031325", "GO:0048856", "GO:0016020"
OG0003741	kinase BLUS1	"GO:0046777", "GO:0000139", "GO:0043268", "GO:0005798", "GO:0043547", "GO:0015629", "GO:0005829", "GO:0004674", "GO:0006972", "GO:0032956", "GO:0010628", "GO:0050801", "GO:0051019", "GO:0018105", "GO:0018107", "GO:0043407", "GO:0007231", "GO:1902456", "GO:0005654", "GO:0000287", "GO:0005524", "GO:0072686", "GO:0050891", "GO:0042803", "GO:1901017", "GO:0009267", "GO:0048471", "GO:0012506", "GO:0043066", "GO:0019898", "GO:0007163", "GO:0005769", "GO:0005802", "GO:0005886", "GO:0019901", "GO:0000910", "GO:0001558", "GO:0002218", "GO:0002237", "GO:0002252", "GO:0006996", "GO:0009682", "GO:0009737", "GO:0009755", "GO:0009888", "GO:0009966", "GO:0010015", "GO:0035556", "GO:0042127", "GO:0048638", "GO:0071396", "GO:0090567", "GO:0090698", "GO:1901701", "GO:1903426", "GO:0006979", "GO:0010035", "GO:0022414", "GO:0005515", "GO:0006810", "GO:0002376", "GO:0031347", "GO:0042742", "GO:0015630", "GO:0016020", "GO:0003006", "GO:0006468", "GO:0009617", "GO:0009791", "GO:0010033", "GO:0048646", "GO:0098542", "GO:0099402", "GO:0065008"
OG0003742	finger protein CONSTANS-LIKE 13	"GO:0010099", "GO:0042802", "GO:0010161", "GO:0000976", "GO:0048579", "GO:0009637", "GO:0007623", "GO:0009658", "GO:0005634", "GO:0003700", "GO:0045892", "GO:0009909", "GO:0048576", "GO:2000032", "GO:0071482", "GO:0010629", "GO:0010218", "GO:0030674", "GO:0005515", "GO:0046872", "GO:0006355", "GO:0009639", "GO:2000030", "GO:0008270", "GO:0048577", "GO:0010018", "GO:0010114"
OG0003758	and ribitol dehydrogenase	"GO:0009507", "GO:0008106", "GO:0019438", "GO:0032787", "GO:0005777", "GO:0006066", "GO:0006721", "GO:0006725", "GO:0006952", "GO:0008610", "GO:0010033", "GO:0044255", "GO:0046394", "GO:0044283", "GO:0044281", "GO:0006950", "GO:0016114"

OG0003764	domain-containing protein 19	"GO:0061630", "GO:0090333", "GO:0009787", "GO:0009610", "GO:0043069", "GO:0043621", "GO:0005886", "GO:0098542", "GO:0031648", "GO:0005634", "GO:0002237", "GO:0005737", "GO:0009609", "GO:0010029", "GO:2000022", "GO:2000028", "GO:0051865", "GO:0009617", "GO:0005515", "GO:0016020", "GO:0005622", "GO:0006950", "GO:0048856", "GO:0009966", "GO:0004842", "GO:0071215"
OG0003789	019703187.2uncharacterized protein LOC105036460	GO:0016020
OG0003824	protein pKIWI502	"GO:0000275", "GO:0009535", "GO:0005515", "GO:0005524", "GO:0016887", "GO:0046933", "GO:0046961", "GO:0015986", "GO:1902600", "GO:0009536", "GO:0016491"
OG0003852	protein 27	"GO:0009416", "GO:0009409", "GO:0005515", "GO:0009737", "GO:0045892", "GO:0009637", "GO:0009615", "GO:0042752", "GO:2000028", "GO:0010114", "GO:0009646", "GO:0009628"
OG0003860	011658492.1uncharacterized protein LOC101219972	"GO:0016491", "GO:0016020", "GO:0016627", "GO:0006091"
OG0003867	026440406.1uncharacterized protein LOC113339329	GO:0016020
OG0003938	reticulum oxidoreductin-1	"GO:0005789", "GO:0005515", "GO:0015035", "GO:0016972", "GO:0071949", "GO:0006979", "GO:0018401", "GO:0022417", "GO:0030198", "GO:0030968", "GO:0034975", "GO:0042593", "GO:0045454", "GO:0071456", "GO:0007165", "GO:0034976", "GO:0042592", "GO:0051604"
OG0004016	039115653.1uncharacterized protein LOC120251182 isoform X2	"GO:0004252", "GO:0006508"
OG0004022	iron transporter 1	"GO:0005381", "GO:0005384", "GO:0042803", "GO:0046872", "GO:0006874", "GO:0006880", "GO:0030026", "GO:0034755", "GO:0071421", "GO:0005774"
OG0004025	ENHANCED DISEASE RESISTANCE 2-like	"GO:0005789", "GO:0005886", "GO:0010008", "GO:0070273", "GO:0009723", "GO:0009751", "GO:1900056", "GO:1900150", "GO:0016020", "GO:0005515", "GO:0017018", "GO:0046872", "GO:0009846", "GO:0035970", "GO:0042742"
OG0004033	galactinol--sucrose galactosyltransferase 2	"GO:0047268", "GO:0047274", "GO:0052692", "GO:0006979", "GO:0009312", "GO:0009414", "GO:0034484", "GO:0008378"
OG0004062	044442448.1uncharacterized protein LOC123168633	NA
OG0004085	4.1	"GO:0005886", "GO:0019900", "GO:0043621", "GO:0009414", "GO:0009651", "GO:0009738", "GO:0010555", "GO:0005515", "GO:0006950", "GO:0009628", "GO:1900458"
OG0004158	factor BOA	"GO:0003676", "GO:0000122", "GO:0005634", "GO:0009409", "GO:0005667", "GO:0003700", "GO:0009909", "GO:0005737", "GO:0010492", "GO:0042802", "GO:0010082", "GO:0010150", "GO:0080022", "GO:0010380", "GO:0000976", "GO:0080036", "GO:0080113", "GO:0009873", "GO:0042753", "GO:0000156", "GO:0009414", "GO:1990110", "GO:0031537", "GO:0045893", "GO:0010119", "GO:0090506", "GO:0048576", "GO:2000031", "GO:0009787", "GO:2000022", "GO:0051093"
OG0004185	synthase 2, chloroplastic	"GO:0005739", "GO:0009507", "GO:1990234", "GO:0004311", "GO:0004337", "GO:0005515", "GO:0046872", "GO:0006744", "GO:0009793", "GO:0010236", "GO:0045337", "GO:0009570", "GO:0008654", "GO:0010033", "GO:0016114", "GO:0051707", "GO:0044687"
OG0004254	esterase	"GO:0005634", "GO:0005737", "GO:0012505", "GO:0016020", "GO:0030054", "GO:0005515", "GO:0016298", "GO:0052689", "GO:0006631", "GO:0006950", "GO:0010035", "GO:0010646", "GO:0023051", "GO:0005783", "GO:0071944", "GO:0016747", "GO:0006979", "GO:0009966", "GO:0010038", "GO:0043231", "GO:0016787", "GO:0003824"
OG0004262	protein kinase inhibitor SMR4	"GO:0005634", "GO:0005515", "GO:0006974", "GO:0010564"
OG0004308	PIN-LIKES 6	"GO:0005789", "GO:0010329", "GO:0009734", "GO:0010252", "GO:0010311", "GO:0040009", "GO:0080162"
OG0004377	partner of ACD11 1	"GO:0005886", "GO:0005515", "GO:0034051", "GO:0005737", "GO:0016020", "GO:0000976", "GO:0003700", "GO:0046983",

		"GO:0006355", "GO:0009740", "GO:0009742", "GO:0009826", "GO:0010086", "GO:0048510", "GO:0080113", "GO:0003676", "GO:0050832"
OG0004398	020705493.1uncharacterized protein LOC110116303	GO:0016020
OG0004421	dehydrogenase 2, mitochondrial	"GO:0005654", "GO:0005739", "GO:0004657", "GO:0071949", "GO:0006562", "GO:0006970", "GO:0006979", "GO:0009414", "GO:0010942", "GO:0042742"
OG0004430	039830763.1uncharacterized protein LOC120691681	NA
OG0004442	038980334.1uncharacterized protein LOC103701037 isoform X1	"GO:0016020", "GO:0016740"
OG0004444	010905737.1uncharacterized protein LOC105032855	NA
OG0004551	010920260.1uncharacterized protein LOC105044153 isoform X1	"GO:0005634", "GO:0005737", "GO:0004860", "GO:0005509", "GO:0005622", "GO:0043086"
OG0004631	A1 PLIP2, chloroplastic	"GO:0009534", "GO:0016020", "GO:0008970", "GO:0047714", "GO:0052739", "GO:0002213", "GO:0015908", "GO:0019432", "GO:0031349"
OG0004682	010904871.1uncharacterized protein LOC105032189	NA
OG0004738	OG0004738 Membrin-11	"GO:0005789", "GO:0005801", "GO:0012507", "GO:0031201", "GO:0031902", "GO:0000149", "GO:0005484", "GO:0006906", "GO:0045088", "GO:0050708"
OG0004762	protein At3g17800, chloroplastic	"GO:0009536", "GO:0009611", "GO:0010193", "GO:0010224"
OG0004778	ion channel protein 1, mitochondrial	"GO:0005743", "GO:0008381", "GO:0006811", "GO:0034599", "GO:0055085", "GO:0006810", "GO:0000307", "GO:0005515", "GO:0016538", "GO:0000079", "GO:0010332", "GO:0044772", "GO:0009526", "GO:0034220"
OG0004958	020088735.1uncharacterized protein LOC109710514	"GO:0016740", "GO:0016020"
OG0004963	transporter 1	"GO:0005773", "GO:0005886", "GO:0015079", "GO:0009932", "GO:0048825", "GO:0071805", "GO:0016020", "GO:0009674", "GO:1990573", "GO:0006811", "GO:0005737", "GO:0043231", "GO:0006813"
OG0004981	008802418.1non-lysosomal glucosylceramidase-like	"GO:0016139", "GO:0065008", "GO:0016757", "GO:0006680", "GO:0008422", "GO:0000139", "GO:0005886", "GO:0005789", "GO:0004348", "GO:0051493", "GO:0008202", "GO:1901615", "GO:0044281", "GO:0016020", "GO:0005975"
OG0004984	protein SKIP22	GO:0005515
OG0005084	NEN1	"GO:0005622", "GO:0008408", "GO:0003676", "GO:0046872", "GO:0090305", "GO:0004527"
OG0005116	alkenal/one oxidoreductase, chloroplastic	"GO:0005737", "GO:0043227", "GO:0003723", "GO:0003960", "GO:0042803", "GO:0048038", "GO:0070402", "GO:0006739", "GO:0044248", "GO:0043231", "GO:0008168", "GO:0016417", "GO:0016628", "GO:0016829", "GO:0006637", "GO:0008610", "GO:0009888", "GO:0030154", "GO:0044255", "GO:0044550", "GO:0048731", "GO:0009536", "GO:0016020", "GO:0071704"
OG0005124	protein 5	"GO:0010482", "GO:0098755", "GO:0009793", "GO:0048765", "GO:0010029", "GO:0051567", "GO:0010026"
OG0005233	039124591.1uncharacterized protein LOC120261005	"GO:0016020", "GO:0043231", "GO:0048471", "GO:0004722", "GO:0005515", "GO:0044877", "GO:0007010", "GO:0007059", "GO:0007165", "GO:0044238", "GO:0048523", "GO:0071704", "GO:0000922", "GO:0005829", "GO:0051301"
OG0005234	010905495.1uncharacterized protein LOC105032685	GO:0016020
OG0005252	008792168.1multiple inositol polyphosphate phosphatase 1 isoform X1	"GO:0052745", "GO:0006796", "GO:0044281", "GO:0071704", "GO:0003993", "GO:0016791"
OG0005304	phosphatase, chloroplastic	"GO:0009507", "GO:0009579", "GO:0016020", "GO:0043621", "GO:0006468", "GO:0009231", "GO:0016311", "GO:0042651", "GO:0016301", "GO:0046872", "GO:0010196", "GO:0016787"

OG0005520	kDa class IV heat shock protein	"GO:0005783", "GO:0043621", "GO:0051082", "GO:0006457", "GO:0009408", "GO:0009651", "GO:0042542", "GO:0045471", "GO:0046685", "GO:0046686", "GO:0046688", "GO:0010286", "GO:0044183", "GO:0051259", "GO:0005788", "GO:0032991", "GO:0042802", "GO:0050821"
OG0005540	010931027.1uncharacterized protein LOC105052034	NA
OG0005565	protein At1g01500	"GO:0004617", "GO:0016020"
OG0005566	008776159.3uncharacterized protein LOC103696343	GO:0016020
OG0005619	chlorophyll(ide) b reductase NYC1, chloroplastic	"GO:0009535", "GO:0005515", "GO:0034256", "GO:0008610", "GO:0010304", "GO:0015996", "GO:0044255", "GO:0044281", "GO:0065008", "GO:0006631"
OG0005662	010922582.1uncharacterized protein LOC105045858	character(0
OG0005704	protein At1g32220, chloroplastic	"GO:0005737", "GO:0043231", "GO:0016616", "GO:0006744", "GO:0006979", "GO:0008202", "GO:0043229"
OG0005736	proteinase inhibitor 12	"GO:0005576", "GO:0005773", "GO:0004869", "GO:0005515", "GO:0006952", "GO:0006972", "GO:0006979", "GO:0009409", "GO:0010951", "GO:0010030", "GO:0034605", "GO:0042631", "GO:0009414", "GO:0009611"
OG0005738	stress protein A-like protein	"GO:0002238", "GO:0005737", "GO:0016208"
OG0005919	protein 2	"GO:0009570", "GO:0005504", "GO:0071704", "GO:0006631"
OG0005999	SGR2	"GO:0005739", "GO:0005783", "GO:0005794", "GO:0005856", "GO:0009705", "GO:0005515", "GO:0008970", "GO:0035091", "GO:0046872", "GO:0007165", "GO:0009416", "GO:0009590", "GO:0009660", "GO:0009959", "GO:0019953", "GO:0022414", "GO:0033036", "GO:0046488", "GO:0048856", "GO:0071702", "GO:0005548", "GO:0004620"
OG0006018	transfer protein SFH2	"GO:0016020", "GO:0009653", "GO:0048731"
OG0006089	019704652.1uncharacterized protein LOC109505593	GO:0016020
OG0006116	reductase	"GO:0005829", "GO:0009507", "GO:0016324", "GO:0004032", "GO:0005515", "GO:0016229", "GO:0070401", "GO:0006979", "GO:0009409", "GO:0009414", "GO:0009651", "GO:0019853", "GO:0042593", "GO:0046185", "GO:0048870", "GO:0110095", "GO:1990641"
OG0006132	OG0006132 Synaptotagmin-3	"GO:0005783", "GO:0016020", "GO:0008289", "GO:0006810", "GO:0005737", "GO:0012505", "GO:0043231"
OG0006197	DOG1-like 4	"GO:0005634", "GO:0003677", "GO:0005515", "GO:0006355", "GO:0007165", "GO:0048523", "GO:0050793", "GO:0051239", "GO:0071310", "GO:0098542", "GO:0009737", "GO:0010033", "GO:1901701", "GO:0009725", "GO:0033993", "GO:0042802", "GO:0043565", "GO:0009617", "GO:0009791"
OG0006268	020090737.1uncharacterized protein LOC109711848	"GO:0043229", "GO:0016779", "GO:0005524", "GO:0046872", "GO:0009534"
OG0006367	GTPase-activating protein 22	"GO:0005576", "GO:0005769", "GO:0005776", "GO:0005829", "GO:0030659", "GO:0055037", "GO:0005096", "GO:0031267", "GO:0030154", "GO:0043547", "GO:0045944", "GO:0009507", "GO:0003729", "GO:0005515", "GO:0034046", "GO:0009793", "GO:0016125", "GO:0016554", "GO:0019287", "GO:0019288", "GO:0031425", "GO:0031426", "GO:0050790"
OG0006397	domain-containing protein 16	"GO:0005737", "GO:0005515", "GO:0016740", "GO:0004842", "GO:0051707"
OG0006446	3'-O-beta-glucosyltransferase	"GO:0005515", "GO:0080043", "GO:0006725", "GO:0006950", "GO:0009628", "GO:0051707", "GO:0035251", "GO:0032787", "GO:0033554", "GO:1901615", "GO:1901701", "GO:0080044", "GO:0009636", "GO:0008299", "GO:0010033", "GO:0005737", "GO:0050403", "GO:0050502", "GO:0080046", "GO:0010224", "GO:0051555", "GO:0016131", "GO:0098754", "GO:0009813", "GO:0044238"
OG0006473	NAR1	"GO:0005634", "GO:0005829", "GO:0097361", "GO:0005515", "GO:0046872", "GO:0051539", "GO:0001666", "GO:0010468", "GO:0016226", "GO:0070482"

OG0006500	transferase At4g12130, mitochondrial	"GO:0005759", "GO:0016226"
OG0006556	bisphosphate carboxylase/oxygenase large subunit N-methyltransferase, chloroplastic,,,	"GO:0005737", "GO:0016020", "GO:0043231", "GO:0005515", "GO:0008170", "GO:0008757", "GO:0016043", "GO:0018022", "GO:0009536", "GO:0008168", "GO:0032259"
OG0006629	chloroplastic	"GO:0005739", "GO:0009535", "GO:0031969", "GO:0004325", "GO:0042803", "GO:0046872", "GO:0051537", "GO:0006783", "GO:0006979", "GO:0055035"
OG0006703	protein At4g17486	"GO:0005829", "GO:0032991", "GO:0016929", "GO:0042802", "GO:0101005", "GO:0006611", "GO:0016926", "GO:0032434"
OG0006835	008792341.2uncharacterized protein LOC103708985	NA
OG0006873	hydrolase 19, chloroplastic	"GO:0005777", "GO:0009507", "GO:0035529", "GO:0046872", "GO:0006734", "GO:0006742", "GO:0010468", "GO:0019677", "GO:0000210"
OG0006875	008783204.2dipeptidyl aminopeptidase 4 isoform X1	"GO:0005737", "GO:0016020", "GO:0042995", "GO:0043229", "GO:0005515", "GO:0008233", "GO:0012501", "GO:0005730", "GO:0005771", "GO:0005776", "GO:0005886", "GO:0008270", "GO:0032183", "GO:0042803", "GO:0061630", "GO:0006511", "GO:0009411", "GO:0010228", "GO:0016567", "GO:0080148", "GO:1902584", "GO:2000785", "GO:0004177", "GO:0008236", "GO:0008239", "GO:0006508"
OG0006894	chloroplastic	"GO:0009507", "GO:0009579", "GO:0016020", "GO:0005515", "GO:0080124", "GO:0015996"
OG0006899	009406110.1PREDICTED: uncharacterized protein LOC103989082	"GO:0016811", "GO:0006672", "GO:0016020"
OG0006994	beta-amylase 9	"GO:0009570", "GO:0005515", "GO:0016161", "GO:0000024", "GO:0005983", "GO:0009409", "GO:0009414", "GO:0080027", "GO:0009507", "GO:0004553", "GO:0006950", "GO:0009628"
OG0007089	3',8-cyclase, mitochondrial,,,	"GO:0005634", "GO:0005759", "GO:0005829", "GO:0009507", "GO:0019008", "GO:0005515", "GO:0005525", "GO:0046872", "GO:0051539", "GO:0061798", "GO:0061799", "GO:0006777", "GO:0032324"
OG0007096	050119657.1uncharacterized protein LOC126596974	"GO:0000932", "GO:0005685", "GO:0005688", "GO:0005730", "GO:0005732", "GO:0046540", "GO:0071013", "GO:1990726", "GO:0003729", "GO:0005515", "GO:0000290", "GO:0000398", "GO:0030490", "GO:0016020"
OG0007115	039126196.1uncharacterized protein LOC120262186	"GO:0042802", "GO:0009793", "GO:0005085", "GO:0048767", "GO:0009531", "GO:2001108", "GO:0005829", "GO:2000012", "GO:0050832", "GO:0016324", "GO:0080092", "GO:0090406", "GO:0016020"
OG0007135	transporter 1	"GO:0009536", "GO:0009705", "GO:0016324", "GO:0090406", "GO:0002020", "GO:0005366", "GO:0015149", "GO:0051117", "GO:0015749", "GO:0023052", "GO:1902004", "GO:0005886", "GO:0006812", "GO:0015798"
OG0007267	inactive ATP-dependent zinc metalloprotease FTSHI 3, chloroplastic	"GO:0005745", "GO:0009534", "GO:0031969", "GO:0004176", "GO:0004222", "GO:0005515", "GO:0005524", "GO:0008270", "GO:0016887", "GO:0010206", "GO:0030163", "GO:0034982", "GO:0065003", "GO:0005743", "GO:0006508", "GO:0010073"
OG0007674	038973392.1uncharacterized protein LOC103701491	GO:0016020
OG0007729	031268187.1uncharacterized protein LOC116126655	GO:0051213
OG0007848	60S subunit biogenesis factor REI1 homolog 2	"GO:0005634", "GO:0005829", "GO:0030687", "GO:0000976", "GO:0003700", "GO:0005515", "GO:0046872", "GO:0006355", "GO:0006364", "GO:0009631", "GO:0042273", "GO:0031981", "GO:0090070"
OG0008124	ubiquitin thioesterase 2	"GO:0090316", "GO:0043328", "GO:0022607", "GO:0005770", "GO:0009653", "GO:0005774", "GO:0061578", "GO:0005654", "GO:0048285", "GO:0000281", "GO:0005829", "GO:0019904", "GO:0140492", "GO:0000502", "GO:0006897", "GO:0042127", "GO:0046872", "GO:0044090", "GO:0071108", "GO:0070536", "GO:0005515", "GO:0006508"

OG0008149	020104188.1uncharacterized protein LOC109721156	NA
OG0008196	010925823.1splicing factor ESS-2 homolog	"GO:0005681", "GO:0071013"
OG0008203	038972598.1uncharacterized protein LOC103724163	"GO:0005634", "GO:0019005", "GO:0003700", "GO:0043565", "GO:0006355", "GO:0031146"
OG0008345	peroxiredoxin	"GO:0005615", "GO:0005634", "GO:0005739", "GO:0005829", "GO:0048471", "GO:0004602", "GO:0008379", "GO:0042802", "GO:0047184", "GO:0000302", "GO:0009269", "GO:0010231", "GO:0042744", "GO:0045454", "GO:0046475", "GO:0048026", "GO:0050832", "GO:0098869", "GO:0009526"
OG0008348	009392047.1PREDICTED: LOW QUALITY PROTEIN: uncharacterized protein LOC103978068	NA
OG0008353	020087055.1uncharacterized protein LOC109709302	"GO:0016020", "GO:0016301", "GO:0046872", "GO:0016310", "GO:0044238"
OG0008378	ubiquitin-protein ligase AIP2	"GO:0061630", "GO:0009414", "GO:0009788", "GO:0005634", "GO:0043161", "GO:0043162", "GO:0005829", "GO:0070534", "GO:0051865", "GO:0008270", "GO:2000070", "GO:0071629", "GO:0009651", "GO:0000209", "GO:1902006", "GO:0009630", "GO:0006513", "GO:0009789", "GO:0061635", "GO:0005789", "GO:0047484", "GO:0009938", "GO:0051787", "GO:0042742", "GO:0050793", "GO:0046872"
OG0008390	response protein 4	"GO:0005886", "GO:0043424"
OG0008395	receptor UVR8	"GO:0005694", "GO:0012505", "GO:0015630", "GO:0016020", "GO:0031410", "GO:0031981", "GO:0004842", "GO:0008289", "GO:0019899", "GO:0042802", "GO:0002376", "GO:0006511", "GO:0006974", "GO:0009411", "GO:0016043", "GO:0030154", "GO:0036211", "GO:0048523", "GO:0048731", "GO:0050790", "GO:0051707", "GO:0005622", "GO:0005737", "GO:0043229"
OG0008415	lipase 2	"GO:0005737", "GO:0043231", "GO:0016298", "GO:0006629"
OG0008475	3, chloroplastic	"GO:0009536", "GO:0048046", "GO:0004556", "GO:0005515", "GO:0046872", "GO:0005983", "GO:0005987", "GO:0009737", "GO:0009739"
OG0008476	de-epoxidase, chloroplastic	GO:0005622
OG0008481	020099241.1uncharacterized protein LOC109717759	"GO:0005634", "GO:0005789", "GO:0032991", "GO:0019899", "GO:0031593", "GO:0009968", "GO:0036503", "GO:0043161", "GO:0048522", "GO:0034098", "GO:0030433", "GO:0071712", "GO:0006511"
OG0008536	043698318.1lactoylglutathione lyase-like	GO:0016829
OG0008571	protein homolog	"GO:0005783", "GO:0005795", "GO:0020037", "GO:0006778", "GO:0009651", "GO:0016020", "GO:0009536", "GO:0009737"
OG0008602	010934531.1uncharacterized protein LOC105054657	NA
OG0008681	038984348.1uncharacterized protein YciO-like	GO:0003725
OG0008749	esterase	"GO:0005783", "GO:0016020", "GO:0071944", "GO:0016298", "GO:0016747", "GO:0052689", "GO:0006631", "GO:0006979", "GO:0010038", "GO:0010646", "GO:0023051", "GO:0065008", "GO:0005737", "GO:0012505", "GO:0043231", "GO:0016787"
OG0008861	finger AN1 domain-containing stress-associated protein 12	"GO:0005634", "GO:0005515", "GO:0009737", "GO:0009651", "GO:0005737", "GO:0046872", "GO:0097501", "GO:0016020", "GO:0000976", "GO:0008270"
OG0008997	MATURATION PROTEIN 1	"GO:0044183", "GO:0009408", "GO:0006457", "GO:0010231"
OG0009032	020106422.1uncharacterized protein LOC109722716	NA
OG0009081	poly(A) polymerase 3	"GO:0005737", "GO:0016604", "GO:0000166", "GO:0004652", "GO:0005515", "GO:0046872", "GO:0008285", "GO:0031124", "GO:0034470", "GO:0043631", "GO:0045824", "GO:0048366", "GO:0048451", "GO:0006396", "GO:0006397", "GO:0031123", "GO:0016740", "GO:0048367"

OG0009095	tocopherol cyclase, chloroplastic	"GO:0009706", "GO:0010287", "GO:0009976", "GO:0016853", "GO:0006631", "GO:0006979", "GO:0009266", "GO:0009644", "GO:0009651", "GO:0009915", "GO:0010189", "GO:0015994", "GO:0016122", "GO:0031347", "GO:0044255"
OG0009119	038979801.1uncharacterized protein LOC120109958 isoform X2	character(0
OG0009160	024031873.1LOW QUALITY PROTEIN: uncharacterized protein LOC21397006	NA
OG0009350	020247030.1uncharacterized protein LOC109824768	GO:0005886
OG0009382	(S)-NAD(P)H-hydrate dehydratase	"GO:0005759", "GO:0005829", "GO:0009507", "GO:0005515", "GO:0005524", "GO:0047453", "GO:0006734", "GO:0006739", "GO:0034356", "GO:0110051"
OG0009767	scaffold protein A homolog	"GO:0005654", "GO:0005694", "GO:0000993", "GO:0006283", "GO:0009411"
OG0010072	020108721.1uncharacterized protein LOC109724339	GO:0009507
OG0010082	synthase	"GO:0005783", "GO:0005794", "GO:0031966", "GO:0071617", "GO:0007006", "GO:0009888", "GO:0032049", "GO:0016020", "GO:0016747", "GO:0006644", "GO:0016746"
OG0010162	kinase STUNTED	"GO:0019901", "GO:1900150", "GO:0046777", "GO:0004672", "GO:0002221", "GO:1900426", "GO:1900459", "GO:0005777", "GO:0051020", "GO:0045088", "GO:0071323", "GO:0032502", "GO:0005886", "GO:0051781", "GO:1905393", "GO:0010476"
OG0010414	008789958.1spermatogenesis-associated protein 20	"GO:0005515", "GO:0005975"
OG0010741	domain-containing protein At3g04780	"GO:0005515", "GO:0045893", "GO:0061136"
OG0010949	OG0010949 -	"GO:0005507", "GO:0016151", "GO:0009611", "GO:0009631", "GO:0009737", "GO:0009961", "GO:0009414", "GO:0005543"
OG0011026	LAZ1 homolog 2	"GO:0005768", "GO:0005829", "GO:0009705", "GO:0030659", "GO:0007033", "GO:0012501", "GO:0098876", "GO:1900458"
OG0011044	stress transcription factor B-1	"GO:0005634", "GO:0005737", "GO:0000978", "GO:0003700", "GO:0042802", "GO:0006357", "GO:0008356", "GO:0034605", "GO:0042803", "GO:0000302", "GO:0045892", "GO:0045893", "GO:0000976", "GO:0005515", "GO:0006355"
OG0011092	010937495.1uncharacterized protein LOC105056860	NA
OG0011251	039135486.1uncharacterized protein LOC120272676 isoform X1	NA
OG0011375	F-box protein At5g04010	NA
OG0011483	FATTY ACID EXPORT 4, chloroplastic	"GO:0031969", "GO:0009793", "GO:1905885"
OG0011563	029122799.1uncharacterized protein LOC105052891 isoform X1	GO:0016020
OG0011800	OG0011800 -	NA
OG0011904	protein kinase regulatory subunit gamma-1	NA
OG0011986	RING protein 1	"GO:0005634", "GO:0005770", "GO:0005783", "GO:0005794", "GO:0005886", "GO:0003677", "GO:0005515", "GO:0046872", "GO:0061630", "GO:0006511", "GO:0009416", "GO:0009651", "GO:0009687", "GO:0009739", "GO:0009742", "GO:0009789", "GO:0010200", "GO:0016567", "GO:0033591", "GO:0047484", "GO:1901371", "GO:0000976", "GO:0006952", "GO:0005737", "GO:0031982", "GO:0012505", "GO:0016020", "GO:0009793"
OG0011989	heat shock protein, chloroplastic	"GO:0000427", "GO:0042644", "GO:0101031", "GO:0043621", "GO:0006355", "GO:0009408", "GO:0009416", "GO:0006970", "GO:0009658"
OG0012085	022874281.1uncharacterized protein LOC111393118	NA

OG0012263	OG0012263 -	NA
OG0012349	OG0012349 -	"GO:0005789", "GO:0006888", "GO:0015031", "GO:0070973"
OG0012465	039133531.1uncharacterized protein LOC120270558	NA
OG0012590	nuclease 2	"GO:0005622", "GO:0004518", "GO:0006807", "GO:0044238", "GO:0050832"
OG0013117	OG0013117 -	NA
OG0013274	family molecular chaperone regulator 5, mitochondrial	NA
OG0013438	embryogenesis abundant protein 31	"GO:0005730", "GO:0005515", "GO:0006873", "GO:0009845", "GO:0010226"
OG0013450	039126234.1uncharacterized protein LOC120262222	NA
OG0013639	molecular patterns-induced protein A70	"GO:0006950", "GO:0009617"
OG0014192	009412886.1PREDICTED: uncharacterized protein LOC103994282	NA
OG0014365	OG0014365 -	NA
OG0014681	stress-inducible protein Rab21	"GO:0005507", "GO:0016151", "GO:0009611", "GO:0009631", "GO:0009737", "GO:0009961", "GO:1902075"
OG0014683	OG0014683 -	NA
OG0014684	OG0014684 -	NA
OG0014701	element-binding protein 2A	"GO:0005634", "GO:0000976", "GO:0003700", "GO:0005515", "GO:0009414", "GO:0009555", "GO:0009651", "GO:0009737", "GO:0009751", "GO:0009753", "GO:0009834", "GO:0009873", "GO:0010286", "GO:0019760", "GO:0034605", "GO:0045893", "GO:0050832", "GO:2000070", "GO:1900036", "GO:0042542", "GO:0071497", "GO:0005886", "GO:0005983", "GO:0009723", "GO:0009738", "GO:0009744", "GO:0009749", "GO:0010119", "GO:0010182", "GO:0010224", "GO:0010353", "GO:0010449", "GO:0010896", "GO:0031930", "GO:0032880", "GO:0048316", "GO:0048527", "GO:2000082"
OG0015108	OG0015108 -	NA
OG0016736	OG0016736 -	NA
OG0016761	004976673.1late embryogenesis abundant protein At5g17165	NA
OG0018792	OG0018792 -	NA
OG0018837	DOG1-like 4	"GO:0005622", "GO:0003676", "GO:0005515", "GO:0006952", "GO:0007165", "GO:0009725", "GO:0051707", "GO:0042802", "GO:0043565", "GO:0009791", "GO:0010033"
OG0020486	dehydrin	GO:0009415
OG0020490	OG0020490 -	NA
OG0021889	OG0021889 -	NA
OG0022246	OG0022246 -	NA
OG0022255	b561 and DOMON domain-containing protein At5g35735	GO:0016020
OG0022271	OG0022271 -	NA
OG0022283	isoprenylcysteine alpha-carbonyl methylesterase ICMEL1	"GO:0000139", "GO:0005789", "GO:0010296", "GO:0009737", "GO:0044238", "GO:0044248", "GO:0008236", "GO:0006508"
OG0022297	kDa class II heat shock protein	"GO:0005737", "GO:0005515", "GO:0006972", "GO:0009408", "GO:0042542", "GO:0045471", "GO:0046685", "GO:0046686", "GO:0005829", "GO:0043621", "GO:0044183", "GO:0051082", "GO:0006457", "GO:0009651", "GO:0046688", "GO:0051259", "GO:0051260"

OG0022298	kDa proline-rich protein DC2.15	"GO:0005783", "GO:0009505", "GO:0009506", "GO:0009707", "GO:0043621", "GO:0009409", "GO:0009651", "GO:0009682", "GO:0009733", "GO:0009737", "GO:0010102", "GO:0050832"
OG0024634	zipper protein HAT3	"GO:0000976", "GO:0003700", "GO:0005515", "GO:0009414", "GO:0009641", "GO:0009734", "GO:0009735", "GO:0009738", "GO:0009826", "GO:0010016", "GO:0010218", "GO:0010311", "GO:0045892", "GO:0042803", "GO:0010017", "GO:0080191"
OG0024638	OG0024638 -	NA
OG0024669	OG0024669 -	NA
OG0024721	OG0024721 -	NA
OG0024801	embryogenesis abundant protein 31	"GO:0005730", "GO:0005515", "GO:0006873", "GO:0009845", "GO:0010226"
OG0024806	OG0024806 -	NA
OG0027777	ACID-INSENSITIVE 5-like protein 5	"GO:0042802", "GO:0090575", "GO:1901002", "GO:0000978", "GO:1902584", "GO:0005794", "GO:0001228", "GO:0009911", "GO:0043621", "GO:0009789", "GO:1990440", "GO:0010508", "GO:0031625", "GO:0046982", "GO:0043065", "GO:0000976", "GO:0003700", "GO:0005515", "GO:0006355", "GO:0006950", "GO:0007165", "GO:0009628", "GO:0009737", "GO:0009791", "GO:0048522", "GO:0071310", "GO:1901701", "GO:0007275"
OG0027799	OG0027799 -	NA
OG0027905	OG0027905 -	GO:0009793

Appendix B.4 List of down-regulated AHL motif-containing orthogroups and their associated GO terms

OG ID	OG name	GO
OG0000030	SMALL AUXIN UP-REGULATED RNA 12	"GO:0009266", "GO:1900057", "GO:0009741", "GO:0009641", "GO:0009646", "GO:0009734", "GO:0051510", "GO:0030307", "GO:0005515", "GO:0005737", "GO:2000012", "GO:0010029", "GO:0019897", "GO:0005634", "GO:1900140", "GO:0009733", "GO:0009737", "GO:0010202", "GO:0016020", "GO:0009639", "GO:0009642", "GO:0005886"
OG0000041	pectate lyase 8	"GO:0005576", "GO:0030570", "GO:0046872", "GO:0009624", "GO:0009664", "GO:0042547", "GO:0045490", "GO:0098542", "GO:0016829", "GO:0005886", "GO:0009705", "GO:0043424", "GO:0016020"
OG0000043	factor MYB61	"GO:1903086", "GO:1900384", "GO:0000902", "GO:0006970", "GO:0009611", "GO:0000976", "GO:0006952", "GO:0009834", "GO:0009800", "GO:0048364", "GO:0005634", "GO:1901957", "GO:0003700", "GO:0005515", "GO:0009737", "GO:0045892", "GO:0009909", "GO:0010119", "GO:0010214", "GO:0010089", "GO:0035017", "GO:0010224", "GO:1901348", "GO:0045723", "GO:0002213", "GO:0000162", "GO:0045893", "GO:0010438", "GO:0050832", "GO:0010597", "GO:1901332", "GO:0000987", "GO:0010091", "GO:0009759", "GO:0071365", "GO:0005737", "GO:1901141", "GO:0009094", "GO:1901002", "GO:2000652", "GO:0048226", "GO:0009423", "GO:0007623", "GO:0040008", "GO:0009825", "GO:0006723", "GO:0080091", "GO:0048658", "GO:0009555", "GO:0003682", "GO:0010090", "GO:0048354", "GO:0010087", "GO:0009409", "GO:0048765", "GO:0045165", "GO:0030154", "GO:1990841", "GO:0010018", "GO:0009740", "GO:0009867", "GO:0010345", "GO:0009892", "GO:0009411", "GO:0009809", "GO:0001708", "GO:2000039", "GO:0032880", "GO:0048629", "GO:0080187", "GO:0010026", "GO:0046394", "GO:0031327", "GO:0009628", "GO:2000762", "GO:0032787", "GO:0052545", "GO:0007154", "GO:0023052"
OG0000052	factor TCP15	"GO:0042803", "GO:1900056", "GO:0000978", "GO:0008361", "GO:0009653", "GO:0043433", "GO:0048578", "GO:0001216", "GO:0009735", "GO:0042753", "GO:0048364", "GO:0005634", "GO:0009739", "GO:0009737", "GO:0045893", "GO:0010229", "GO:0048510", "GO:0140537", "GO:0010029", "GO:0051301", "GO:0048467", "GO:0010252", "GO:0080086", "GO:0042023",

		"GO:0031540", "GO:0000987", "GO:0048438", "GO:0009725", "GO:0033993", "GO:0042802", "GO:0003700", "GO:0031347"
OG0000065	homeodomain protein 3	"GO:0005634", "GO:0005737", "GO:0000976", "GO:0003700", "GO:0042803", "GO:0046872", "GO:0009414", "GO:0009640", "GO:0009733", "GO:0009735", "GO:0009738", "GO:0009739", "GO:0009741", "GO:0009793", "GO:0010371", "GO:0010431", "GO:0019760", "GO:0043392", "GO:0045892", "GO:0045893", "GO:0048509", "GO:0009737", "GO:0009791", "GO:0006355", "GO:0009416", "GO:0005515", "GO:0009628", "GO:0048574", "GO:0003677", "GO:0048316", "GO:0010033", "GO:0010582", "GO:0043565", "GO:0001173", "GO:0009637"
OG0000089	synthase A catalytic subunit 9 [UDP-forming]	"GO:0005794", "GO:0010005", "GO:0010330", "GO:0016760", "GO:0042802", "GO:0046872", "GO:0006970", "GO:0009414", "GO:0009825", "GO:0009833", "GO:0009834", "GO:0010192", "GO:0010214", "GO:0010400", "GO:0030244", "GO:0042742", "GO:0043622", "GO:0050832", "GO:0005886", "GO:0043621"
OG0000114	XAT2	"GO:0000139", "GO:0035252", "GO:0047517", "GO:0052636", "GO:0009664", "GO:0048354", "GO:0006486", "GO:0006493", "GO:0010192"
OG0000135	OG0000135 Expansin-A1	"GO:0005576", "GO:0016020", "GO:0006949", "GO:0009635", "GO:0009739", "GO:0009826", "GO:0009828", "GO:0010114", "GO:0010311", "GO:0009664", "GO:0080022"
OG0000181	repressor OFP8	"GO:0005634", "GO:0005515", "GO:0045892", "GO:0005737", "GO:1900457", "GO:0051510", "GO:0009553", "GO:0043622", "GO:0005730", "GO:2000652", "GO:0005856", "GO:0030863"
OG0000202	metal-associated isoprenylated plant protein 36	"GO:0005634", "GO:0005737", "GO:0016020", "GO:0071944", "GO:0005515", "GO:0046870", "GO:0009908", "GO:0010015", "GO:0010233", "GO:0046872", "GO:0055073", "GO:0019904", "GO:0006878", "GO:0055078", "GO:0006811", "GO:0006950", "GO:0043231", "GO:0071585", "GO:0005622", "GO:0012505"
OG0000237	H4	"GO:0000228", "GO:0005576", "GO:0005654", "GO:0000987", "GO:0019904", "GO:0031490", "GO:0046982", "GO:0006334", "GO:0006335", "GO:0006352", "GO:0009414", "GO:0000786", "GO:0003677", "GO:0030527"
OG0000252	protein knotted-1-like 10	"GO:0005634", "GO:0005768", "GO:0005886", "GO:0009506", "GO:0015630", "GO:0000978", "GO:0000981", "GO:0003723", "GO:0042803", "GO:0001708", "GO:0006357", "GO:0009691", "GO:0009736", "GO:0009901", "GO:0009934", "GO:0010051", "GO:0010089", "GO:0010094", "GO:0010497", "GO:0010582", "GO:0010930", "GO:0019827", "GO:0045892", "GO:0000976", "GO:0048440"
OG0000271	xyloglucan glycosyltransferase 5	"GO:0000139", "GO:0042803", "GO:0047259", "GO:0051753", "GO:0009294", "GO:0009617", "GO:0009793", "GO:0009860", "GO:0048359", "GO:0071555", "GO:0099402", "GO:0048868"
OG0000275	domain-containing protein Os02g0683500	"GO:1901371", "GO:0010073", "GO:0000976", "GO:0080113", "GO:0009873", "GO:0009741", "GO:0009910", "GO:0048527", "GO:0048573", "GO:0005634", "GO:0003700", "GO:0005515", "GO:0045892", "GO:0019760", "GO:0010358", "GO:2000241", "GO:0009725", "GO:0003677", "GO:0009791", "GO:0048367", "GO:0050793", "GO:0099402"
OG0000307	Zinc finger 1	"GO:0000932", "GO:0005634", "GO:0005829", "GO:0019900", "GO:0019902", "GO:0002213", "GO:0009625", "GO:0009737", "GO:0009744", "GO:0009749", "GO:0042594", "GO:0090351", "GO:1902074", "GO:0010494", "GO:0010162", "GO:0071368", "GO:0046872", "GO:1905582"
OG0000310	repeat receptor-like kinase protein FLORAL ORGAN NUMBER1	"GO:0000325", "GO:0005789", "GO:0005886", "GO:0009506", "GO:0090406", "GO:0000166", "GO:0001653", "GO:0004674", "GO:0033612", "GO:0042277", "GO:0042802", "GO:0043621", "GO:0009755", "GO:0009838", "GO:0009934", "GO:0010067", "GO:0010078", "GO:0010080", "GO:0010088", "GO:0010089", "GO:0010183", "GO:0010223", "GO:0036289", "GO:0045595", "GO:0048229", "GO:0048437", "GO:0048833", "GO:0051301", "GO:0010102", "GO:0010227", "GO:0010468", "GO:0045490", "GO:0050829", "GO:0060866", "GO:0010082", "GO:0005524", "GO:0004712", "GO:0006979", "GO:0009845", "GO:0045087", "GO:2000280", "GO:1901141", "GO:0080113", "GO:0048831",

		"GO:0017046", "GO:0051428", "GO:0010311", "GO:2000652", "GO:1902025", "GO:1901333", "GO:0031540", "GO:0090548"
OG0000311	factor TCP2	"GO:0005634", "GO:0009507", "GO:0001216", "GO:0005515", "GO:1990837", "GO:0006355", "GO:0008285", "GO:0009408", "GO:0009733", "GO:0009908", "GO:0010150", "GO:0031347", "GO:0048826", "GO:1903508", "GO:2000032", "GO:0000976", "GO:0009637", "GO:2000306", "GO:0009799", "GO:0048831", "GO:0045893", "GO:0045944"
OG0000317	GLUTAMINE DUMPER 3	"GO:0005515", "GO:0006521", "GO:0009615", "GO:0010585", "GO:0019048", "GO:0016020", "GO:0080143"
OG0000318	alpha-3 chain	"GO:0005737", "GO:0005874", "GO:0003924", "GO:0005200", "GO:0005525", "GO:0000226", "GO:0000278", "GO:0045298", "GO:0005515", "GO:0071258", "GO:0005634", "GO:0005819", "GO:0016787", "GO:0046872"
OG0000347	auxin efflux carrier component 1c	"GO:0016328", "GO:0009555", "GO:0009925", "GO:0009749", "GO:0001666", "GO:0045177", "GO:0009908", "GO:0010358", "GO:0010338", "GO:0010315", "GO:0080162", "GO:0010252", "GO:0009640", "GO:1901332", "GO:0010051", "GO:0048767", "GO:0005783", "GO:0048766", "GO:0009505", "GO:0048826", "GO:0000323", "GO:0009986", "GO:0009958", "GO:0005515", "GO:0048830", "GO:0010329", "GO:0010229", "GO:0010105", "GO:0010540", "GO:0009416", "GO:0009942", "GO:0012506"
OG0000348	serine/threonine-protein kinase At1g01540	"GO:0005777", "GO:0005886", "GO:0004674", "GO:0004712", "GO:0005524", "GO:0019901", "GO:0006468", "GO:0006950", "GO:0009738", "GO:0009845", "GO:0019722", "GO:0048364", "GO:1905393", "GO:0000166", "GO:0004672", "GO:0009611", "GO:1900150", "GO:0080141", "GO:0080142", "GO:0046777", "GO:0002221", "GO:1900459", "GO:1900426", "GO:0005634", "GO:0002237", "GO:0005768", "GO:0010119", "GO:0045088", "GO:0071323", "GO:0033612", "GO:0009742", "GO:0009793", "GO:0010227", "GO:0016020", "GO:0032502", "GO:0016310", "GO:0000976", "GO:1902458", "GO:0042742", "GO:0005737", "GO:0043231", "GO:0042802", "GO:0090351"
OG0000351	factor LATE FLOWERING	"GO:0005634", "GO:0000978", "GO:0000981", "GO:0003697", "GO:0003725", "GO:0005524", "GO:0030983", "GO:0033699", "GO:0046872", "GO:0046983", "GO:0047627", "GO:1990165", "GO:0000012", "GO:0006260", "GO:0006302", "GO:0006357", "GO:0006790", "GO:0009150", "GO:0009266", "GO:0009733", "GO:0010197", "GO:0010500", "GO:0045893", "GO:0048235", "GO:0048462", "GO:0048586", "GO:0048587", "GO:0048766", "GO:0048767", "GO:0080126", "GO:0090305", "GO:2000012", "GO:2000032", "GO:0000166", "GO:0042335", "GO:0009637", "GO:0009911", "GO:0045824", "GO:0010187", "GO:0009704", "GO:0010218", "GO:0009567", "GO:0009959", "GO:0006970", "GO:0009737", "GO:0031347", "GO:1902074", "GO:2000031", "GO:0005840", "GO:1990904", "GO:0003729", "GO:0003735", "GO:0006412"
OG0000355	transcription factor GT-2	"GO:0042803", "GO:0010192", "GO:0008361", "GO:0000976", "GO:0046621", "GO:0010090", "GO:0042631", "GO:0005634", "GO:0003700", "GO:0045892", "GO:0009909", "GO:0030308", "GO:0048498", "GO:0019760", "GO:0004518", "GO:0048442", "GO:0032876", "GO:0019900", "GO:2000038", "GO:2000037", "GO:0090428", "GO:0042802", "GO:0000987", "GO:0048441", "GO:0005516", "GO:0045893", "GO:0005515", "GO:0048438", "GO:0048437", "GO:0048827", "GO:0006355", "GO:0009414", "GO:0009653", "GO:0010605", "GO:0045926", "GO:0045934", "GO:0048580", "GO:0048523"
OG0000376	motif-containing protein 4	"GO:0005515", "GO:0043433", "GO:0051245"
OG0000381	factor bHLH130	"GO:0000978", "GO:0048767", "GO:0046983", "GO:0009637", "GO:0009911", "GO:0042335", "GO:0045824", "GO:0042127", "GO:0000981", "GO:0006357", "GO:0005634", "GO:0009739", "GO:0048235", "GO:2000488", "GO:0010119", "GO:0048573", "GO:1903286", "GO:0043562", "GO:1902456", "GO:0043621", "GO:0009414", "GO:0009409", "GO:0009408", "GO:0071215", "GO:0010378", "GO:0042803", "GO:2000031", "GO:0006970", "GO:0005737", "GO:0006808", "GO:0071368", "GO:2000028",

		"GO:0080147", "GO:0003700", "GO:0045893", "GO:0016036", "GO:0010372", "GO:0000987", "GO:0051511", "GO:2000024", "GO:0006355", "GO:1902074", "GO:0071396", "GO:0051510", "GO:0009737", "GO:0010187", "GO:0048440", "GO:0010114"
OG0000402	GTPase-activating protein 2	"GO:0005769", "GO:0005886", "GO:0005938", "GO:0009531", "GO:0015629", "GO:0030427", "GO:0032153", "GO:0055037", "GO:0005096", "GO:0031267", "GO:0007266", "GO:0009664", "GO:0016477", "GO:0034059", "GO:0043547", "GO:0007275", "GO:0009653", "GO:0048523", "GO:0005515", "GO:0044087", "GO:0050790", "GO:0030054", "GO:0031410", "GO:0042995", "GO:0043231", "GO:0033043", "GO:0005768", "GO:0048646", "GO:0080090", "GO:0007165"
OG0000431	PATTERNING FACTOR-like protein 1	GO:0010052
OG0000446	finger protein CONSTANS-LIKE 3	"GO:0010099", "GO:0042802", "GO:2000032", "GO:0010161", "GO:0000976", "GO:0048579", "GO:0007623", "GO:0009658", "GO:0005634", "GO:0010629", "GO:0003700", "GO:0045892", "GO:0009909", "GO:0048577", "GO:0010031", "GO:0048576", "GO:0046872", "GO:0009641", "GO:0005730", "GO:0045893", "GO:0006355", "GO:0009637", "GO:0010018", "GO:0005515", "GO:0009507", "GO:0003729", "GO:0009409", "GO:0009737", "GO:1901259"
OG0000452	esterase/lipase At5g33370	"GO:0005576", "GO:0005737", "GO:0043231", "GO:0005515", "GO:0016788", "GO:0009751", "GO:0010226", "GO:0016042", "GO:0042335", "GO:0042538", "GO:0005783", "GO:0009627", "GO:0016297"
OG0000455	transporter-like protein 2	"GO:0005768", "GO:0005794", "GO:0005886", "GO:0009986", "GO:0005515", "GO:0010011", "GO:0010328", "GO:0015171", "GO:0015293", "GO:0001736", "GO:0006865", "GO:0009734", "GO:0009926", "GO:0010311", "GO:0010588", "GO:0048829", "GO:0060919", "GO:0003333", "GO:0009958", "GO:0048765"
OG0000463	repressor OFP13	"GO:0005634", "GO:0005515", "GO:0045892", "GO:0005737", "GO:0005730", "GO:0005856", "GO:0043622", "GO:0051510", "GO:1900457", "GO:0030863", "GO:0009553", "GO:2000652", "GO:0046872"
OG0000493	020264663.1uncharacterized protein LOC109840429 isoform X2	NA
OG0000495	protein 6	"GO:0005576", "GO:0005737", "GO:0005886", "GO:0009505", "GO:0005515", "GO:0009651", "GO:0009737", "GO:0009740", "GO:0009744", "GO:0009749", "GO:0009750", "GO:0009751", "GO:0010286", "GO:0045454", "GO:2000377"
OG0000531	NSP-INTERACTING KINASE 1	"GO:0010262", "GO:1900150", "GO:0009556", "GO:0060548", "GO:0046777", "GO:0005654", "GO:0009729", "GO:0005524", "GO:0004712", "GO:0004714", "GO:0051607", "GO:0034504", "GO:0033612", "GO:0010152", "GO:0015026", "GO:0042803", "GO:0010150", "GO:1901653", "GO:0009742", "GO:0004674", "GO:0005886", "GO:0007639", "GO:0045089", "GO:0005737", "GO:0048653", "GO:0010227", "GO:0004713", "GO:0019199", "GO:0000166", "GO:0008219", "GO:0004675", "GO:0010008", "GO:0008289", "GO:0007178", "GO:0030154", "GO:0090351"
OG0000550	synthase 6	"GO:0005789", "GO:0005515", "GO:0009922", "GO:0102756", "GO:0006970", "GO:0009416", "GO:0009611", "GO:0009826", "GO:0010025", "GO:0010345", "GO:0042761", "GO:0048868", "GO:0070417", "GO:0005783", "GO:0016020"
OG0000571	SOSEKI 5	"GO:0016324", "GO:0031234", "GO:0042803", "GO:0006970", "GO:0010229", "GO:0010600", "GO:0010928", "GO:0051258", "GO:0051302", "GO:0090708", "GO:1902074", "GO:2000024", "GO:0009925", "GO:2000067", "GO:0000118", "GO:0035098", "GO:0035102", "GO:0003682", "GO:0007049", "GO:0016020", "GO:0005515"
OG0000578	domain-containing protein NPY1	"GO:0009860", "GO:0010051", "GO:0005770", "GO:0009911", "GO:0042742", "GO:0005886", "GO:0048825", "GO:0009904", "GO:0009958", "GO:0005515", "GO:0010229", "GO:0045176", "GO:0009653", "GO:0010087", "GO:0080022", "GO:0010588",

		"GO:0010305", "GO:0007165", "GO:0009637", "GO:0010540", "GO:0016020", "GO:0006952", "GO:0071944"
OG0000583	phosphoribosyltransferase 2,,,,,	"GO:0005576", "GO:0005654", "GO:0005829", "GO:0009507", "GO:0012505", "GO:0031982", "GO:0003999", "GO:0005515", "GO:0015114", "GO:0016208", "GO:0006168", "GO:0009690", "GO:0032263", "GO:0032264", "GO:0035435", "GO:0044209"
OG0000607	receptor-like protein kinase At5g18500,,,,,	"GO:0005777", "GO:0005886", "GO:0004674", "GO:0004712", "GO:0005524", "GO:0019901", "GO:0002221", "GO:0031663", "GO:0042742", "GO:0045087", "GO:0046777", "GO:1905393", "GO:0009611", "GO:0000166", "GO:0004672", "GO:0006468", "GO:0006950", "GO:0015026", "GO:0033612", "GO:0007639", "GO:0009793", "GO:0010227", "GO:0048653", "GO:1900459", "GO:0016310"
OG0000621	SHI RELATED SEQUENCE 1,,,,,	"GO:0005634", "GO:0003700", "GO:0042803", "GO:0043565", "GO:0046982", "GO:0009299", "GO:0009555", "GO:0009640", "GO:0009733", "GO:0009739", "GO:0045893", "GO:0048364", "GO:0000976", "GO:0009938", "GO:0009755", "GO:0048653", "GO:0046872", "GO:0009734", "GO:0009851", "GO:0046983", "GO:0006355"
OG0000678	OG0000678 Cyclin-D3-2,,,,,	"GO:0005634", "GO:0005737", "GO:0005515", "GO:0007049", "GO:0010444", "GO:0048316", "GO:0005622", "GO:0010033", "GO:0010440", "GO:0044772", "GO:0009744", "GO:1901371", "GO:0009735", "GO:0009791"
OG0000731	IV inositol polyphosphate 5-phosphatase 7,,,,,	"GO:0007010", "GO:0008022", "GO:0046855", "GO:0046856", "GO:0044877", "GO:0005829", "GO:0052658", "GO:0048766", "GO:0005881", "GO:0009845", "GO:0032957", "GO:0005634", "GO:0048016", "GO:0048015", "GO:0052629", "GO:0010588", "GO:0010305", "GO:2000369", "GO:0010067", "GO:0006661", "GO:0004445", "GO:0009932", "GO:0071472", "GO:0004438", "GO:0004439", "GO:2000377", "GO:0031410", "GO:0043813", "GO:0043812", "GO:0034485", "GO:0048471", "GO:0009737", "GO:0048312", "GO:0012506", "GO:0015812", "GO:0005768", "GO:0022607", "GO:0005874", "GO:0005905", "GO:0019904", "GO:0007032", "GO:0005739", "GO:0098590", "GO:0012505", "GO:0006811", "GO:0061024", "GO:0071705", "GO:0071702", "GO:0016050", "GO:0051050", "GO:0005886", "GO:0005515", "GO:0046030", "GO:0009743", "GO:0071310", "GO:0090351", "GO:1901701", "GO:0007165"
OG0000735	H2A,,,,,	"GO:0000786", "GO:0005634", "GO:0005721", "GO:0003677", "GO:0003682", "GO:0046982", "GO:0000792", "GO:0030527", "GO:0070828"
OG0000738	2-alpha-L-fucosyltransferase,,,,,	"GO:0005794", "GO:0016020", "GO:0031127", "GO:0042803", "GO:0009651", "GO:0009969", "GO:0031985", "GO:0008107", "GO:0042546", "GO:0071555"
OG0000753	WVD2-like 3,,,,,	"GO:0010031", "GO:0007163", "GO:0010091", "GO:0043622", "GO:0008017", "GO:0051511", "GO:0009825", "GO:0001578", "GO:0009737", "GO:0071369", "GO:0072657", "GO:0055028", "GO:0010015", "GO:0009570", "GO:0009651", "GO:0004462", "GO:0051213", "GO:0009409", "GO:0006979", "GO:0005777", "GO:0019243", "GO:0016151"
OG0000807	oxidase-like protein SKU5,,,,,	"GO:0005576", "GO:0009505", "GO:0016491", "GO:0046872", "GO:0006950", "GO:0009932", "GO:0005886"
OG0000819	OG0000819 Cyclin-B1-1,,,,,	"GO:0000307", "GO:0005634", "GO:0005737", "GO:0005515", "GO:0016538", "GO:0000079", "GO:0001558", "GO:0010332", "GO:0044772", "GO:0051301"
OG0000841	3,,,,,	"GO:0005576", "GO:0009505", "GO:0005515", "GO:0008810", "GO:0007389", "GO:0009624", "GO:0009828", "GO:0010047", "GO:0030245", "GO:0042547", "GO:1990059", "GO:0009835"
OG0000850	protein ABP19a,,,,,	"GO:0005576", "GO:0009506", "GO:0031012", "GO:0046872", "GO:0010497", "GO:0050829", "GO:0050832", "GO:0005737", "GO:0004784", "GO:0030145", "GO:0042802", "GO:0050162", "GO:0019430", "GO:2000280", "GO:0009734"
OG0000868	protein SAUR76,,,,,	"GO:0005634", "GO:0005737", "GO:0019897", "GO:0005515", "GO:0009733", "GO:0009958", "GO:0030307", "GO:0060918", "GO:0090057", "GO:0009725", "GO:0005622", "GO:0009639"

OG0000893	PATTERNING FACTOR-like protein 6,,,,,	"GO:0005576", "GO:0010052", "GO:0016787"
OG0000900	zipper protein ATHB-13,,,,,	"GO:0042803", "GO:0009651", "GO:0080022", "GO:0000976", "GO:0009637", "GO:0048826", "GO:0000981", "GO:0009414", "GO:0009788", "GO:0009733", "GO:0006357", "GO:0009744", "GO:0048573", "GO:0005634", "GO:0009739", "GO:0045893", "GO:0030308", "GO:0048510", "GO:0017148", "GO:0010311", "GO:0009965", "GO:0009615"
OG0000905	synthase 12,,,,,	"GO:0005783", "GO:0016020", "GO:0005515", "GO:0009922", "GO:0006970", "GO:0009416", "GO:0009611", "GO:0009826", "GO:0010025", "GO:0010345", "GO:0042761", "GO:0048868", "GO:0070417", "GO:0016747", "GO:0006633", "GO:0009409", "GO:0048856"
OG0000935	S-transferase F10,,,,,	"GO:0000325", "GO:0016020", "GO:0004364", "GO:0043169", "GO:0043295", "GO:0006979", "GO:0009414", "GO:0009635", "GO:0051707", "GO:0071704", "GO:0098754", "GO:0005634", "GO:0009705", "GO:0016740", "GO:0046283", "GO:0050832", "GO:1900384", "GO:0009628", "GO:0009507", "GO:0032991", "GO:0042803", "GO:0002239", "GO:0009407", "GO:0009410", "GO:0000302", "GO:0010033", "GO:0005737", "GO:0043231", "GO:0006950", "GO:0009636"
OG0000951	OG0000951 Cyclin-D4-1,,,,,	"GO:0005634", "GO:0005737", "GO:0005515", "GO:0009744", "GO:0010444", "GO:0048316", "GO:0051726", "GO:0000307", "GO:0016538", "GO:0000079", "GO:0042023", "GO:0044772", "GO:1901371", "GO:0009735"
OG0000958	010926363.2uncharacterized protein LOC105048670,,,,,	GO:0005515
OG0000972	042018473.1uncharacterized protein LOC121766208,,,,,	NA
OG0000984	protein A,,,,,	"GO:0000785", "GO:0005730", "GO:0005829", "GO:0043565", "GO:0016043", "GO:0000786", "GO:0005634", "GO:0003690", "GO:0031492", "GO:0006334", "GO:0030261", "GO:0045910", "GO:2000014", "GO:0005737"
OG0000989	BIG GRAIN 1,,,,,	"GO:0016020", "GO:0009733", "GO:0060918", "GO:0010929", "GO:0080113", "GO:0009630", "GO:0005886"
OG0001010	inactive receptor kinase At1g48480,,,,,	"GO:0005886", "GO:0045177", "GO:0000166", "GO:0004672", "GO:0042802", "GO:0009610", "GO:0009834", "GO:0016310", "GO:2000605", "GO:0009856", "GO:0016020", "GO:0071944", "GO:0005737", "GO:0090404", "GO:0010183"
OG0001018	inactive receptor kinase At5g58300,,,,,	"GO:0016020", "GO:0004672", "GO:0042802", "GO:0009610", "GO:0009834", "GO:2000605", "GO:0000166", "GO:0016310", "GO:0005886", "GO:0045177", "GO:0080092", "GO:0005515", "GO:0071944"
OG0001025	KINESIN LIGHT CHAIN-RELATED 1,,,,,	"GO:0043231", "GO:0055028", "GO:0005515", "GO:0006810", "GO:0006996", "GO:0007018", "GO:0007368", "GO:0009860", "GO:0022607", "GO:0031347", "GO:0048598", "GO:0050793", "GO:0051640", "GO:0051649", "GO:0005634", "GO:0005871", "GO:0016020", "GO:0031982", "GO:0008092", "GO:0008104", "GO:0032991", "GO:0046907", "GO:0048731"
OG0001027	factor bHLH49,,,,,	"GO:0000978", "GO:0048767", "GO:0046983", "GO:0048446", "GO:0009637", "GO:0009911", "GO:0045824", "GO:1902448", "GO:0042127", "GO:0000981", "GO:0006357", "GO:0005634", "GO:0009739", "GO:0048235", "GO:2000488", "GO:0071368", "GO:1901701", "GO:0009755", "GO:0071396", "GO:0009742", "GO:0080147", "GO:0009740", "GO:0040008", "GO:0000976", "GO:0006355", "GO:0003700", "GO:2000762", "GO:0010372", "GO:0051511", "GO:0045893", "GO:2000024", "GO:0016036"
OG0001036	EXORDIUM-like 3,,,,,	"GO:0005615", "GO:0048046", "GO:0001666", "GO:0005576"
OG0001046	008798667.2uncharacterized protein LOC103713491,,,,,	"GO:0016020", "GO:0004489", "GO:0044238", "GO:0071704", "GO:0044281"
OG0001051	010924057.1uncharacterized protein LOC105046995,,,,,	GO:0016020
OG0001059	029119795.1uncharacterized protein LOC105043044 isoform X2,,,,,	"GO:0000118", "GO:0003712", "GO:0006355"

OG0001088	of constitutive active ROPs 2, chloroplastic,,,,	"GO:0016020", "GO:0005634", "GO:0005875", "GO:0005886", "GO:0090404", "GO:0016043", "GO:0005856", "GO:0043231", "GO:0043229", "GO:0005874", "GO:0005515", "GO:0043622", "GO:0005737"
OG0001096	metal-associated isoprenylated plant protein 7,,,,,	"GO:0005730", "GO:0016020", "GO:0005515", "GO:0008270", "GO:0046870", "GO:0009910", "GO:0006950", "GO:0046916", "GO:0005737", "GO:0055078", "GO:0010233", "GO:0005634", "GO:0019904", "GO:0046914", "GO:0071585"
OG0001102	factor TCP4,,,,,	"GO:0005634", "GO:0009507", "GO:0001216", "GO:0005515", "GO:1990837", "GO:0006355", "GO:0008285", "GO:0009408", "GO:0009637", "GO:0009733", "GO:0009908", "GO:0010150", "GO:0031347", "GO:0048826", "GO:1903508", "GO:2000032", "GO:0003700", "GO:0043565", "GO:0009965", "GO:0048825", "GO:2000306", "GO:0045944", "GO:0003677"
OG0001106	010918212.1uncharacterized protein LOC105042627,,,,,	GO:0016020
OG0001119	P450 86A1,,,,,	"GO:0005789", "GO:0005506", "GO:0005515", "GO:0016709", "GO:0018685", "GO:0020037", "GO:0052694", "GO:0102033", "GO:0002213", "GO:0009611", "GO:0009694", "GO:0010214", "GO:0010345", "GO:0010584", "GO:0035336", "GO:0042761", "GO:0048480", "GO:0048653", "GO:0070330", "GO:0080110", "GO:0006694", "GO:0006952", "GO:0048437", "GO:0048438", "GO:0016020"
OG0001170	008790043.1uncharacterized protein LOC103707369,,,,,	GO:0016740
OG0001185	protein 70-2,,,,,	"GO:0005819", "GO:0009524", "GO:0010005", "GO:0008017", "GO:0007010", "GO:0009832", "GO:0010051", "GO:0071555"
OG0001246	029121699.1uncharacterized protein LOC105049460,,,,,	NA
OG0001305	protein MYBAS2,,,,,	"GO:1902074", "GO:1901002", "GO:0043266", "GO:0000976", "GO:0009411", "GO:0009409", "GO:0003700", "GO:0008219", "GO:0045892", "GO:0009909", "GO:1990841", "GO:0045893", "GO:0009809", "GO:0010119", "GO:0010214", "GO:0016036", "GO:0010015", "GO:0010597", "GO:2000652", "GO:0055062", "GO:0010373", "GO:0080086", "GO:0080187", "GO:1902584", "GO:0009620", "GO:0009740", "GO:0006952", "GO:0007623", "GO:0009505", "GO:0009867", "GO:0009646", "GO:0005634", "GO:0005515", "GO:0009737", "GO:0019632", "GO:0120195", "GO:0010089", "GO:0035865", "GO:1903086", "GO:0045723", "GO:0010017", "GO:0000987", "GO:0010090", "GO:0048354", "GO:0010224", "GO:0010345", "GO:0009555", "GO:0009423", "GO:1903338", "GO:0048653", "GO:0050826", "GO:0043068", "GO:1901348", "GO:0050832", "GO:1901371", "GO:0009789", "GO:1990019", "GO:0080092", "GO:0090406", "GO:2000762", "GO:0009585", "GO:0048765", "GO:0045165", "GO:0010026"
OG0001332	receptor-like serine/threonine-protein kinase RGI3,,,,,	"GO:0009790", "GO:2000280", "GO:0042802", "GO:0010087", "GO:0010082", "GO:0009266", "GO:0009791", "GO:0048229", "GO:0048646", "GO:0004672", "GO:0042277", "GO:0005783", "GO:0009725", "GO:0006952", "GO:0006468", "GO:0005886", "GO:0000166", "GO:0001653", "GO:0045595", "GO:0048367", "GO:0010078", "GO:0080092", "GO:0048878", "GO:0046777", "GO:0010088", "GO:0048437", "GO:0048833", "GO:0010080", "GO:0009934", "GO:0043621", "GO:0005789", "GO:0018193", "GO:0033612", "GO:0006810", "GO:0006950", "GO:2000023", "GO:1905393", "GO:0010183", "GO:0051301", "GO:0003002", "GO:0010089", "GO:0010067", "GO:0010223", "GO:0090406", "GO:1901141", "GO:0060866", "GO:0080113", "GO:0048831", "GO:0017046", "GO:0051428", "GO:0010311", "GO:2000652", "GO:0050829", "GO:1902025", "GO:1901333", "GO:0010468", "GO:0031540", "GO:0090548", "GO:0009506", "GO:0036289", "GO:0004674"
OG0001357	domain and ankyrin repeat-containing protein NPR5,,,,,	"GO:0005634", "GO:0005737", "GO:0000976", "GO:0005515", "GO:0009628", "GO:0009864", "GO:0009944", "GO:0009954", "GO:0009965", "GO:0010227", "GO:0010254", "GO:0010434", "GO:0010582", "GO:0010646", "GO:0010865", "GO:0016567", "GO:0023051", "GO:0005829", "GO:0032991", "GO:0009620",

		"GO:0048439", "GO:0009627", "GO:0009966", "GO:1902074", "GO:0006355", "GO:0071407"
OG0001377	repeat-containing thioredoxin TTL1,,,,,	"GO:0009651", "GO:0032780", "GO:0009742", "GO:0006457", "GO:0005886", "GO:0009789", "GO:0009734", "GO:0000003", "GO:0005634", "GO:0004721", "GO:0009408", "GO:0042030", "GO:0005829", "GO:0010305", "GO:0051879", "GO:0101031", "GO:0030544", "GO:0042802", "GO:0006996", "GO:0031982", "GO:0012505", "GO:0033365", "GO:0016787", "GO:0031072", "GO:0061077", "GO:0006626", "GO:0097255", "GO:0031410", "GO:0031347", "GO:0071816", "GO:0043621", "GO:0050821", "GO:1903070", "GO:0005515", "GO:0048731", "GO:0043231", "GO:0051131", "GO:0033554", "GO:0070678", "GO:0009266", "GO:0009611", "GO:0006986", "GO:0034605", "GO:0070417"
OG0001392	serine/threonine-protein kinase PBL8,,,,,	"GO:1901141", "GO:0080141", "GO:0080142", "GO:1902458", "GO:0046777", "GO:0009620", "GO:0004674", "GO:0002221", "GO:0005886", "GO:1900426", "GO:0005634", "GO:0005524", "GO:0004713", "GO:0005768", "GO:0004712", "GO:0030957", "GO:0031663", "GO:0050777"
OG0001486	008793736.2uncharacterized protein LOC103709963,,,,,	NA
OG0001501	ubiquitin-protein ligase ATL42,,,,,	"GO:0005739", "GO:0016020", "GO:0004842", "GO:0046872", "GO:0010200", "GO:0016567", "GO:0050832", "GO:0009416", "GO:0033591", "GO:0098542", "GO:0009617", "GO:0002238", "GO:0031625", "GO:0009793", "GO:0043068", "GO:0005886", "GO:0051865", "GO:0061630", "GO:0009628", "GO:0031667", "GO:0042742"
OG0001502	domain-containing protein 12,,,,,	"GO:0005773", "GO:0009505", "GO:0009827", "GO:0010154", "GO:0007275", "GO:0005576", "GO:0005737", "GO:0043231", "GO:0021700", "GO:0042547", "GO:0009835"
OG0001510	CHUP1, chloroplastic,,,,	"GO:0009707", "GO:0009902"
OG0001547	ribosomal protein S13,,,,,	"GO:0005730", "GO:0022627", "GO:0003735", "GO:0048027", "GO:0070181", "GO:0000462", "GO:0006412"
OG0001572	039142605.1uncharacterized protein LOC120279982,,,,,	"GO:0016020", "GO:0005576", "GO:0070012"
OG0001577	NSP-INTERACTING KINASE 2,,,,,	"GO:0016020", "GO:0004672", "GO:0005515", "GO:0038023", "GO:0006468", "GO:0006950", "GO:0007154", "GO:0009653", "GO:0009725", "GO:0009791", "GO:0030154", "GO:0042592", "GO:0048827", "GO:0050793", "GO:0005622", "GO:0019199", "GO:0007165", "GO:0009888", "GO:0010016", "GO:0040008", "GO:0071310", "GO:0090567", "GO:0090698", "GO:0098542", "GO:1905392", "GO:0003006", "GO:0048869", "GO:0051179", "GO:0032502", "GO:0004674", "GO:0031347", "GO:0005102", "GO:0005886", "GO:0015026", "GO:0033612", "GO:0042802", "GO:0002237", "GO:0007639", "GO:0009625", "GO:0048653", "GO:0050826", "GO:0009555", "GO:0009741", "GO:0010227", "GO:0016301", "GO:0016310", "GO:0008219", "GO:0009742", "GO:0010150", "GO:0090351", "GO:0006952", "GO:0014070", "GO:0042803", "GO:0048437"
OG0001598	GPI-anchored protein At4g28100,,,,,	GO:0016020
OG0001631	protein,,,,,	"GO:0005802", "GO:0005515", "GO:0006892", "GO:0009734", "GO:0010087", "GO:0010305"
OG0001643	WALLS ARE THIN 1,,,,,	"GO:0090358", "GO:0090355", "GO:0015186", "GO:0080144", "GO:0048316", "GO:0009851", "GO:0006952", "GO:0009834", "GO:0034639", "GO:0009705", "GO:0009826", "GO:0005515", "GO:0000162", "GO:0098712", "GO:0005938", "GO:0010315", "GO:0071555", "GO:0032973", "GO:0043090", "GO:0005737", "GO:0005886", "GO:0009073", "GO:0008652", "GO:0006520", "GO:0046394"
OG0001657	finger protein GIS,,,,,	"GO:0005634", "GO:0000976", "GO:0003700", "GO:0046872", "GO:0046982", "GO:0006355", "GO:0009640", "GO:0009736", "GO:0009740", "GO:0009788", "GO:0009910", "GO:0010090", "GO:0010582", "GO:0019760", "GO:0042752", "GO:0048579", "GO:0060862", "GO:0005515", "GO:0009909", "GO:0010008", "GO:0019866", "GO:0008236", "GO:0008474", "GO:0006508",

		"GO:0009739", "GO:0032880", "GO:0048364", "GO:0098734", "GO:0048510", "GO:0048766", "GO:0048767", "GO:0009873"
OG0001659	029118542.1uncharacterized protein LOC105038912 isoform X1,,,,,	GO:0005643
OG0001664	010934792.1uncharacterized protein LOC105054863,,,,,	"GO:0005576", "GO:0070012"
OG0001667	molecular patterns-induced protein A70,,,,,	"GO:0009611", "GO:0009753", "GO:0042742", "GO:0006950", "GO:0009617"
OG0001677	domain-containing protein 75,,,,,	"GO:0071472", "GO:0061630", "GO:0005515", "GO:0005737", "GO:1901001", "GO:0006952", "GO:1900457", "GO:0005886", "GO:0016567", "GO:0098542", "GO:0031648", "GO:2000022", "GO:0043621", "GO:0051865", "GO:0090333", "GO:0070696"
OG0001679	xyloglucan endotransglucosylase/hydrolase protein 32,,,,,	"GO:0005886", "GO:0048046", "GO:0016762", "GO:0030247", "GO:0033946", "GO:0006950", "GO:0009266", "GO:0009664", "GO:0009725", "GO:0010087", "GO:0010154", "GO:0010411", "GO:0016998", "GO:0030243", "GO:0042546", "GO:0048573", "GO:0080086", "GO:0009416", "GO:0009827", "GO:0010033", "GO:0016049", "GO:0009645", "GO:0009826", "GO:0009831", "GO:0009834", "GO:0051301", "GO:0071365", "GO:0010218", "GO:0016020", "GO:0071555", "GO:0071669", "GO:0071944"
OG0001685	RING-H2 finger protein ATL69,,,,,	"GO:0009507", "GO:0016020", "GO:0031982", "GO:0004842", "GO:0009416", "GO:0009737", "GO:0016567", "GO:0033591", "GO:0042742", "GO:0043562", "GO:0061630", "GO:0010200", "GO:0050832", "GO:0005739", "GO:0016740", "GO:0046872", "GO:0006950", "GO:0009617", "GO:0002238", "GO:0005515", "GO:0043068", "GO:0005886", "GO:0051865", "GO:0009909", "GO:0010966", "GO:0070417", "GO:0043227", "GO:0006513"
OG0001686	LRR receptor-like serine/threonine-protein kinase IRK,,,,,	"GO:0005886", "GO:0000166", "GO:0004672", "GO:0005515", "GO:0038023", "GO:0006468", "GO:0006810", "GO:0009628", "GO:0010015", "GO:0010016", "GO:0010073", "GO:0040008", "GO:0050793", "GO:0051302", "GO:0090567", "GO:0090698", "GO:0098542", "GO:0004674", "GO:0005102", "GO:0019199", "GO:0042277", "GO:0009755", "GO:0010051", "GO:0010102", "GO:0048229", "GO:0048437", "GO:0048638", "GO:0065001", "GO:1905421", "GO:2000023", "GO:0003002", "GO:0006833", "GO:0009790", "GO:0009888", "GO:0010286", "GO:0030154", "GO:0042742", "GO:0048646", "GO:0048827", "GO:0048878", "GO:0071555", "GO:0043231", "GO:0005524", "GO:0019901", "GO:0033612", "GO:0042803", "GO:0008219", "GO:0009729", "GO:0009742", "GO:0010150", "GO:0010227", "GO:0010262", "GO:0045089", "GO:1900140", "GO:1900150", "GO:0001653", "GO:0004383", "GO:0042802", "GO:0005976", "GO:0009266", "GO:0009838", "GO:0010074", "GO:0010082", "GO:0031347", "GO:0045087", "GO:0080092", "GO:1901141", "GO:0080113", "GO:0046777", "GO:0048831", "GO:0006979", "GO:0017046", "GO:0051428", "GO:0010078", "GO:0010311", "GO:2000652", "GO:1902025", "GO:1901333", "GO:0009845", "GO:0031540", "GO:0090548", "GO:0015026", "GO:0016310", "GO:0090351", "GO:0005737"
OG0001734	protein 2,,,,,	"GO:0045814", "GO:0042802", "GO:0016607", "GO:0061087", "GO:0035064", "GO:1900111", "GO:0005677", "GO:0032922", "GO:0001666", "GO:0048587", "GO:0031519", "GO:0051571", "GO:0070417", "GO:0005515", "GO:0009409", "GO:0010228", "GO:0031062", "GO:0040029", "GO:0010048", "GO:0048572", "GO:0009791", "GO:0010468"
OG0001760	008775845.1uncharacterized protein LOC103696095,,,,,	NA
OG0001770	protein kinase HSL1,,,,,	"GO:0000325", "GO:0005789", "GO:0005886", "GO:0009506", "GO:0090406", "GO:0000166", "GO:0001653", "GO:0004674", "GO:0017046", "GO:0033612", "GO:0042802", "GO:0043621", "GO:0051428", "GO:0006970", "GO:0006979", "GO:0009845", "GO:0009934", "GO:0009960", "GO:0010051", "GO:0010075", "GO:0010078", "GO:0010088", "GO:0010183", "GO:0010227", "GO:0010311", "GO:0010468", "GO:0010555", "GO:0031540", "GO:0036289", "GO:0045087", "GO:0045490", "GO:0045595",

		"GO:0048229", "GO:0048831", "GO:0050829", "GO:0060866", "GO:0080113", "GO:0090548", "GO:1901141", "GO:1901333", "GO:1902025", "GO:2000652", "GO:0010067", "GO:0010089", "GO:0010223", "GO:0051301", "GO:0004672", "GO:0018193", "GO:0046777", "GO:0010074", "GO:0010082", "GO:0048833", "GO:0010080", "GO:0004713", "GO:2000280", "GO:0042277", "GO:0005524", "GO:0010102"
OG0001823	arabinogalactan protein 2,,,,,	"GO:0048364", "GO:0048367", "GO:0016020"
OG0001880	protease AED3,,,,,	"GO:0009627", "GO:0005737", "GO:0043231", "GO:0016020", "GO:0043067", "GO:0008233", "GO:0044238", "GO:0071704", "GO:0005789", "GO:0004175", "GO:0070001", "GO:0010033", "GO:0005576", "GO:0004190", "GO:0006508"
OG0001902	leucine zipper 2,,,,,	"GO:0005654", "GO:0005829", "GO:0048471", "GO:0000976", "GO:0003700", "GO:0031490", "GO:0042803", "GO:0043621", "GO:0051019", "GO:0007231", "GO:0008272", "GO:0009294", "GO:0009555", "GO:0009652", "GO:0009970", "GO:0010628", "GO:0010629", "GO:0045596", "GO:0045893", "GO:0051170", "GO:0090567", "GO:0005515", "GO:0006355"
OG0001942	ribosomal protein L17-1,,,,,	"GO:0005634", "GO:0005844", "GO:0022625", "GO:0003735", "GO:0005515", "GO:0070180", "GO:0002181", "GO:0034198", "GO:0042788", "GO:0003729"
OG0001950	ubiquitin-protein ligase XB3,,,,,	"GO:0005634", "GO:0005737", "GO:0012505", "GO:0004842", "GO:0005515", "GO:0016279", "GO:0046872", "GO:0007275", "GO:0009408", "GO:0010033", "GO:0018022", "GO:0019222", "GO:0042742", "GO:0051865", "GO:0043231", "GO:0098590", "GO:0007165", "GO:0042391", "GO:0048522", "GO:0061024", "GO:0072659", "GO:0005886", "GO:0006810"
OG0001977	010943541.1uncharacterized protein LOC105061252,,,,,	"GO:0004553", "GO:0071704"
OG0002006	indeterminate-domain 14,,,,,	"GO:0009590", "GO:0000976", "GO:0002221", "GO:0045604", "GO:0043621", "GO:0009536", "GO:0048364", "GO:0051302", "GO:0003700", "GO:0045893", "GO:0048444", "GO:0010336", "GO:2000012", "GO:0010431", "GO:0034504", "GO:0019900", "GO:0010031", "GO:0010075", "GO:0042803", "GO:0010150", "GO:0008356", "GO:0009965", "GO:0005634", "GO:0009959", "GO:2000904", "GO:0048510", "GO:0048575", "GO:0048574", "GO:0009939", "GO:2000122", "GO:0010029", "GO:0046872", "GO:0010601"
OG0002020	pectinesterase/pectinesterase inhibitor 51,,,,,	"GO:0005576", "GO:0016020", "GO:0030599", "GO:0046910", "GO:0009409", "GO:0009741", "GO:0042545", "GO:0043086", "GO:0045490", "GO:0048358", "GO:0048359", "GO:0050829", "GO:0050832", "GO:0052542", "GO:1902066", "GO:0004857", "GO:0016788", "GO:0005737", "GO:0009617", "GO:1990110", "GO:0090406", "GO:0003729", "GO:0009624", "GO:0045488", "GO:0071555", "GO:0009620", "GO:0005515", "GO:0010043", "GO:0010187", "GO:0010468", "GO:0051510", "GO:0080147"
OG0002035	stress transcription factor B-4,,,,,	"GO:0005634", "GO:0005737", "GO:0000978", "GO:0003700", "GO:0042802", "GO:0006357", "GO:0008356", "GO:0034605", "GO:0009408", "GO:0033554", "GO:0045892", "GO:0005515"
OG0002047	038989672.1uncharacterized protein LOC120113062,,,,,	character(0
OG0002054	3-beta-dioxygenase 1,,,,,	"GO:0005737", "GO:0005515", "GO:0016707", "GO:0009686", "GO:0009740", "GO:0010114", "GO:0048367", "GO:0031347", "GO:0044550", "GO:0009639", "GO:0009739", "GO:0002238", "GO:0009805"
OG0002067	ribosomal protein L26-1,,,,,	"GO:0005654", "GO:0005730", "GO:0022625", "GO:0042788", "GO:0003735", "GO:0005515", "GO:0048027", "GO:0002181", "GO:0006364", "GO:0042273", "GO:0045727", "GO:0071480", "GO:0003723", "GO:0015934", "GO:0003729", "GO:0006412"
OG0002130	010910969.2LOW QUALITY PROTEIN: uncharacterized protein LOC105036948,,,,,	GO:0016787
OG0002165	010930495.1uncharacterized protein LOC105051663,,,,,	GO:0016020

OG0002181	protein At4g14100,,,,,	NA
OG0002186	polygalacturonase,,,,,	"GO:0016798", "GO:0048609", "GO:0003006", "GO:0007275", "GO:0042803", "GO:0009651", "GO:0080163", "GO:0038023", "GO:1902584", "GO:0022414", "GO:0044389", "GO:0006952", "GO:0009845", "GO:0009867", "GO:0005886", "GO:0009789", "GO:0009409", "GO:0004864", "GO:0010427", "GO:0005829", "GO:0016787", "GO:0004553"
OG0002187	039116327.1uncharacterized protein LOC120251750,,,,,	NA
OG0002199	arabinogalactan protein 17,,,,,	GO:0005576
OG0002205	030939381.1uncharacterized protein LOC115964170,,,,,	GO:0016020
OG0002233	010923183.1uncharacterized protein LOC105046322 isoform X2,,,,,	"GO:0005622", "GO:0050403", "GO:0050502", "GO:0080043", "GO:0080044"
OG0002247	OG0002247 Calreticulin,,,,,	"GO:0005794", "GO:0030866", "GO:0005788", "GO:0005506", "GO:0005509", "GO:0003729", "GO:0005829", "GO:0017148", "GO:0034504", "GO:0008270", "GO:0042981", "GO:0006611", "GO:0006457", "GO:0042742", "GO:0005764", "GO:0005635", "GO:0031625", "GO:0010628", "GO:0032355", "GO:0008284", "GO:0009897", "GO:0045787", "GO:0042277", "GO:0009410", "GO:0005844", "GO:0000122", "GO:0046283", "GO:0044183", "GO:0030246", "GO:0040020", "GO:0051082", "GO:0005615", "GO:0048471", "GO:0030433", "GO:0009626", "GO:0005789"
OG0002262	YABBY 4,,,,,	"GO:0010022", "GO:0010154", "GO:1902183", "GO:0010450", "GO:0010093", "GO:0000976", "GO:0048833", "GO:0006355", "GO:0009933", "GO:0009944", "GO:0005634", "GO:0003700", "GO:0005515", "GO:0009909", "GO:2000024", "GO:0090706", "GO:0048481", "GO:0010158", "GO:0048440"
OG0002266	transporter G family member 10,,,,,	"GO:0042910", "GO:0009893", "GO:0007275", "GO:0051707", "GO:0022607", "GO:0009897", "GO:0051050", "GO:1901701", "GO:0005773", "GO:0044281", "GO:0000166", "GO:0005768", "GO:0140359", "GO:0048522", "GO:0071396", "GO:0098754", "GO:0140115", "GO:0065008", "GO:0071705", "GO:0046907", "GO:0009725", "GO:0008514", "GO:0006725", "GO:0005634", "GO:0005515", "GO:0070013", "GO:0042908", "GO:0010888", "GO:0071407", "GO:0010243", "GO:0019218", "GO:0016324", "GO:0005775", "GO:0009531", "GO:0042802", "GO:0007034", "GO:0051239", "GO:0055065", "GO:0071470", "GO:0016020", "GO:0042626", "GO:0033993", "GO:0055080", "GO:0055085", "GO:0071704", "GO:0098771", "GO:0010345", "GO:1903825"
OG0002280	IQ-DOMAIN 19,,,,,	"GO:0070507", "GO:0055074", "GO:0090333", "GO:0009574", "GO:0016607", "GO:0005730", "GO:0005875", "GO:0009409", "GO:2001006", "GO:0019722", "GO:0055028", "GO:2000652", "GO:0010091", "GO:0042542", "GO:0005886", "GO:0009524", "GO:0007105", "GO:0005635", "GO:0005876", "GO:0005516", "GO:0051211", "GO:0009738", "GO:0071244", "GO:0051592", "GO:0072699", "GO:2000073", "GO:0010089", "GO:0005874", "GO:0016020", "GO:0005515", "GO:0008017"
OG0002285	inactive receptor kinase At4g23740,,,,,	"GO:0005886", "GO:0000166", "GO:0004672", "GO:0042802", "GO:0009610", "GO:0009834", "GO:0016310", "GO:2000605", "GO:0045177", "GO:0009856", "GO:0016020", "GO:0071944", "GO:0080092", "GO:0005737", "GO:0043231", "GO:0090406", "GO:0005524", "GO:0046777"
OG0002290	homeodomain protein 2,,,,,	"GO:0042659", "GO:0015630", "GO:0090575", "GO:0000978", "GO:0009610", "GO:0001228", "GO:0045944", "GO:0009954", "GO:0005654", "GO:0048363", "GO:0046982", "GO:0009908", "GO:0015629", "GO:0005829", "GO:0034504", "GO:0010074", "GO:0042803", "GO:0010197", "GO:0008134", "GO:0048523", "GO:0009965", "GO:0003785", "GO:0051015", "GO:0009737", "GO:0048510", "GO:1905393", "GO:0010077", "GO:0010076", "GO:0000785", "GO:0045931", "GO:0010229", "GO:0010228", "GO:0010223", "GO:0000122", "GO:0080006", "GO:0010154", "GO:0048457", "GO:0010051", "GO:0010089", "GO:0000981", "GO:0006357", "GO:0008285", "GO:0010201", "GO:0010227",

		"GO:0010371", "GO:0045892", "GO:0090470", "GO:0003677", "GO:0006355", "GO:0000976", "GO:0003700"
OG0002334	factor bHLH93,,,,,	"GO:0010371", "GO:0010162", "GO:0048317", "GO:0048658", "GO:0000987", "GO:0046983", "GO:0045487", "GO:0009960", "GO:0001046", "GO:0005634", "GO:0003700", "GO:0009738", "GO:0045892", "GO:0045893", "GO:0005737", "GO:0010115", "GO:0031542", "GO:0050826", "GO:2000022", "GO:0031347", "GO:0010444", "GO:0009611", "GO:0010629", "GO:0048657", "GO:0009753", "GO:0010039", "GO:0034756", "GO:0009409", "GO:0005515", "GO:0000976", "GO:0048316", "GO:0006355", "GO:0009888", "GO:0009651", "GO:0010026"
OG0002337	tolerance receptor-like cytoplasmic kinase 1,,,,,	"GO:0019901", "GO:1902074", "GO:1901000", "GO:0009793", "GO:0009611", "GO:0009631", "GO:0009960", "GO:0004674", "GO:0043621", "GO:0042742", "GO:0005886", "GO:0009414", "GO:0005516", "GO:0004713", "GO:0010008", "GO:0010310", "GO:1900459", "GO:0009845", "GO:0048364", "GO:0009738", "GO:0019722", "GO:0006468", "GO:0016020", "GO:0004672", "GO:0005515", "GO:0009409", "GO:0016310", "GO:0048316", "GO:0098542", "GO:0031410", "GO:0009791", "GO:0090698", "GO:0000166", "GO:0090392", "GO:0010311", "GO:0042803", "GO:0009786", "GO:0030139", "GO:0032877"
OG0002339	transporter 12,,,,,	"GO:0005737", "GO:0009925", "GO:0043229", "GO:0008514", "GO:0015081", "GO:0015145", "GO:0015210", "GO:0015293", "GO:0035344", "GO:0098655", "GO:0098721", "GO:0006812", "GO:0034220", "GO:0048731", "GO:0005886", "GO:0098702"
OG0002370	IQ-DOMAIN 32,,,,,	"GO:0005730", "GO:0005737", "GO:0005874", "GO:0005875", "GO:0005886", "GO:0005516", "GO:0009409", "GO:0009738", "GO:0010091", "GO:0019722", "GO:0042542", "GO:0051592", "GO:0055074", "GO:0071244", "GO:0005819", "GO:0009524", "GO:0009574", "GO:0016607", "GO:0007105", "GO:0015630", "GO:0090333", "GO:0005856"
OG0002382	038976083.1uncharacterized protein LOC120107009,,,,,	NA
OG0002386	lectin-domain containing receptor kinase VIII.1,,,,,	"GO:0005737", "GO:0005886", "GO:0000166", "GO:0004675", "GO:0005515", "GO:0002229", "GO:0006468", "GO:0007166", "GO:0009555", "GO:0022607", "GO:0042742", "GO:0048522", "GO:0071318", "GO:0007165", "GO:0004674", "GO:0002376", "GO:0009751", "GO:0031349", "GO:0004888"
OG0002414	ALTERED PHOSPHATE STARVATION RESPONSE 1,,,,,	"GO:0005634", "GO:0005515", "GO:0015706", "GO:0010167", "GO:0071705", "GO:0071249"
OG0002479	factor 6,,,,,	"GO:0048364", "GO:0005634", "GO:0009409", "GO:0009739", "GO:0005515", "GO:0045893", "GO:0048366", "GO:0008285", "GO:0000976", "GO:0061062", "GO:0048316", "GO:0009624", "GO:0010218", "GO:0005524", "GO:0010114"
OG0002506	008781987.1uncharacterized protein LOC103701627,,,,,	GO:0016020
OG0002541	damage-repair/toleration protein DRT100,,,,,	"GO:0009505", "GO:0009507", "GO:0012505", "GO:0016020", "GO:0031410", "GO:0000166", "GO:0004672", "GO:0005515", "GO:0006807", "GO:0006952", "GO:0006974", "GO:0009791", "GO:0044238", "GO:0048229", "GO:0050793", "GO:0099402", "GO:0006281"
OG0002573	008792216.1serine/threonine -protein phosphatase 6 regulatory ankyrin repeat subunit C-like,,,,,	"GO:0045595", "GO:0031410", "GO:0030100", "GO:0007165", "GO:0007267", "GO:0007389", "GO:0048646", "GO:0048468", "GO:0005886", "GO:0023051", "GO:0048598", "GO:0012505", "GO:0010646", "GO:0033365", "GO:0016740", "GO:0016567", "GO:0019899"
OG0002648	008776689.1uncharacterized protein LOC103696750,,,,,	character(0
OG0002716	NETWORKED 4B,,,,,	"GO:0005774", "GO:0005783", "GO:0005884", "GO:0005886", "GO:0009506", "GO:0031965", "GO:0051015"
OG0002736	protein S-acyltransferase 22,,,,,	"GO:0005768", "GO:0005783", "GO:0030659", "GO:0016409", "GO:0016417", "GO:0018345", "GO:0033036", "GO:0045087", "GO:0048522", "GO:0071702", "GO:0005794", "GO:0005886", "GO:0006950", "GO:0005515", "GO:0005737", "GO:0012505", "GO:0016020", "GO:0043231", "GO:0016747", "GO:0006807",

		"GO:0044238", "GO:0016746", "GO:0009574", "GO:0009793", "GO:0008284", "GO:0009615", "GO:0000398", "GO:0009414", "GO:1902806", "GO:0009409", "GO:0005524", "GO:0050792", "GO:0016310", "GO:0010235", "GO:1902290", "GO:2000031", "GO:0040020", "GO:0008356", "GO:0042023", "GO:0004674", "GO:1900426", "GO:0006357", "GO:0010005", "GO:0032991", "GO:0098725", "GO:0032953", "GO:0010584", "GO:0033206", "GO:0010444"
OG0002751	IQ-DOMAIN 18,,,,,	"GO:0070507", "GO:0016604", "GO:0009574", "GO:0007165", "GO:2000073", "GO:1901701", "GO:0005886", "GO:0006950", "GO:0009524", "GO:0005635", "GO:0005876", "GO:0005516", "GO:0051211", "GO:0009737", "GO:2001006", "GO:0072699", "GO:0055028", "GO:0010035", "GO:0010089", "GO:0010033", "GO:0016607", "GO:0010091", "GO:0007105", "GO:0005730", "GO:0005737", "GO:0005874", "GO:0009409", "GO:0009738", "GO:0009739", "GO:0019722", "GO:0042542", "GO:0051179", "GO:0051592", "GO:0055074", "GO:0071244", "GO:0090333", "GO:0005819", "GO:0005875"
OG0002782	diphosphate reductase, chloroplastic,,,,	"GO:0009941", "GO:0016020", "GO:0005515", "GO:0016628", "GO:0045550", "GO:0010189", "GO:0015995", "GO:0031969", "GO:0071949", "GO:0102067", "GO:0015979", "GO:0009838", "GO:0009900", "GO:0090693"
OG0002851	CELLULOSE SYNTHASE INTERACTIVE 1,,,,,	"GO:0016020", "GO:0005737", "GO:0043229", "GO:0005622"
OG0002870	reductase,,,,,	"GO:0005634", "GO:0005783", "GO:0005829", "GO:0005856", "GO:0005516", "GO:0019899", "GO:0050614", "GO:0071949", "GO:0006979", "GO:0007265", "GO:0008104", "GO:0008285", "GO:0009725", "GO:0009808", "GO:0009826", "GO:0009834", "GO:0009888", "GO:0016132", "GO:0061024", "GO:0005789", "GO:0016020", "GO:0051537", "GO:0051539", "GO:0016226"
OG0002907	transporter G family member 23,,,,,	"GO:1902074", "GO:0055075", "GO:1901002", "GO:0055078", "GO:0009753", "GO:0007034", "GO:0009751", "GO:1903825", "GO:0005775", "GO:0009733", "GO:0044281", "GO:0000166", "GO:0071472", "GO:0009408", "GO:0005768", "GO:0140359", "GO:0071456", "GO:0071705", "GO:2000032", "GO:0098590", "GO:0048226", "GO:0008514", "GO:0048869", "GO:0009739", "GO:0005515", "GO:0009737", "GO:0016043", "GO:0010345", "GO:0005773", "GO:0031410", "GO:0070013", "GO:0042802", "GO:0046983", "GO:0006725", "GO:0009628", "GO:0009725", "GO:0015918", "GO:0033554", "GO:0033993", "GO:0048878", "GO:0055085", "GO:0016020", "GO:0071944", "GO:0042626", "GO:0071704", "GO:0005886", "GO:0009531", "GO:0016787", "GO:0055080", "GO:0071470", "GO:0098771"
OG0002937	of constitutive active ROPs 4,,,,,	"GO:0005634", "GO:0005737", "GO:0005886", "GO:0090404", "GO:0005515", "GO:0009664", "GO:0043622", "GO:0043231"
OG0002945	kinase Nek2,,,,,	"GO:0035264", "GO:0043622", "GO:0006468", "GO:0000278", "GO:0005654", "GO:0005524", "GO:0004712", "GO:0045893", "GO:0005829", "GO:0030145", "GO:0055028", "GO:0010212", "GO:0010311", "GO:0004674", "GO:0009913", "GO:0030010", "GO:2000001", "GO:0010366", "GO:0005515", "GO:0000910", "GO:0002221", "GO:1900150", "GO:1900424", "GO:0009875", "GO:0009611", "GO:0042542", "GO:0009414", "GO:0002237", "GO:0004708"
OG0002957	cell nuclear antigen,,,,,	"GO:0000307", "GO:0000785", "GO:0005652", "GO:0016604", "GO:0043596", "GO:0043626", "GO:0000701", "GO:0003682", "GO:0003684", "GO:0008022", "GO:0030337", "GO:0042802", "GO:0070182", "GO:0000122", "GO:0006272", "GO:0006287", "GO:0006298", "GO:0031297", "GO:0032355", "GO:0034644", "GO:0042276", "GO:0045732", "GO:0045739", "GO:0045740", "GO:0046686", "GO:0051726", "GO:0070207", "GO:0070301", "GO:0071548", "GO:1902065", "GO:0009617", "GO:0005515", "GO:0050790"
OG0002974	IQ-DOMAIN 2,,,,,	"GO:0010033", "GO:0070507", "GO:0009574", "GO:0016607", "GO:0005730", "GO:0005886", "GO:0009524", "GO:0007105", "GO:0008017", "GO:0005635", "GO:0005876", "GO:0051211", "GO:0051592", "GO:2001006", "GO:0072699", "GO:0055028",

		"GO:0010089", "GO:2000073", "GO:0010091", "GO:0005516", "GO:0055074", "GO:0090333", "GO:0042542", "GO:0009409", "GO:0009738", "GO:0071244", "GO:0016020", "GO:0019722", "GO:0009739", "GO:0005515"
OG0003000	transcription factor-like E2FE,,,,,	"GO:0090575", "GO:0016607", "GO:0000978", "GO:0008284", "GO:0001228", "GO:0001227", "GO:0045944", "GO:0006367", "GO:0009733", "GO:0000122", "GO:2000134", "GO:0042802", "GO:0043433", "GO:0005737", "GO:0006606", "GO:0032876", "GO:0000977", "GO:0000987", "GO:0042981", "GO:0001217", "GO:0003682", "GO:0001216", "GO:0000981", "GO:0003677", "GO:0005515", "GO:0005667", "GO:0003700", "GO:0045893", "GO:0051446", "GO:0051302", "GO:0000902", "GO:0000976", "GO:0006355", "GO:0046983", "GO:0046982", "GO:0051782", "GO:0019760", "GO:0070176"
OG0003055	transporter 1,,,,,	"GO:0005739", "GO:0009705", "GO:0015098", "GO:0090414"
OG0003075	microtubule-associated protein 7,,,,,	"GO:0005739", "GO:0009524", "GO:0009574", "GO:0055028", "GO:1990023", "GO:0008017", "GO:0046983", "GO:0000280", "GO:0000911", "GO:0043622", "GO:0005634", "GO:0048528"
OG0003288	protein At5g65660,,,,,	GO:0016020
OG0003313	OG0003313 Patellin-6,,,,,	"GO:0005737", "GO:0012505", "GO:0016020", "GO:0043231", "GO:0002020", "GO:0008289", "GO:0007049", "GO:0009860", "GO:0051301", "GO:0071365", "GO:0071702", "GO:0071944", "GO:0010053", "GO:1901703", "GO:0048731"
OG0003351	domain-containing protein At3g50780,,,,,	NA
OG0003526	HOTHEAD,,,,,	"GO:0005576", "GO:0005737", "GO:0043231", "GO:0016614", "GO:0046593", "GO:0050660", "GO:0007267", "GO:0009058", "GO:0009553", "GO:0010430", "GO:0016491"
OG0003542	OG0003542 Cyclin-D6-1,,,,,	"GO:0005634", "GO:0005737", "GO:0005515", "GO:0010440", "GO:0042023", "GO:0010444", "GO:0048316", "GO:0009744", "GO:0051726", "GO:1901371", "GO:0010033", "GO:0009735"
OG0003616	010928432.1uncharacterized protein LOC105050200,,,,,	NA
OG0003619	finger protein ATL13,,,,,	"GO:0004842", "GO:0031625", "GO:0046872", "GO:0009620", "GO:0009793", "GO:0010033", "GO:0016567", "GO:0098542", "GO:0033591", "GO:0061630", "GO:0043068", "GO:0043562", "GO:0042742", "GO:0009416", "GO:0005886", "GO:0002238", "GO:0009737", "GO:0005739", "GO:0050832", "GO:0010200", "GO:0051865", "GO:0009617"
OG0003649	transcription factor ASR3,,,,,	"GO:0005515", "GO:0006355"
OG0003676	family protein At2g38370,,,,,	"GO:0005737", "GO:0005829", "GO:0005515", "GO:0009903", "GO:0009904"
OG0003678	038975680.1uncharacterized protein LOC120106715,,,,,	NA
OG0003841	ASPARTIC PROTEASE IN GUARD CELL 1,,,,,	"GO:0009627", "GO:0009737", "GO:0070001", "GO:0016020", "GO:0004175", "GO:0005783", "GO:0005576", "GO:0009414", "GO:0048868", "GO:0044238", "GO:0071704", "GO:0071944"
OG0003871	ECERIFERUM 2,,,,,	"GO:0005634", "GO:0005783", "GO:0016410", "GO:0009555", "GO:0009699", "GO:0010025", "GO:0042761", "GO:0008374", "GO:0050734", "GO:0009698", "GO:0005737", "GO:0043231", "GO:0008610", "GO:0010033", "GO:0044085", "GO:0044255", "GO:0045229"
OG0004005	020104672.1uncharacterized protein LOC109721438,,,,,	NA
OG0004067	esterase,,,,,	"GO:0005783", "GO:0016020", "GO:0071944", "GO:0016298", "GO:0016747", "GO:0052689", "GO:0006979", "GO:0010038", "GO:0016042", "GO:0044255", "GO:0005737", "GO:0012505", "GO:0043231", "GO:0006631", "GO:0006950", "GO:0010035", "GO:0010646", "GO:0023051", "GO:0065008", "GO:0016787", "GO:0003824"
OG0004093	020094225.1uncharacterized protein LOC109714168,,,,,	NA
OG0004115	endotransglucosylase protein 34,,,,,	"GO:0048046", "GO:0004553", "GO:0016762", "GO:0030247", "GO:0009408", "GO:0009409", "GO:0009414", "GO:0009612",

		"GO:0009645", "GO:0009664", "GO:0009733", "GO:0009741", "GO:0009826", "GO:0009834", "GO:0010218", "GO:0010411", "GO:0005737", "GO:0009835", "GO:0071555"
OG0004157	domain-containing protein At1g67900,,,,,	"GO:0005886", "GO:0005515", "GO:0009860", "GO:0009904", "GO:0009908", "GO:0009958", "GO:0010051", "GO:0010229", "GO:0042742", "GO:0010305", "GO:0010588", "GO:0080022", "GO:0009638", "GO:0009785", "GO:0016567", "GO:0016020", "GO:0071944", "GO:0006952", "GO:0007165", "GO:0009637", "GO:0048825"
OG0004281	CHROMOSOME TRANSMISSION FIDELITY 7,,,,,	"GO:0005634", "GO:0005694", "GO:0008080", "GO:0000724", "GO:0007064", "GO:0009553", "GO:0009793", "GO:0016573", "GO:0034089", "GO:0048364", "GO:0048609", "GO:0048653", "GO:0060772", "GO:0071922", "GO:0080186", "GO:0043229", "GO:0016407", "GO:0000819", "GO:0007062", "GO:0009791", "GO:0045132", "GO:0099402", "GO:0000070"
OG0004296	family molecular chaperone regulator 1,,,,,	"GO:0005634", "GO:0005829", "GO:0005515", "GO:0006612", "GO:0070971", "GO:0009409", "GO:0009651", "GO:0010119", "GO:0010228", "GO:0043268", "GO:0071629"
OG0004322	JASON,,,,,	GO:0051321
OG0004389	protein 3,,,,,	"GO:0005576", "GO:0005764", "GO:0016020", "GO:0004566", "GO:0009826", "GO:0030203", "GO:0048522", "GO:2000026"
OG0004393	MIZU-KUSSEI 1,,,,,	"GO:0005789", "GO:0032541", "GO:0009658", "GO:0010274"
OG0004401	protein ATH1,,,,,	"GO:0005654", "GO:0005829", "GO:0005856", "GO:0000978", "GO:0001228", "GO:0003779", "GO:0046983", "GO:0008284", "GO:0008285", "GO:0009640", "GO:0009880", "GO:0009965", "GO:0010051", "GO:0010076", "GO:0010077", "GO:0010089", "GO:0010154", "GO:0010223", "GO:0010227", "GO:0010228", "GO:0010229", "GO:0010371", "GO:0030154", "GO:0045892", "GO:0045944", "GO:0048363", "GO:0048457", "GO:0048510", "GO:0080006", "GO:0042659", "GO:0015630", "GO:0090575", "GO:0009954", "GO:0046982", "GO:0015629", "GO:0034504", "GO:0010197", "GO:0000785", "GO:0003785", "GO:0051015", "GO:0009610", "GO:0090470", "GO:0042803", "GO:0003682", "GO:0008134", "GO:0009737", "GO:0009506", "GO:0000981", "GO:0003723", "GO:0006357", "GO:0010201", "GO:0010497", "GO:0000976", "GO:0003700", "GO:0006355", "GO:0048438", "GO:0001708", "GO:0010074", "GO:1905393", "GO:0048437"
OG0004403	helix-loop-helix protein 79,,,,,	"GO:0000978", "GO:0048767", "GO:0046983", "GO:0048446", "GO:0009637", "GO:0009911", "GO:0045824", "GO:1902448", "GO:0042127", "GO:0000981", "GO:0006357", "GO:0005634", "GO:0009739", "GO:0048235", "GO:2000488", "GO:0071368", "GO:0000976", "GO:0006355", "GO:0003700", "GO:2000762", "GO:0010372", "GO:0009740", "GO:0051511", "GO:0045893", "GO:2000024", "GO:0016036"
OG0004433	inactive leucine-rich repeat receptor kinase XIAO,,,,,	"GO:0005886", "GO:0012505", "GO:0000166", "GO:0004672", "GO:0005515", "GO:0038023", "GO:0006468", "GO:0006952", "GO:0009555", "GO:0009741", "GO:0009755", "GO:0010015", "GO:0010074", "GO:0045229", "GO:0048638", "GO:0048657", "GO:0048878", "GO:0051239", "GO:0051321", "GO:0051707", "GO:0006810", "GO:0009617", "GO:0022603", "GO:0030154", "GO:0048229", "GO:0048646", "GO:0048658", "GO:0070727", "GO:0090696", "GO:0098542", "GO:0005524", "GO:0015026", "GO:0033612", "GO:0042803", "GO:0007639", "GO:0008219", "GO:0009729", "GO:0009742", "GO:0010150", "GO:0010227", "GO:0010262", "GO:0045089", "GO:0048653", "GO:1900150", "GO:0042802", "GO:0009793", "GO:0031347", "GO:0016310", "GO:0046983", "GO:0048366", "GO:0044238"
OG0004496	NEOXANTHIN-DEFICIENT 1,,,,,	GO:0016123
OG0004601	transporter B family member 19,,,,,	"GO:0009640", "GO:0008361", "GO:0048767", "GO:0090691", "GO:0009637", "GO:0008559", "GO:0009735", "GO:0005886", "GO:0060919", "GO:0005524", "GO:0009958", "GO:0005515", "GO:0010329", "GO:0043481", "GO:0010218", "GO:0048443", "GO:0010315", "GO:0010541", "GO:0010540", "GO:0016887"

OG0004630	1,,,,,	"GO:0005576", "GO:0005773", "GO:0009044", "GO:0046556", "GO:0009627", "GO:0010214", "GO:0031222", "GO:0045493"
OG0004649	protein 7,,,,,	"GO:0010187", "GO:0000976", "GO:0009610", "GO:0006355", "GO:0006950", "GO:0051301", "GO:0009938", "GO:0005634", "GO:0009639", "GO:1903508", "GO:0005515", "GO:0003712", "GO:0051179", "GO:0009737", "GO:0048367", "GO:0051606", "GO:2000033", "GO:0001708", "GO:0009653", "GO:1901701", "GO:0009755", "GO:0003700", "GO:0071396", "GO:0009966", "GO:0009888", "GO:0009739", "GO:0010604", "GO:0042803", "GO:0007584", "GO:0005737", "GO:0010247", "GO:0009628", "GO:0140110", "GO:0031667", "GO:0045944", "GO:0016036", "GO:0022414", "GO:0051093", "GO:0005622", "GO:0006357", "GO:0009937", "GO:0051241", "GO:0010029"
OG0004659	020242150.1uncharacterized protein LOC109820421 isoform X2,,,,,	GO:0016020
OG0004740	transcription factor Y subunit A-10,,,,,	"GO:0010262", "GO:0080182", "GO:0016602", "GO:0000978", "GO:0035065", "GO:0009567", "GO:0009785", "GO:0001228", "GO:0001217", "GO:0009414", "GO:0005654", "GO:0006109", "GO:0009408", "GO:0009738", "GO:0045892", "GO:0048510", "GO:0055046", "GO:0032993", "GO:0000981", "GO:0005515", "GO:0006357", "GO:0045893", "GO:0000976", "GO:0003700"
OG0004759	008775950.2uncharacterized protein LOC103696192,,,,,	"GO:0003924", "GO:0005525", "GO:0006412", "GO:0016020"
OG0004769	methyltransferase At1g29790,,,,,	character(0
OG0004798	arabinogalactan protein 7,,,,,	"GO:0009834", "GO:0048731", "GO:0005576", "GO:0005886", "GO:0031982", "GO:0047911", "GO:0009555", "GO:0009838", "GO:0009846", "GO:0009900", "GO:0045490", "GO:0048437", "GO:0048868", "GO:0009651"
OG0004806	009414858.1PREDICTED: uncharacterized protein LOC103995863,,,,,	GO:0016020
OG0004872	endotransglucosylase/hydrolase protein 9,,,,,	"GO:0005576", "GO:0004553", "GO:0016762", "GO:0030247", "GO:0009408", "GO:0009409", "GO:0009414", "GO:0009612", "GO:0009645", "GO:0009664", "GO:0009733", "GO:0009741", "GO:0009826", "GO:0009834", "GO:0010218", "GO:0010411", "GO:0009828", "GO:0009737", "GO:0009835", "GO:0071370", "GO:0005975"
OG0004982	receptor-like serine/threonine-protein kinase RGI1,,,,,	"GO:0009790", "GO:2000280", "GO:0042802", "GO:0010087", "GO:0010082", "GO:0009266", "GO:0009791", "GO:0048878", "GO:0048229", "GO:0048646", "GO:0004672", "GO:0042277", "GO:0009725", "GO:0006468", "GO:0005886", "GO:0000166", "GO:0098542", "GO:0001653", "GO:0006955", "GO:0048367", "GO:0010078", "GO:0080092", "GO:0010088", "GO:1901141", "GO:0010183", "GO:0048437", "GO:0080113", "GO:0048831", "GO:0009934", "GO:0043621", "GO:0051301", "GO:0005789", "GO:0009506", "GO:0045595", "GO:0017046", "GO:0051428", "GO:0033612", "GO:0010311", "GO:2000652", "GO:0036289", "GO:1902025", "GO:1901333", "GO:0004674", "GO:0031540", "GO:0010089", "GO:0010067", "GO:0090548", "GO:0010223", "GO:0090406", "GO:0060866", "GO:0050829", "GO:0010468", "GO:0010102"
OG0005038	protein TANGLED1,,,,,	"GO:0005875", "GO:0009574", "GO:0005515", "GO:0000914", "GO:0005730", "GO:0009524", "GO:0008017", "GO:2000694", "GO:0005737", "GO:0015630"
OG0005053	nucleotide-binding protein subunit gamma 4,,,,,	"GO:0005634", "GO:0005886", "GO:0007186", "GO:0009737", "GO:0080050", "GO:0005834", "GO:0005515", "GO:0009845", "GO:0010540", "GO:0018342", "GO:0018345", "GO:0048527", "GO:0036211"
OG0005077	009410166.1PREDICTED: uncharacterized protein LOC103992257,,,,,	"GO:0005634", "GO:0005524", "GO:0006351", "GO:2000070", "GO:0061630", "GO:0065003", "GO:0009651", "GO:1902006", "GO:0009630", "GO:0009789", "GO:0009788", "GO:0006511", "GO:0047484", "GO:0009938", "GO:0031625", "GO:0046872", "GO:0016020", "GO:0005829", "GO:0071218", "GO:0051865"

OG0005085	a-b binding protein 4, chloroplastic,,,,	"GO:0009523", "GO:0009535", "GO:0009782", "GO:0016168", "GO:0031409", "GO:0046872", "GO:0006950", "GO:0009639", "GO:0009644", "GO:0009645", "GO:0009768", "GO:0005515", "GO:0010033", "GO:0009409", "GO:0019904"
OG0005118	009390971.1PREDICTED: uncharacterized protein LOC103977236,,,,,	"GO:0005737", "GO:0043229"
OG0005158	esterase/lipase At3g48460,,,,,	"GO:0008126", "GO:0006631"
OG0005176	NETWORKED 3C,,,,,	"GO:0005634", "GO:0005774", "GO:0005884", "GO:0005886", "GO:0009506", "GO:0012505", "GO:0031965", "GO:0051015"
OG0005387	47,,,,,	"GO:0005576", "GO:0005737", "GO:0009505", "GO:0043231", "GO:0004601", "GO:0020037", "GO:0046872", "GO:0006979", "GO:0009269", "GO:0009409", "GO:0042538", "GO:0042744", "GO:0071456", "GO:0098869", "GO:0002215", "GO:0009908", "GO:0140825", "GO:0012505", "GO:0005509"
OG0005500	017700156.2uncharacterized protein LOC103714829,,,,,	"GO:0005886", "GO:0009506", "GO:0019900", "GO:0043621", "GO:0009414", "GO:0009651", "GO:0009738", "GO:0009751", "GO:0010555", "GO:0051607", "GO:0051665", "GO:1900458"
OG0005502	oxidase 1,,,,,	"GO:0005634", "GO:0005737", "GO:0032452", "GO:0050660", "GO:1990534", "GO:0010468", "GO:0016570", "GO:0046208", "GO:0048510"
OG0005544	010919185.1fasciclin-like arabinogalactan protein 8,,,,,	"GO:0009834", "GO:0048364", "GO:0016020", "GO:0048367", "GO:0005886"
OG0005549	topoisomerase 2,,,,,	"GO:0000228", "GO:0000791", "GO:0000792", "GO:0000793", "GO:0005654", "GO:0005730", "GO:0005814", "GO:0005829", "GO:0009330", "GO:1990904", "GO:0000182", "GO:0000287", "GO:0000400", "GO:0003682", "GO:0003729", "GO:0003918", "GO:0005080", "GO:0005524", "GO:0008022", "GO:0008301", "GO:0030332", "GO:0042803", "GO:0042826", "GO:0043021", "GO:0043130", "GO:0046982", "GO:0000712", "GO:0006260", "GO:0006265", "GO:0006266", "GO:0006974", "GO:0007060", "GO:0007076", "GO:0007568", "GO:0009410", "GO:0010212", "GO:0031507", "GO:0042752", "GO:0043065", "GO:0045944", "GO:0051306", "GO:0007143", "GO:0005737", "GO:0003677", "GO:0046872", "GO:0000819", "GO:0000166", "GO:0003916"
OG0005584	RNA-binding protein ARP1,,,,,	"GO:0061158", "GO:0009651", "GO:0008285", "GO:0003690", "GO:0003697", "GO:0005654", "GO:0009414", "GO:0009409", "GO:0000381", "GO:0003727", "GO:1990428", "GO:0005829", "GO:1990825", "GO:0035198", "GO:0042802", "GO:0035197", "GO:1900864", "GO:0005615", "GO:0097157", "GO:0009737", "GO:0035925", "GO:0005739", "GO:0010029", "GO:0009693", "GO:0080156", "GO:0008219", "GO:0010150", "GO:0006970", "GO:0008380", "GO:1901000", "GO:0006858", "GO:1990904", "GO:0006397", "GO:0010228", "GO:0050688", "GO:0010043", "GO:0000380", "GO:0032508", "GO:0007623", "GO:0006406", "GO:0045087", "GO:0010501", "GO:0003729"
OG0005676	pectin methyltransferase QUA3,,,,,	"GO:0000139", "GO:0008757", "GO:0042546", "GO:0045489", "GO:0052546"
OG0005741	receptor-like serine/threonine-protein kinase ER1,,,,,	"GO:0009790", "GO:0010087", "GO:1901002", "GO:1905421", "GO:0048878", "GO:0046777", "GO:0042277", "GO:0009553", "GO:0007178", "GO:0051302", "GO:0005524", "GO:0004712", "GO:0045595", "GO:0048481", "GO:0050832", "GO:2000038", "GO:0033612", "GO:0048281", "GO:0042802", "GO:0010073", "GO:1902584", "GO:0009664", "GO:0005783", "GO:0009944", "GO:0042742", "GO:0005886", "GO:0009965", "GO:0004675", "GO:0070370", "GO:0001558", "GO:0010148", "GO:0030155", "GO:0010103", "GO:2000280", "GO:0042659", "GO:0043621", "GO:0009755", "GO:0005789", "GO:0009826", "GO:0045184", "GO:0048653", "GO:0090708", "GO:0031347", "GO:0010088", "GO:0055075", "GO:1903224", "GO:0009611", "GO:0009934", "GO:0006468", "GO:0010078", "GO:0015026", "GO:0009741", "GO:0001653", "GO:0007639", "GO:0048354", "GO:2000067", "GO:0016310", "GO:0042803", "GO:0009742", "GO:0019901", "GO:0007165"
OG0005838	007215314.1uncharacterized protein LOC18783714,,,,,	"GO:0016740", "GO:0006004", "GO:0016020"

OG0005926	010928808.1uncharacterized protein LOC105050470,,,,,	"GO:0003824", "GO:0016787", "GO:0006281"
OG0006078	protein kinase-like protein ZAR1,,,,,	"GO:0005886", "GO:0009505", "GO:0090406", "GO:0000166", "GO:0004674", "GO:0005515", "GO:0006950", "GO:0009888", "GO:0010069", "GO:0030154", "GO:0046777", "GO:0048229", "GO:0048437", "GO:0048438", "GO:0048646", "GO:0048827", "GO:0048878", "GO:0050793", "GO:0051321", "GO:0071554", "GO:0090698", "GO:1905392", "GO:0042802", "GO:0009610", "GO:0040008"
OG0006082	inhibitor PPE8B,,,,,	"GO:0005886", "GO:0009505", "GO:0030599", "GO:0046910", "GO:0010119", "GO:0050829", "GO:0071555", "GO:0005576", "GO:0005737", "GO:0003729", "GO:0009620", "GO:0009624", "GO:1990110", "GO:0004857", "GO:0005515", "GO:0010043", "GO:0010187", "GO:0010468", "GO:0045490", "GO:0050832", "GO:0051510", "GO:0080147"
OG0006088	only protein 6,,,,,	"GO:0010928", "GO:0010468", "GO:0010305", "GO:0060776"
OG0006109	010916425.1uncharacterized protein LOC105041244,,,,,	NA
OG0006125	I reaction center subunit N, chloroplastic,,,,	"GO:0030093", "GO:0019904", "GO:0015979"
OG0006150	factor GHD7,,,,,	"GO:0010099", "GO:0008270", "GO:0042802", "GO:2000032", "GO:0010161", "GO:0000976", "GO:0048579", "GO:0045036", "GO:0009641", "GO:0005730", "GO:0007623", "GO:0009637", "GO:0009658", "GO:0010629", "GO:0003700", "GO:0045892", "GO:0009909", "GO:0048577", "GO:0045893", "GO:0048576", "GO:0030154", "GO:0009536", "GO:0010018", "GO:0010223"
OG0006279	STICHEL-like 2,,,,,	"GO:0005634", "GO:0005663", "GO:0000166", "GO:0003689", "GO:0006261", "GO:0006281", "GO:0007049", "GO:0010091", "GO:0032991", "GO:0043229", "GO:0006260", "GO:0006259", "GO:0010026"
OG0006334	POLLENLESS 3-LIKE 2,,,,,	"GO:0005634", "GO:0017053", "GO:0005515", "GO:0006792", "GO:0007140", "GO:0009556", "GO:0009658", "GO:0010438", "GO:0010439"
OG0006372	leucine-rich repeat receptor-like serine/threonine-protein kinase At1g60630,,,,,	"GO:0005737", "GO:0005886", "GO:0004672", "GO:0005515", "GO:0040008", "GO:0016020", "GO:0043231", "GO:0071944", "GO:0042802", "GO:0006468", "GO:0009610"
OG0006440	TIFY 8,,,,,	GO:0005515
OG0006460	SOSEKI 2,,,,,	"GO:0016324", "GO:0031234", "GO:0042803", "GO:0051258", "GO:0051302", "GO:0090708", "GO:2000067", "GO:1902074", "GO:0006970", "GO:0007049", "GO:0010928", "GO:0010229", "GO:0010600", "GO:2000024", "GO:0009925"
OG0006602	lipid phosphate phosphatase 3, chloroplastic,,,,	"GO:0005774", "GO:0009507", "GO:0012505", "GO:0003993", "GO:0008195", "GO:0016740", "GO:0042802", "GO:0002376", "GO:0006644", "GO:0006952", "GO:0010224", "GO:0046839", "GO:0090279", "GO:0004672", "GO:0016310", "GO:0048856", "GO:0005743", "GO:0031969", "GO:0009626", "GO:0090351"
OG0006645	protein At1g76660,,,,,	NA
OG0006651	protein At5g48480,,,,,	NA
OG0006716	protein,,,,,	"GO:0003729", "GO:0004672", "GO:0009615", "GO:0009617", "GO:0009620", "GO:0009627", "GO:0009651", "GO:0009723", "GO:0009737", "GO:0009751", "GO:0010224", "GO:0031540", "GO:0046686"
OG0006793	038979907.1protein BRANCHLESS TRICHOME-like,,,,,	GO:0010090
OG0006881	010926075.1uncharacterized protein LOC105048466,,,,,	NA
OG0006974	protein-tyrosine kinase CEPR1,,,,,	"GO:0005886", "GO:0000166", "GO:0001653", "GO:0004713", "GO:0017046", "GO:0042802", "GO:0051428", "GO:0006970", "GO:0006979", "GO:0009845", "GO:0009960", "GO:0010051", "GO:0010074", "GO:0010075", "GO:0010087", "GO:0010227", "GO:0010311", "GO:0010468", "GO:0010555", "GO:0018193", "GO:0031540", "GO:0045087", "GO:0045490", "GO:0046777", "GO:0048831", "GO:0050829", "GO:0060866", "GO:0080113",

		"GO:0090548", "GO:1901141", "GO:1901333", "GO:1902025", "GO:2000652", "GO:0042659", "GO:0010183", "GO:0009553", "GO:0043621", "GO:0006833", "GO:0033612", "GO:0045184", "GO:0090708", "GO:0010067", "GO:0010223", "GO:0010082", "GO:0055075", "GO:1903224", "GO:0009611", "GO:0009934", "GO:0051302", "GO:0010078", "GO:2000067", "GO:0010089", "GO:0090406", "GO:0004672"
OG0007036	receptor-like serine/threonine-protein kinase GHR1,,,,,	"GO:0090333", "GO:0009791", "GO:0048646", "GO:0004672", "GO:0006468", "GO:0040008", "GO:0048507", "GO:0005886", "GO:0009789", "GO:0048869", "GO:0000166", "GO:1901528", "GO:0050793", "GO:0005515", "GO:0071244", "GO:0048367", "GO:0005737", "GO:0043231", "GO:0099402", "GO:0071485", "GO:0051239", "GO:0051707", "GO:0048658", "GO:0048229", "GO:0004674", "GO:0006952", "GO:0051321", "GO:0030154", "GO:0012505", "GO:1905392", "GO:0090404", "GO:0042802", "GO:0010183", "GO:0009610", "GO:0016310"
OG0007116	mobility group B protein 6,,,,,	"GO:0006281", "GO:0051707", "GO:0008284", "GO:0000976", "GO:0051052", "GO:0080135", "GO:0008301", "GO:1902533", "GO:0000794", "GO:0003700", "GO:0030527", "GO:0006338", "GO:0003723", "GO:0045892", "GO:0071310", "GO:0045595", "GO:0005829", "GO:0031410", "GO:0050776", "GO:0045935", "GO:0003682", "GO:0008134", "GO:0006952", "GO:0006996", "GO:0000785", "GO:0005102", "GO:0006357", "GO:0048731", "GO:0016020", "GO:0012505", "GO:0070898", "GO:2000026", "GO:0003677", "GO:0006325"
OG0007225	membrane-associated kinase regulator 1,,,,,	"GO:0005829", "GO:0005886", "GO:0009536", "GO:0019210", "GO:0005737", "GO:0016020", "GO:0009741"
OG0007251	008785030.1uncharacterized protein LOC103703811,,,,,	"GO:0016301", "GO:0016310"
OG0007368	051124850.1uncharacterized protein LOC127247156,,,,,	NA
OG0007495	peeling cupredoxin,,,,,	GO:0016020
OG0007498	008775695.1uncharacterized protein LOC103695999,,,,,	NA
OG0007646	acyltransferase DCR,,,,,	"GO:0005737", "GO:0016410", "GO:0010090", "GO:0010143", "GO:0019438", "GO:0051179", "GO:0050734", "GO:0009699", "GO:0009698"
OG0007662	factor bHLH57,,,,,	"GO:0090547", "GO:0042803", "GO:0061086", "GO:0000976", "GO:0009631", "GO:0045597", "GO:0001216", "GO:0047484", "GO:0005634", "GO:0045893", "GO:0051782", "GO:2000038", "GO:0010444", "GO:0003700", "GO:0046983", "GO:0006950", "GO:0009507", "GO:0003735", "GO:0070180", "GO:0006412", "GO:0003677"
OG0007682	008798782.2WD repeat-containing protein WRAP73,,,,,	"GO:0005515", "GO:0090307", "GO:0005815", "GO:0072686", "GO:1990811", "GO:0000070", "GO:1902440"
OG0007739	ubiquitin-protein ligase SGR9, amyloplastic,,,,	"GO:0005634", "GO:0005829", "GO:0009536", "GO:0051787", "GO:0061630", "GO:0000209", "GO:0006970", "GO:0009414", "GO:0009737", "GO:0009968", "GO:0051865", "GO:0061635", "GO:0071629", "GO:0009630", "GO:0009788", "GO:2000070", "GO:0009651", "GO:1902006", "GO:0006511", "GO:0009938", "GO:0047484", "GO:0005515", "GO:0071218", "GO:0009789", "GO:0005789", "GO:0016020"
OG0007743	maintenance complex-binding protein,,,,,	"GO:0005634", "GO:0042555", "GO:0005515", "GO:0006260", "GO:0006301", "GO:0007062"
OG0007765	kinase WAG1,,,,,	"GO:0005634", "GO:0005737", "GO:0009925", "GO:0009986", "GO:0004674", "GO:0005546", "GO:0005547", "GO:0009882", "GO:0010314", "GO:0019901", "GO:0032266", "GO:0070273", "GO:0070300", "GO:0080025", "GO:0009638", "GO:0009734", "GO:0009785", "GO:0009860", "GO:0009908", "GO:0009926", "GO:0009958", "GO:0046777", "GO:0048766", "GO:0048767", "GO:0048825", "GO:0062075", "GO:2000114", "GO:0007623", "GO:0010362"
OG0007781	domain receptor-like kinase 3,,,,,	"GO:0019901", "GO:0008061", "GO:0042802", "GO:1900150", "GO:0009593", "GO:0004672", "GO:0006468", "GO:0043621", "GO:0005773", "GO:0009789", "GO:1900426", "GO:1900459",

		"GO:0000166", "GO:0005777", "GO:0002237", "GO:0045088", "GO:0071323", "GO:0031348", "GO:0032491", "GO:0042803", "GO:0046777", "GO:2001080", "GO:0004674", "GO:0042742", "GO:0005886", "GO:0005775", "GO:0002752", "GO:0019199", "GO:0009609", "GO:0032499", "GO:0050832", "GO:0071219", "GO:0035556", "GO:0045087", "GO:0016301"
OG0007790	RALF-like 34,,,,,	"GO:0048046", "GO:0005179", "GO:0007267", "GO:0090406", "GO:0009741", "GO:0019722", "GO:0045926", "GO:0005576", "GO:0048018", "GO:0007165", "GO:0080092", "GO:0005515"
OG0007855	008801864.1uncharacterized protein At3g61260,,,,,	"GO:0005886", "GO:0009506", "GO:0005515", "GO:0009651", "GO:0009738", "GO:0009751", "GO:0010555", "GO:0051607", "GO:0051665", "GO:1900458"
OG0007867	like protein 29,,,,,	"GO:2000280", "GO:0042659", "GO:0070727", "GO:0010082", "GO:1901002", "GO:0048878", "GO:0042277", "GO:0009553", "GO:0051302", "GO:0010078", "GO:2000038", "GO:1902584", "GO:0048646", "GO:0009620", "GO:0048226", "GO:0006810", "GO:0005886", "GO:0004675", "GO:0098542", "GO:0001653", "GO:0005515", "GO:0009737", "GO:0090708", "GO:0032870", "GO:2000067", "GO:0090626", "GO:0016020"
OG0008010	020108176.1syntaxin-related protein KNOLLE,,,,,	"GO:0005737", "GO:0016020", "GO:0015031", "GO:0016192", "GO:0022607", "GO:0010817", "GO:0010119", "GO:0000281", "GO:0019900", "GO:0010256", "GO:0051128", "GO:0009860", "GO:0005484", "GO:0000149", "GO:0006612", "GO:0009504", "GO:0009524", "GO:0005815", "GO:0006906", "GO:0006904", "GO:0031981", "GO:0031201", "GO:0040008", "GO:0005886", "GO:0030133", "GO:0006887", "GO:0048278"
OG0008145	domain-containing protein 45,,,,,	"GO:0010033", "GO:0043069", "GO:0098542", "GO:0004842", "GO:0009617", "GO:0005515", "GO:0005737", "GO:0016020", "GO:2000028", "GO:0016567", "GO:0016740"
OG0008278	009407490.1PREDICTED: uncharacterized protein LOC103990161,,,,,	NA
OG0008625	010932933.1uncharacterized protein LOC105053469,,,,,	"GO:0042175", "GO:0005509", "GO:0016740", "GO:0006004", "GO:0016020"
OG0008718	protein,,,,,	"GO:0005886", "GO:0016020", "GO:0009610"
OG0009030	sugar phosphate/phosphate translocator At1g12500,,,,,	"GO:0005783", "GO:0005794", "GO:0008514", "GO:0015165", "GO:0015297", "GO:0008643", "GO:0015780", "GO:0048359", "GO:0098656", "GO:0005459", "GO:0005460", "GO:1905039"
OG0009126	010913261.1uncharacterized protein LOC105039000,,,,,	"GO:0009507", "GO:0016020", "GO:0043531", "GO:0000725", "GO:0006811", "GO:0007165", "GO:0055085", "GO:0016887"
OG0009140	19,,,,,	"GO:0009505", "GO:0004601", "GO:0005515", "GO:0045926", "GO:0003824", "GO:0006950", "GO:0016491"
OG0009191	042386700.1serine/threonine -protein kinase WNK4-like,,,,,	GO:0016740
OG0009321	nodulin-like protein 1,,,,,	GO:0016020
OG0009322	pectinesterase 68,,,,,	"GO:0005737", "GO:0009505", "GO:0090406", "GO:0005515", "GO:0030599", "GO:0009846", "GO:0009860", "GO:0045490", "GO:0050829", "GO:0071555", "GO:0005576", "GO:0042545"
OG0009621	receptor-like serine/threonine-protein kinase SIK1,,,,,	"GO:0010087", "GO:1901002", "GO:1905421", "GO:0048878", "GO:0042277", "GO:0009553", "GO:0007178", "GO:0006468", "GO:0051302", "GO:0005524", "GO:0004712", "GO:0045595", "GO:0048481", "GO:0050832", "GO:2000038", "GO:0033612", "GO:0048281", "GO:0042802", "GO:0010073", "GO:1902584", "GO:0009664", "GO:0005783", "GO:0009944", "GO:0042742", "GO:0005886", "GO:0009965", "GO:0004675", "GO:0070370", "GO:0001558", "GO:0010148", "GO:0030155", "GO:0010103", "GO:0042659", "GO:1901141", "GO:0048831", "GO:0043621", "GO:0009826", "GO:0010075", "GO:0019901", "GO:0045184", "GO:0090708", "GO:0031540", "GO:0090548", "GO:0055075", "GO:1903224", "GO:0009611", "GO:0080113", "GO:0009934", "GO:0017046", "GO:0051428", "GO:0010311", "GO:2000652", "GO:1902025", "GO:1901333", "GO:0001653", "GO:0048354", "GO:2000067", "GO:0016310", "GO:0048653", "GO:0015026", "GO:0007639"

OG0009939	010930061.1DNA polymerase alpha subunit B,,,,,	"GO:0005654", "GO:0005658", "GO:0005829", "GO:0003887", "GO:0005515", "GO:0006269", "GO:0006270", "GO:0003677"
OG0010255	protein 7,,,,,	NA
OG0010379	043810419.1keratin, type II cytoskeletal 1-like,,,,	NA
OG0010537	replication licensing factor MCM6,,,,,	"GO:0000347", "GO:0000785", "GO:0005656", "GO:0005737", "GO:0031298", "GO:0042555", "GO:0003682", "GO:0003688", "GO:0003697", "GO:0003727", "GO:0005524", "GO:0009378", "GO:0016887", "GO:0042802", "GO:0046872", "GO:1990518", "GO:0000727", "GO:0006268", "GO:0006271", "GO:0006279", "GO:0030174", "GO:1902975", "GO:0005515", "GO:0006270", "GO:0007276", "GO:0009555", "GO:0090329", "GO:0140013", "GO:1902969"
OG0010747	inactive leucine-rich repeat receptor-like protein kinase At5g06940,,,,,	"GO:0005737", "GO:0005886", "GO:0043231", "GO:0004672", "GO:0005102", "GO:0038023", "GO:0042277", "GO:0006952", "GO:0009628", "GO:0010033", "GO:0010074", "GO:0010075", "GO:0010087", "GO:0010102", "GO:0018193", "GO:0046777", "GO:0048437", "GO:1905393", "GO:2000023", "GO:2000241", "GO:1901141", "GO:0010082", "GO:0080113", "GO:0048831", "GO:0009934", "GO:0043621", "GO:0009506", "GO:0017046", "GO:0051428", "GO:0010078", "GO:0033612", "GO:0010311", "GO:2000652", "GO:0036289", "GO:0042802", "GO:1902025", "GO:1901333", "GO:0004674", "GO:0001653", "GO:0031540", "GO:0090548", "GO:0010088", "GO:0010183", "GO:0009416", "GO:0009755", "GO:0005789", "GO:0045595", "GO:0009741", "GO:0006950", "GO:0009838", "GO:0016043", "GO:0090406"
OG0010775	LRR receptor-like serine/threonine-protein kinase At5g45780,,,,,	"GO:0010262", "GO:1900150", "GO:0009556", "GO:0060548", "GO:0046777", "GO:0005654", "GO:0000166", "GO:0009729", "GO:0004713", "GO:0051607", "GO:0034504", "GO:0033612", "GO:0010152", "GO:0015026", "GO:0042803", "GO:0010150", "GO:1901653", "GO:0009742", "GO:0004674", "GO:0005886", "GO:0007639", "GO:0045089", "GO:0005737", "GO:0048653", "GO:0019199", "GO:0010227", "GO:0010008", "GO:0004675", "GO:0004714", "GO:0005524", "GO:0007178", "GO:0008219", "GO:0090351"
OG0011001	010673369.2uncharacterized protein LOC104889764 isoform X4,,,,,	GO:0016020
OG0011319	phosphatase 1,,,,,	"GO:0016787", "GO:0006950", "GO:0003993", "GO:0006952", "GO:0009611", "GO:0009625", "GO:0009753"
OG0011975	020591475.1uncharacterized protein LOC110032249,,,,,	NA
OG0012257	050877967.1protein E6-like,,,,,	NA
OG0015996	OG0015996 -,,,,,	NA
OG0016028	OG0016028 -,,,,,	NA
OG0016747	transcription factor ERF073,,,,,	"GO:2000280", "GO:0010030", "GO:0042802", "GO:0010286", "GO:0009880", "GO:0009864", "GO:0000976", "GO:0009735", "GO:0005886", "GO:0048825", "GO:0005634", "GO:0009739", "GO:0003700", "GO:0008219", "GO:0045893", "GO:0071454", "GO:0019760", "GO:0010105", "GO:0090708", "GO:0005829", "GO:0009611", "GO:1900057", "GO:0009873", "GO:0009736", "GO:0009416", "GO:0009414", "GO:0009409", "GO:0071472", "GO:0045892", "GO:0045595", "GO:0005737", "GO:2000082", "GO:0009651", "GO:0010182", "GO:0009753", "GO:0009751", "GO:0009658", "GO:1990110", "GO:0009749", "GO:0034605", "GO:0071497", "GO:0010119", "GO:0070483", "GO:0010896", "GO:0071456", "GO:0031930", "GO:0050832", "GO:0010353", "GO:0062211", "GO:0032880", "GO:0005983", "GO:0009788", "GO:0048527", "GO:0009744", "GO:0005515", "GO:0010449", "GO:0048510", "GO:0010186", "GO:0051707", "GO:0090332", "GO:0009734", "GO:0009789", "GO:0006952", "GO:0009738", "GO:0005789"

OG0018690	OG0018690 -,,,,,	NA
OG0018770	73E1,,,,,	"GO:0080043", "GO:0080044", "GO:0080046", "GO:0009698", "GO:0051555", "GO:0005515", "GO:0045089", "GO:0098754", "GO:0016131", "GO:0050502", "GO:0010224", "GO:0050403", "GO:0042802"
OG0018871	OG0018871 -,,,,,	NA
OG0020489	OG0020489 -,,,,,	NA
OG0022264	OG0022264 -,,,,,	NA

Appendix B.5 Gene ontology terms enriched in *Xerophyta* species

Appendix B5.1 GO terms enriched in poikilochlorophyllous *Xerophyta schlechteri* and *X. humilis*. These were generated by examining orthogroups that were only up-regulated or down-regulated in the two poikilochlorophyllous species but were not differentially expressed in *X. elegans*.

Up-regulated GO terms

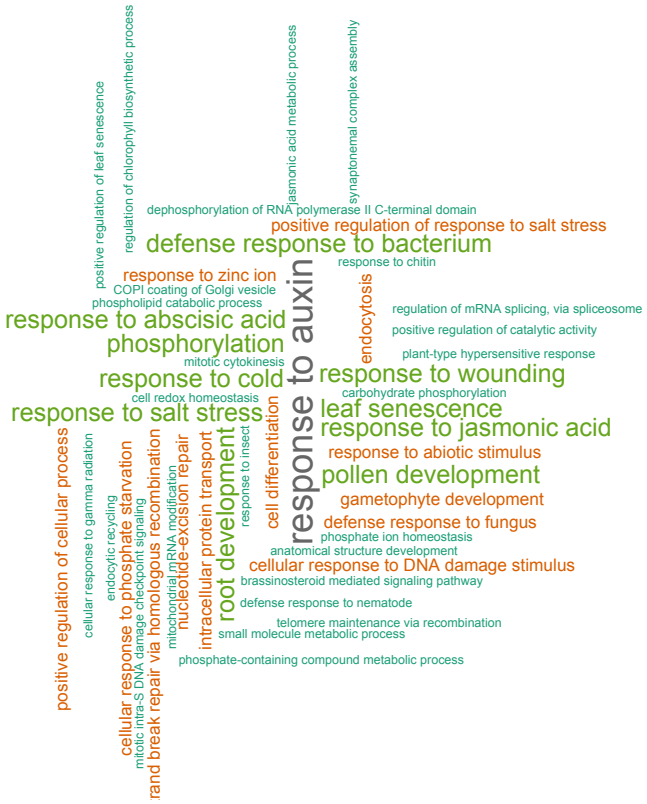

Down-regulated GO terms

Appendix B5.2 GO terms enriched in the homoiochlorophyllous *Xerophyta elegans*. These were generated by examining orthogroups that were only up-regulated or down-regulated in *X. elegans* but were not differentially expressed in *X. schlechteri* and *X. humilis*.

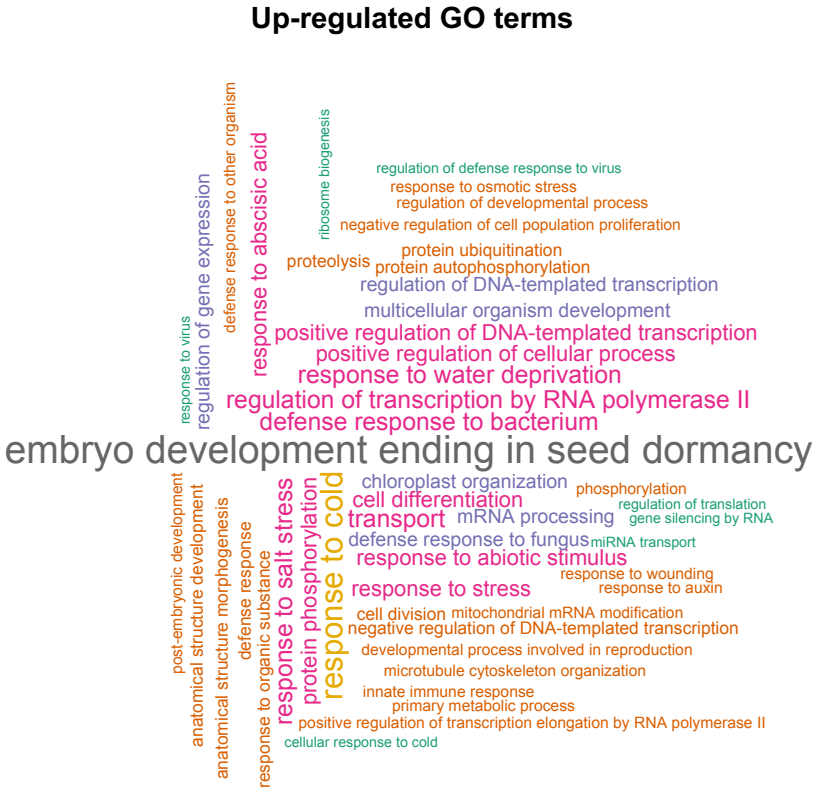

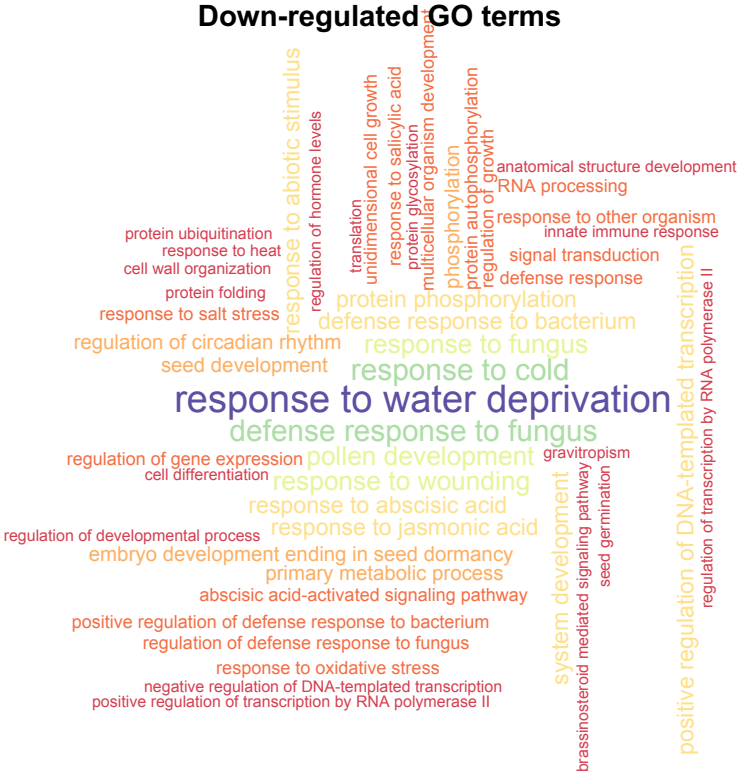

Appendix C. Primary and secondary metabolite plots

Appendix C.1 Volcano plots showing significant differences in primary metabolites

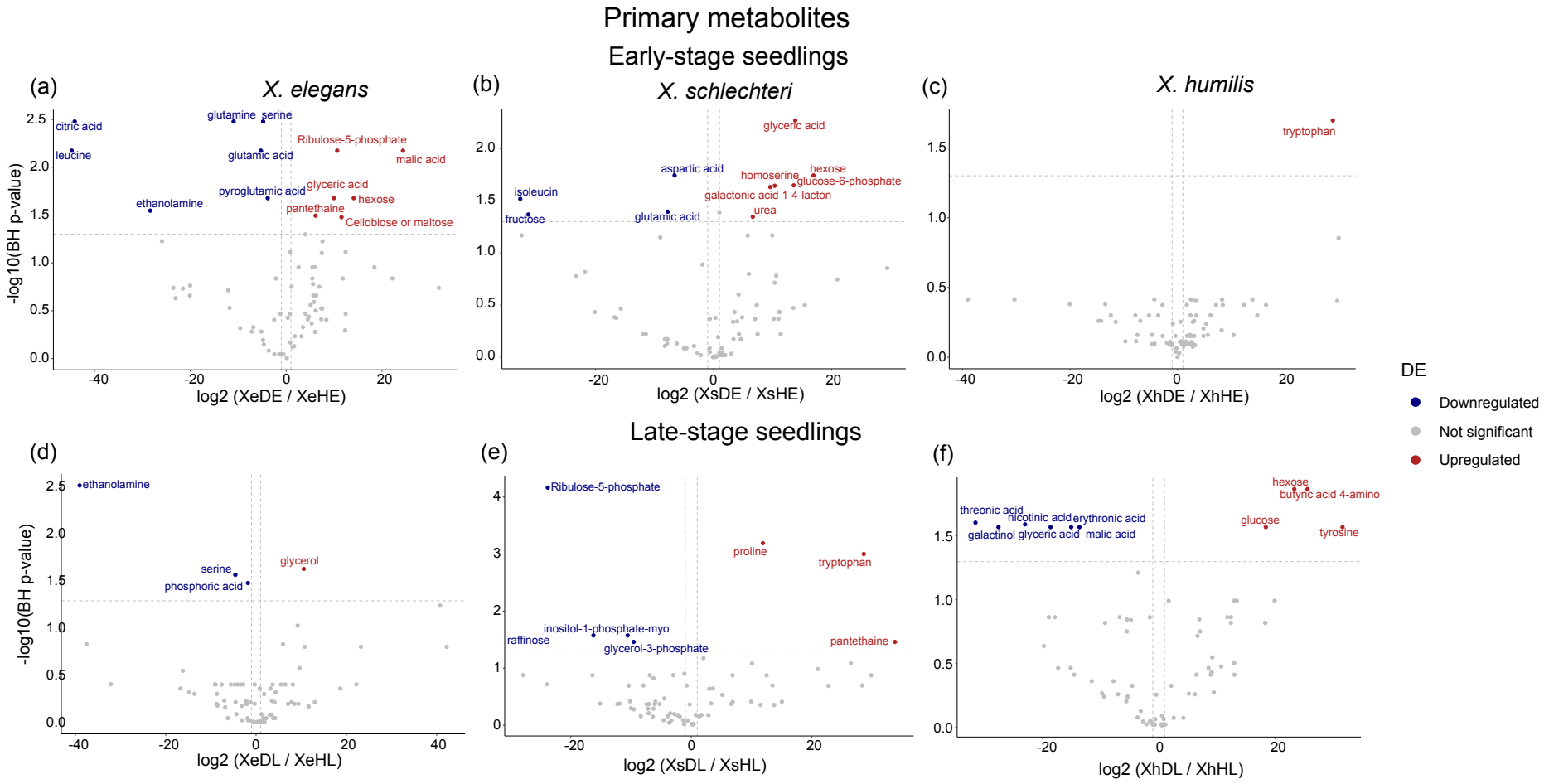

Appendix C.2. Volcano plots illustrating pairwise comparisons between hydrated and dehydrated seedlings of *Xerophyta* species.

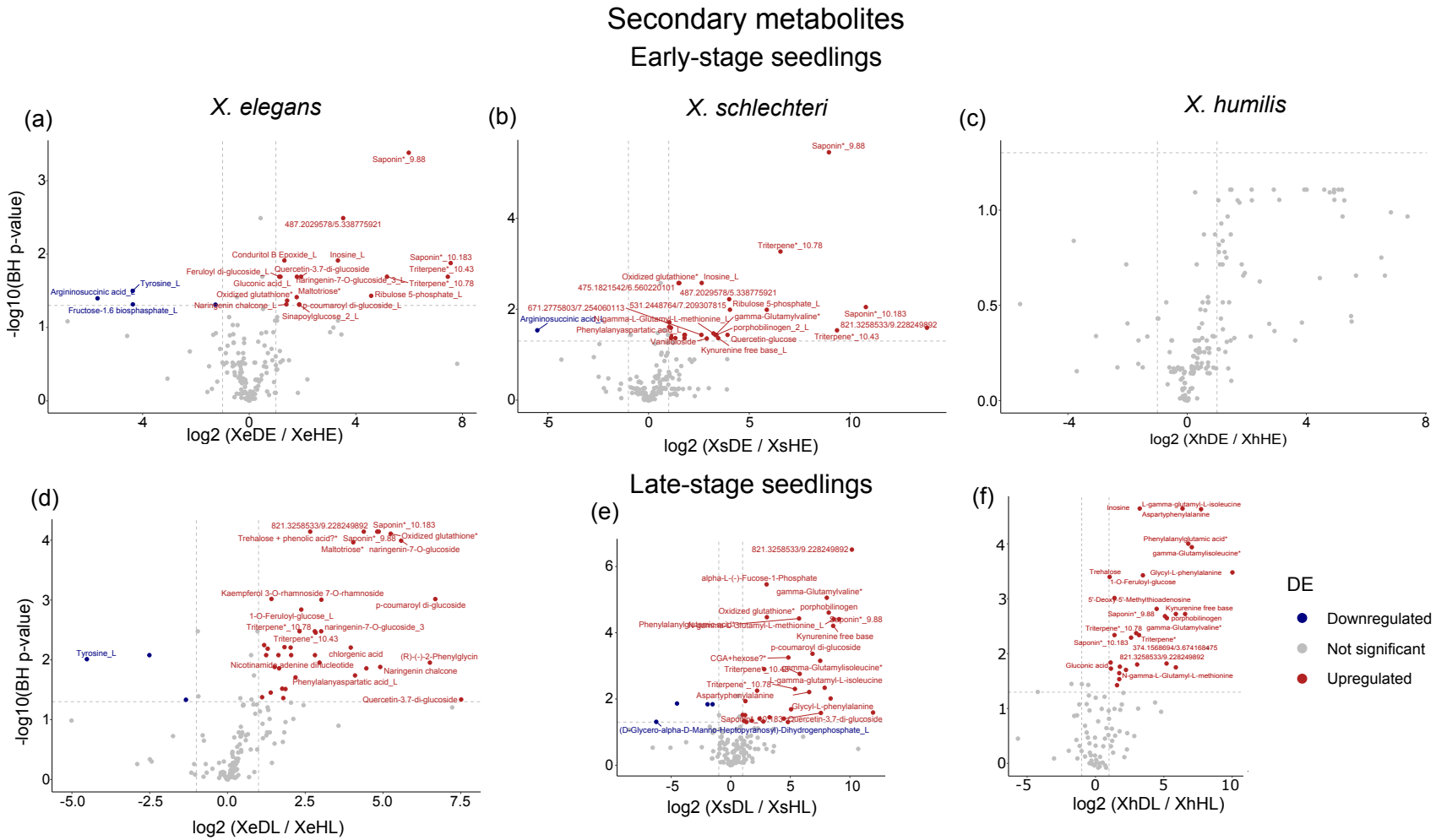

Appendix D. Quantification of chloroplast structures

Appendix D.1. Number of plastoglobules and starch grains from TEM images of *X. elegans* and *X. schlechteri* chloroplasts under desiccating conditions. Quantification was done in 15 different chloroplasts using ImageJ software

		X. elegans		*X. schlechteri*	
Time (hours)	Chloroplast number	Plastoglobules	Starch	Plastoglobules	Starch
0	1	18	0	18	4
	2	18	0	19	3
	3	22	0	19	2
	4	13	0	19	3
	5	20	0	14	1
	6	14	0	18	1
	7	14	0	11	0
	8	19	0	18	1
	9	14	0	12	2
	10	19	0	12	1
	11	20	2	11	2
	12	22	2	19	2
	13	20	1	12	0
	14	20	2	14	0
	15	21	2	11	2
3	1	15	4	7	3
	2	15	6	15	5
	3	12	4	8	3
	4	11	2	7	4
	5	14	4	9	6
	6	15	4	16	8
	7	14	5	17	6
	8	14	3	13	2
	9	16	5	17	2
	10	11	2	15	3
	11	15	3	7	3
	12	17	2	11	2
	13	14	4	14	7
	14	11	2	10	4
	15	17	2	11	4
6	1	6	3	11	3
	2	6	3	16	5
	3	7	4	12	5
	4	9	3	18	4
	5	9	2	18	5
	6	7	2	10	3
	7	12	2	10	3
	8	14	4	18	4

	9	14	5	13	5
	10	11	3	10	3
	11	15	2	10	3
	12	14	5	10	4
	13	15	3	18	4
	14	12	2	11	4
	15	10	3	18	5
	1	7	3	11	2
	2	9	4	10	1
	3	7	3	13	1
	4	7	4	15	1
	5	10	4	15	2
	6	14	4	12	2
	7	14	6	16	3
9	8	16	5	16	3
	9	10	4	18	6
	10	14	2	13	1
	11	15	6	15	2
	12	15	4	13	2
	13	14	2	10	1
	14	11	6	11	1
	15	11	4	11	4
	1	15	5	9	2
	2	10	5	11	1
	3	16	4	13	1
	4	11	5	14	1
	5	11	7	14	2
	6	11	5	12	2
	7	10	5	14	3
12	8	8	5	16	3
	9	18	3	16	4
	10	9	3	11	1
	11	10	4	14	2
	12	11	2	14	2
	13	13	3	9	1
	14	10	7	12	1
	15	16	3	10	4
	1	5	6	20	1
	2	11	4	20	4
	3	5	3	22	3
	4	5	4	25	2
	5	11	6	26	3
	6	8	2	20	4

	7	9	4	28	2
15	8	6	2	29	6
	9	11	5	25	5
	10	11	2	27	3
	11	10	4	28	1
	12	12	2	25	4
	13	8	3	25	2
	14	12	5	28	2
	15	11	4	20	4
	1	25	4	19	1
	2	25	6	20	6
	3	23	7	15	6
	4	18	2	11	3
	5	17	2	15	2
	6	21	3	10	3
	7	21	2	8	3
24	8	20	3	17	4
	9	17	3	10	1
	10	22	5	11	4
	11	25	2	14	5
	12	22	6	11	1
	13	25	3	9	5
	14	17	6	13	2
	15	17	5	11	2
	1	9	0	16	0
	2	15	0	16	0
	3	9	0	21	0
	4	15	0	23	0
	5	12	0	18	0
	6	15	0	23	0
72	7	15	0	25	0
	8	9	0	17	0
	9	10	0	16	0
	10	9	0	17	0
	11	11	0	16	0
	12	12	0	22	0
	13	11	0	22	0
	14	10	0	23	0
	15	12	0	17	0

Appendix D.2. Number of plastoglobules and starch grains from TEM images of *X. elegans* and *X. schlechteri* chloroplasts under rehydrating conditions. Quantification was done in 15 different chloroplasts using ImageJ software

		X. elegans		*X. schlechteri*	
Time (hour)	Chloroplast number	Plastoglobules	Starch	Plastoglobules	Starch
1	1	21	0	35	0
	2	24	0	37	0
	3	24	0	24	0
	4	20	0	35	0
	5	28	0	38	0
	6	28	0	27	0
	7	33	0	44	0
	8	20	0	37	0
	9	20	0	35	0
	10	29	0	25	0
	11	22	0	26	0
	12	28	0	39	0
	13	23	0	32	0
	14	21	0	24	0
	15	23	0	25	0
2	1	21	2	33	0
	2	22	1	27	0
	3	15	0	32	0
	4	22	0	32	0
	5	17	0	23	0
	6	15	0	37	0
	7	15	0	22	0
	8	20	0	22	0
	9	22	0	24	0
	10	15	3	24	0
	11	17	0	23	0
	12	23	0	34	0
	13	32	0	30	0
	14	20	0	26	0
	15	21	0	21	0
	1	15	2	25	0
	2	14	2	25	0
	3	21	0	20	0
	4	20	1	24	0
	5	25	0	19	0
	6	19	0	16	0
	7	20	0	19	0
	8	14	1	23	0

4	9	21	0	18	0
	10	17	0	19	0
	11	16	2	20	0
	12	28	5	28	0
	13	17	1	18	0
	14	15	0	19	0
	15	18	2	24	0
8	1	14	5	14	2
	2	24	7	17	2
	3	14	1	28	2
	4	19	0	17	0
	5	13	0	28	4
	6	14	0	15	2
	7	14	0	16	3
	8	24	5	28	1
	9	19	2	19	0
	10	13	4	20	0
	11	20	5	25	0
	12	19	4	15	1
	13	25	4	15	3
	14	22	3	28	0
	15	15	2	21	0
12	1	13	8	8	5
	2	13	7	9	4
	3	15	5	8	4
	4	15	8	9	3
	5	22	3	12	3
	6	12	4	19	2
	7	12	7	22	1
	8	21	6	8	2
	9	12	5	10	3
	10	15	6	10	4
	11	16	3	10	4
	12	17	5	10	3
	13	13	4	11	3
	14	21	8	14	1
	15	17	5	21	5
	1	12	5	26	7
	2	16	2	18	4
	3	14	8	20	5
	4	10	5	28	6
	5	17	2	24	5
	6	13	2	26	7

	7	20	3	21	5
48	8	16	6	16	6
	9	11	3	14	4
	10	17	5	26	5
	11	10	5	16	6
	12	16	2	14	4
	13	22	6	27	4
	14	19	5	19	5
	15	13	4	20	6